NAVIGATIONAL RISK OF CONTAINER FALLS IN THE STRAIT OF MALACCA

ARTICLES FOR FACULTY MEMBERS

Title/Author	AIS-enabled weather routing for cargo loss prevention / Spyrou-Sioula, K., Kontopoulos, I., Kaklis, D., Makris, A., Tserpes, K., Eirinakis, P., & Oikonomou, F..
Source	*Journal of Marine Science and Engineering* Volume 10 Issue 11 (2022) 1755 Pages 1-16 https://doi.org/10.3390/JMSE10111755 (Database: MDPI)

Title/Author	A new evaluation approach to control maritime transportation accidents: A study case at the Straits of Malacca / Md Hanafiah, R., Zainon, N. S., Karim, N. H., Abdul Rahman, N. S. F., Behforouzi, M., & Soltani, H. R.
Source	*Case Studies on Transport Policy* Volume 10 Issue 2 (2022) Pages 751–763 https://doi.org/10.1016/j.cstp.2022.02.004 (Database: ScienceDirect)

Title/Author	Assessing the influence of sudden propulsion loss on a ship's manoeuvrability in various wave heights utilizing CFD / Kim, D., Song, S., & Tezdogan, T.
Source	*Ocean Engineering* Volume 311 Part 2 (2024) 119022 Pages 1-13 https://doi.org/10.1016/J.OCEANENG.2024.119022 (Database: ScienceDirect)

27th October 2024

PSNZ

NAVIGATIONAL RISK OF CONTAINER FALLS IN THE STRAIT OF MALACCA

ARTICLES FOR FACULTY MEMBERS

Title/Author	Assessment of human error contribution to container loss risk under fault tree analysis and interval type-2 fuzzy logic-based SLIM approach / Erdem, P., Akyuz, E., Aydin, M., Celik, E., & Arslan, O.
Source	*Proceedings of the Institution of Mechanical Engineers Part M: Journal of Engineering for the Maritime Environment* Volume 238 Issue 3 (2024) Pages 553–566 https://doi.org/10.1177/14750902231203074 (Database: SagePub)

Title/Author	Crude oil transportation route choices: A connectivity reliability-based approach / Wang, S., Jia, H., Lu, J., & Yang, D.
Source	*Reliability Engineering and System Safety* Volume 235 (2023) 109254 Pages 1-11 https://doi.org/10.1016/j.ress.2023.109254 (Database: ScienceDirect)

Title/Author	Evaluation of the factors causing container lost at sea through fuzzy-based Bayesian network / Öztürk, O. B.
Source	*Regional Studies in Marine Science* Volume 73 (2024) 103466 Pages 1-12 https://doi.org/10.1016/J.RSMA.2024.103466 (Database: ScienceDirect)

📅 **27th October 2024**

PSNZ

NAVIGATIONAL RISK OF CONTAINER FALLS IN THE STRAIT OF MALACCA

ARTICLES FOR FACULTY MEMBERS

Title/Author	Exploring spatial patterns and environmental risk factors for global maritime accidents: A 20-year analysis / Zhou, X., Ruan, X., Wang, H., & Zhou, G.
Source	*Ocean Engineering* Volume 286 Part 1 (2023) 115628 Pages 1-10 https://doi.org/10.1016/j.oceaneng.2023.115628 (Database: ScienceDirect)
Title/Author	Simulating the impact of the sustained melting arctic on the global container sea–rail intermodal shipping / Sun, Z., Zhang, R., & Zhu, T.
Source	*Sustainability (Switzerland)* Volume 14 Issue 19 (2022) 12214 Pages 1-19 https://doi.org/10.3390/su141912214 (Database: MDPI)
Title/Author	Quantitive HAZOP and D-S evidence theory-fault tree analysis approach to predict fire and explosion risk in inert gas system on-board tanker ship / Durukan, O., Akyuz, E., Destanoğlu, O., Arslanoğlu, Y., & Sezer, S. I.
Source	*Ocean Engineering* Volume 308 (2024) 118274 Pages 1-12 https://doi.org/10.1016/J.OCEANENG.2024.118274 (Database: ScienceDirect)

27th October 2024

PSNZ

ARTICLES FOR FACULTY MEMBERS

NAVIGATIONAL RISK OF CONTAINER FALLS IN THE STRAIT OF MALACCA

Title/Author	**AIS-enabled weather routing for cargo loss prevention / Spyrou-Sioula, K., Kontopoulos, I., Kaklis, D., Makris, A., Tserpes, K., Eirinakis, P., & Oikonomou, F.**
Source	***Journal of Marine Science and Engineering*** **Volume 10 Issue 11 (2022) 1755 Pages 1-16** **https://doi.org/10.3390/JMSE10111755** **(Database: MDPI)**

Article

AIS-Enabled Weather Routing for Cargo Loss Prevention

Kalliopi Spyrou-Sioula [1,*], Ioannis Kontopoulos [1], Dimitrios Kaklis [2], Antonios Makris [1], Konstantinos Tserpes [1], Pavlos Eirinakis [3] and Fotis Oikonomou [2]

[1] Department of Informatics and Telematics, Harokopio University of Athens, 17778 Athens, Greece
[2] Danaos Research Center, Danaos Shipping Co., Ltd., 18545 Piraeus, Greece
[3] Department of Industrial Management & Technology, University of Piraeus, 18545 Piraeus, Greece
[*] Correspondence: itp20129@hua.gr

Abstract: The operation of any vessel includes risks, such as mechanical failure, collision, property loss, cargo loss, or damage. For modern container ships, safe navigation is challenging as the rate of innovation regarding design, speed profiles, and carrying capacity has experienced exponential growth over the past few years. Prevention of cargo loss in container ship liners is of high importance for the Maritime industry and the waterborne sector as it can lead to potentially disastrous, harmful, or even life-threatening outcomes for the crew, the shipping company, the marine environment, and aqua-culture. With the installment of onboard decision support system(s) (DSS) that will provide the required operational guidance to the vessel's master, we aim to prevent and overcome such events. This paper explores cargo losses in container ships by employing a novel weather routing optimization DS framework that aims to identify excessive motions and accelerations caused by bad weather at specific times and locations; it also suggests alternative routes and, thus, ultimately prevents cargo loss and damage.

Keywords: safety; parametric-roll; AIS; routing optimization; container ships

1. Introduction

Optimal ocean route planning is strongly connected to the safety and energy consumption of vessels as well as to the minimization of CO_2 emissions that reduce cost and the overall environmental footprint of shipping. Among other factors, it depends on efficient and robust ship tracking and weather forecasting. There exists a wealth of spatiotemporal data-driven solutions related to these issues that build upon a multitude of features from vessel tracking devices and structural properties of ships, weather conditions, and internal machinery sensors. Tracking can be performed using synthetic aperture radar (SAR) images and data from an automatic identification system (AIS) [1] or other surveillance systems [2]. The spatial dimensions focus on local conditions, e.g., wave-energy spectra and currents, which affect the costs of the overseas movement of a ship, while the temporal aspects correspond to environmental and ship-system conditions, and examine how they evolve with time (e.g., speed, power absorbed by the ship propulsion system, rotational motions along the three axes of the vessel).

Over the past few years, a high rate of innovation was observed concerning the designs (size increase, speed profile, cargo stored on deck) and operational profiles (loading profile, estimated time of arrival, charter party contracts) of container ship liners. This has led to increased risks for Maritime companies as they have little to no experience when it comes to safe and cost-efficient navigation of large, newly-built vessels. Container-carrying capacity has increased by around 1500% since 1968 and has almost doubled in the past decade (this is indicative of the innovation and scale expansion rate). While serious shipping accidents worldwide have declined, incidents involving large vessels—namely container ships—are resulting in disproportionately high losses. Large container ships are prone to onboard accidents and cargo losses due to excessive motions and accelerations in bad weather

conditions, leading to environmental pollution and financial damages for Maritime and insurance companies following container loss claims. Parametric roll due to bad weather conditions is one of the main reasons for cargo losses in container ships. Such situations can be avoided if identified along a vessel's course; these situations can be potentially prevented by employing a decision support (DS) toolkit, which offers the vessel's master an alternative route that takes into account the weather forecasts, the profile of the vessel, as well as navigational standards.

The research conducted in this paper is supported, enhanced, and validated by a large Maritime company [1] operating more than 70 container ships of various sizes, with a long-term commitment and expertise on the subject of safe navigation. Coupling and incorporating their input with guidelines extracted from the International Maritime Organisation (IMO) regulatory framework, this paper introduces a consolidated approach for routing optimization based on historical AIS and weather data in order to prevent parametric roll of the vessel and, therefore, container loss and damage. The envisaged framework will assist shipowners in achieving efficiency in fleet management with tangible benefits in terms of environmental compliance and protection of cargo and crew safety.

The remainder of the paper is organized as follows. Section 2 presents work related to weather routing. Section 3 provides the methodology followed in this work, including the necessary preprocessing for route extraction (Section 3.1), handling adverse conditions (Section 3.2), and the weather routing algorithm (Section 3.3). Section 4 presents the results of the corresponding computational study, while Section 5 concludes the paper.

2. Related Work

Weather routing has received increased attention in recent years due to increased available computational power, the improved quality of weather data and predictions, the increased interest in autonomous vessels and the drive to reduce emissions from ships. To that end, nowadays there is much better information on weather forecasts, with much higher spatial and temporal resolutions. The improvements in data quality and availability have facilitated the development of online algorithms for optimal routes during voyages. One must consider finding the optimal route and sailing speed for a given voyage considering the environmental conditions, mainly involving wind and waves. The objectives typically involve minimizing operating costs, travel time, fuel consumption, and risk of passage ([3]), with a focus on safety (i.e., parametric rolling or surf riding), comfort (passengers seasickness), and reducing cargo loss and damage. In [4], Fabbri et al. considered navigation risk based on sailing conditions following the IMO guidelines for navigators [2]. Moreover, other approaches have targeted multiple objectives [5,6].

Walther et al. [7] evaluated different modeling approaches, optimization algorithms, and their applications in weather routing systems. The analysis shows that the weather routing problem is treated as a single-objective or multi-objective optimization problem that can be modeled as a constrained graph problem, a constrained nonlinear optimization problem, or a combination of both. Depending on the modeling approach, different methods were used to solve it, ranging from Dijkstra's algorithm [8], dynamic programming [9,10], calculus of variations [11], and optimal control methods, to isochrone methods or iterative approaches for solving nonlinear optimization problems.

Zis et al. [3] presented a taxonomy of weather routing and voyage optimization research in Maritime transportation, explaining the main methodological approaches and key disciplines. Apart from the aforementioned methodologies, the use of pathfinding algorithms and heuristics as well as more recent applications using artificial intelligence and machine learning technologies were included.

Delitala et al. [12] presented two climatological simulations for ship routing. Simulations represented two theoretical long-distance routes in the central–eastern Mediterranean, which were analyzed across various simulated climatic conditions; the results were compared with those of control routes. Furthermore, a route simulator was developed for 7 Mediterranean routes and 15 different ships: passenger, cargo, and RO-PAX (i.e., dedi-

cated to carry both passengers and tracks). The results were analyzed in terms of passenger and crew comfort, bunker consumption by ships, and crossing time. The route simulator, based on the available wind and wave forecasts, takes into account the optimal velocity, corresponding to the desired arrival time, the optimal power, corresponding to the expected fuel consumption, and the minimum comfort index, corresponding to the best possible comfort conditions for passengers.

Shigunov et al. [13] presented some considerations regarding ship-specific operational guidance in order to avoid cargo loss and damage due to conditions of excessive roll motions and large accelerations in heavy weather. Furthermore, limiting values were defined, taking into account the actual lashing systems and mass distributions in container stacks, as well as the standards for probabilistic safety criteria on the basis of the required safety level and cost–benefit considerations. Maki et al. [14] presented a genetic weather routing algorithm that incorporated three different types of objective functions with different weights to balance between fuel efficiency and ship safety, taking into account parametric rolling, and numerically validating that there is a trade-off between ship safety and fuel efficiency.

Veneti et al. [5] proposed a weather routing algorithm based on an exact time-dependent bi-objective shortest path algorithm for ship routes in the area of the Aegean Sea, Greece. The two objectives of the problem involved the minimization of fuel consumption and the total risk of the ship route while taking into account the prevailing weather conditions and the total travel time. In the proposed model, the risk was defined as the combination of the results of a marine accident probability with the severity of its consequences. These accidents can be divided into nine categories: foundered, missing vessel, fire/explosion, collision, contact, grounding/wrecked/stranded, war loss/hostilities, hull/machinery damage, and miscellaneous. For the risk assessment information, such as the vessel type, size, age, flag, navigation area characteristics, traffic data, and historic data about accidents, weather and sea conditions were considered.

Perera et al. [15] presented an overview of weather routing and safe ship handling approaches in the shipping industry, which should be implemented simultaneously to achieve optimal and safe ship navigation conditions and minimize the respective environmental pollution. In particular, weather routing and safe ship handling were combined by selecting an optimal route with appropriate ship orientations and engine power configurations with vessel design characteristics under forecasted and actual weather conditions (i.e., wind, waves and tides/currents).

In July 2002, Regulation 19 of the International Convention for the Safety of Life at Sea (SOLAS-V) came into force, i.e., large cargo vessels were obliged to fit and use AIS for reporting their position, speed, and heading, and for serving surveillance purposes. This regulation resulted in an abundance of data that completely changed the Maritime surveillance scenario ([16]). Since then, there have been vast amounts of data on the sailing speeds and positions of ships globally. AIS data can be particularly useful to identify when ships deviate due to weather from traditional routes and provide real information on the actual benefits achieved through weather routing, particularly regarding savings in total voyage time.

AIS data are extensively utilized to examine and predict vessel trajectories. In this regard, a dual linear autoencoder approach for vessel trajectory prediction using AIS data was proposed in [17]. Chen et al. [18] proposed a ship movement classification based on AID data using convolutional neural networks. Volkova et al. [19] also utilized neural networks based on AIS data to predict a vessel's trajectory to reduce the likelihood of collisions or other incidents. A data mining approach was proposed by Rong et al. [20] to characterize shipping routes and offer anomaly detection, while pattern recognition for the vessel's handling behavior using an AIS sub-trajectory clustering analysis was proposed in [21].

Further, Varlamis et al. [22] presented a methodology for extracting information from the navigation network for an area, using data from the trajectories of multiple vessels, which are collected using AIS. The resulting information was modeled using a network

abstraction, which allows identifying the various movement patterns of vessels across an edge of the network and can be the basis for outlying behavior detection using off-the-shelf methods.

Kontopoulos et al. [16] extended the concept of the network abstraction model proposed in [22] and presented a distributed framework that captured the cargo vessel's behavior and extracted the pattern of its movement using AIS data. Specifically, it employs sparse historic AIS data and polynomial interpolation in order to extract shipping lanes. It modifies a well-established clustering algorithm, called density-based spatial clustering of applications with noise (DBSCAN) in order to achieve more coherent trajectory clusters, which are then composed to create the shipping lanes. Each itinerary that is represented as a set of convex hulls manages to accurately represent the spatial boundaries of the vessel movement indicating that any future AIS position can be effectively predicted and placed in a certain geographic region. Simultaneously, the convex hulls represent the behaviors of the vessel movements in terms of speed and headings and detect possible anomalies and deviations. This Maritime traffic model assumes that large vessels of the same type, such as cargo vessels or passenger ships, which mainly employ AIS, travel between the same waypoints by following the same routes and similar speeds, locations, and directions.

Kim et al. [23] calculated the energy efficiency operational indicator (EEOI) for monitoring the operational efficiency of a ship by using big data technologies to handle the large amount of ship dynamic data, which can be obtained from AIS in combination with the ship's static data and weather data. The latter is used for the estimation of additional resistance acting on the ship in order to calculate the engine power of the ship.

Kaklis et al. [24] presented a big data framework for the real-time monitoring of the operational state of a vessel as well as for simulation and model deployment purposes. This tool was utilized accordingly to extend and enhance the methodology initially proposed in [25,26] regarding fuel oil consumption (FOC) estimation. More specifically, a novel recurrent neural network architecture was introduced that ideally approximates the underlying function describing the vessel's FOC by taking into account historical operational and weather data. Finally, it was demonstrated how the FOC deep learning model could be coupled with a weather routing algorithm, proposing the optimal route for a vessel in terms of fuel consumption efficiency.

The scope of this work is to define a weather routing approach as a decision-making process to select the optimal route in a given voyage, taking into account the expected weather and sea conditions in order to prevent cargo loss and damage in container ships utilizing AIS data. The optimality of the selected route depends on the objective of reducing risk by avoiding certain areas with adverse weather. For this reason, we set some boundaries (standards) for unacceptable combinations of ship speed and course with respect to the mean wave direction, mean seaway periods, and significant wave heights. In order for the ship master to avoid these combinations, an alternative route was proposed in real time to satisfy the standards calculated from the ship's dynamic data (AIS) and weather data.

3. Methodology

In this section, a detailed description of the weather routing methodology is provided. Initially, a preprocessing phase takes place to extract the routes from the AIS messages. Then, the proper thresholds of the weather conditions when following Maritime routes are investigated and, finally, the weather routing algorithm is described.

3.1. Preprocessing

In this first phase, Maritime routes need to be extracted to be used as the baseline. To do so, previous works on extracting Maritime traffic patterns [16,22] were exploited. In these works, a series of steps were followed to extract the most commonly used vessel routes. Figure 1 illustrates these steps.
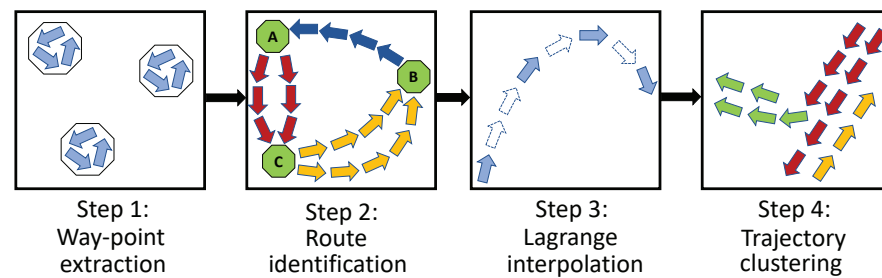
Figure 1. Preprocessing steps for extracting Maritime traffic routes.

Initially, the DBSCAN clustering algorithm was used to identify clusters or regions at sea, called waypoints, where the vessels stop. These waypoints correspond to ports and anchorage areas. Then, the AIS trajectories of each vessel were segmented based on the waypoints, thus routes from waypoint to waypoint were identified for each vessel. Because the vessel trajectories may be more sparse at certain points in time and space due to bad signal reception or other factors, interpolation was applied to the trajectories in step 3. Therefore, for each vessel route, dense and rich information trajectories were available. The final step employed a modified version of the DBSCAN algorithm to cluster multi-vessel trajectories of the same route (waypoint to waypoint) based on the location, speed, and heading of the AIS positions. As a result, several clusters along each route were created; each cluster represented the area in which vessels moved with a certain speed and heading. More details can be found in [16].

Figure 2 illustrates the final Maritime route network of the Mediterranean Sea that was extracted from the preprocessing phase. For each departure and destination point (e.g., from Piraeus to Port Said), a set of clusters and their centroids are available, which specify the ways the vessels move in terms of space, speed, and headings between the departure and destination points.
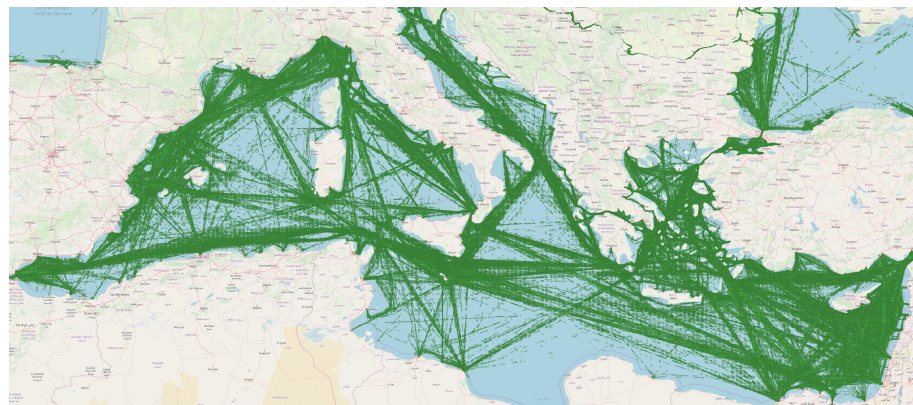
Figure 2. The final Maritime route network.

3.2. Adverse Weather Conditions for Container Ships

To identify changes in the route based on the weather, the Copernicus Marine Service [3] (CMEMS) and the Copernicus Climate Change Service [4] (C3S) were used for the wave and wind data, respectively. Data from these services are gridded, meaning that weather data are provided for each cell in the grid. The grid resolution for the former service is $0.083°$, while for the latter service is $0.25°$. To create a uniform grid for all the weather data at the same time, bilinear interpolation of the wind data onto the wave data was employed. As a result, the final weather grid that contains both wind and wave information had a resolution of $0.083°$. This resolution was chosen in order to have a more fine-grained grid, creating a richer pool of spatial options to choose from when considering alternate routes. Due to a large amount of weather data for our study area, a three-hourly temporal resolution was chosen. So, each route was generalized and divided into three-hourly

intervals to synchronize with the weather data. In particular, the timestamp of each route's centroid was matched to the nearest available timestamp of the weather data grid.

After careful examination of the IMO guidelines [5,6], the literature review conducted in Section 2 and incorporating the expertise of a major container ship operator (Danaos Shipping), it was decided that the significant wave height, the mean wave period, the mean wind speed, the wave direction, and their corresponding thresholds—adverse condition thresholds—as shown in Table 1, will be used for the implementation of the weather routing algorithm. Danaos's expertise originated from the investigation of operational incidents resulting in cargo loss. Investigation reports include weather conditions at the time of the incident as potential root causes for the loss of cargo. The definition of the Weather threshold contains an empirical analysis in reference to the investigation of past incidents as reported in the organizational assets of Danaos shipping.

Table 1. Weather thresholds of adverse conditions.

Significant Wave Height h_s (m)	Peak Wave Period T_p (s)	Mean Wind Speed (m/s) V_w	Wave Direction (Range in °)
≤ 6.0	$7.0 \leq T_p \leq 15.0$	≤ 22.6	60–120° and 240–300°

Specifically, regarding the wave period, it was decided to use the metric of the mean wave period. According to IMO guidelines, when a ship rides on the wave crest, there is a great possibility of its stability reduction. This may become critical for wavelengths (λ) within the range of 0.6 to 2.3 L (where L is the ship's length in meters). So, considering the wavelength as 0.6 L, the mean wave period was calculated in relation to the wavelength (λ) following the equation $0.8 \cdot sqrt(\lambda)$.

Regarding the wave direction, thresholds according to [13] were used, in which unacceptable combinations of the ship heading, with respect to the mean wave direction, are displayed. If the ship master avoids the lateral wave direction (beam-to-quartering waves) as shown in Table 1, the risk of excessive motions and accelerations will reduce and, thus, the prevention of cargo loss and damage increases.

Our study focused on vessels that have lengths below 200 m (i.e., with the length between perpendiculars (lpp): lpp < 200). This means that at any given time point: (i) the wave must not exceed a height of 4.5 m, (ii) the mean wave period must not exceed 8 s, (iii) the wind must not exceed a mean speed of 19 m per second, and (iv) the difference between the direction of the wave and the direction of the vessel must not be in the specified ranges.

3.3. Weather Routing Algorithm

To calculate an alternate route option based on the adverse weather conditions as defined in Table 1, and given an initial departure/destination point, and departure time, the set of centroids (see Section 3.1) along that route is iterated. The following steps are made during the weather routing process and are depicted in Algorithm 1:

1. Based on the current timestamp [7], the mean speed provided by the current centroid of the route [8], and the Haversine [9] distance between the current centroid and the next one along that route, the timestamp of the next centroid is calculated (line 4).
2. The position of the next centroid is used to find the cell of the weather grid at which the vessel will be located.
3. Given the timestamp and the grid cell of the next centroid, the weather conditions from the Copernicus services are retrieved (line 5).
4. If the weather conditions are adverse (see Section 3.2), the nearest cell of the weather grid in the space–time that satisfies the weather thresholds is found (line 7). The centroid of the weather grid acts as the proposed alternative for the vessel to move to (line 8). If the weather conditions are not adverse, the initial centroid is used for the route (line 10). To speed up the process, the search space is limited to the distance the vessel would have traveled, given the mean speed of the centroid and the three-hour

time horizon. To find the nearest cell, the nearest neighbor algorithm is employed, which finds the nearest cell in relation to distance from the route centroid using spatial indexing (R-tree). R-trees allow indexing data values, which are defined in two (or more) dimensions. The search strategy uses the best-first-search to query the index, where the values are provided in order of the increasing distance. We limited the search to a maximum of 10 nearest points.

5. Finally, the next centroid of the initial route is considered the current one and the entire process repeats itself until there are no more centroids along the route.

Algorithm 1 Weather Routing algorithm

Input: A set of centroids along the initial route R, Weather Thresholds WT
Output: A set of centroids along the optimized route R_o

1: **function** ROUTEOPTIMIZATION($R[\ ]$)
2: $\quad R_o \leftarrow []$
3: $\quad$ **for** $i \leftarrow 1$ to $length(R)$ **do**
4: $\quad\quad t(c_{i+1}) \leftarrow distance(c_i, c_{i+1})/v(c_i)$
5: $\quad\quad w \leftarrow getWeatherConditions(t(c_{i+1}), cell(c_{i+1}))$
6: $\quad\quad$ **if** w exceeds WT **then**
7: $\quad\quad\quad cellCentroid \leftarrow getNearestNeighbor(cell(c_{i+1}))$
8: $\quad\quad\quad R_o.append(cellCentroid)$
9: $\quad\quad$ **else**
10: $\quad\quad\quad R_o.append(c_{i+1})$
11: $\quad$ **return** R_o

Figures 3–5 illustrate three examples of the alternate route recommendation via the weather routing algorithm and the adverse condition thresholds. The red lines indicate the initial route the vessel is supposed to follow and the yellow lines indicate the route proposed by the algorithm.
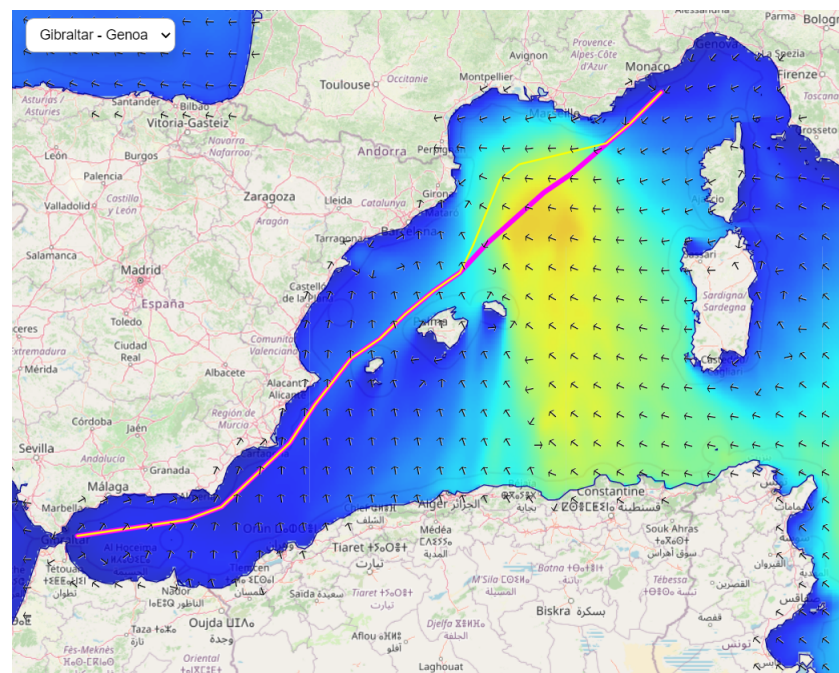
Figure 3. Alternate route recommendation on route Gibraltar–Genoa.
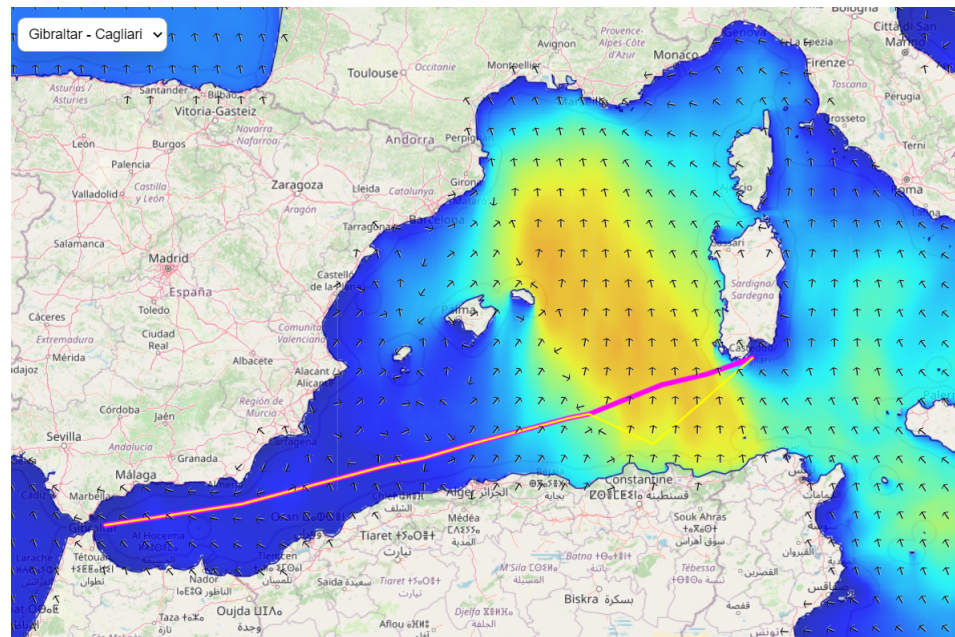
Figure 4. Alternate route recommendation on route Gibraltar–Cagliari.
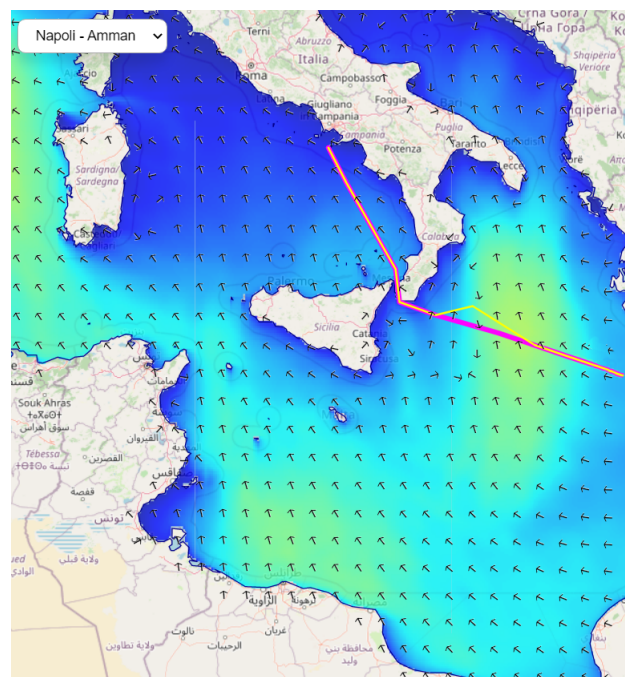
Figure 5. Alternate route recommendation on route Napoli–Amman.

4. Results

To evaluate the proposed weather routing algorithm, we used a dataset that was produced during the study of Kontopoulos et al. [16] and composed of several routes in the Mediterranean sea during the period from January 2022 to March 2022. For evaluation purposes, we chose 15 frequent routes with varying trajectory durations, from one day to several weeks.

The proposed weather routing algorithm takes into account four different weather thresholds. To properly evaluate the algorithm on each threshold, we compared the prevailing weather conditions between the initial routes and the alternate ones. Specifically, for the wave height, we measured its mean value $\overline{h_s^a}$ along the portion (set of centroids) of the route where the adverse conditions were in effect. Then, we measured the mean wave

height $\overline{h_s^b}$ of the alternate route during the same period of time. The difference between the mean values to the initial mean value $\overline{h_s^a}$ indicates the percentage of the decrease of the significant wave height h_s (Equation (1)). The percentage-wise decrease of the wave height for each route is demonstrated in Figure 6.

$$H = \frac{\overline{h_s^a} - \overline{h_s^b}}{\overline{h_s^a}} \qquad (1)$$
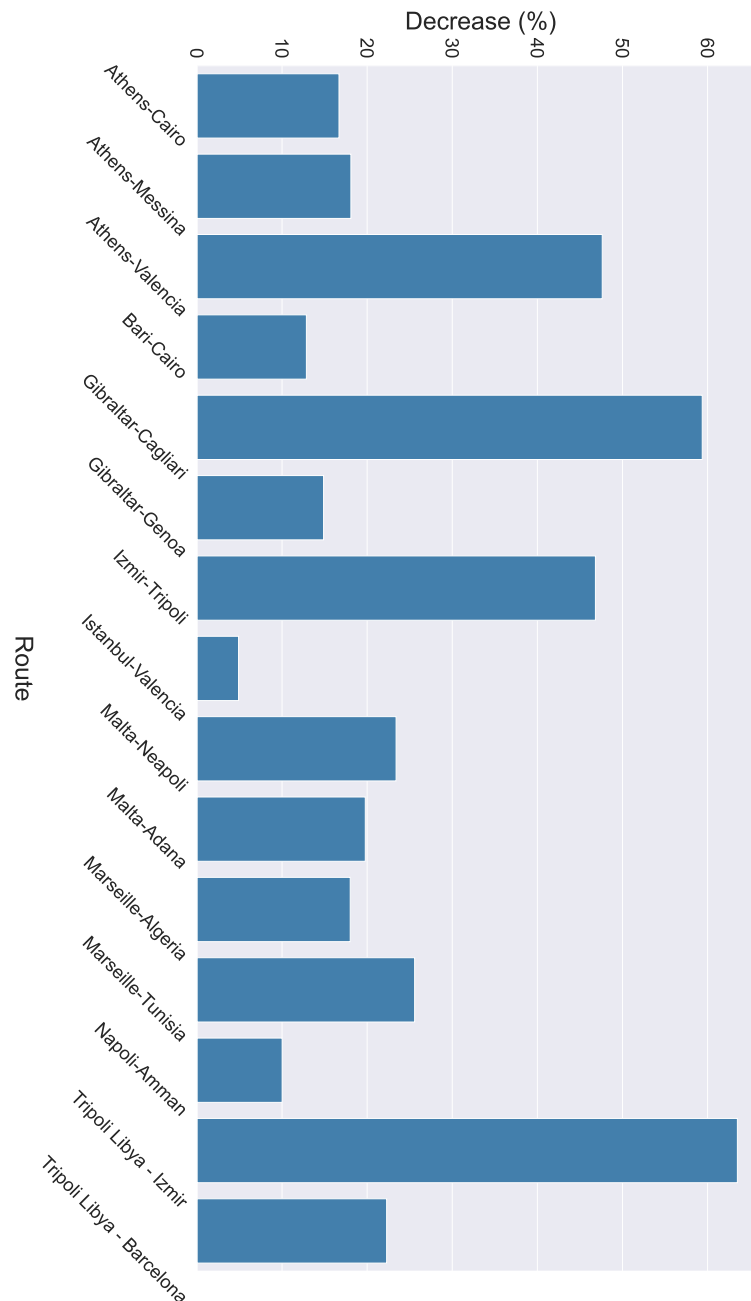
Figure 6. Decrease of the wave height when the alternate routes are followed.

We can observe that the minimum decrease was 5% in the route from Napoli to Amman and the maximum decrease was approximately 60% in the route from Gibraltar to Cagliari. Furthermore, the mean decrease overall was at about 22%. The same process was followed for the other weather thresholds as well. Specifically, for the wave period and the wind speed, we measured their mean values ($\overline{p_s^a}$ and $\overline{v_s^a}$, respectively) along the portion

of the route where the adverse conditions were in effect. In the next step, we measured the mean wave period $\overline{p_s^b}$ and the mean wind speed $\overline{v_s^b}$ of the alternate route during the same period of time. The difference between the mean values to the initial mean values indicates the percentage of the decrease of the wave period p_s (Equation (2)) and the wind speed (Equation (3)), respectively. The percentage-wise decrease of the wave period is demonstrated in Figure 7 and the percentage-wise decrease of the wind speed is illustrated in Figure 8 for each route.

$$P = \frac{\overline{p_s^a} - \overline{p_s^b}}{\overline{p_s^a}} \tag{2}$$

$$V = \frac{\overline{v_s^a} - \overline{v_s^b}}{\overline{v_s^a}} \tag{3}$$
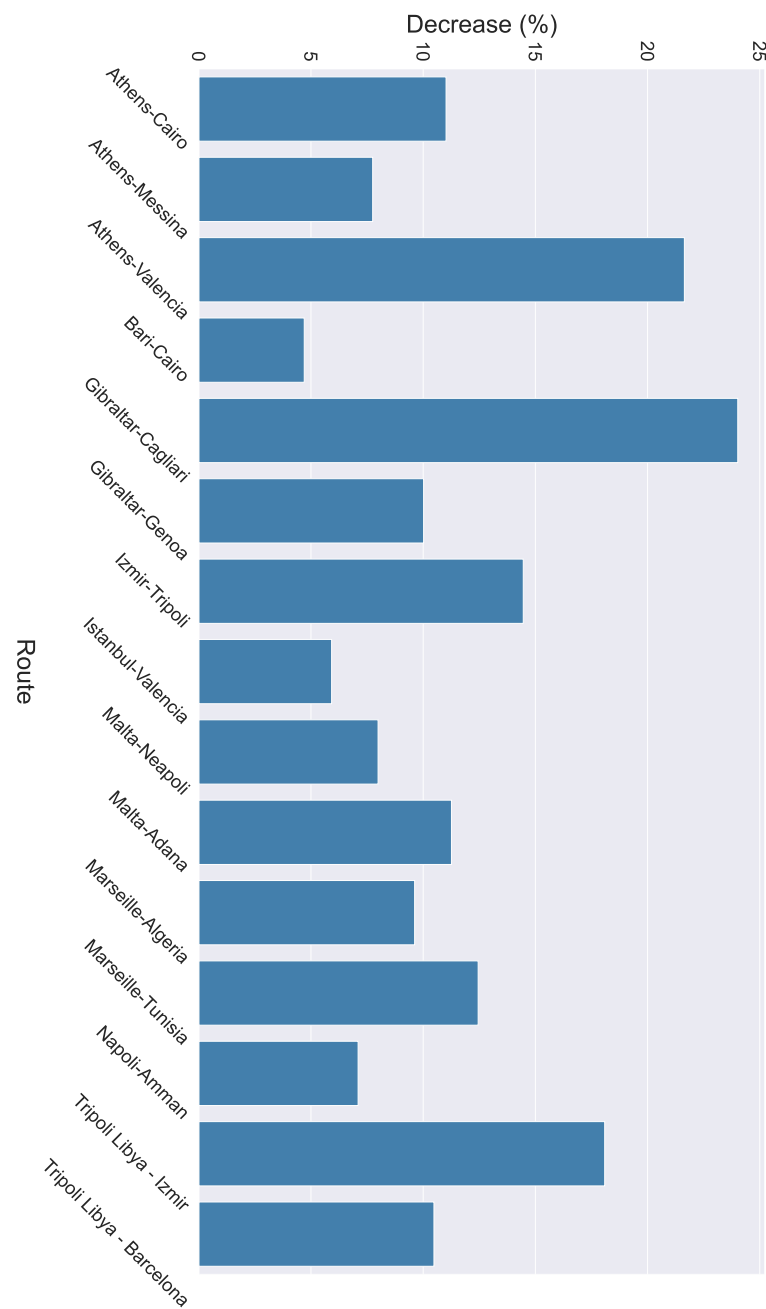
Figure 7. Decrease of the wave period when the alternate routes are followed.

Regarding the wave period, it is observed that there was a decrease of approximately 11% with a maximum decrease of 24% and a minimum decrease of 4%. In terms of wind speed, only the routes of Marseille–Algeria and Napoli–Amman demonstrated a decrease of 8% and 18%, respectively. This is due to the fact that in the other routes the wind speed threshold was not exceeded.
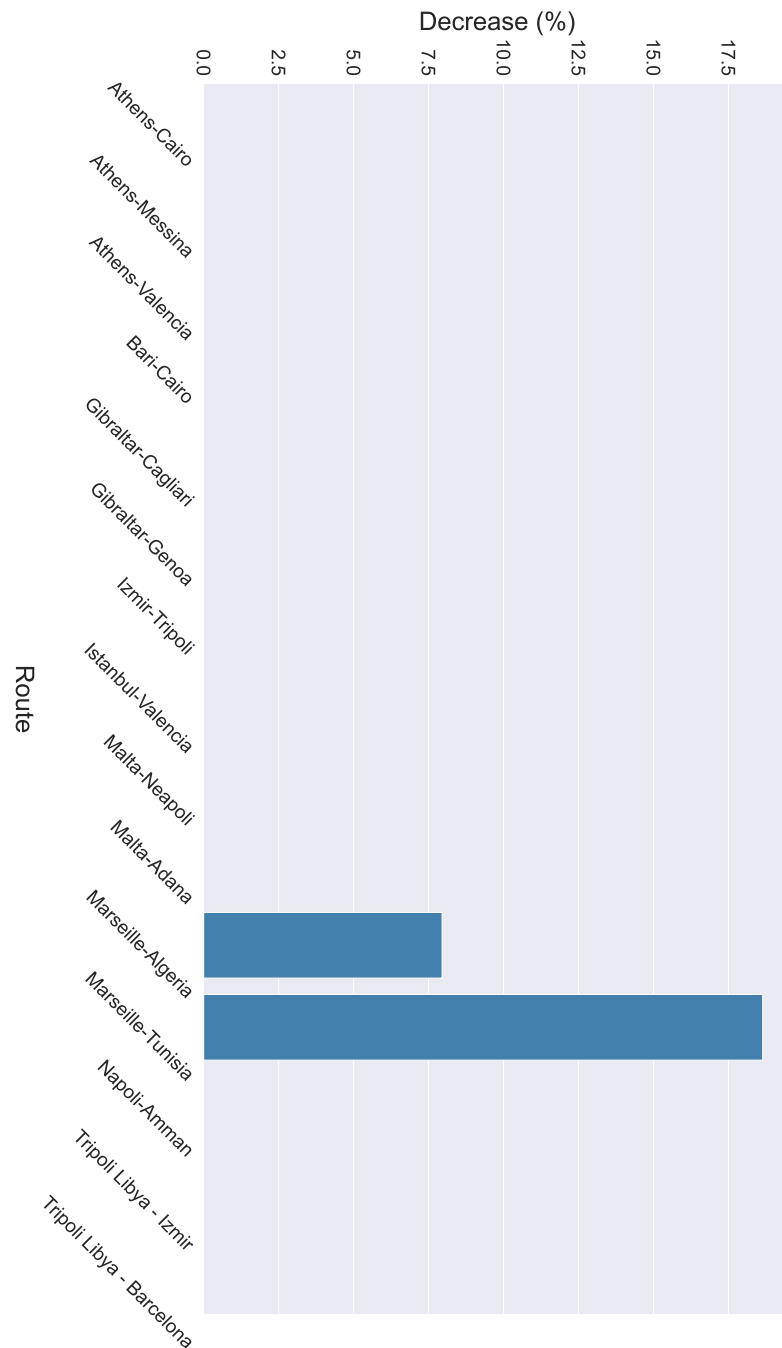
Figure 8. Decrease of the wind speed when the alternate routes are followed.

Similar to the previous thresholds, the mean direction of the relative difference between the vessel's heading and the wave's direction was measured in both routes (initial and alternate). As the denominator, the mean wave direction of the initial route was used and the difference in the wave direction of the routes was used as the numerator. As a result, the percentage-wise deviation of the wave direction between the routes is illustrated in

Figure 9. Based on the results, the maximum deviation reached 24% and the minimum deviation was approximately 0.5%.
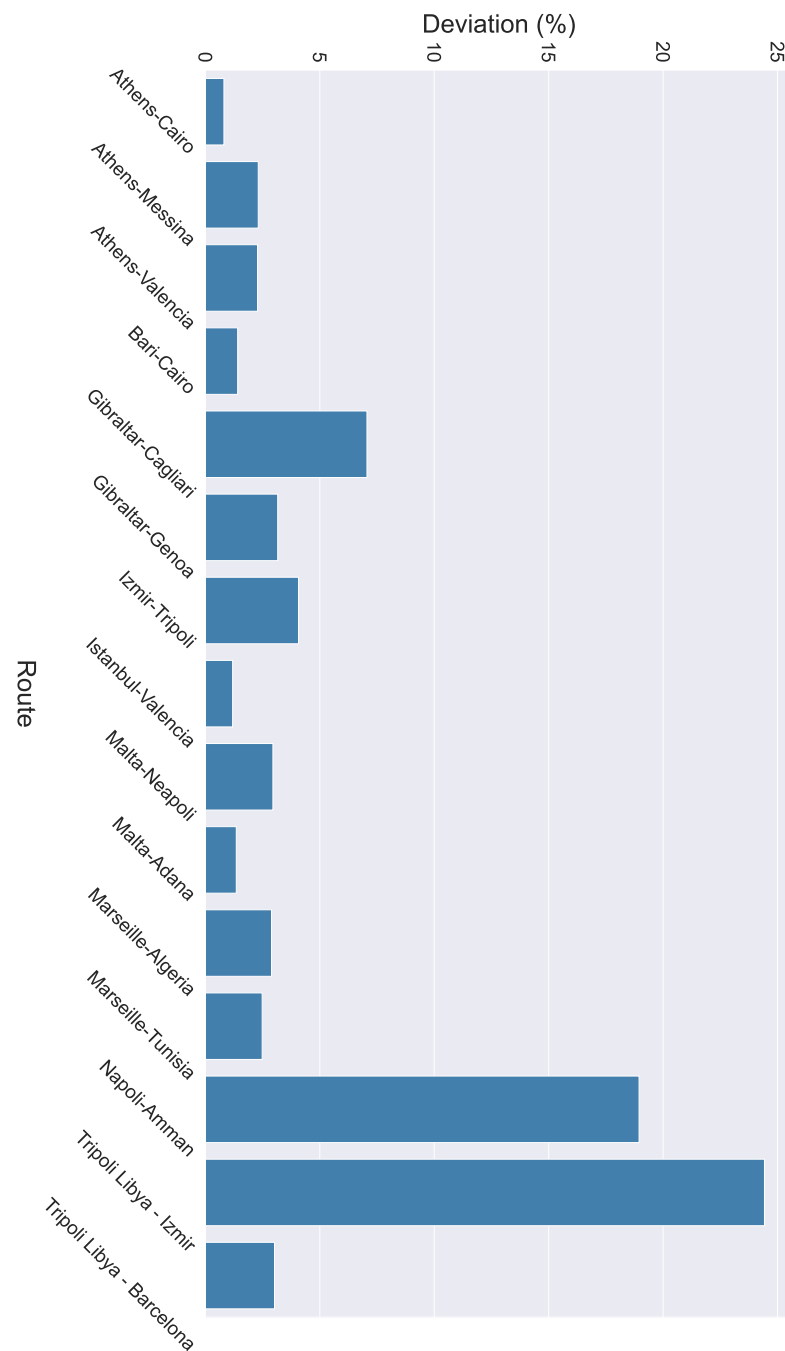
Figure 9. Deviation of wave direction when the alternate routes are followed.

Finally, Figure 10 displays the length of the trajectories for both the initial and the recommended routes, and Figure 11 displays the difference in length between the initial and the recommended routes. It can be observed that the maximum difference in length is approximately 200 km in the case of the Istanbul–Valencia route. Taking into account that the initial route is over 2500 km, a difference of 200 km is only an ≈8% difference, which is an acceptable deviation compared to the cargo loss and potential impact on the regional marine ecology and environment.
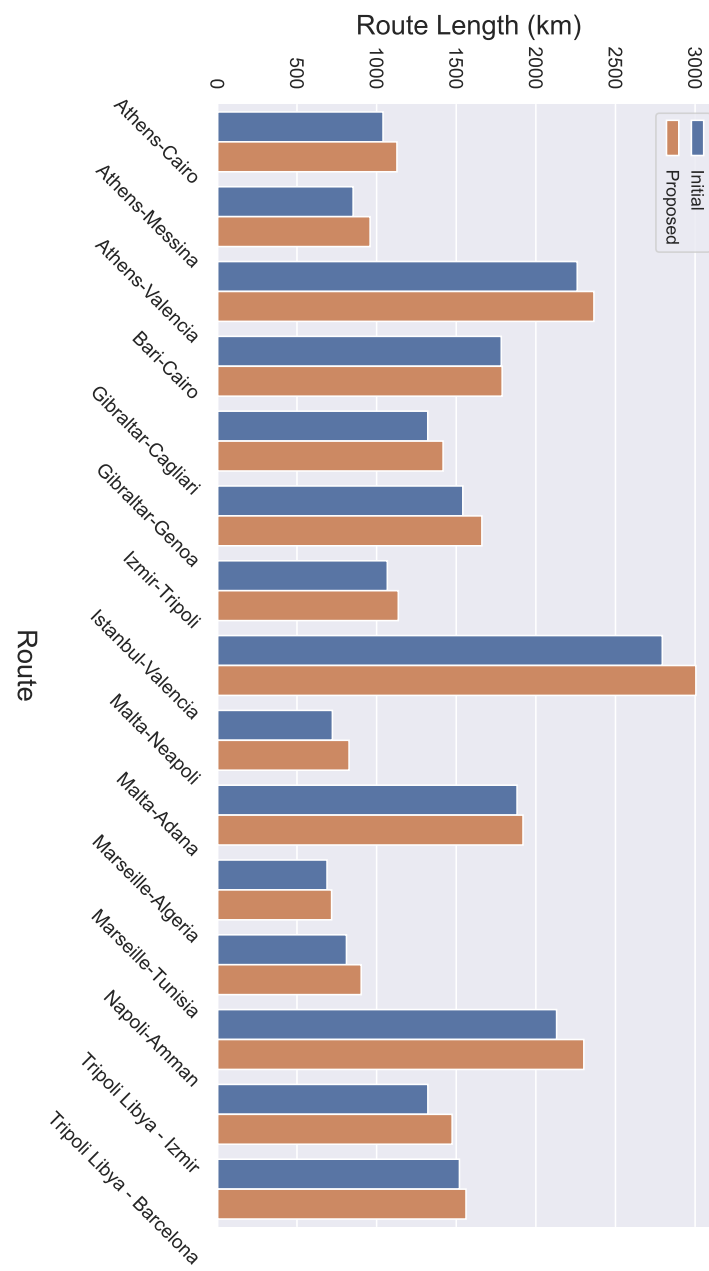
Figure 10. The length of the routes for both the initial and recommended routes.
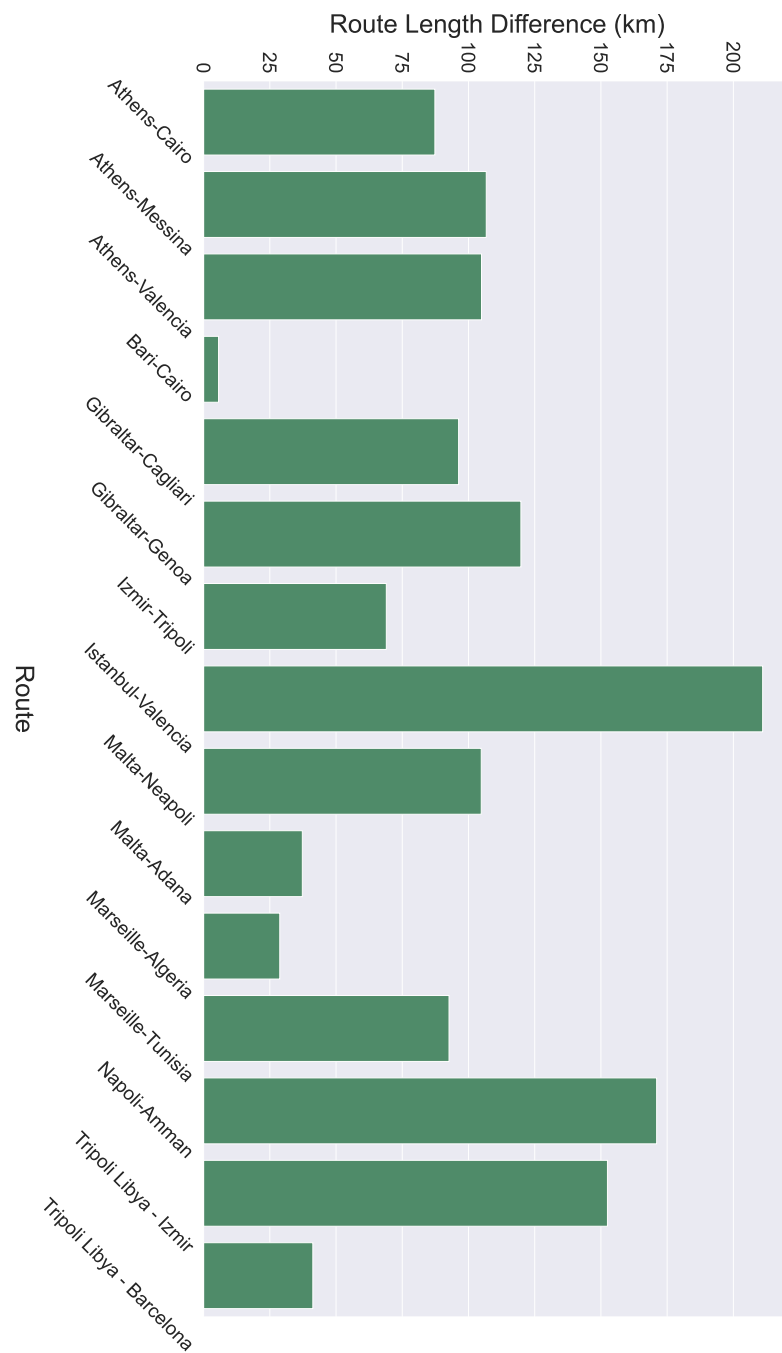
Figure 11. The difference in length between the initial and the recommended routes.

5. Conclusions

This paper proposed a weather routing optimization algorithm for cargo loss prevention based on historical AIS data. The proposed algorithm employed historical AIS trajectories to extract the Maritime routes of container ships. IMO guidelines, pertinent literature on the subject, and Maritime expertise from marine engineers and operators were exploited and combined accordingly to outline a consolidated framework, defining the appropriate thresholds of adverse weather conditions for container ships. The evaluation of the algorithm demonstrated a significant decrease in bad weather conditions (e.g., wind speed, wave height) when the (alternative) optimal routes were followed instead of the initial ones.

In future work, we will aim to apply the weighted thresholds for adverse weather conditions. This will eventually result in a more refined, adaptive routing optimization

scheme as different weather thresholds (e.g., wind speed and wave direction) will be considered distinctively when planning an alternative route. Therefore, a variety of other factors will be taken into account, such as vessel-specific variables (size, deadweight, displacement, etc.) as well as real-time operational features (speed, power, heading, etc.) acquired from onboard sensor installments.

Author Contributions: Conceptualization, I.K.; Methodology, K.S.-S. and I.K.; writing—original draft preparation, I.K., K.S.-S. and D.K.; writing—review and editing, A.M., K.T., P.E. and F.O. All authors have read and agreed to the published version of the manuscript.

Institutional Review Board Statement: Not applicable.

Informed Consent Statement: Not applicable.

Data Availability Statement: Not applicable.

Conflicts of Interest: The authors declare no conflict of interest.

Notes

1. Danaos Shipping, https://danaos.com/ (accessed on 2 November 2022).
2. https://wwwcdn.imo.org/localresources/en/OurWork/Safety/Documents/Stability/MSC.1-CIRC.1228.pdf (accessed on 2 November 2022).
3. https://marine.copernicus.eu/ (accessed on 2 November 2022).
4. https://climate.copernicus.eu/ (accessed on 2 November 2022).
5. https://wwwcdn.imo.org/localresources/en/OurWork/Safety/Documents/Stability/MSC.1-CIRC.1228.pdf (accessed on 2 November 2022).
6. https://wwwcdn.imo.org/localresources/en/OurWork/Environment/Documents/MEPC.1-CIRC.850-REV2.pdf (accessed on 2 November 2022).
7. (the first timestamp is the departure time).
8. (initially, this is the departure point).
9. (the Haversine—or great circle—distance is the angular distance between two points on the surface of a sphere).

References

1. Zhao, Z.; Ji, K.; Xing, X.; Zou, H.; Zhou, S. Ship surveillance by integration of space-borne SAR and AIS–review of current research. *J. Navig.* **2014**, *67*, 177–189. [CrossRef]
2. Chen, S.; Hong, X.; Khalaf, E.; Morfeq, A.; Alotaibi, N.D. Adaptive B-spline neural network based nonlinear equalization for high-order QAM systems with nonlinear transmit high power amplifier. *Digit. Signal Process.* **2015**, *40*, 238–249. [CrossRef]
3. Zis, T.P.; Psaraftis, H.N.; Ding, L. Ship weather routing: A taxonomy and survey. *Ocean. Eng.* **2020**, *213*, 107697. [CrossRef]
4. Fabbri, T.; Vicen-Bueno, R.; Hunter, A. Multi-criteria weather routing optimization based on ship navigation resistance, risk and travel time. In Proceedings of the 2018 International Conference on Computational Science and Computational Intelligence (CSCI), Las Vegas, NV, USA, 12–14 December 2018; pp. 135–140.
5. Veneti, A.; Makrygiorgos, A.; Konstantopoulos, C.; Pantziou, G.; Vetsikas, I.A. Minimizing the fuel consumption and the risk in Maritime transportation: A bi-objective weather routing approach. *Comput. Oper. Res.* **2017**, *88*, 220–236. [CrossRef]
6. Yang, J.; Wu, L.; Zheng, J. Multi-Objective Weather Routing Algorithm for Ships: The Perspective of Shipping Company's Navigation Strategy. *J. Mar. Sci. Eng.* **2022**, *10*, 1212. [CrossRef]
7. Walther, L.; Rizvanolli, A.; Wendebourg, M.; Jahn, C. Modeling and optimization algorithms in ship weather routing. *Int. J. -Navig. Marit. Econ.* **2016**, *4*, 31–45. [CrossRef]
8. Pennino, S.; Gaglione, S.; Innac, A.; Piscopo, V.; Scamardella, A. Development of a new ship adaptive weather routing model based on seakeeping analysis and optimization. *J. Mar. Sci. Eng.* **2020**, *8*, 270. [CrossRef]
9. Shao, W.; Zhou, P.; Thong, S.K. Development of a novel forward dynamic programming method for weather routing. *J. Mar. Sci. Technol.* **2012**, *17*, 239–251. [CrossRef]
10. Wei, S.; Zhou, P. Development of a 3D dynamic programming method for weather routing. *Transnav Int. J. Mar. Navig. Saf. Sea Transp.* **2012**, *6*, 79–85.
11. Papadakis, N.A.; Perakis, A.N. Deterministic minimal time vessel routing. *Oper. Res.* **1990**, *38*, 426–438. [CrossRef]

12. Delitala, A.M.S.; Gallino, S.; Villa, L.a.; Lagouvardos, K.; Drago, A. Weather routing in long-distance Mediterranean routes. *Theor. Appl. Climatol.* **2010**, *102*, 125–137. [CrossRef]

13. Shigunov, V.; Moctar, O.E.; Rathje, H. Operational guidance for prevention of cargo loss and damage on container ships. *Ship Technol. Res.* **2010**, *57*, 8–25. [CrossRef]

14. Maki, A.; Akimoto, Y.; Nagata, Y.; Kobayashi, S.; Kobayashi, E.; Shiotani, S.; Ohsawa, T.; Umeda, N. A new weather-routing system that accounts for ship stability based on a real-coded genetic algorithm. *J. Mar. Sci. Technol.* **2011**, *16*, 311–322. [CrossRef]

15. Perera, L.P.; Soares, C.G. Weather routing and safe ship handling in the future of shipping. *Ocean. Eng.* **2017**, *130*, 684–695. [CrossRef]

16. Kontopoulos, I.; Varlamis, I.; Tserpes, K. A distributed framework for extracting Maritime traffic patterns. *Int. J. Geogr. Inf. Sci.* **2021**, *35*, 767–792. [CrossRef]

17. Murray, B.; Perera, L.P. A dual linear autoencoder approach for vessel trajectory prediction using historical AIS data. *Ocean. Eng.* **2020**, *209*, 107478. [CrossRef]

18. Chen, X.; Liu, Y.; Achuthan, K.; Zhang, X. A ship movement classification based on Automatic Identification System (AIS) data using Convolutional Neural Network. *Ocean. Eng.* **2020**, *218*, 108182. [CrossRef]

19. Volkova, T.A.; Balykina, Y.E.; Bespalov, A. Predicting ship trajectory based on neural networks using AIS data. *J. Mar. Sci. Eng.* **2021**, *9*, 254. [CrossRef]

20. Rong, H.; Teixeira, A.; Soares, C.G. Data mining approach to shipping route characterization and anomaly detection based on AIS data. *Ocean. Eng.* **2020**, *198*, 106936. [CrossRef]

21. Gao, M.; Shi, G.Y. Ship-handling behavior pattern recognition using AIS sub-trajectory clustering analysis based on the T-SNE and spectral clustering algorithms. *Ocean. Eng.* **2020**, *205*, 106919. [CrossRef]

22. Varlamis, I.; Kontopoulos, I.; Tserpes, K.; Etemad, M.; Soares, A.; Matwin, S. Building navigation networks from multi-vessel trajectory data. *GeoInformatica* **2021**, *25*, 69–97. [CrossRef]

23. Kim, S.H.; Roh, M.I.; Oh, M.J.; Park, S.W.; Kim, I.I. Estimation of ship operational efficiency from AIS data using big data technology. *Int. J. Nav. Archit. Ocean. Eng.* **2020**, *12*, 440–454. [CrossRef]

24. Kaklis, D.; Eirinakis, P.; Giannakopoulos, G.; Spyropoulos, C.; Varelas, T.J.; Varlamis, I. A big data approach for Fuel Oil Consumption estimation in the Maritime industry. In Proceedings of the 2022 IEEE Eighth International Conference on Big Data Computing Service and Applications (BigDataService), Newark, CA, USA, 15–18 August 2022; 2022; pp. 39–47.

25. Kaklis, D.; Giannakopoulos, G.; Varlamis, I.G.; Spyropoulos, C.; Varelas, T.J. A data mining approach for predicting main-engine rotational speed from vessel-data measurements. In Proceedings of the IDEAS'19: Proceedings of the 23rd International Database Applications & Engineering Symposium, Athens, Greece, 10–12 June 2019; ACM: New York, NY, USA, 2019; pp. 1–10.

26. Kaklis, D.; Giannakopoulos, G.; Varlamis, I.G.; Spyropoulos, C.; Varelas, T.J. Online Training for Fuel Oil Consumption Estimation: A Data Driven Approach. In Proceedings of the 23rd IEEE International Conference on Mobile Data Management (MDM), Paphos, Cyprus, 6–9 June 2022; pp. 1–10.

ARTICLES FOR FACULTY MEMBERS

NAVIGATIONAL RISK OF CONTAINER FALLS IN THE STRAIT OF MALACCA

Title/Author	**A new evaluation approach to control maritime transportation accidents: A study case at the Straits of Malacca / Md Hanafiah, R., Zainon, N. S., Karim, N. H., Abdul Rahman, N. S. F., Behforouzi, M., & Soltani, H. R.**
Source	*Case Studies on Transport Policy* **Volume 10 Issue 2 (2022) Pages 751–763** **https://doi.org/10.1016/j.cstp.2022.02.004** **(Database: ScienceDirect)**

A new evaluation approach to control maritime transportation accidents: A study case at the Straits of Malacca

Rudiah Md Hanafiah [a], Nurul Sakinah Zainon [b], Nur Hazwani Karim [c],
Noorul Shaiful Fitri Abdul Rahman [d,*], Mehrdad Behforouzi [e], Hamid Reza Soltani [e]

[a] *Faculty of Maritime Studies, Universiti Malaysia Terengganu, 21300 Kuala Terengganu, Terengganu, Malaysia*
[b] *DB Schenker Logistics (Malaysia) Sdn. Bhd, Malaysia*
[c] *Faculty of Maritime Studies, Universiti Malaysia Terengganu, 21300 Kuala Terengganu, Terengganu, Malaysia*
[d] *Faculty of Business, Higher Colleges of Technology, Abu Dhabi 25035, United Arab Emirates*
[e] *Department of Maritime, International Maritime College Oman, 322 Sohar, Sultanate of Oman*

A B S T R A C T

The Strait of Malacca (SOM) has a high vessel traffic density, making it a bustling region with a significant risk of accidents. The safety of navigation will be jeopardised as trading and the number of vessels passing through the chokepoint increase. Additionally, the attempts to maintain security and safety in the region impose significant expenses on the government. A continuous effort is crucial to sustaining these numbers at bay in the future. As a result, this research aims to evaluate the traffic situation and develop a decision-making model to reduce maritime accidents at SOM. Following that, two Multiple-Criteria Decision-Making (MCDM) techniques were employed: the Analytic Hierarchy Process (AHP) and the Technique for Order of Preference by Similarity to Ideal Solution (TOPSIS). The proposed decision-making model will assist the Marine Department of Malaysia and other related entities to promote safety awareness.

1. Introduction

International trade and economic development have relied heavily on maritime transportation from the dawn of time. It has played a crucial part in the geographic discovery, cultural exchange, and economic growth throughout history. Over 90% of global commerce takes place on the ocean (UNCTAD, 2019). It is by far the most cost-effective method of transporting products and raw materials worldwide. A strait is a narrow passage of water that connects two larger bodies of water and is critical for both international and domestic navigation (Roberts, 2006). With respect to the Law of the Sea Convention 1982 (LOSC), the Straits of Malacca and Singapore are treated as a single strait (Rusli, 2020), which are also among the busiest maritime routes in the world, and play a significant role in the global commerce.

The Malacca Strait is the world's longest strait and a vital shipping route (Zaman et al., 2015). Trade between the Indian Ocean, the South China Sea, and the Pacific Ocean has traditionally used this route. The SOM is an important economic corridor that passes through 60% of the world's marine commerce. It is also one of the main oil transit routes

because it is the quickest way to get Middle Eastern oil to China, South Korea, and Japan, all in the Far East (China Team Power, 2017; Rusli, 2012). Its physical location is critical for the Indo-Pacific area that connects Malaysia, Indonesia, and Singapore, referring to the SOM as the "national assets" (Dahalan et al., 2013; Handani et al., 2018). The Malacca Strait connects the east coast of Sumatra Island in Indonesia with the west coast of Peninsular Malaysia and is situated between the two seas. Its southern end connects with the Strait of Singapore.

The SOM plays a vital role in international seaborne trade. Container ships, oil tankers, and bulk carriers are the most common ships that pass the Malacca Strait (Abdul Rahman et al., 2016). Accident rates are high at seaports all around the world, making maritime transportation at sea a dangerous place to navigate. The bigger the significance of shipping in international commerce, the greater the effect of maritime accidents on the global economy. In addition, the geographical location of the Malacca Strait, which makes it so crucial for world trade, also places it at high risk due to the heavy traffic that has led to many marine tragedies (Rusli, 2020; Yasin et al., 2019). Maritime accidents often occur in waterways such as straits and canals with a high traffic volume and are

---

constrained by geography (Luo and Shin, 2019). Keeping up with the ever-increasing traffic has become a major safety and security concern of maritime transportation at the SOM. Thus, the study of maritime traffic safety in the Malacca Strait is critical for improving navigational safety.

According to the existing records from the Marine Department of Malaysia, the number of maritime accidents in the SOM witnessed an upward trend between 1999 and 2017. A cumulative number of 92 maritime accidents occurred between 1999 and 2017 (Marine Department of Malaysia, 2017). Fig. 1 depicts the type of accidents involved in the SOM from 1999 to 2017, including collision, grounding, sinking, collision on fire, medical evacuation (Medevac), wrecking, engine problems, man overboard, unstable, hijacked and on fire. Collision showed the most common type of accidents over the timeframe, followed by grounding and sinking, respectively. Moreover, between 2014 and 2015, it reached a peak accounted for 13 accidents, respectively, before dropping drastically in 2016. The latest data obtained from the government agency was in 2017, recording two grounding cases and one sinking at the SOM.

The SOM is a well-known waterway utilised by sailors from all over the globe for safe passage. It is a narrow strait measuring twenty-two and a half metres deep with 805 km (500 nautical miles), making it the longest in Southeast Asia (Kamran Dastjerdi and Hosseini Nasrabady, 2020). The SOM is designated as a strait posing a significant risk of ship collisions. This area has a greater level of risk. One of the concerns that authorities and policymakers are grappling with is identifying the variables contributing to maritime accidents resulting in oil spills to create effective prevention and mitigation measures (Cakir et al., 2021). As such, this study aims to develop a decision-making model that can be used by national or maritime organisations to develop specific safety plans, allocate resources, and make better decisions regarding the prevention and handling of maritime accidents thereby improving shipping safety. The remainder of the paper is organised as follows: Section 2 conducts a literature review to describe the present state of research on maritime accidents. Section 3 presented the paper's hybrid model of AHP and TOPSIS techniques. Section 4 addressed the process of determining the appropriate criteria for determining the best option for preventing maritime accidents at SOM. Section 4 explains how the various parameters were determined, and Section 5 summarises the paper's findings and future research.

2. Literature review

Now and again, the globe is startled by a maritime disaster. "A marine casualty" is defined as an occurrence or a series of events that happened firmly attributable to the operation of a ship. It does not cover intentional misconduct. Casualties in the maritime industry are divided into two categories: "serious casualty", and "very significant marine casualty". Consequently, the lowest degree of gravity is assigned to 'marine incidents' (MI) and the greatest level of gravity is assigned to very severe marine casualties' (VSC), as indicated in Table 1.

Historically, there has been a lengthy and comprehensive list of maritime incidents, with a disproportionately high number of deaths and injuries. As a result of these accidents, the marine world has been

Table 1
Taxonomy of marine incidents and casualties.

Taxonomy	Marine incident	Marine casualty Serious casualty	Very serious casualty
Definition	- Endangers the safety of the ship, its occupants or any other person or the environment	- Fire - Explosion - Collision - Grounding - Contact - Heavy weather damage - Ice damage - Hull cracking - Suspected hull defect - Material damage to a ship - Stranding or disabling of a ship - Material damage to marine infrastructure • Severe damage to the environment	- -Total loss of the ship - -Death - -Severe damage to the environment - -Loss, presumed loss or abandonment of a ship

Source:International Maritime Organization, 2008; Fedi et al., 2020.
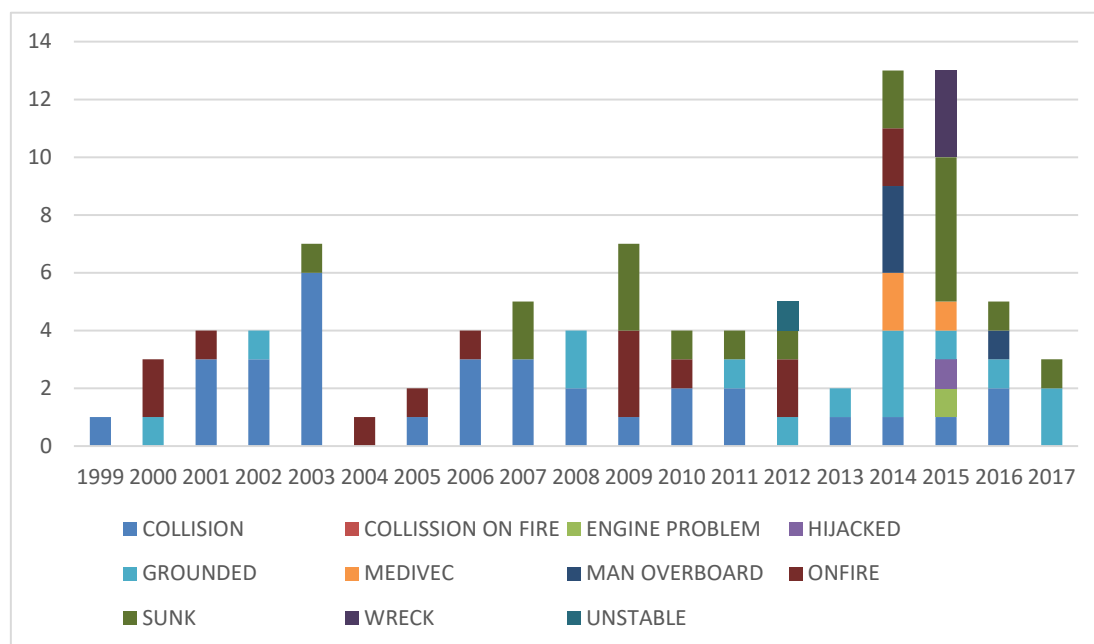

Fig. 1. Casualty breakdowns in the SOM from 1999 to 2017. Source: Illustrated by the Authors.

compelled to create international conventions on safety, responsibility, and environmental safeguards during the past hundred years. According to Allianz 2021 Safety and Shipping Review 2021, the top three causes of total losses in 2020 have been foundered (sunk/submerged) (54 %), wrecked/stranded (20%), and fire/explosion (11 %), accounting for 85% of all total losses. The number of recorded shipping casualties or incidents decreased significantly from 2,818 in 2015 to 2,703 in 2020, representing a decrease of around 4% in total. In response to accidents, maritime safety rules have evolved to be more reactive. Fig. 2 represents Awal's chronology that may be regarded in this respect. It depicts the most significant marine incidents during the last century and the subsequent actions taken due to those events. This method has been effective for ongoing vessels when prior experiences helped establish a solid foundation for safety management (Lim et al., 2018).

The control of narrow channels that serve a significant amount of international marine traffic is a major challenge. The ramifications of a marine disaster are serious and will have far-reaching economic and environmental implications. In addition, this chokepoint is responsible for transporting one-third of the world's traded goods, and its efficient operation necessitates installing an adequate and functional support system (Jeevan et al., 2020). Hutabarat et al. (2020) highlighted that maintaining shipping security in the SOM through Integrated Piloting Strategy as the vessel across the straits. It is projected that a spectacular rise of the future total vessel collision frequency due to the expansion of the Indonesian port near the SOM (Handani et al., 2018). Even so, limited scholars have comprehensively studied the causes of accident rates at SOM and how to mitigate them from the perspective of the government agency. Consequently, existing safety measures need to be improved to address the difficulties of increasing marine traffic, and this development has to be accompanied by complimentary services.

Maritime accidents are complicated events that often include more than one cause (Kristiansen, 2013). As a result, figuring out what set of circumstances led to a particular accident occurrence becomes more challenging. Consequently, compared to the number of mishaps, the growth in maritime safety research and resulting discoveries in the literature is minimal (Soner et al., 2015). Human factors are generally acknowledged as significant contributors to the failures of marine accident prevention systems in the maritime industry (Coraddu et al.,

2020; Kim & Na, 2017; Othman et al., 2015). Many scholars have highlighted that human mistake is responsible for more than 80% of all maritime fatalities and injuries (Sánchez-Beaskoetxea et al., 2021; Berg et al., 2013). Even if a ship or its systems are fully automated, human error still plays a role in the design or operation of the vessel or its systems (Ramos et al., 2018). The non-human elements, on the other hand, are concerned with equipment and machinery issues (Sahin & Yip, 2020) and vessel conditions (Fan et al., 2020) to influence navigation safety procedures (Celik and Cebi, 2009).

2.1. Factors leading to the maritime accidents

2.1.1. Human factor

a. Negligence by the seafarers

In legal terms, negligence is defined as carelessness that causes damage to a person or property. James Reason's (2000) taxonomy of human mistakes is a frequently used analytical framework for classifying various types of errors, namely (a) slips, (b) lapses, (c) errors, and (d) violations. A slip is when adequate planning and intention, but the desired outcome is inefficient or wrong. Inattention or poor memory are lapses that result in missed actions, also known as "sleeping rules" since they were forgotten or unknown. For an action to be a mistake, it must have been led by an ineffective strategy. Actions that deviate from established norms, regulations, or procedures are called violations. Therefore, lapses and violations result from procedural negligence/carelessness since the formal processes are either not followed, are disregarded, or are violated (Nævestad et al., 2018). Moreover, the term "lookout failure" refers to the failure to recognise a potentially hazardous situation outside the ship (Li et al., 2012). It is widely believed that all of these sorts of marine disasters are caused by negligence, including improper navigation, poor crew training, a lack of acceptable safety equipment or training, insufficient supervisory oversight of crew operations, and faulty vessel maintenance (Kozanhan, 2019).
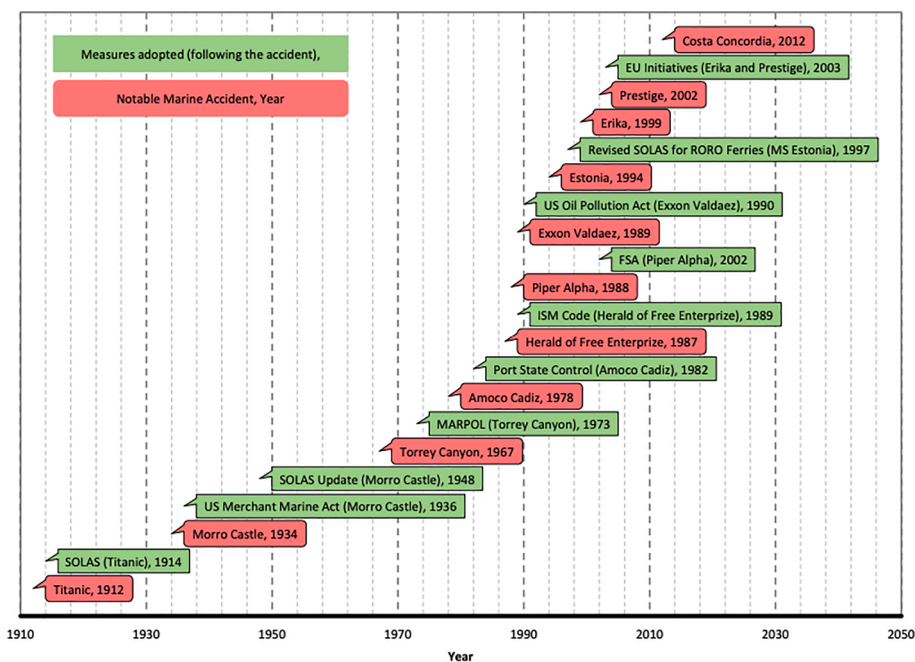
b. Fatigue

Fig. 2. A timeline of notable maritime accidents and reactive measures taken by international communities.
Source: Awal (2016).

Lützhöft et al. (2011) mentioned that fatigue results from a cumulative set of factors such as an individual being deprived of sleep and not having proper rest. Fatigue can combine with other fatigue-inducing factors such as long working hours and perhaps also adverse weather conditions to cause a state of fatigue. Previously published research by Jepsen et al. (2015) concluded that fatigue is a physical or mental weakness that will impact the surrounding environment regardless of occupation or cultural influences. Personal crew readiness is crucial to avoid fatigue during the job. Inadequate rest and sleep, lapses in judgment, such as doing intensive tasks just before another, and a physical fitness deficit contribute to marine accidents (Galieriková, 2019). Therefore, fatigue can cause a human error in manoeuvring the ship navigation (Erol and Başar, 2015).

c. Communication Breakdown

'Communication breakdown' is the third most often cited cause of accidents. It is the primary immediate cause of groundings and the second immediate cause of collisions (Acejo et al., 2018). On-board a ship, communication takes place between crew and operator and shore staff (Kececi and Arslan, 2017). Additionally, human interactions are hindered by a lack of communication due to a language barrier between crew members, particularly among multi-national crews (Othman et al., 2015). Approximately 68 maritime communication functions were classified into 14 major categories in the maritime world, including radio communication, onboard communication, communication with external agencies, routine works and operations, shipping particulars, shipping manuals, cargo operations, watchkeeping, safety and security, emergency, and medical procedure, reporting, weather, and terminology use (Ahmmed et al., 2020a). As such, it covers instances when crew members do not cooperate or when people are unable to coordinate operations (Galieriková, 2019). When communication fails, it is often impossible to determine the root cause of the problem. Information may be withheld because of a lack of communication, language, or hierarchical barriers (James et al., 2018).

2.1.2. Machinery equipment

a. Inadequate equipment design

A technology-driven approach to bridge system deployment may result in designs that do not support users or operational sensemaking (Johnsen, Kilskar & Danielsen, 2019). Without incorporating professional user knowledge throughout the design process, a gap may develop between the final ship design, including onboard technology, and how the crew operates (Mallam, Lundh & MacKinnon, 2015). This may result in poor and dangerous work habits, thus increasing the risk of mistakes and accidents. Similarly, in the maritime aspect of a ship's bridge, the quality and consistency of design spanning interfaces and interaction devices between navigator and equipment are essential for minimising user mistakes and boosting productivity. Design should convey pertinent information and effectively explain how to accomplish its users' desired job or activities. Whether physical or digital, interaction with an item, interface, or system should be simple to understand and facilitate the user's optimum decision-making for their intended activities (Mallam & Nordby, 2021). For example, the Helge Ingstad collision investigation determined insufficient equipment backup, ineffective navigation equipment that was not programmed to utilise all safety features, and watchkeepers who failed to use the Electronic Chart Display and Information System (ECDIS) properly, were all contributory factors (Johnsen, 2021).

b. Lack of Proper Maintenance

The vast majority of the country's vessels are not adequately maintained at all times. Minor issues are often overlooked and may not get full attention. Inadequate maintenance raises safety issues and increases the total operating cost of the facility (Mia et al., 2021). Poorly maintained and operated vessels have a higher probability of causing loss of human life, loss of vessels, and impacting the marine and coastal environment (Wróbel et al., 2017). Additionally, inadequate and irregular monitoring of the cargo-securing system's condition during maritime transport (Onyshchenko et al., 2021). All documentation about routine maintenance, repairs, and replacements should be examined to determine whether such activities were performed on the vessel or its machinery.

c. Ship system too complicated

Moreover, crew network contact is strongly linked to interactions with system functions since marine systems are socio-technical in nature. Lee and Chung (2018) criticality indicates that the present system and human network are incapable of adequately enabling cooperation, and therefore the system or human network must be enhanced to handle variability. Interactions between crew members, hardware, and software are required for the systems onboard ships to function properly (man–machine interfaces). Advanced technologies have two distinct effects. While advancements in the marine sector help reduce the likelihood and severity of maritime accidents, the connection between the accident and human error has developed due to technological advancements (Liu et al., 2020). Simultaneously, as technology advanced, there was a rise in human, machine, and software interactions. The increased interaction increased the complexity of the systems (Ceylan et al., 2021).

2.1.3. Ship condition

a. Unseaworthiness of the ships

The term "unseaworthy" would be used to describe a vessel that is incapable of accepting cargo and delivering it safely and appropriately to its ultimate destination (Hanzu-Pazara et al., 2016). Improving marine seaworthiness is essential for preserving ship safety, increasing maritime security, reducing ship pollution, and enhancing crew ability (Lin and Cheng, 2020). When an accident occurs due to the ship's state, the crew members are responsible for being prosecuted for negligent operation (Menon, 2021). The probability of a ship sustaining a lower level of seaworthiness while in operation is calculated as the product of two probabilities: 1) the probability of the ship being involved in the accident (event probability), and 2) the probability that the ship will sustain a lower level of seaworthiness after the accident has occurred (lower-seaworthiness conditional probability) (Talley, 1999). A vessel owner is responsible for ensuring that the vessel is equipped with adequate safety equipment before it is used. This is done to prevent a maritime accident at sea. The unseaworthy vessel should not have been on the water's surface because it could have caused an accident. The vessel may be known as unseaworthy when: (i) failure to provide updated equipment; (ii) using old or broken machinery or tools for maintenance; (iii) failure to perform regular inspections on equipment; (iv) unsafe pathways or access points to and from the vessel; (v) failure to train seafarers; (vi) lack of an adequate number of seafarers for the work assigned. A ship in poor condition cannot be deemed seaworthy at all times. Loss of stability is a significant factor in marine accidents, posing a significant danger to navigation safety (Hanzu-Pazara et al., 2016).

b. Obsolete

In the definition of obsolete, a vessel can no longer be used or has passed its useful life span. The risk of an accident occurring increases if the vessel is used at sea and the risk of ship uncontrollability at sea and other issues resulting from engine and hull failure. Walmsley (2013) also

mentioned that if over ten years, the owners have to register them with less reputable flags states to continue trading. This can establish a downward cycle of potentially lowering standards and cutting corners on safety. Ships are in danger of spontaneously combusting because of the source of the fire, which is due to outdated components (Priatno and Sunaryo, 2020). Additionally, obsolete ships contain combustible chemicals that often catch fire in hazardous shipbreaking/recycling environments (Chowdhury et al., 2017).

c. Defectives

Defective refers to something that has a flaw in it and does not function properly. The use of defective or out-of-station navigational markings can result in accidents occurring anywhere, at any time, and under any circumstances (Akten, 2006). Fan et al. (2019) indicated that when a ship is discovered to be defective, the likelihood of serious risk is always lower than when the ship is not encountered to be defective. This outcome is comprehensible since when a ship is discovered to be defective, the operator will devote more attention and effort to ship maintenance, actively repairing and making the ship safer. As a result, the likelihood of the ship being classified as high-risk falls proportionately. Moreover, Utama and Chen (2018) concluded that the primary causes of the sinking of a RoRo vessel are defects in the stability and damage to the compartments.

2.2. Alternatives to control the maritime accidents

The Malacca Strait is the longest strait in the world and a significant shipping route. Global commerce is greatly influenced by it. However, the Malacca Strait's geographical location puts it at risk owing to heavy traffic, which has resulted in several maritime accidents. As a result, it is critical to investigate other strategies for enhancing navigational safety. Theoretically, there are mitigation measures that can be taken to reduce maritime accidents at the SOM. The literature identifies several critical approaches, i) regulation and enforcement, ii) working schedule, iii) proper maintenance, iv) continuous training seafarers, v) safety in the workplace, and vi) maritime English.

2.2.1. Regulation and enforcement

Effective maritime law enforcement is critical to safeguarding marine areas and national interests (Chang, 2021). A proactive strategy is needed to constantly evaluate and improve all related elements for legislative and regulatory advancement in the area of maritime accident risk investigation (Van Hoof et al., 2020). This includes encouraging port and shipping companies and individual practitioners to abide by applicable rules and regulations and standardise their operations, and improve maritime management (Changhai and Shenping, 2019), encompassing restriction of the entry of any unqualified shipping companies and low-standard ships into the maritime sector, improving ship inspection quality and conducting rigorous ship inspections. As such, it is crucial to improve the professional training of law enforcement officers to enforce maritime rules, regulations, and common sense to mitigate maritime accidents.

2.2.2. Working schedule

Ships often operate 24 h a day, seven days a week, resulting in a wide range of work schedules and watchkeeping patterns. Two sets of schedules were used: those with two watchkeepers/watch keeping teams (2-watch systems) and those with three watchkeepers/watch keeping teams (3-watch systems) (Oldenburg et al., 2013). This means the first set of schedules has an average working day length of 12 h, while the second set has an average working day length of 8 h. Incorporating a comprehensive evaluation of work schedules and sleep difficulties by international regulatory authorities, helping seafarers cope with changing industrial conditions, decreasing environmental challenges, and building a culture of safety aboard ships. Fatigue resulting from longer working schedule significantly affect one's performance and its consequences for efficiency, productivity, and workplace standards are some of the most common causes of deadly mistakes at human errors (Turedi & Ozer-Caylan, 2021). By promoting rotating systems, midnight shifts might be evenly distributed among the various watch crews, while non-rotating schedules might benefit sleep and tiredness, considering seafarers' daytime preferences (van Leeuwen et al., 2021).

2.2.3. Proper maintenance

Maintenance is composed of three distinct components: risk assessment, strategy selection, and the process of calculating the best interval for doing the maintenance work. As mentioned by International Labour Organization (1997), all breathing apparatus, rescue harnesses, lifelines, resuscitation equipment, and any other equipment provided for use in or in connection with entrance into dangerous locations or emergencies should be maintained and frequently inspected and checked for correct operation by a competent person. In addition, a record of the inspections and checks should be kept. Before and after each usage, all breathing devices should be inspected and tested to ensure that they are in proper working order. Moreover, the equipment used to test the environment of dangerous locations should be kept in good condition and, when applicable, serviced and calibrated on a regular basis. Also, the manufacturer's guidelines should be retained and followed. The key to maximising ship system dependability and safety is important to implement a strong maintenance management system capable of minimising or eliminating equipment/component failures (Emovon et al., 2018).

2.2.4. Continuous training seafarers

Maritime education and training are essential to mitigate the risk of maritime accidents. According to Eliopoulou et al. (2016), there is a need to enhance training for seafarers, acquaint them with new technology, and teach them emergency management skills based on previous ship mishaps. Kim et al. (2016) recommended some enhancements to the safety system training, including a decision-support system for traffic safety, enhancements to ship safety design, instructions that prioritise ship and passenger safety, and the provision of suitable training. Moreover, it is necessary for a seafarer with more than 10 years of experience to continue training in order to develop his or her skills and abilities (Chan et al., 2019). The fact that demand for future advanced training requirements of operators and the infrastructure in navigational equipment, 3D modeling, robotics, automation and other maritime technology are needed to supply cadets for Industry 4.0 (Zainol Abidin & Ismail, 2021).

2.2.5. Safety in workplace

The maritime sector is known as an industry at risk in which maritime safety is primarily concerned with human and organisational factors. The ship's operations are filled with comprehensive regulations, instructions, and standards that officers and personnel are required to understand and follow. There are four main components of safety at sea namely safety of navigation, technological and operational ships' safety, the safety of the crew in an emergency, and prevention of pollution of the environment from ships (Kopacz et al., 2002) that should be applicable in any ships on voyage. Therefore, it is crucial that the crew must have the necessary knowledge, expertise, abilities, and safety equipment on any maritime expedition to ensure the safety of the crew and passengers on board (Formela et al., 2019).

2.2.6. Maritime English (ME)

The inability to communicate effectively in English results in misunderstanding, which often results in maritime catastrophes, endangering the safety of lives and the security of ships. "Safety of shipping" is the most important term when it comes to deriving a definition of ME and standardising this language. To begin with, the ability to communicate effectively was the most significant aspect in on-board positions. The importance of radio communication over Very High

Frequency (VHF) Radio and with Vessel Traffic Service (VTS) is particularly relevant (Fan et al., 2017) communicating with multicultural nationalities and port authorities, participating in inter-and intra-ship communication from ship to shore and shore to ship, negotiating with international clients and providing emergency instructions to passengers or crews (Mercado et al., 2018). Interview recruitment mostly assessed the applicants' oral communication abilities, however, standardised English language tests like the Marlins and IELTS were also used by certain recruiting organisations to assess their English language proficiency (Ahmmed et al., 2020b) including speaking, writing, reading and listening. Therefore, Maritime and Education Training (MET) instituitions need to pay subsequent attention to ME communication skills of students at the same time, achieving expected level of proficiency.

3. Research methodology

In order to control maritime accidents at the Straits of Malacca, this study used a combination of different decision-making methods, namely, a Cause-and-Effect Analysis, AHP, and TOPSIS (i.e., a hybrid method). As shown in Fig. 3, a flow chart depicting the proposed methodology in sequential order has been developed to establish the calculation process for this study. AHP and TOPSIS is well known as powerful multi-criteria decision-making (MCDM) tools. However, there are a number of disadvantages in both methods. One disadvantage of AHP is the subjectivity of the assessor's expert opinion and the degree of interdependence between the criteria and variants, since the criteria chosen may bias the results for a particular variant (Nefeslioglu et al., 2013). Meanwhile, TOPSIS's disadvantages include correlations between criteria, the uncertainty inherent in determining weights solely through objective or subjective approaches, and the potential of
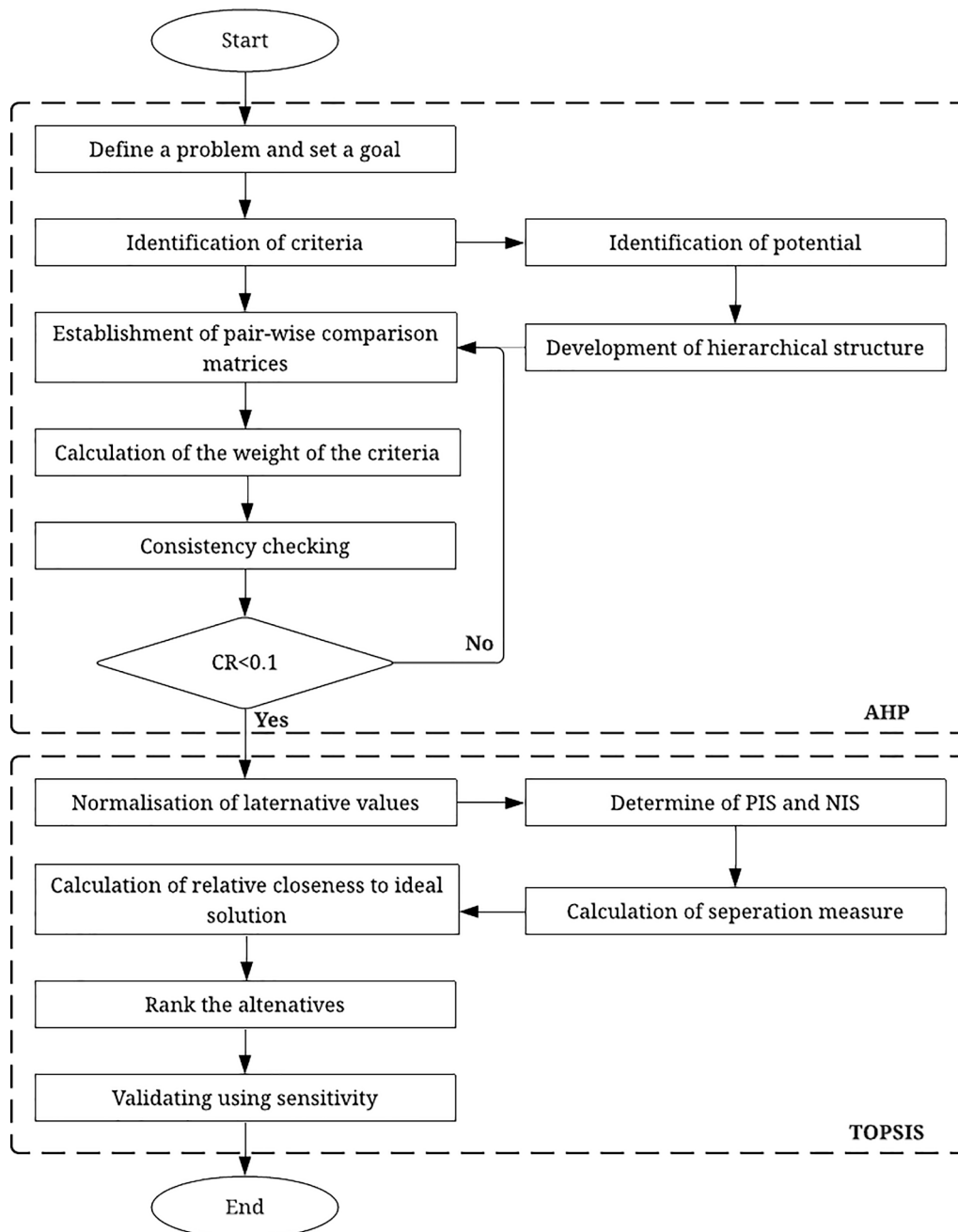

Fig. 3. Research design.

alternative closed to ideal and nadir points coexisting (Li et al., 2011). Consequently, the hybrid method is being used since it is a practical and helpful methodology for ranking and selecting a number of alternatives using distance separation measures. This strategy assists decision makers in organising the issues that must be addressed as well as doing systematic analysis comparisons. Finally, all alternatives will be ranked according to the order of preference.

3.1. Criteria identification and filtration (Steps 1, 2, and 3)

The criteria discussed in this paper were discovered through a review of the literature (see Table 2) and further discussed with the assistance of experts. There were 14 professional maritime experts that were interviewed for this study in which each of the 14 experts from various firms was interviewed individually, as seen in Table 3. The face-to-face survey lasted roughly 20–30 min and was conducted at the respondent's place of employment at a time that was mutually agreed upon by all participants. The researchers began by explaining the selection procedure and guiding relevant respondents through the pairwise comparison. Following consultation with knowledgeable professionals, a filtration process was conducted. Three significant criteria and nine sub-criteria were discovered to be responsible for maritime accidents due to this research.

Following that, after the criteria had been identified, revised, and further filtered, a generic model was developed, as illustrated in Fig. 4.

3.2. AHP weight assessment (Step 4)

Using the AHP method, each factor contributing to maritime accidents was assigned a weight based on its importance. A total of five formulae were used in this method. Table 4 shows a preferable scale ranging from 1 to 9, where 1 indicates the equivalent between factors, while nine shows that one criterion is relatively much more important than the other factors (Saaty, 1988).

To quantify the judgments, a construction of pair-wise comparison matrix ($n \times n$) that shows the preference of one criterion A_i over the other, A_j is built using a scale in Table 2 (Saaty, 1988).

The a_{ij} entries are defined by rules as follows:

- Rule 1: if $a_{ij} = \alpha, 1/\alpha, \alpha \neq 0$
- Rule 2: if A_i is judge to be of an equal number of equal relative number as A_j, then $\alpha_{ij} = a_{ji} = 1$

The following matrix D was created in accordance with the aforementioned rules:

$$D = a_{ij} = \begin{bmatrix} 1 & a_n \cdots & a_{1n} \\ 1/a_n & 1 \cdots & a_{2n} \\ 1/a_{1n} & 1/a_{2n} \cdots & 1 \end{bmatrix} \quad (1)$$

Next, in order to determine the priorities of each criterion or also known as a weight vector value (W_k), the value of each comparison is calculated by using Equation (2) as follows:

$$W_k = \frac{1}{n}\sum_{j=1}^{n} \left(\frac{a_{kj}}{\sum_{j=1}^{n} a_{ij}} \right) (k = 1, 2, 3, \cdots, n) \quad (2)$$

where a_{ij} stands for the entry of row i and column j in a comparison

Table 2
Main criteria and sub-criteria.

No.	Main Criteria	Sub-Criteria
1	Human Error	Negligence by Seafarers, Fatigue, Communications breakdown
2	Machinery Equipment	Inadequate Equipment, Lack of Proper Maintenance, Complicated Ship System
3	Ship Condition	Unseaworthiness, Obsolete, Defective

Table 3
Experts knowledge and experience.

Expert	Position	Years of Experience
1	Researcher	10 – 15 years
2	Marine Officer	More than 20 years
3	Researcher	More than 20 years
4	Vessel Manager	15 – 20 years
5	Marine Superintendent	10 – 15 years
6	QHSSE Superintendent	15 – 20 years
7	Vessel Manager	15 – 20 years
8	Manning Advisor	More than 20 years
9	Assistant Officer	Less than 10 years
10	Operator and Traffic Manager	10 – 15 years
11	Operator and Traffic Manager	10 – 15 years
12	Operator and Traffic Manager	15 – 20 years
13	Operator and Traffic Manager	More than 20 years
14	Advisor Commercial	More than 20 years

matrix of order n.

After that, the Consistency Ratio (CR) will be calculated in order to ensure the judgement made by the experts are consistent. The equation of the CR is expressed in Equation (3)–(5) as follows:

$$CR = \frac{CI}{RI} \quad (3)$$

$$CI = \frac{\lambda_{max} - n}{n - 1} \quad (4)$$

$$\lambda_{max} = \frac{\sum_{j=1}^{n} \left[\frac{\sum_{k=1}^{n} W_k a_{jk}}{W_j} \right]}{n} \quad (5)$$

where Random Index (RI) refers to the value of average random index (Table 5).

The inconsistency of a pair-wise comparison can be measured by calculating the Consistency Ratio (CR). A CR value of 0.10 or less can be considered reasonable when evaluating the consistency of a pair-wise comparison, allowing the AHP to proceed with the calculation of weight vectors (Md Hanafiah, 2017). As an alternative, when the CR is greater than 0.10, it indicates that the pair-wise judgments are inconsistent. As a result, before proceed with the next step, the decision-maker should review the pair-wise judgments.

3.3. TOPSIS method (Step 5)

The Technique for Order Preference by Similarity to Ideal Solutions (TOPSIS) method was originally proposed by Hwang and Yoon in 1981 (Md Hanafiah, 2017). TOPSIS defines the index of the positive-ideal solution, called similarity (or relative proximity), with remoteness from the negative-ideal solution (Kahraman, 2008; Othman et al., 2015). The method then selects the alternative with the greatest similarity to the positive-ideal solution. The TOPSIS methodology consists of six main steps for generating accurate data, as follows:

Step 5.1: Calculate the normalised decision matrix

The normalised decision matrix value r_{ij} is calculated using Equation (6) as follows:

$$r_{ij} = \frac{x_{ij}}{\sqrt{\sum_{i=1}^{m} x^2_{ij}}}, i = 1, 2, \cdots, m; j = 1, 2, \cdots, n \quad (6)$$

Where R_{ij} and X_{ij} are the original and normalised scores of the decision matrix, respectively.

Step 5.2: Calculate the weighted normalised decision matrix

The weighted normalised decision matrix was obtained by multiplying the normalised decision matrix in Step 1 with other associated weights. The weighted normalised value was calculated using Equation (7):
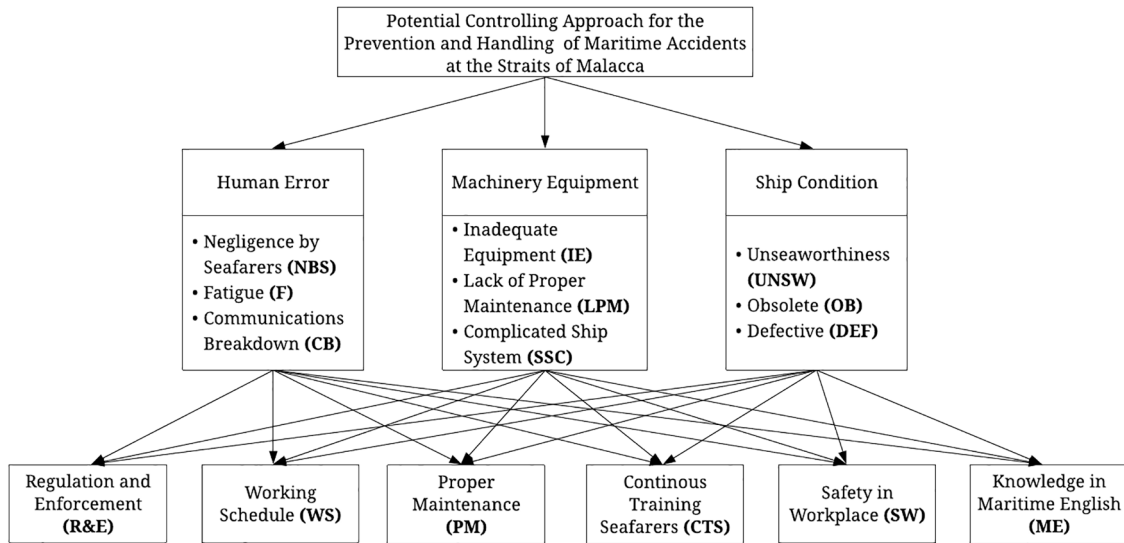
Fig. 4. The generic model of potential controlling approach for the prevention and handling of maritime accidents at the SOM.

Table 4
Comparison scale.

Numerical Assessment (Scale)	Linguistic Meaning
1	Equally Important
3	Weakly Important
5	Strongly Important
7	Very Strongly Important
9	Extremely Important
2, 4, 6, 8	Intermediate values between the two adjacent judgments.

$$V_{ij} = W_j \times R_{ij}, i = 1, 2, \cdots, m; j = 1, 2, \cdots, n \qquad (7)$$

Where, w_j represents the weight of the jth criterion

Step 5.3: Determine the Positive Ideal Solution (PIS) and the Negative Ideal Solution (NIS)

In this step, the positive ideal solutions V^+, and the negative-ideal solutions V^-, were determined by obtaining both the maximum and minimum values of the weighted normalised elements in each column, where solution V^+ is for maximum and solution V^- is for minimum. The solutions can be expressed through Equations (8) and (9):

$$V^+ = \left\{ V_1^+, V_2^+, V_3^+, \ldots, V_n^+ \right\} = \left\{ \left(\max_j V_{ij} | j \in J \right) \right\}, \left\{ \left(\min_j V_{ij} | j \in J' \right) \right\} \qquad (8)$$

$$V^- = \left\{ V_1^-, V_2^-, V_3^-, \ldots, V_n^- \right\} = \left\{ \left(\min_j V_{ij} | j \in J \right) \right\}, \left\{ \left(\max_j V_{ij} | j \in J' \right) \right\} \qquad (9)$$

where by J is associated with the benefit criteria and J' is associated with the cost criteria.

Step 5.4: Calculate the separation measure for each alternative from the PIS and NIS

The separation of each alternative from the positive ideal solution is given by Equation (10):

$$D^+_i = \sqrt{\sum_{j=1}^n \left(V_{ij} - V^+_j \right)^2}, i = 1, 2, \cdots, m \qquad (10)$$

On the other hand, the separation from the NIS is given by Equation (11):

$$D_i^- = \sqrt{\sum_{j=1}^n \left(V_{ij} - V_j^- \right)^2}, i = 1, 2, \cdots, m \qquad (11)$$

Step 5.5: Calculate the relative closeness of each alternative.

Calculate the relative closeness to the ideal solution using Equation (12):

$$RC_i^+ = \frac{D_i^-}{D_i^- + D_i^+}, i = 1, 2, \cdots, m \qquad (12)$$

$$RC_i^+ = 1 \, if A_i = A^+; RC_i^+ = 0 \, if A_i = A^- \qquad (13)$$

where the index value is $0 \leq RC_i^+ \leq 1$. An alternative A_i is closer to V^+ as RC_i^+ approaches 1.

Step 5.6: Rank the order of preference for all the alternatives.

Based on the relative closeness to the ideal solution in Step 5.5, the alternative with CC_i closest to 1 is the better-performing alternative. Moreover, it allows the ranking of alternatives used in the study according to the values calculated to identify the most affected group. Hence, a greater relative closeness represents a higher-ranking order among the alternatives, and thus, this alternative is chosen as the recommended alternative.

4. Analysis results and findings

This section presents the analysis and the findings obtained from the research. The Straits of Malacca was chosen as a case study. This research developed a scientific model using a hybrid method, namely a combination of the Analytic Hierarchy Process (AHP) and the Technique for Order Preferred by Similarity to Ideal Solution (TOPSIS), to rank the

Table 5
Value of average random index.

N	1	2	3	4	5	6	7	8	9	10
RI	0	0	0.58	0.9	1.12	1.24	1.32	1.41	1.45	1.49

factor and alternatives for the Malacca Straits.

In the data collecting procedure, all of the required information was gathered from industry experts. This study engaged a total of 14 professional experts in Malaysia's maritime industry with at least ten years of experience in the subject area. The face-to-face survey took about 30–40 min at the interviewee's workplace, at a time mutually agreed upon by all parties. The researchers explained the selection process and directed experts through the pairwise comparison.

By attributing Step 4, criteria that contribute to maritime accidents have been analysed and identified. Table 6 depicts the global weight and consistency ratio of the main criteria of maritime accidents and its respective sub-criteria. This study found that the most important main criteria in maritime accidents is human error, consisting of weight of 0.7373. Followed by machinery equipment (0.1432) and the ship condition (0.1194). Moreover, the global weights of criteria that attribute to maritime accidents in the SOM have been addressed that negligence by seafarers is the most important criterion affecting maritime accidents with the weight of 0.4007, followed by fatigue (0.1667), communication breakdown (0.1698), inadequate equipment (0.0492), lack of proper maintenance (0.0583), ship system complicated (0.0357), unseaworthiness (0.0487), obsolete (0.0356) and defective (0.0356).

In Step 5, to establish the normalised decision matrix, Equation (6) was used based on the evaluation data of Table 4. The results of the normalised decision matrix are shown in Table 7.

By identifying the weighted normalised decision matrix, the positive and negative ideal solutions were determined using Equation (7) – (8) and the results are depicted in Tables 8 and 9, respectively.

To determine the distance separation measures from the positive and negative ideal solutions, Equations (9) and (10) were used. Table 10 lists the results of the distance separation values:

At the final step of the analysis, the values in Table 8 are used in Equation (11), the relative closeness to the ideal solution was calculated and ranked accordingly. The alternative with a more excellent relative closeness value was chosen as the best alternative for controlling maritime accidents. Table 11 represents the rank of the alternatives for controlling maritime accidents at the Malacca Straits. Proper maintenances scored the highest closeness value at 0.7829, making it the best alternative to control maritime accidents at the SOM. This can be seen that knowledge in maritime English came in second, which followed by working schedule accounted for 0.5065 and 0.5049, respectively. Meanwhile, safety in workplace alternative generated 0.4388, which was twice as much as that of regulation and enforcement (0.2417). The least closeness value is the continuous training seafarers alternative, which stood at only 0.2373.

Table 6
Global weights and consistency ratio of the criteria contribute to maritime accidents at the SOM.

Main Criteria	Weights of Main Criteria	Sub-Criteria	Local Weight of Sub-Criteria	Global Weight
Human Error	0.7373	Negligence by seafarer	0.5435	**0.4007**
		Fatigue	0.2262	**0.1667**
		Communication Breakdown	0.2303	**0.1698**
			CR: 0.0001	
Machinery Equipment	0.1432	Inadequate Equipment	0.3433	0.0492
		Lack of Proper Maintenance	0.4072	0.0583
		Ship System Complicated	0.2495	0.0357
			CR: 0.0013	
Ship Condition	0.1194	Unseaworthiness	0.4082	0.0487
		Obsolete	0.2983	0.0356
		Defective	0.2983	0.0356
	CR: 0.0033		*CR: 0.0003*	

5. Discussion

Based on the findings of this study, hence, ranking the alternatives for mitigating the contribution of human errors to shipping collision. The outcome was finalised that proper ship maintenance is ideal for mitigation of maritime accidents, followed by knowledge in Maritime English and working schedule. Marine equipment is well-developed and engineered to withstand the rigours of the world's seas and waterways, which all vessels have to encounter. However, it is becoming more and more challenging to manage due to the sheer number of moving types of machinery. An engine breakdown, an issue with electrical systems or another equipment failure may lead to maritime accidents. While harsh weather and rough waves may lead to equipment failure, many other variables might also play. In such a way, if the ship's crew does not have specialised knowledge and understanding of the machine or system maintenance, the ship may experience a catastrophic breakdown. The crews must review all paperwork related to regular maintenance, repairs, and replacements to establish whether such operations were done on the vessel or its equipment. Additionally, the Standards for Training, Certification and Watchkeeping (STCW) 1995 rule, the 2010 Manila Amendments, and SOLAS (Safety of Life at Sea) standards require maritime cadets to be proficient in English. Insufficient English proficiency leads to misunderstanding, which frequently results in maritime disasters, endangering life and security. Miscommunication is a significant cause of maritime accidents. Other than that, human errors can be overcome through a balance working schedule to maintain the productivity of the cadets in charge.

In light of the well-known fact that human error is responsible for 80–85% of all maritime accidents, the workplace's safety comes at forth. It concerns safety improvements that involve the minimization of distractions, and the vessel is equipped with the necessary safety equipment to handle emergencies and provide the best chance of survival for all on board. The IMO was established to increase safety aboard ships by implementing various rules, regulations, and specifications to be followed by vessels on the operation. Improvements may be seen in the design, stability, equipment, engine, and human factors of ships, among other things. In many circumstances, proper safety precautions and training may dramatically reduce maritime incidents. As a result, it is anticipated to boost SOM's maritime safety, and both commercial players and government agencies should make security with adequate rescue resources and adequate actions.

6. Recommendation to control maritime accidents

Fig. 5 shows the important structure and pillars that play an essential role in reducing and preventing accidents. As the backbone of maritime management, Flag State is responsible for drafting and enforcing national and International Maritime Organization (IMO) laws and regulations. Therefore, synergy and active participation between the leading players can effectively reduce risks and accidents. The four most important players directly related to Flag State include ship-owners (owners, shipping management), inspectors (Flag state control, Port state control, classification society and auditors), training centres, and vessel traffic service providers.

Increasing the interaction of each of these four pillars with each other, in the form of a particular working group, under the supervision of Flag state, to implement and execute the instructions correctly, and updating the knowledge of active personnel on the fleets, can be very effective in reducing risks and accidents. In this regard, the role of the shipmaster, as a representative of the ship-owner, is vital to interact with inspectors to prepare and implement preventive measures. These preventive measures to mitigate accidents can be classified into four main areas.

The first part is related to the field of management and managerial actions. These measures can be defined as holding meetings, examining the risks in the study route, human resource management, and personnel

Table 7
Normalised decision matrix.

	NBS	F	CB	IE	LPM	SSC	UNSW	OB	DEF
R&E	0.1782	0.0733	0.0769	0.0309	0.0298	0.0131	0.0351	0.0233	0.0261
WS	0.1622	0.1013	0.0425	0.0157	0.0142	0.0094	0.0123	0.0078	0.0090
PM	0.1082	0.0483	0.0344	0.0233	0.0339	0.0139	0.0188	0.0164	0.0131
CTS	0.2004	0.0624	0.0965	0.0142	0.0248	0.0234	0.0156	0.0110	0.0095
SW	0.1622	0.0655	0.0491	0.0198	0.0212	0.0111	0.0169	0.0146	0.0135
ME	0.1559	0.0405	0.0884	0.0091	0.0096	0.0131	0.0104	0.0078	0.0077

Table 8
The Positive Ideal Solution (PIS),V^+

	NBS	F	CB	IE	LPM	SSC	UNS	OB	DEF
R&E	0.1782	0.0733	0.0769	0.0309	0.0298	0.0131	0.0351	0.0233	0.0261
WS	0.1622	0.1013	0.0425	0.0157	0.0142	0.0094	0.0123	0.0078	0.0090
PM	0.1082	0.0483	0.0344	0.0233	0.0339	0.0139	0.0188	0.0164	0.0131
CTS	0.2004	0.0624	0.0965	0.0142	0.0248	0.0234	0.0156	0.0110	0.0095
SW	0.1622	0.0655	0.0491	0.0198	0.0212	0.0111	0.0169	0.0146	0.0135
ME	0.1559	0.0405	0.0884	0.0091	0.0096	0.0131	0.0104	0.0078	0.0077

Table 9
The Negative Ideal Solution (NIS),V^-

	NBS	F	CB	IE	LPM	SSC	UNS	OB	DEF
R&ER	0.1782	0.0733	0.0769	0.0309	0.0298	0.0131	0.0351	0.0233	0.0261
WS	0.1622	0.1013	0.0425	0.0157	0.0142	0.0094	0.0123	0.0078	0.0090
PM	0.1082	0.0483	0.0344	0.0233	0.0339	0.0139	0.0188	0.0164	0.0131
CTS	0.2004	0.0624	0.0965	0.0142	0.0248	0.0234	0.0156	0.0110	0.0095
SW	0.1622	0.0655	0.0491	0.0198	0.0212	0.0111	0.0169	0.0146	0.0135
ME	0.1559	0.0405	0.0884	0.0091	0.0096	0.0131	0.0104	0.0078	0.0077

Table 10
Distance separation values of each alternative.

Alternative	D+	D-
Regulation and Enforcement	0.0993	0.0317
Working Schedule	0.0822	0.0838
Proper Maintained	0.0324	0.1167
Continuous Training Seafarers	0.1155	0.0359
Safety in workplace	0.0883	0.0691
Maritime English	0.0722	0.0741

Table 11
The rank of the distance separation values for each alternative.

Alternative	Relatives Closeness	Rank
Proper Maintenances	0.7829	1
Maritime English	0.5065	2
Working Schedule	0.5049	3
Safety in Workplace	0.4388	4
Regulation and Enforcement	0.2417	5
Continuous Training Seafarers	0.2373	6

capabilities in relation to the assigned responsibilities. Also, formulating and presenting incentive policies in coordination with the shipping management or the ship-owner can effectively motivate personnel.

Ensuring the quality of continuous training of personnel and increasing their ability level is another part that the ship's master must pursue. Although these exercises are carried out in the form of various drills and training on board the ship, it seems that a detailed analysis and evaluation of the qualitative results of these exercises is not available,

and usually, these trainings have been considered in quantitative terms.

The third part includes the subject matter of accurate communication and implementation of rules and regulations, the importance of training standards, the standardisation of staff work hours and rest periods, the importance of close cooperation and interaction with class and flag inspectors, and finally, the importance of ensuring the availability of vital equipment related with shipping certificates.

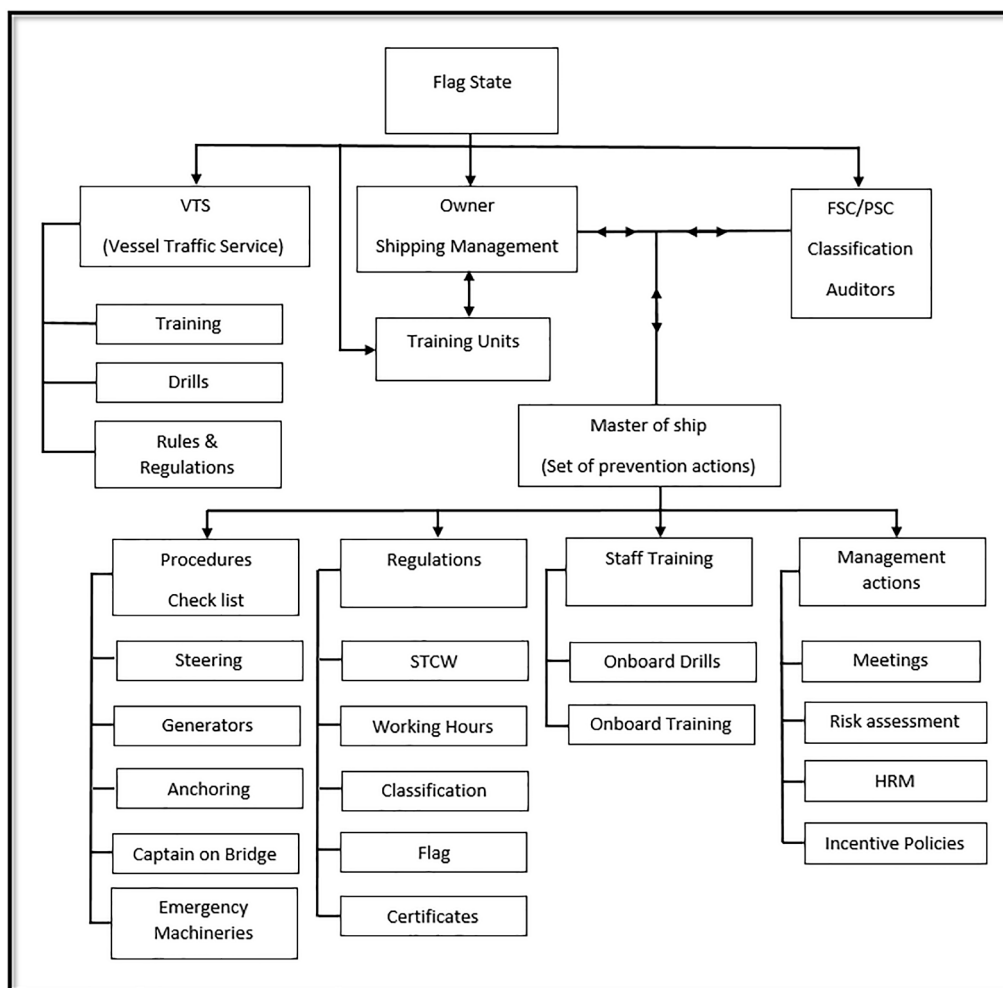The last section includes a set of machinery and equipment related to

Fig. 5. A proposed framework to control maritime accidents.

the safe operation of the ship. It is also necessary to develop operational checklists related to preventive measures, given the nature of the risks associated with the traffic route. The presence of the shipmaster on the bridge when the ship is manoeuvring in a high traffic separation area and an officer with less experienced is on a bridge can significantly reduce the risk of accidents. In addition to training and ensuring the quality of personnel working in the fleet, continuous training in vessel traffic service has an undeniable role in reducing risk. These exercises and training can help increase the quality level of people working in this sector and the safe guidance of ships. However, this can also effectively improve proper and coordinated communication with the ship, especially in critical situations.

7. Conclusion

Although the strait is regulated by a traffic separation system (TSS) and a Vessel Traffic System (VTS) in compliance with Collision Regulations (COLREG) 1972, collision incidents continue to occur attributed to the existence of SOM's natural structure. As a maritime country situated next to the world's busiest straits, through the incorporation of the proposed decision-making model to control maritime accidents. This study contributes to assist the Marine Department Malaysia (MARDEP) and other related entities in raising safety awareness and preventing maritime accidents by putting in place all of the necessary preventative measures for the future. In addition, this study proposes a new framework (Fig. 5) for striking the efficiency of stakeholders, maintaining safety and security for sea transport services, and attaining operational

effectiveness for law enforcement on the water.

Recognising the impediment, this study shows that the main factor that contributes to maritime accidents are due to human errors. As a result, a comprehensive assessment of human behaviour is becoming more important. The vast number of events occurred due to one of the following reasons or a combined effect of them: inadequate equipment, a communication breakdown, fatigue, lack of proper maintenance, complicated ship system, unseaworthiness, obsolete and defective.

The newly discovered information may then be utilised to aid in the development of new rules and practices aimed at preventing future marine catastrophes. In addition, government agencies are dedicated to preparing highly competent seafarers for international maritime operations. This is an area where improved training and recruiting procedures are anticipated to have a beneficial effect, paving the way for the sector to move ahead constructively in terms of accident reduction.

Future studies should expand the number of accident analyses and standardise accident investigation reports to aid in data quantification. It should also have a model for shipping management to assess their crews' negligence levels and predict the potential outcomes of different risk-reduction measures. In addition, it can be expanded to include other accident types and various geographical locations across the globe. This reflects a better knowledge of variables that may have contributed to an accident and various perspectives on the complex context of a disaster.

CRediT authorship contribution statement

Rudiah Md Hanafiah: Methodology. **Nurul Sakinah Zainon:**

Conceptualization. **Nur Hazwani Karim:** Conceptualization. **Noorul Shaiful Fitri Abdul Rahman:** Methodology. **Mehrdad Behforouzi:** Recommendation and Conclusion. **Hamid Reza Soltani:** Recommendation and Conclusion.

Declaration of Competing Interest

The authors declare that they have no known competing financial interests or personal relationships that could have appeared to influence the work reported in this paper.
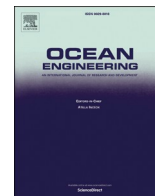
Acknowledgement

References

Abdul Rahman, N.S.F., Abdul, S., Rasdi, R., 2016. Decision strategies for boosting maritime economy in Malaysia due to the opening of Northern Sea Route. Journal of Maritime Research 13 (3).

Acejo, I., Sampson, H., Turgo, N., Ellis, N., & Tang, L. (2018). The causes of maritime accidents in the period 2002-2016.

Ahmmed, R., Sinha, B.S., Khan, D.R., Islam, D.M., 2020a. A needs analysis of Maritime English language skills for Bangladeshi seafarers to work onboard ships. Marine Policy 119, 104041. https://doi.org/10.1016/j.marpol.2020.104041.

Ahmmed, R., Sinha, B.S., Khan, D.R., Islam, D.M., 2020b. A needs analysis of Maritime English language skills for Bangladeshi seafarers to work on-board ships. Marine Policy 119, 104041. https://doi.org/10.1016/j.marpol.2020.104041.

Akten, N., 2006. Shipping accidents: a serious threat for marine environment. J. Black Sea/Mediterr. Environ. 12 (3), 269–304.

Awal, Z. I. (2016). Development of Logic Programming Technique (LPT) for Marine Accident Analysis. A Dissertation Submitted to the Department of Naval Architecture and Ocean Engineering, Graduate School of Engineering, Osaka University.

Berg, N., Storgård, J., Lappalainen, J., 2013. The impact of ship crews on maritime safety. Publications of the Centre for Maritime Studies, University of Turku A 64, 1–48.

Cakir, E., Sevgili, C., Fiskin, R., 2021. An analysis of severity of oil spill caused by vessel accidents. Transportation Research Part D: Transport and Environment 90, 102662.

Celik, M., Cebi, S., 2009. Analytical HFACS for investigating human errors in shipping accidents. Accid. Anal. Prev. 41 (1), 66–75.

Ceylan, B.O., Akyuz, E., Arslan, O., 2021. Systems-Theoretic Accident Model and Processes (STAMP) approach to analyse socio-technical systems of ship allision in narrow waters. Ocean Eng. 239, 109804. https://doi.org/10.1016/j. oceaneng.2021.109804.

Chan, S.R., Hamid, N.A., Mokhtar, K., 2019. The Impact of Safety Climate on Malaysian Seafarers' Safety Performance: A Pilot Study. Malaysian Journal Of Consumer And Family Economics 11–23.

Chang, Y.-C., 2021. The use of force during law enforcement in disputed maritime areas. Marine Policy 124, 104382. https://doi.org/10.1016/j.marpol.2020.104382.

Changhai, H., Shenping, H.u., 2019. Factors correlation mining on maritime accidents database using association rule learning algorithm. Cluster Computing 22 (S2), 4551–4559.

China Power Team, 2017. August 2) How much trade transits the South China Sea? Retrieved from: https://chinapower.csis.org/much-trade-transits-south-china-sea/.

Chowdhury, K.A., Mili, M.I.J., Akhter, S., Ahmed, K.A., 2017. Pollution by shipping industry in the northern Bay of Bengal: a review study. Imp J Interdiscip Res 3 (3), 1352–1362.

Coraddu, A., Oneto, L., Navas de Maya, B., Kurt, R., 2020. Determining the most influential human factors in maritime accidents: A data-driven approach. Ocean Eng. 211, 107588. https://doi.org/10.1016/j.oceaneng.2020.107588.

Dahalan, W.S.A.W., Zainol, Z.A., Hassim, J., Ting, C.H., 2013. E-Navigation in the Straits of Malacca and Singapore. International Journal of Computer Theory and Engineering 388–390. https://doi.org/10.7763/IJCTE.2013.V5.715.

Emovon, I., Norman, R.A., Murphy, A.J., 2018. Hybrid MCDM based methodology for selecting the optimum maintenance strategy for ship machinery systems. J. Intell. Manuf. 29 (3), 519–531. https://doi.org/10.1007/s10845-015-1133-6.

Eliopoulou, E., Papanikolaou, A., Voulgarellis, M., 2016. Statistical analysis of ship accidents and review of safety level. Saf. Sci. 85, 282–292.

Erol, S., Başar, E., 2015. The analysis of ship accident occurred in Turkish search and rescue area by using decision tree. Maritime Policy & Management 42 (4), 377–388.

Fan, L., Fei, J., Schriever, U., Fan, S.i., 2017. The communicative competence of Chinese seafarers and their employability in the international maritime labour market. Marine Policy 83, 137–145.

Fan, L., Wang, M., Yin, J., 2019. The impacts of risk level based on PSC inspection deficiencies on ship accident consequences. Research in Transportation Business & Management 33, 100464. https://doi.org/10.1016/j.rtbm.2020.100464.

Fan, S., Blanco-Davis, E., Yang, Z., Zhang, J., Yan, X., 2020. Incorporation of human factors into maritime accident analysis using a data-driven Bayesian network. Reliab. Eng. Syst. Saf. 203, 107070. https://doi.org/10.1016/j.ress.2020.107070.

Fedi, L., Faury, O., Etienne, L., 2020. Mapping and analysis of maritime accidents in the Russian Arctic through the lens of the Polar Code and POLARIS system. Marine Policy 118, 103984. https://doi.org/10.1016/j.marpol.2020.103984.

Formela, K., Weintrit, A., Neumann, T., 2019. Overview of definitions of maritime safety, safety at sea, navigational safety and safety in general. International Journal on Marine Navigation and Safety of Sea Transportation, TransNav, p. 13.

Galieriková, A., 2019. The human factor and maritime safety. Transp. Res. Procedia 40, 1319–1326.

Handani, D.W., Ariana, I.M., Dinariyana, A.A.B., Adhita, I.S., 2018. Modelling of Ship Collision Frequency in The Strait of Malacca and Singapore (SOMS) Influenced by Indonesian Port Development. Maritime Safety International Conference (MASTIC.

Hanzu-Pazara, R., Duse, Varsami, C., Andrei, C., Dumitrache, R., 2016. The influence of ship's stability on safety of navigation. IOP Conf. Ser.: Mater. Sci. Eng. 145 (8), 082019. https://doi.org/10.1088/1757-899X/145/8/082019.

Hutabarat, T.S.N.B., Ma'arif, S., Zulbainarni, N., Yusgiantoro, P., 2020. The Use of Integrated Piloting Strategy to Achieve a Balance of Economic Efficiency and Security Effectiveness in the Strait of Malacca. International Journal of Management 11 (9).

International Labour Organization, 1997. Accident prevention on board ship at sea and in port. Retrieved from. https://www.ilo.org/safework/info/standards-and-inst ruments/codes/WCMS_107798/lang–en/index.htm.

International Maritime Organization, 2008. Casualty Investigation Code: Code of the International Standards and Recommended Practices for a Safety Investigation Into a Marine Casualty Or Marine Incident. IMO Publishing.

James, A.J., Schriever, U.G., Jahangiri, S., Girgin, S.C., 2018. Improving maritime English competence as the cornerstone of safety at sea: a focus on teaching practices to improve maritime communication. WMU Journal of Maritime Affairs 17 (2), 293–310.

Jeevan, J., Mohd Salleh, N.H., Md Hanafiah, R., Ngah, A.H., 2020. Emergence of Emergency Logistics Centre (ELC): Humanitarian Logistics Operations at the Straits of Malacca. Transactions on Maritime Science 9 (02), 279–292.

Jepsen, J.R., Zhao, Z., van Leeuwen, W.M., 2015. Seafarer fatigue: a review of risk factors, consequences for seafarers' health and safety and options for mitigation. International maritime health 66 (2), 106–117.

Johnsen, S.O., Kilskar, S.S., Danielsen, B.E., September 2019. Hannover. ESREL, Germany, p. 2019.

Johnsen, S.O., 2021. In: The Challenges of Sensemaking and Human Factors in the Maritime Sector-Exploring the Helge Ingstad Accident. CRC Press, pp. 85–96.

Kahraman, C., 2008. Multi-Criteria Decision Making Methods and Fuzzy Sets. https:// doi.org/10.1007/978-0-387-76813-7_1.

Kamran Dastjerdi, H., Hosseini Nasrabady, N., 2020. Role of malacca strait with a geopolitical and strategic approach. Geopolitics Quarterly 16 (60), 264–287.

Kececi, T., Arslan, O., 2017. SHARE technique: A novel approach to root cause analysis of ship accidents. Saf. Sci. 96, 1–21.

Kim, H.T., Na, S., 2017. Development of a Human Factors Investigation and Analysis Model for Use in Maritime Accidents: A Case Study of Collision Accident Investigation. Journal of Navigation and Port Research 41 (5), 303–318.

Kim, T.-E., Nazir, S., Øvergård, K.I., 2016. A STAMP-based causal analysis of the Korean Sewol ferry accident. Saf. Sci. 83, 93–101.

Kopacz, Z., Morgaś, W., Urbański, J., 2002. The maritime navigation, its environment and its safety system. Annual of Navigation 45–57.

Kozanhan, M.K., 2019. Maritime tanker accidents and their impact on marine environment. Scientific Bulletin" Mircea cel Batran" Naval Academy 22 (1), 1–20.

Kristiansen, S., 2013. Maritime transportation: safety management and risk analysis. Routledge.

Lee, J., Chung, H., 2018. A new methodology for accident analysis with human and system interaction based on FRAM: Case studies in maritime domain. Saf. Sci. 109, 57–66.

Li, X.F., Liu, Z.X., Peng, Q.E., 2011. Improved Algorithm of TOPSIS Model and Its Application in River Health Assessment. Journal of Sichuan University 43 (2), 14–21.

Li, S., Meng, Q., Qu, X., 2012. An overview of maritime waterway quantitative risk assessment models. Risk Analysis: An International Journal 32 (3), 496–512.

Lim, G.J., Cho, J., Bora, S., Biobaku, T., Parsaei, H., 2018. Models and computational algorithms for maritime risk analysis: a review. Ann. Oper. Res. 271 (2), 765–786.

Lin, W.C., Cheng, H.H., 2020. Improving maritime safety through enhancing marine process management: The application of balanced scorecard. Manag. Decis.

Liu, Z., Wu, Z., Zheng, Z., 2020. A novel model for identifying the vessel collision risk of anchorage. Appl. Ocean Res. 98, 102130. https://doi.org/10.1016/j. apor.2020.102130.

Luo, MEIFENG, Shin, SUNG.-HO., 2019. Half-century research developments in maritime accidents: Future directions. Accid. Anal. Prev. 123, 448–460.

Lützhöft, M., Grech, M.R., Porathe, T., 2011. Information environment, fatigue, and culture in the maritime domain. Reviews of human factors and ergonomics 7 (1), 280–322.

Mallam, S.C., Nordby, K., 2021. In: Supporting Consistent Design and Sensemaking Across Ship Bridge Equipment Through Open Innovation. CRC Press, pp. 155–171.

Marine Department of Malaysia (2017). The Number of Vessels Entering entering the Straits of Malacca.

Md Hanafiah, R. (2017). A Decision Making Model for Assessing the Influence of Steaming Speed on the Revenue Performance of Tanker on Time Charter. Universiti Teknologi MARA.

Menon (2021, September). What is seaworthiness and why is it important? Marine Insight. Retrieved from https://www.marineinsight.com/naval-architecture/what-is-seaworthiness-and-why-it-is-important/.

Mercado, F.M., Mogol, C.R., Sarmiento, J.L., Jalbuena, M.C.M., 2018. The Philippine Context of the Teaching and Learning of Maritime English. The Normal Lights 12 (1).

Mia, M. J., Islam, M. S., Islam, M. A., Islam, M., & Uddin, M. I. (2021, April). Brief Analysis Of Inland Waterway Accidents In Bangladesh: Causes And Solutions. 12th International Conference on Marine Technology (MARTEC 2020) At: Faculty of Engineering – Pattimura University, Ambon, Indonesia.

Nævestad, T.O., Vedal Størkersen, K., Phillips, R.O., 2018. Procedure negligence in coastal cargo: what can be done to reduce the gap between formal and informal aspects of safety? Safety 4 (3), 34.

Nefeslioglu, H.A., Sezer, E.A., Gokceoglu, C., Ayas, Z., 2013. A modified analytical hierarchy process (M-AHP) approach for decision support systems in natural hazard assessments. Comput. Geosci. 59, 1–8.

Oldenburg, M., Hogan, B., Jensen, H.-J., 2013. Systematic review of maritime field studies about stress and strain in seafaring. Int. Arch. Occup. Environ. Health 86 (1), 1–15.

Onyshchenko, S., Shibaev, O., Melnyk, O., 2021. Assessment of Potential Negative Impact of the System of Factors on the Ship's Operational Condition During Transportation of Oversized and Heavy Cargoes. Transactions on Maritime Science 10 (1), 126–134.

Othman, M.K., Fadzil, M.N., Abdul Rahman, N.S.F., 2015. The Malaysian Seafarers psychological distraction assessment using a TOPSIS method. International Journal of e-Navigation and Maritime Economy 3, 40–50.

Priatno, D.H., Sunaryo, 2020. Study of Pioneer Sea Transportation's Safety with Formal Safety Assessment Method. IOP Conf. Ser.: Earth Environ. Sci. 557 (1), 012016. https://doi.org/10.1088/1755-1315/557/1/012016.

Ramos, M.A., Utne, I.B., Vinnem, J.E., Mosleh, A., 2018. In: Accounting for human failure in autonomous ship operations. CRC Press, pp. 355–363.

Roberts, J., 2006. Compulsory pilotage in international straits: The Torres Strait PSSA proposal. Ocean Development & International Law 37 (1), 93–112.

Rusli, M.H.B.M., 2012. Bridges across Critical International Shipping Ways: A Study of the Proposed Strait of Malacca Bridge. China Oceans L, Rev., p. 14

Rusli, M.H.M., 2020. Navigational hazards in international maritime chokepoints: A study of the Straits of Malacca and Singapore. Journal of International Studies 8, 47–75.

Saaty, T.L., 1988. What is the analytic hierarchy process? In: Mitra, G., Greenberg, H.J., Lootsma, F.A., Rijkaert, M.J., Zimmermann, H.J. (Eds.), Mathematical Models for Decision Support. Springer Berlin Heidelberg, Berlin, Heidelberg, pp. 109–121. https://doi.org/10.1007/978-3-642-83555-1_5.

Sahin, B., Yip, T.L., 2020. June). Analysis of root causes for maritime accidents originated from human factor. The International Association of Maritime Economists (*IAME*). Hong Kong.

Sánchez-Beaskoetxea, J., Basterretxea-Iribar, I., Sotés, I., Machado, M.D.L.M.M., 2021. Human error in marine accidents: Is the crew normally to blame? Maritime Transport Research 2, 1–16.

Soner, O., Asan, U., Celik, M., 2015. Use of HFACS–FCM in fire prevention modelling on board ships. Saf. Sci. 77, 25–41.

Talley, W.K., 1999. Determinants of ship accident seaworthiness. International journal of maritime economics 1 (2), 1–14.

Turedi, O., Ozer-Caylan, D., 2021. Developing a grounded theory of national maritime policies based on safety, security and environment. Journal of International Maritime Safety, Environmental Affairs, and Shipping 5 (2), 84–97.

Unctad, 2019. United Nations Conference on Trade and Development. United Na- tions Publications, Review of Maritime Transport.

Van Hoof, L., Van den Burg, S.W.K., Banach, J.L., Röckmann, C., Goossen, M., 2020. Can multi-use of the sea be safe? A framework for risk assessment of multi-use at sea. Ocean Coast. Manag. 184, 1–13.

van Leeuwen, W.M.A., Pekcan, C., Barnett, M., Kecklund, G., 2021. Mathematical modelling of sleep and sleepiness under various watch keeping schedules in the maritime industry. Marine Policy 130, 104277. https://doi.org/10.1016/j.marpol.2020.104277.

Wróbel, K., Montewka, J., Kujala, P., 2017. Towards the assessment of potential impact of unmanned vessels on maritime transportation safety. Reliab. Eng. Syst. Saf. 165, 155–169.

Yasin, Z., Hwai, A.T.S., Abdullah, A.L., Razalli, N., 2019. The Ocean Legacy of Malaka and Sustainability in the Straits of Malacca. Journal of Ocean and Culture 2, 58–73.

Zainol Abidin & Ismail (2021). Challenges and Opportunities for Malaysian Seafarers. In Harun and Ja'afar (Eds.) Malaysia: A Maritime Nation (pp. 193-205). Kuala Lumpur: Maritime Institute of Malaysia.

Zaman, M.B., Kobayashi, E., Wakabayashi, N., Maimun, A., 2015. Risk of navigation for marine traffic in the Malaka Strait using AIS. Procedia Earth Planet. Sci. 14, 33–40.

ARTICLES FOR FACULTY MEMBERS

NAVIGATIONAL RISK OF CONTAINER FALLS IN THE STRAIT OF MALACCA

Title/Author	Assessing the influence of sudden propulsion loss on a ship's manoeuvrability in various wave heights utilizing CFD / Kim, D., Song, S., & Tezdogan, T.
Source	*Ocean Engineering* Volume 311 Part 2 (2024) 119022 Pages 1-13 https://doi.org/10.1016/J.OCEANENG.2024.119022 (Database: ScienceDirect)

Research paper

Assessing the influence of sudden propulsion loss on a ship's manoeuvrability in various wave heights utilizing CFD

Daejeong Kim [a], Soonseok Song [b,*], Tahsin Tezdogan [c]

[a] *Divison of Navigation Convergence Studies, Korea Maritime & Ocean University, 727, Taejong-ro, Yeongdo-gu, Busan, Republic of Korea*
[b] *Department of Naval Architecture & Ocean Engineering, College of Engineering, Inha University, 100 Inha-ro, Incheon, Republic of Korea*
[c] *Department of Civil, Maritime and Environmental Engineering, School of Engineering, University of Southampton, Boldrewood Innovation Campus, Building 176, SO16 7QF, UK*

ARTICLE INFO

Keywords:
Free-running ship
Manoeuvrability
Seakeeping
Computational fluid dynamics
Control

ABSTRACT

The prevalence of ship propulsion failure remains a significant concern at sea, posing a recurring risk to maritime safety. As a ship's ability to manoeuvre heavily relies on its propulsive power generated by a rotating propeller, any loss in propulsion can lead to potential hazards such as collisions, contacts, or groundings, particularly in a real seaway. Therefore, accurately assessing the manoeuvring capabilities of ships experiencing propulsion failure is crucial for ensuring navigation safety. This paper aims to examine the impacts of sudden propulsion loss on the manoeuvring capability of the KCS (KRISO Container Ship) model under different wave heights, utilizing URANS (Unsteady Reynolds-Averaged Navier-Stokes) simulations. Through a series of case studies comparing ship performances under normal conditions versus propulsion loss scenarios, particularly during turning circle manoeuvres in different wave height conditions, the study sheds light on the significant impact of propulsion failure on ship manoeuvrability. When examining the ship's turning performance under identical wave heights, it became evident that the ship's advance increased in instances of propulsion loss compared to normal operational conditions. Specifically, at a wave height of 2.4 m, the ship's advance increased by 23% during propulsion failure. Similarly, at wave heights of 3.6 m, 4.8 m, and 6.0 m, the increases were 19%, 17%, and 12%, respectively. In calm water, there was a 24% increase in advance. Notably, at a wave height of 7.2 m, the ship failed to complete a 90° turn, making it impossible to determine the ship's advance under these conditions. The findings underscore the critical importance of sufficient propulsion power for safe vessel operation. This research not only provides valuable insights for navigators into ship manoeuvring under propulsion failure but also contributes to the development of contingency measures, especially pertinent for autonomous vehicles encountering similar propulsion challenges.

1. Introduction

As the reliance on shipping activities continues to grow, the escalating maritime traffic poses a significant risk to maritime safety. As detailed in the accident investigation report covering the period from 2014 to 2022 (EMSA, 2023), the most prevalent incident at sea has recently been identified as the failure of propulsion power on the ship, as illustrated in Fig. 1. Moreover, there has been a significant rise in propulsion failure incidents in recent years. This specific occurrence was predominantly linked to commercial cargo vessels. The loss of ship's propulsive power emerges as among the most perilous occurrences in maritime shipping, greatly compromising a ship's manoeuvrability

amidst challenging oceanic conditions. Inadequate manoeuvring capability, stemming from the failure of ship propulsion power, may contribute to additional and severe navigation incidents (including collisions, contacts, and groundings) especially in areas with dense traffic or narrow waterways.

Based on the article excerpt from The New York Times (Mike Baker, 2024), the Baltimore bridge collapse underscored the critical significance of propulsion loss in the tragic event. It illustrates how the sequential breakdown of the cargo ship's vital operational systems, notably its electrical generators, resulted in the vessel drifting uncontrollably towards catastrophe. Despite advancements in automation and redundancy systems within the maritime sector, the unforeseen

---

"complete blackout" (which essentially signifies propulsion loss) highlights the intricate nature and potential vulnerabilities of modern vessel operations, which will be thoroughly investigated in this study.

It should be highlighted that a ship's manoeuvring capability is significantly influenced by its thrust, which is directly linked to propulsion power, as stated by Hasnan et al. (2020). In addition, the velocity of the fluid discharged from the propeller and directed towards the rudder blade is a crucial factor in influencing the rudder force that controls the heading of the ship, thereby directly affecting a ship's manoeuvring capability. From this, it can be deduced that as the velocity of the fluid entering towards the rudder increases, it generates control force and moment by the rudder, ensuring the safety of a ship's steering performance. Therefore, sudden thrust loss (meaning propulsion system failure) during navigation would have a detrimental effect on the ship's steering capability due to the decrease in fluid velocity entering towards the rudder, thereby resulting in the insufficient generation of control force and moment for the ship's manoeuvrability. The abrupt breakdown of ship's propulsion (indicating a sudden decrease in the velocity of fluid entering towards the rudder) during ship navigation can directly result in the loss of a ship's control capability. This highlights the necessity of a thorough comprehension of a vessel's manoeuvring performance in cases of propulsion failure to prevent maritime accidents. This study aims to assess the manoeuvrability of ships experiencing sudden propulsion failure in various wave conditions encountered during navigation.

A ship's manoeuvrability has been estimated through several approaches in the field of ship hydrodynamics. As an example, to evaluate ship manoeuvring performance, established mathematical models like the Abkowitz model and the MMG (Manoeuvring Modelling Group) model have been utilized. The hydrodynamic coefficients inherent in these models are determined using empirical formulas, acquired through PMM (Planar Motion Mechanism) experiments, or computed through virtual PMM simulations in a CFD (Computational Fluid Dynamics) environment, thus aiding in the assessment of manoeuvring performance. Furthermore, the emulation of free-running experiments traditionally performed in manoeuvring basins by utilizing CFD-based manoeuvring simulations, presently stands out as an advanced tool for tackling ship manoeuvring challenges within research institutions. This preference is attributed to advancements in computing capacity and mathematical algorithms (ITTC, 2021). The ship manoeuvring simulations conducted in a CFD environment offer significant advantages, especially in their capability to precisely simulate and incorporate the impact of fluid viscosity and the turbulent characteristics of fluid flow, characterized by rapid fluctuations in velocity and pressure, which significantly affect ship motions. Its strengths extend to the provision of highly detailed results, encompassing comprehensive insights into forces exerted by the fluid, changes in fluid surface height, and the patterns of velocity and pressure experienced during the ship's control.

As an example, Broglia et al. (2015) conducted ship manoeuvring simulations in a CFD environment to analyse the manoeuvrability of a vessel in calm seas, employing a URANS (Unsteady Reynolds-Averaged Navier-Stokes) approach. For taking into account the complex flow field around the stern of the hull, a modified actuator disk was integrated into the ship's CFD model and this adaptation ensured an accurate representation, addressing oblique flow effects and enhancing the mode's fidelity in simulating the complex dynamics of the manoeuvring ship. The study compared numerical data, which covered various parameters related to ship manoeuvring performance across different manoeuvres, with experimental trials conducted using a ship model designed for free running, showing significant agreement. Wang et al. (2016) performed ship manoeuvring simulations utilizing the URANS approach on a specific type of ship model developed by the Office of Naval Research, exploring the ship's turning capability in calm seas. In the study, the direct discretisation of the propeller was emphasized, resulting in stringent flow resolution requirements. The study validated the accuracy of free-running CFD models through comparison with experimental data by showing that both trajectories and other important parameters exhibited a comprehensive consistency. In Kim et al. (2021), to evaluate the intrinsic manoeuvring performance of KVLCC2 in calm seas, manoeuvring simulations were conducted using CFD and the results were comprehensively illustrated. Free-manoeuvre simulations in this study were conducted utilizing the CFD software STAR-CCM + as an URANS solver. Their investigation underscored the advantages of manoeuvring simulations in a CFD environment for accurately predicting the vessel's performance in calm water. It can be found from the study that favourable comparisons were drawn between the simulation results and experimental data. It is also important to highlight recent studies that utilized manoeuvring simulations in a CFD environment to estimate the manoeuvring characteristics of a ship in waves using an URANS solver, as demonstrated by D. Kim et al. (2021c), 2021a, 2021b; Kim et al. (2023a), 2023b, 2022b; Kim and Tezdogan (2022) Taking advantage of the benefits of CFD simulations for ship manoeuvring problems, these studies are dedicated to the analysis of manoeuvring and seakeeping performance in diverse wave conditions.

The numerous academic studies in ship manoeuvring research field have only addressed the manoeuvring performance of a ship under typical operational circumstances wherein critical ship components such as propeller and rudder are working functionally. It is indisputably true that research examining ship manoeuvrability in normal operating conditions serves as a valuable resource for understanding ship handling capability and offers practical guidance to navigational officers. However, these findings would not provide helpful information on the ship manoeuvrability during propulsion loss incidents (regarded as the most prevalent incident at sea) wherein a rotating propeller is suddenly rendered non-rotating during manoeuvres. While the author's earlier research (Kim et al., 2022a) examined the effect of abrupt thrust loss on the vessel's manoeuvring capability in various directions of regular waves, there remains a perceived need to explore a broader spectrum of wave conditions for a more comprehensive understanding. Therefore, in light of this necessity, this research was driven to explore the impact of the thrust loss on the vessel's manoeuvring ability across varying wave height scenarios using CFD.

This research presents a comprehensive study on the free-manoeuvres of the KCS model navigating through waves of different
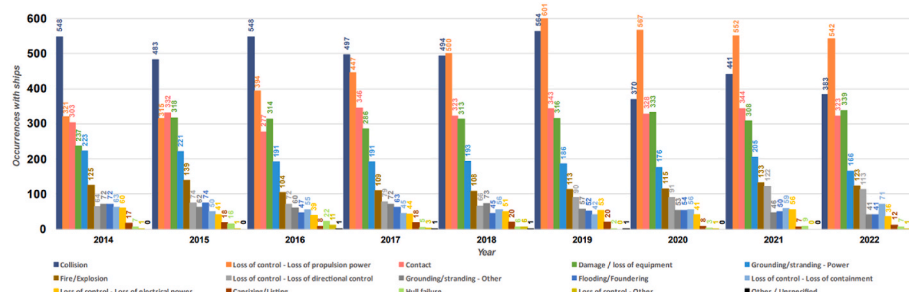

Fig. 1. Types and frequencies of maritime accidents occurring from 2014 to 2022, sourced from EMSA, 2023.

heights, including turning circle manoeuvres, by means of the URANS approach. Manoeuvring simulations in a CFD environment were designed and conducted under both normal operating conditions and scenarios involving propulsion loss, aiming to discern the variation in the manoeuvring performance of the ship moving forward with a specific propeller revolution. In the manoeuvring simulations designed in this study, initially, the stationary ship was constrained until it reached the target forward speed by rotating the propeller at a specific propeller rate, indicating the typical forward movement of the ship at sea. Then, the turning characteristics were examined under both typical operational conditions and sudden thrust loss conditions, following the ship manoeuvring assessment standards proposed by IMO (International Maritime Organization).

2. Methodology

The research approach utilized will be outlined in this section, providing brief explanations within the subsequent sub-sections. Fig. 2 illustrates the methodology for exploring the ship's manoeuvrability under both typical operational conditions and sudden thrust (propulsive power) loss conditions, comprising four primary steps. The selection of representative ship types and the determination of the sea conditions for conducting manoeuvring simulations were decided in the first stage. In the second stage, the numerical modelling conditions were established to generate a ship model capable of free navigation at sea within the CFD environment. This involved defining not only the typical conditions used in ship hydrodynamics but also setting up control mechanisms to simulate an automated auto-pilot system. In the third stage, the step-by-step achievement conditions to estimate the steering capability in the event of propulsion loss were established. This included tasks such as accelerating the stationary ship to reach a specific target speed, creating abrupt thrust loss conditions according to the control mechanism, and finally, implementing rudder blade deflection to perform turning manoeuvres. The concluding fourth stage analysed the manoeuvring and seakeeping characteristics of a ship encountering propulsion system failure, utilizing the simulation results from Step 3. Specifically, this study concentrated on discerning the differences in manoeuvring performance compared to ships unaffected by propulsion loss.

2.1. Goal and scope

The KCS model scaled at $\frac{1}{75.21}$ was chosen in this study, which includes a single rudder and propeller. Fig. 3 illustrates the physical depiction of the adopted KCS model, with detailed specifications provided in Table 1. It is believed that the findings will offer vital insights into the effect of abrupt thrust loss during navigation on the manoeuvrability of currently operating container vessels, considering the KCS hull geometry closely resembling that of commercial container ships. Referencing Table 2 and the accompanying Fig. 4, this study devised twelve distinct simulation scenarios wherein the CFD ship model was employed to simulate the standard turning manoeuvres in bow waves, both under normal operating and propulsion loss conditions. The wave
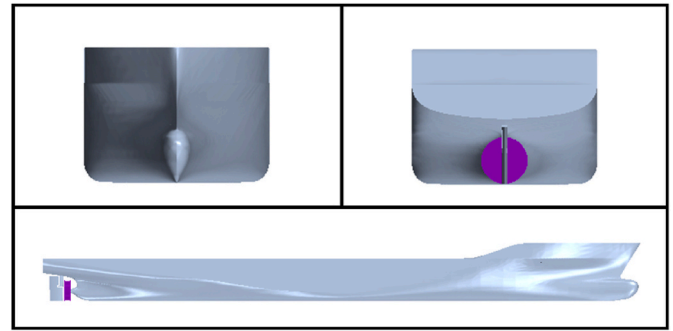
Fig. 3. Geometric representation, sourced from Kim and Tezdogan (2022).

Table 1
Detailed specification of the ship, sourced from SIMMAN, 2020.

Main particulars	Symbols	Model scale (1:75.24)	Full scale
Length between the perpendiculars	L_{BP} (m)	3.057	230.0
Length of waterline	L_{WL} (m)	3.0901	232.5
Beam at waterline	B_{WL} (m)	0.4280	32.2
Draft	D (m)	0.1435	10.8
Displacement	Δ (m³)	0.1222	52,030
Block coefficient	C_B	0.651	0.651
Ship wetted area without rudder	S (m²)	1.6834	9530
Longitudinal centre of buoyancy	% L_{BP}, fwd+	−1.48	−1.48
Metacentric height	GM (m)	0.008	0.6
Radius of gyration	K_{xx}/B	0.49	0.49
Radius of gyration	K_{yy}/L_{BP}, K_{zz}/L_{BP}	0.25	0.25
Propeller diameter	D_P (m)	0.105	7.9
Propeller rotation direction (view from stern)		Right hand side	Right hand side
Rudder turn rate	(deg/s)	20.1	2.32

heights were set as follows: Case 1 had a wave height of H = 0.032 m, corresponding to full-scale heights of 2.4 m. Case 2 had H = 0.048 m, equivalent to full-scale heights of 3.6 m. Case 3 had H = 0.064 m, corresponding to full-scale heights of 4.8 m. Case 4 had H = 0.080 m, equivalent to full-scale heights of 6.0 m. Finally, Case 5 had H = 0.096 m, corresponding to full-scale heights of 7.2 m. Case 6 represents a scenario where the manoeuvring characteristics of the vessel are evaluated in calm seas, where wave loads are absent.

Accelerating the stationary vessel to the target speed is a prerequisite before initiating the turning operation under both typical operational and thrust loss (propulsive power loss) conditions. Throughout the ship's acceleration process, the propeller's rotational rate was adjusted to maintain a constant 13.38 revolutions per second (RPS = 13.38). Due to the varying wave conditions for each case, involving different wave heights, the final forward speed of the ship after acceleration from a stationary condition differed, despite applying the same propeller

Fig. 2. Methodology for conducting manoeuvring simulations in a CFD environment.

Table 2
The simulation conditions established in this study.

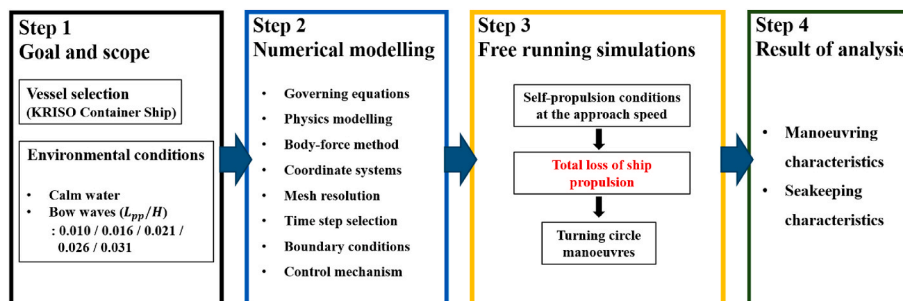| Case no.	Model scale (1:75.24)					
	Approach speed U_0 (m/s)	Propeller rev. (*RPS*)	Wave height H (m)	Encounter Angle μ (degrees)	Encounter Period T_e (s)	Free running manoeuvres
1						
1.1	1.004	**13.38**	0.032	225 (Bow sea)	9.15	Turning manoeuvre
1.2	1.004	**13.38→0**	0.032	225 (Bow sea)	9.15	
2						
2.1	0.945	**13.38**	0.048	225 (Bow sea)	9.29	Turning manoeuvre
2.2	0.945	**13.38→0**	0.048	225 (Bow sea)	9.29	
3						
3.1	0.876	**13.38**	0.064	225 (Bow sea)	9.43	Turning manoeuvre
3.2	0.876	**13.38→0**	0.064	225 (Bow sea)	9.43	
4						
4.1	0.811	**13.38**	0.080	225 (Bow sea)	9.57	Turning manoeuvre
4.2	0.811	**13.38→0**	0.080	225 (Bow sea)	9.57	
5						
5.1	0.737	**13.38**	0.096	225 (Bow sea)	9.74	Turning manoeuvre
5.2	0.737	**13.38→0**	0.096	225 (Bow sea)	9.74	
6						
6.1	1.094	**13.38**	Calm water	–	–	Turning manoeuvre
6.2	1.094	**13.38→0**	Calm water	–	–	

Case no.	Full scale					
	Approach speed U_0 (m/s)	Propeller rev. (*RPS*)	Wave height H (m)	Encounter Angle μ (degrees)	Encounter Period T_e (s)	Free running manoeuvres
1						
1.1	8.709	**1.54**	2.4	225 (Bow sea)	1.055	Turning manoeuvre
1.2	8.709	**1.54→0**	2.4	225 (Bow sea)	1.055	
2						
2.1	8.197	**1.54**	3.6	225 (Bow sea)	1.071	Turning manoeuvre
2.2	8.197	**1.54→0**	3.6	225 (Bow sea)	1.071	
3						
3.1	7.599	**1.54**	4.8	225 (Bow sea)	1.087	Turning manoeuvre
3.2	7.599	**1.54→0**	4.8	225 (Bow sea)	1.087	
4						
4.1	7.035	**1.54**	6.0	225 (Bow sea)	1.104	Turning manoeuvre
4.2	7.035	**1.54→0**	6.0	225 (Bow sea)	1.104	
5						
5.1	6.393	**1.54**	7.2	225 (Bow sea)	1.123	Turning manoeuvre
5.2	6.393	**1.54→0**	7.2	225 (Bow sea)	1.123	
6						
6.1	9.489	**1.54**	Calm water	–	–	Turning manoeuvre
6.2	9.489	**1.54→0**	Calm water	–	–	
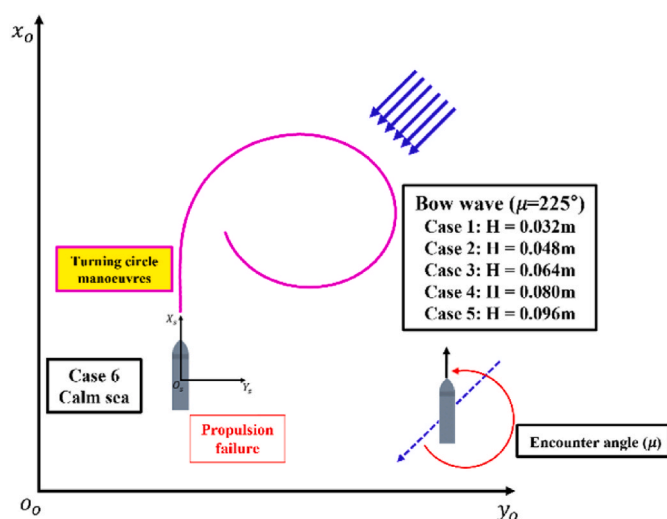
Fig. 4. Schematic depictions of the manoeuvring simulations carried out in this research.

rotational speed. Once the ship attained a constant forward speed, the ability to turn was estimated when the propeller suddenly stopped, and the rudder's rotation was simultaneously adjusted in accordance with the control mechanism. In other words, the propeller operation intentionally transitioned to an abrupt stop condition, signifying a change from an RPS of 13.38 to 0. Simultaneously, the rudder blade was deflected to a hard starboard position, and the turning simulation was conducted.

In maritime operations, sudden propulsion loss can occur due to several practical reasons, including but not limited to mechanical failures, electrical system malfunctions, or human errors. Mechanical failures may involve issues with the propulsion system itself, such as engine malfunctions or gear failures. Electrical system malfunctions could result from faults in the ship's power generation or distribution systems. Additionally, human errors or operational mistakes can contribute to unforeseen propulsion failures. The scenarios simulated in our study aim to reflect these real-world conditions and their impact on ship manoeuvrability. As highlighted by recent incident reports and case studies, such as the Baltimore bridge collapse, these failures can lead to significant navigational hazards, including collisions and groundings, underscoring the importance of addressing these issues.

2.2. Numerical method

Free-manoeuvres for the KCS in a CFD environment were conducted

using the commercial software STAR-CCM+. The subsequent sections will provide a detailed description of the numerical configuration utilized in this study.

2.2.1. Fluid dynamics equations

The URANS equations were employed to develop the CFD ship model for the free-manoeuvre, presented in vector format as follows:

$$\nabla \bullet \mathbf{U} = 0 \tag{1}$$

$$\frac{\partial(\rho\mathbf{U})}{\partial t} + \nabla \bullet \left[\rho\left(\mathbf{U} - \mathbf{U_g}\right)\mathbf{U}\right] = -\nabla p + \nabla \bullet \left(\mu_{eff}\nabla\mathbf{U}\right) + \nabla\mathbf{U} \bullet \nabla\mu_{eff} + q_i \tag{2}$$

Here, we used the standard notation of **U** for the velocity of fluid, $\mathbf{U}_g$ for the velocity of grid, and p and μ_{eff} for the static pressure and the effective dynamic viscosity respectively.

Menter's SST turbulence model was employed in our computations to obtain an efficient and reliable solution for the problem at hand (Menter, 1994). Utilizing the momentum equation's source term, q_i (Eq. (2)), the average effect exerted by a ship's propeller rotating in the wake of its hull was simulated via the momentum source method employing a virtual disk approach. Furthermore, this approach presents a notable advantage in computational efficiency as stated by D. Kim et al. (2021c). The present study adopted the VOF approach, well-known for its efficacy in simulating free-surface flows within engineering contexts. This method is a computational technique used in fluid dynamics to accurately simulate fluid flow behaviours, especially when dealing with the interaction of multiple fluids possessing distinct interfaces. The VOF approach effectively tracks the interface between two or more immiscible fluids by numerically addressing the governing equations that describe fluid motion and interface dynamics within a computational framework. The governing equations were discretised by means of a finite volume scheme. The numerical simulation achieves the process of linking pressure and velocity through the utilisation of a SIMPLE-type algorithm.

2.2.2. Coordinate frames

Fig. 5 depicts the coordinate frames of the CFD ship model utilized in this research. As evident from the figure, Earth-fixed (inertial frame), Ship-fixed (non-inertial frame), Propeller-fixed (non-inertial frame), and Rudder-fixed (non-inertial frame) coordinates were employed in the CFD computations.

2.2.3. Computational domain and boundary conditions

The process of generating the mesh was executed utilizing the automated meshing functionality in the CFD software. Specifically, the

Fig. 5. The illustration of the coordinate frames in this work, sourced from Kim and Tezdogan (2022).

cut-cell method using cartesian grids was employed, notable for its robustness in handling geometric complexities. The utilisation of an overset method was undertaken with the objective of managing the intricate dynamics pertaining to both the ship's 6DoF motions and the rotation of the rudder blade while the ship was operating at sea. The computing domain in the ship CFD model was subdivided into 3 distinct regions (due to an overlapping of overset regions): background, hull, and rudder, as depicted in Fig. 6. In this study, the grid generation process yielded a total of about 7,200,000 cells spanning Cases 1 through 5 for the CFD ship model. Additionally, Case 6 was characterized by a total grid cell count of 5,400,000 cells. A refined grid resolution strategy was adopted (stated in ITTC, 2011) for the prevention of wave dissipation issues in the manoeuvring simulation. It entailed the generation of over eighty mesh count per wavelength along both the x-axis and the y-axis of the horizontal axes, alongside twenty mesh count per wave height along the z-axis, applied to the manoeuvring simulations in waves.

Determining the boundary conditions accurately is a pivotal requirement for ensuring the reliability of solutions in the context of CFD problem-solving. The selection of boundary conditions relies heavily on the specific attributes of the problem to be addressed. Multiple combinations of boundary conditions are available for solving a particular problem. For this study, the selection of boundary conditions aimed to accurately simulate the behaviour of the ship under the normal and thrust loss conditions amidst wave dynamics during self-propulsion at sea. Fig. 7 illustrates the computing domain used for the manoeuvring simulation, incorporating the ship model fitted with a single rudder and virtual disk, as well as the boundary conditions in use.

2.2.4. Ship motion

The CFD ship model developed in this work employed the DFBI (Dynamic Fluid-Body Interaction) method, integrated with the CFD module, to compute the 6DoF (Degrees of Freedom) motion response of the ship under both normal operational conditions and scenarios involving propulsive power loss. In the DFBI method, the ship is regarded as a rigid body, and its motion is computed derived from Newton's equations of motion for 6 degrees of freedom. It is expressed using the following equation. (-)

$$\overrightarrow{F} = \frac{d\left(m\overrightarrow{V}\right)}{dt} \tag{3}$$

$$\overrightarrow{M} = M_b \frac{d(m\overrightarrow{\omega})}{dt} + \overrightarrow{\omega} \times M_b\overrightarrow{\omega} \tag{4}$$

In Eq. (3), $\overrightarrow{F}$, m, and $\overrightarrow{V}$ respectively represent the exerting force vector on the ship, the mass of the ship, and the ship's translation velocity vector. In Eq. (4), $\overrightarrow{M}$, M_b, and $\overrightarrow{\omega}$ respectively represent the exerting moment vector on the ship, the ship's mass tensor, and the ship's rotational speed vector.

2.2.5. Control mechanism

Turning circle manoeuvres were conducted in order to analyse how propulsion failure influences the ship's manoeuvring performance. Prior to initiating the turning manoeuvre simulation following the abrupt thrust loss, the ship, initially at rest with a surge velocity of 0, underwent acceleration by applying a propeller rate of 13.38 per second. When the ship's resistance matched its propulsion force, achieving a steady-state motion, or in other words when the target advance velocity was reached, the propeller rate was abruptly altered per the propeller control module, mimicking the propulsion system failure condition. This modification was introduced to simulate the propulsion failure scenario, as described by the following expression:

$$n(t) = \begin{cases} 13.38 \ (t < t_f) \\ 0 \ (t \geq t_f) \end{cases} \tag{5}$$
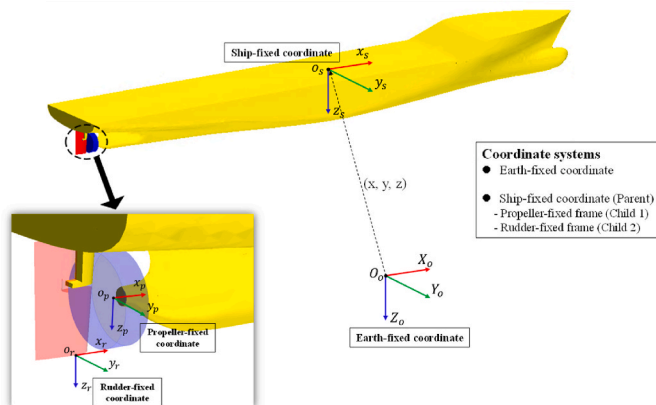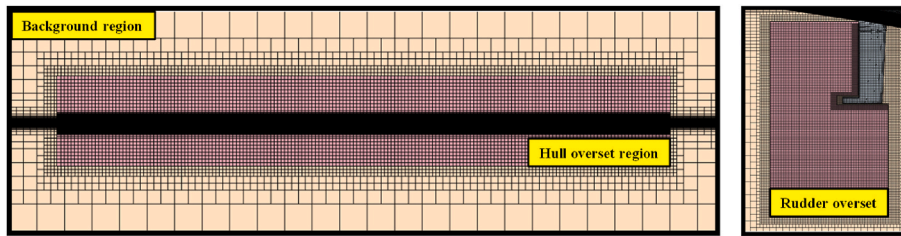
Fig. 6. Computing domain grids in this work.
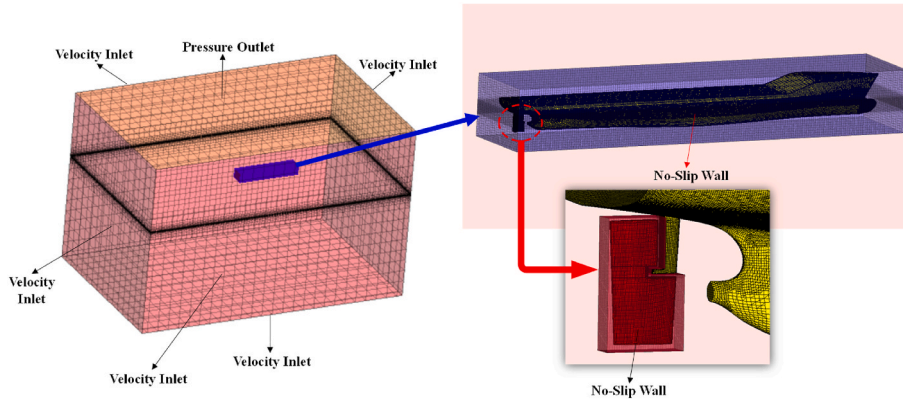
Fig. 7. The boundary conditions imposed on the background, ship hull, and rudder regions.

In Eq. (5), $n(t)$ signify the propeller rate at a specific time t. t_f represents the moment when the propeller rate abruptly becomes 0 during the normal operational condition, marking the onset of propulsive power loss for the ship.

Immediately upon the occurrence of propulsive power loss, specifically when the propeller rate dropped from 13.38 to 0, the ship model initiated the starboard turns, by turning the rudder to its maximum angle of 35°. The rudder rotates around the rudder stock at a speed of 20.1° per second.

3. Results

3.1. Verification and validation study

Readers are directed to a prior study by these authors (D. Kim et al.,

2021c) for detailed information on verification and validation analyses that assessed numerical uncertainties in a CFD model (closely resembled the grid structure of the CFD ship model employed in this work). This previous work utilized the same numerical methodology outlined in the current study, meaning that the CFD ship model presented here is adequately dependable to tackle the propulsion failure issue at hand.

3.2. Turning circle manoeuvre

3.2.1. Turning parameters

This section aims to analyse the contribution of sudden thrust loss to the turning manoeuvres of the ship. It will involve a comparative assessment of key manoeuvring parameters under normal operating conditions versus those experienced in the propulsion loss conditions. Fig. 8 illustrates turning trajectories computed by the free-running CFD
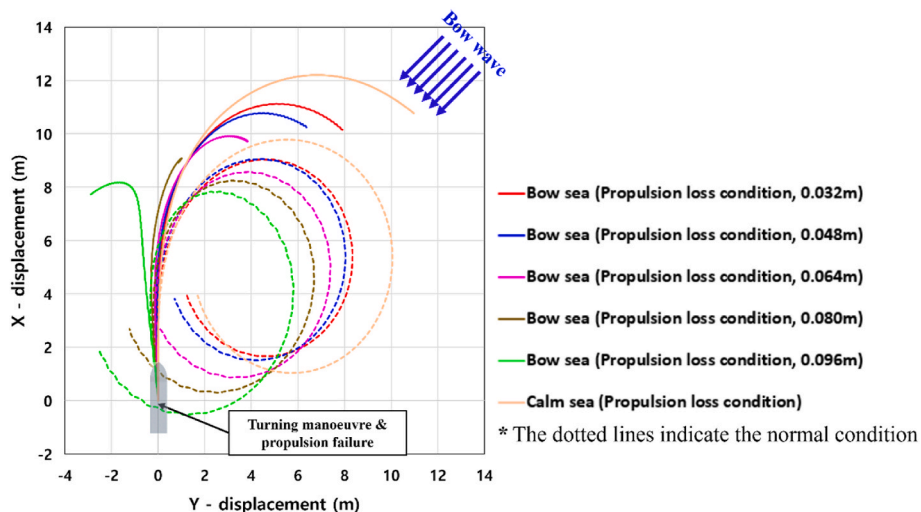
Fig. 8. The trajectories experienced by the ship in all cases (Cases 1–6).

model for all cases, which can be broadly categorized into normal operating conditions, where the vessel undergoes a turning manoeuvre after advancing straight at RPS 13.38, and propulsion loss conditions, where the vessel experiences a propulsion failure at RPS 13.38 and subsequently performs a turning manoeuvre. To ensure consistent evaluation of each case's ship trajectory, the starting coordinates of the turning operation were adjusted to (0,0) in the Earth-fixed frame. Simulations were carried out for both scenarios in each case (i.e., normal operation and propulsion failure) over identical durations, enabling a fair comparison of the impact of thrust loss on the manoeuvrability. It is important to mention that simulations under normal conditions concluded upon achieving a 360° heading angle variation. This decision was made with practical considerations in mind, as a full 360° turn sufficiently represents the ship's turning performance. To analyse the trajectory for each case shown in Fig. 8, Table 3 presents manoeuvring indices for both the normal operational and propulsive power loss conditions, differentiated by the case numbers assigned to each, aiming to enhance clarity. In the segment related to propulsion failure conditions, any "-" signifies that the ship did not complete a turn of 90° or 180°, rendering the advance, transfer, or tactical diameter undefined for those instances.

Firstly, examining the trajectories experienced in the normal operating conditions as depicted in Fig. 8 (the dotted lines), it is evident that as the wave height increased, the size of the circles generated by the

ship's turns noticeably decreased, attributed to the drift force exerted by incident waves. Furthermore, for the same reason, in Cases 1.1, 2.1, and 3.1 (corresponding to wave heights of 0.032, 0.048, and 0.064 m, respectively), the y-coordinate position of the ship upon completing a 360-degree rotation was greater than its y-coordinate position at the initial departure. Conversely, in Cases 5.1 and 6.1, upon completing a 360-degree rotation, the y-coordinate position was observed to be smaller than the y-coordinate position at the initial departure. Cases 5.1 and 6.1 (which correspond to relatively higher wave heights) exhibited characteristics different from the trajectory observed in calm seas, representing the vessel's inherent turning capability. Considering the importance of the vessel's position upon completing a 360-degree turn for masters or navigational officers at sea, it is crucial to understand these characteristics well. As a reference, it is noteworthy that in actual maritime operations, masters or navigational officers often execute 360° turns to avoid collisions or to adjust the Estimated Time of Arrival (ETA) at specific ports before entering. Therefore, understanding the vessel's manoeuvring performance is of paramount importance to them. Examining Cases 1.2 to 6.2 in the figure (solid lines), noticeable differences in results were observed when the vessel conducted a turning manoeuvre due to propulsion failure compared to normal operating conditions. Even in calm water conditions where environmental loads were absent (Case 6.2), the ship was unable to form a circular trajectory through the turn. Furthermore, as wave height increased, it was evident that the ship's turns were nearly impossible to execute. Particularly, at a wave height of 0.080 m (Case 4.1, equivalent to a full-scale wave height of 6.0 m), the ship appeared to initiate a turn but then returned to its original orientation. At a wave height of 0.096 m (Case 5.1, equivalent to a full-scale wave height of 7.2 m), despite attempting a turning manoeuvre, the ship ended up biased towards the port side during straight-line motion before ultimately being strongly pushed in the direction of the incident waves. The figure indicates that the ship, affected by propulsion loss, failed to execute planned starboard turns in all instances. This was primarily due to a sharp decrease in fluid velocity passing over the propeller to the rudder, resulting in diminished turning momentum exerted by the rudder.

In Table 3, when comparing cases with identical wave heights (for example, Cases 1.1 and 1.2 or Cases 2.1 and 2.2), observation revealed that the ship's advance seemed to be greater in the event of propulsion loss than under normal operating conditions. Upon closer examination, it was observed that in Case 1, there was a 23% increase in ship advance when comparing the propulsion failure to the normal operating condition. In Cases 2, 3, 4, and 6, increases of 19%, 17%, 12%, and 24% respectively were observed. Interestingly, in Case 5 (the highest wave height at 0.096 m), the ship was unable to complete a 90° turn, rendering it impossible to define ship advance. For ship transfer, it was observed that when environmental loads were absent (Case 6) or when wave heights were relatively low (Cases 1 and 2), the ship experiencing propulsion failure exhibited larger ship transfers compared to when operating under normal conditions. Conversely, when wave heights were relatively high (Cases 3, 4), ship transfers were smaller in the event of propulsion failure compared to normal operating conditions. Furthermore, the ship's advance decreased as wave height increased, occurring in both normal operation and thrust loss conditions. A similar trend was also apparent in the ship's transfer parameter. The time taken to complete a 90° turn significantly lengthened compared to standard conditions, mainly due to the sudden absence of thrust force, leading to a sharp decrease in fluid velocity directed towards the rudder blade. Intriguingly, Cases 1 to 4, experiencing propulsion loss, failed to achieve a 180° turn, while in Case 5, even a 90° turn was unattainable under propulsion loss conditions. Regarding the time required for a yaw of 90°, compared to normal operating conditions, Case 1 showed a 62% increase under propulsion failure conditions, Case 2 exhibited a 72% increase, Case 3 demonstrated an 82% increase, Case 4 revealed a 107% increase, and Case 6 displayed a 60% increase.

Fig. 9 depicts the temporal evolution of the ship's velocities in the

Table 3
Critical turning parameters.

Parameters (CFD results)	Bow sea (0.032 m) (Case1.1)	Bow sea (0.048 m) (Case 2.1)	Bow sea (0.064 m) (Case 3.1)	Bow sea (0.080 m) (Case 4.1)	Bow sea (0.096 m) (Case 5.1)	Calm sea (Case 6.1)
Normal operating conditions						
Advance (m)	8.79 (2.88 L_{BP})	8.83 (2.89 L_{BP})	8.35 (2.73 L_{BP})	8.04 (2.63 L_{BP})	7.70 (2.52 L_{BP})	9.55 (3.13 L_{BP})
Transfer (m)	3.24 (1.05 L_{BP})	3.09 (1.01 L_{BP})	2.68 (0.88L_{BP})	2.24 (0.73 L_{BP})	1.17 (0.38 L_{BP})	4.07 (1.33 L_{BP})
Time for yaw 90° (s)	12.18	13.08	13.44	14.18	15.10	12.31
Tactical diameter (m)	8.09 (2.65 L_{BP})	7.82 (2.56 L_{BP})	7.17 (2.35L_{BP})	6.54 (2.14 L_{BP})	5.63 (1.84 L_{BP})	9.82 (3.21 L_{BP})
Time for yaw 180° (s)	23.19	24.38	24.93	26.26	27.31	24.20

| Parameters (CFD results)	Bow sea (0.032 m) (Case1.2)	Bow sea (0.048 m) (Case 2.2)	Bow sea (0.064 m) (Case 3.2)	Bow sea (0.080 m) (Case 4.2)	Bow sea (0.096 m) (Case 5.2)	Calm sea (Case 6.2)
Propulsion failure conditions						
Advance (m)	10.83 (3.54 L_{BP})	10.50 (3.43 L_{BP})	9.73 (3.18 L_{BP})	9.03 (2.96 L_{BP})	–	11.87 (3.88 L_{BP})
Transfer (m)	3.57 (1.17 L_{BP})	3.21 (1.05 L_{BP})	2.24 (0.73 L_{BP})	0.94 (0.31 L_{BP})	–	4.82 (1.58 L_{BP})
Time for yaw 90° (s)	19.84	22.47	24.56	29.42	–	19.64
Tactical diameter (m)	–	–	–	–	–	–
Time for yaw 180° (s)	–	–	–	–	–	–
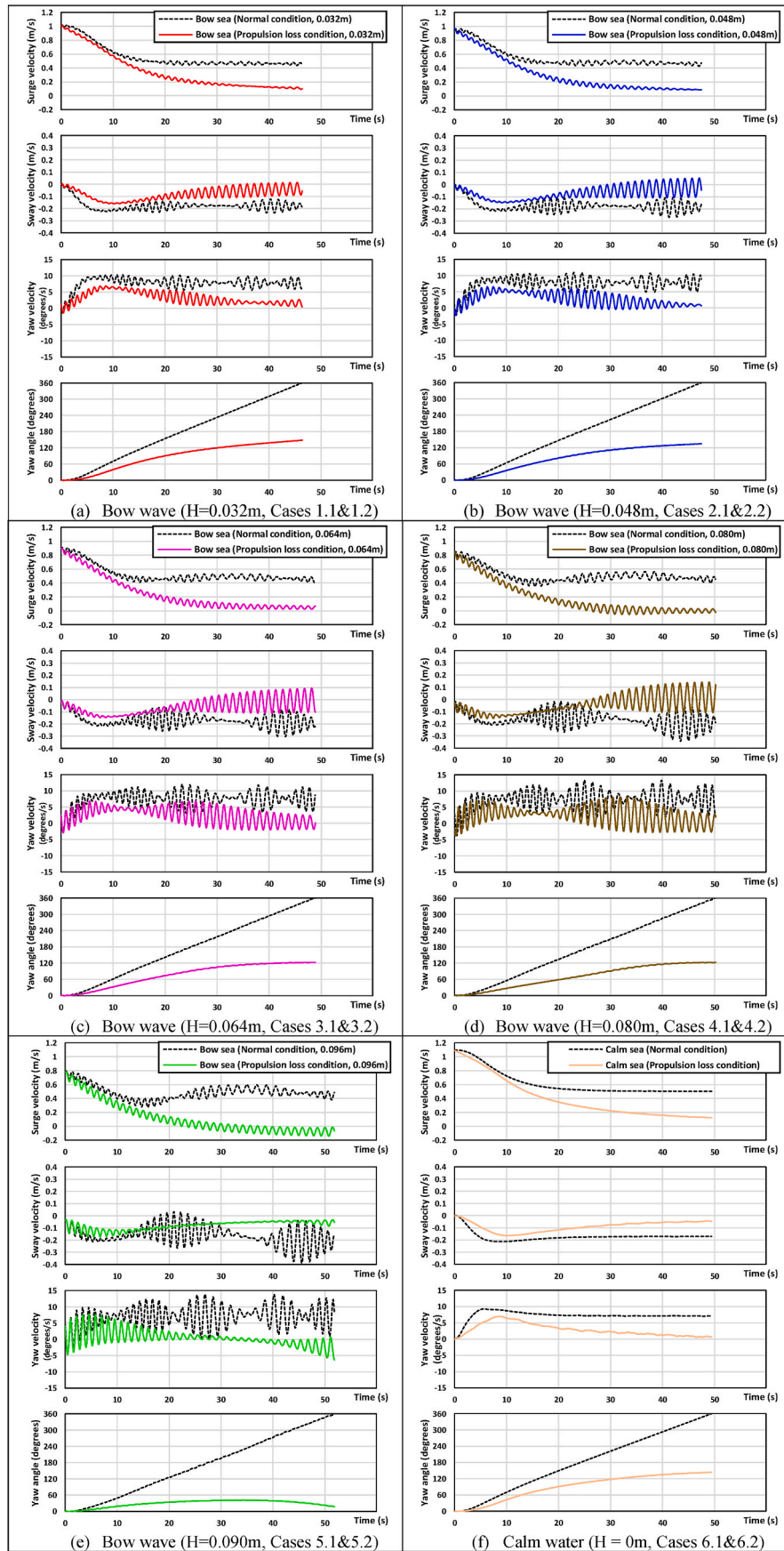
Fig. 9. The temporal changes in the ship's velocities and heading in all cases.

horizontal plane, alongside the heading angle throughout the turning manoeuvre. This aids in comprehensively grasping the variations in ship velocity relative to its turning condition. In the figure, under the normal operation condition, from 0 s until the end of the simulation, the propeller was continuously maintained at a specific RPS. In contrast, for the propulsion loss condition, at 0 s (excluding the pre-simulation phase used to achieve a constant forward speed through self-propulsion computation), the propeller was intentionally and abruptly stopped, transitioning from an RPS of 13.38 to 0. At the same time, the rudder blade was deflected to a hard starboard position, and the turning simulation began from this point. Observations from the figure indicate that the ship, under normal conditions, encountered an involuntary loss in surge speed following a rudder deflection of approximately 35° to starboard. The decrease in speed, ranging from 40% to 55% from the initial velocity at the onset of the starboard turn to the eventually stabilized average, was attributed to increased resistance experienced by the ship induced by a significant angle of drift of the ship. Conversely, when facing propulsive power loss, the ship underwent gradual decreases in surge velocity subsequent to the propulsion power failure and a 35° starboard rudder deflection. The speed decline was primarily attributed to propulsion failure, with the heightened resistance resulting from the angle of drift of the ship. As evidenced by Cases 1.2 to 5.2, while the ship's surge velocity decreased by approximately 40–55% under normal operating conditions, propulsion failure led to a complete drop to about zero within the same duration of turning. Consistent with this, masters of merchant ships typically employ hard starboard or port rudder deflection when the vessel is in a state of stop engine (RPS at 0) to expedite the deceleration of surge speed, leveraging the previously described effect. It was discovered that the sway velocity (translational motion along the y-axis in the ship-fixed frame) and the yaw velocity (rotational motion along the z-axis in the ship-fixed frame) displayed a trend of rapid escalation until reaching a certain threshold after rudder deflection. Subsequently, they gradually stabilized at a consistent level under both normal operational and thrust loss conditions. However, the velocities experienced during the propulsive power issue were significantly lower in comparison to those observed under typical operational conditions. This implies that under the propulsion loss condition, when the propeller was not active, the ship experienced lower fluid velocities entering through the propeller towards the rudder blade side compared to the normal operating condition. This results in relatively lower rudder normal forces, which in turn leads to reduced sway and yaw motions following the initiation of starboard turns, compared to the normal operating condition when the propeller was active. The ship moving forward in relatively low wave heights achieved a shorter time to complete a 90° turn, exhibiting higher yaw velocities in the early transient stage. It is important to emphasize, as evidenced by the yaw angle graph, that in all cases of propulsion loss, the ship failed to complete a 180° turn even with maximum rudder deflection (35°). This highlights the notable disparities in ship trajectory between the typical operational and thrust loss conditions. Taking into account the manoeuvring performance observed under such propulsion loss conditions, it underscores the vessel's inability to swiftly execute substantial course adjustments to evade close-quarter situations within a critical timeframe. This consequently poses a notable threat to navigational safety.

3.2.2. Seakeeping performance and encounter frequencies

Fig. 10 illustrates the temporal changes in the seakeeping performance and heading angles for the KCS as it executed the starboard turns, comparing the typical operational conditions with those in which propulsion was lost. With the exception of the calm water case (Case 6), notable high-frequency fluctuations were noted in the heave, pitch, and roll responses in both conditions, closely linked to the motions resulting from waves. The motions with high frequency caused by waves exhibited continual changes in response to continual and successive changes in the ship's surge speed and the direction where the ship encounters waves. As an illustration, during starboard turns under

conditions where the propeller was generating thrust sufficiently (Cases 1.1 to 5.1), the ship encountered the bow wave from the starboard side at 0° turn, the bow wave from the port side at 90° turn, the quartering wave from the port side at 180° turn, the quartering wave from the starboard side at 270° turn, and again the bow wave from the starboard side at 360° turn, following the initiation of the starboard turns. Fig. 11 depicts the temporal changes in the encounter frequencies computed while the ship was turning to the starboard, alongside the inherent frequencies of the ship motions. A notable contrast in encounter frequency was evident between the normal operational conditions and instances of thrust loss. Consequently, the variations in encounter frequency are expected to influence the seakeeping performance disparities between the normal and propulsive power issue scenarios.

Upon close examination of Fig. 10, it became apparent that the amplitudes of heaving and pitching motions increased as wave heights increased in both the normal and propulsive power loss conditions. Conversely, in calm waters devoid of external disturbances, heave and pitch responses were anticipated to be negligible. Another noteworthy point to highlight is that the ship's manoeuvres in waves revealed noticeable distinctions in seakeeping performance depending on whether thrust loss conditions are present or absent. This discrepancy resulted from significant differences in the ship's heading and surge speed during manoeuvring, which directly influenced the fluctuations in the frequency of wave-encounter and subsequent motion responses. During the manoeuvre, under normal operational conditions, as the ship's heading turned from 0 to 360°, it encountered waves from every direction (including those from the bow, starboard, stern, and port sides). Consequently, the normal condition exhibited pronounced and continual and successive changes in the frequency of wave-encounter, characterized by repetitious fluctuations throughout the turns. On the contrary, when the vessel abruptly lost thrust while moving forward, it led to a narrower range of heading angles in the case of the turns, spanning only from 041° to 148°, with comparatively minimal alterations in the ship's heading throughout the manoeuvres. This limited variation in the ship's heading angle directed the ship to confront waves from particular directions while manoeuvring, thereby causing minimal fluctuations in encounter frequency.

When considering the heave response to waves, the ship experienced its maximum amplitude of heaving motion in the event of encountering waves from the beam. This occurrence is strongly linked to the length ratio between ship and wave. The ship's breadth, acting as the pertinent length in this context, is relatively smaller compared to the wavelength. This discrepancy in size leads to significant vertical motion, with amplitudes early matching the incident waves' height. In the context of the normal operating condition, illustrated in Cases 1.1 to 5.1, as clearly evidenced in Fig. 10, it becomes apparent that during yaw angle turns of 135° and 315°, the ship experienced its maximum response of heaving motion. In the scenario of propulsion failure conditions, observed across Cases 1.2 to 5.2, the majority of instances failed to complete the 135° turn during the manoeuvre, coinciding with encounters of waves from the port beam. Nevertheless, it was noted that as the ship approached this angle, there was a significant rise in heave motion. Differing from the heaving response, it became apparent that waves incident on the beam side of the ship led to minimal pitching response during the turns, a trend observed across both the normal operational and thrust loss conditions. This phenomenon could be attributed to the beam waves' limited generation of pressure differentials between the forward and aft sections of the ship, therefore reducing the moment causing the pitching response. A notable example illustrating the pitching response at the end of the turns for Cases 1.2 to 5.2 is the gradual decrease in pitch amplitude when the ship encounters waves at a 135-degree angle (incident waves from the beam side). A narrower gap between encounter frequency (f_e) and natural frequency (f_n) correlated with increased pitch motion amplitude, as evidenced by the combined analysis of Figs. 10 and 11.

In roll motion, the force and moment exerted on the rudder blade by

Fig. 10. The temporal changes in the seakeeping performance and heading.

(a) Bow wave (H=0.032m, Cases 1.1&1.2)

(b) Bow wave (H=0.048m, Cases 2.1&2.2)

(c) Bow wave (H=0.064m, Cases 3.1&3.2)

(d) Bow wave (H=0.080m, Cases 4.1&4.2)

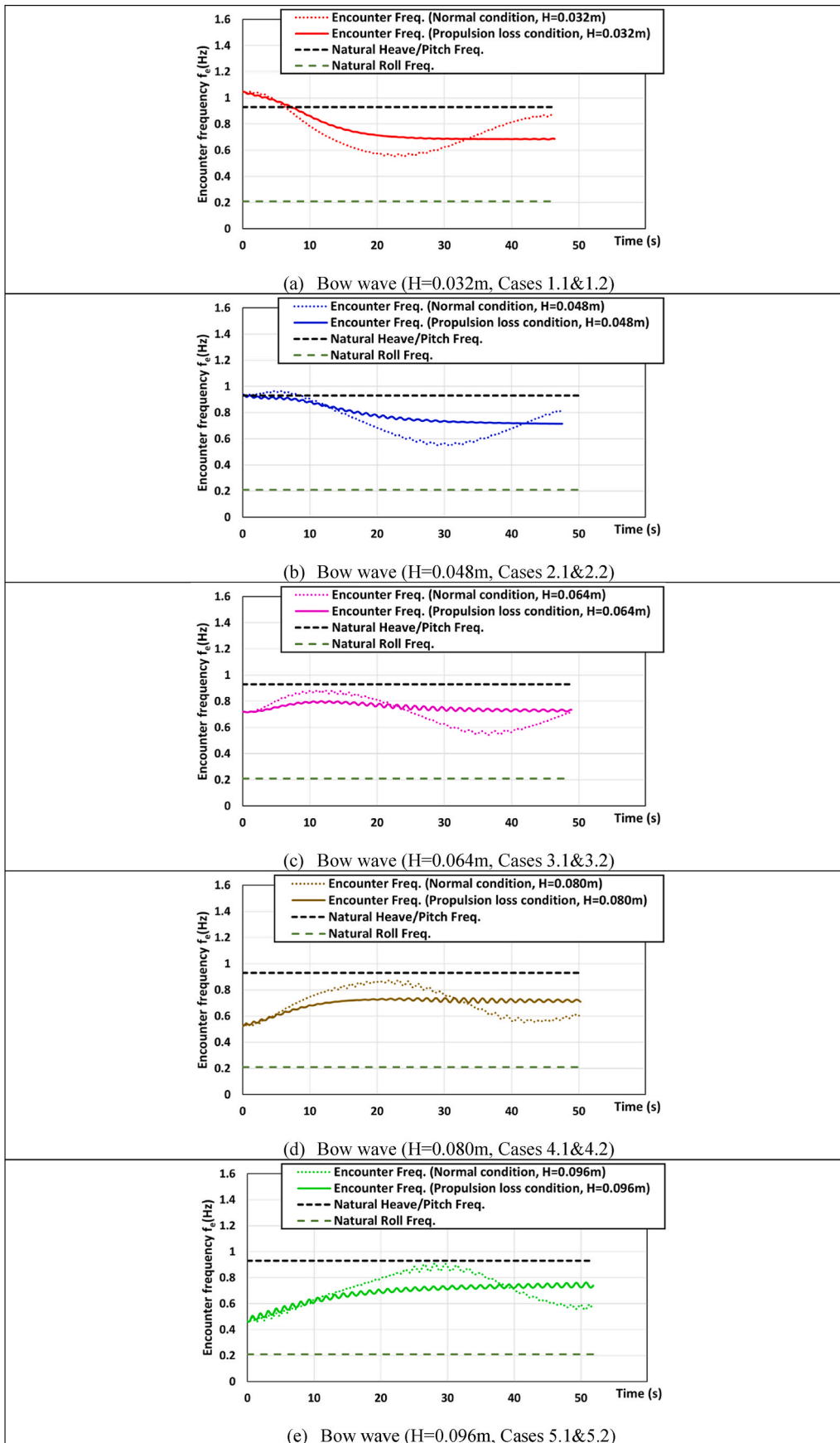(e) Bow wave (H=0.096m, Cases 5.1&5.2)
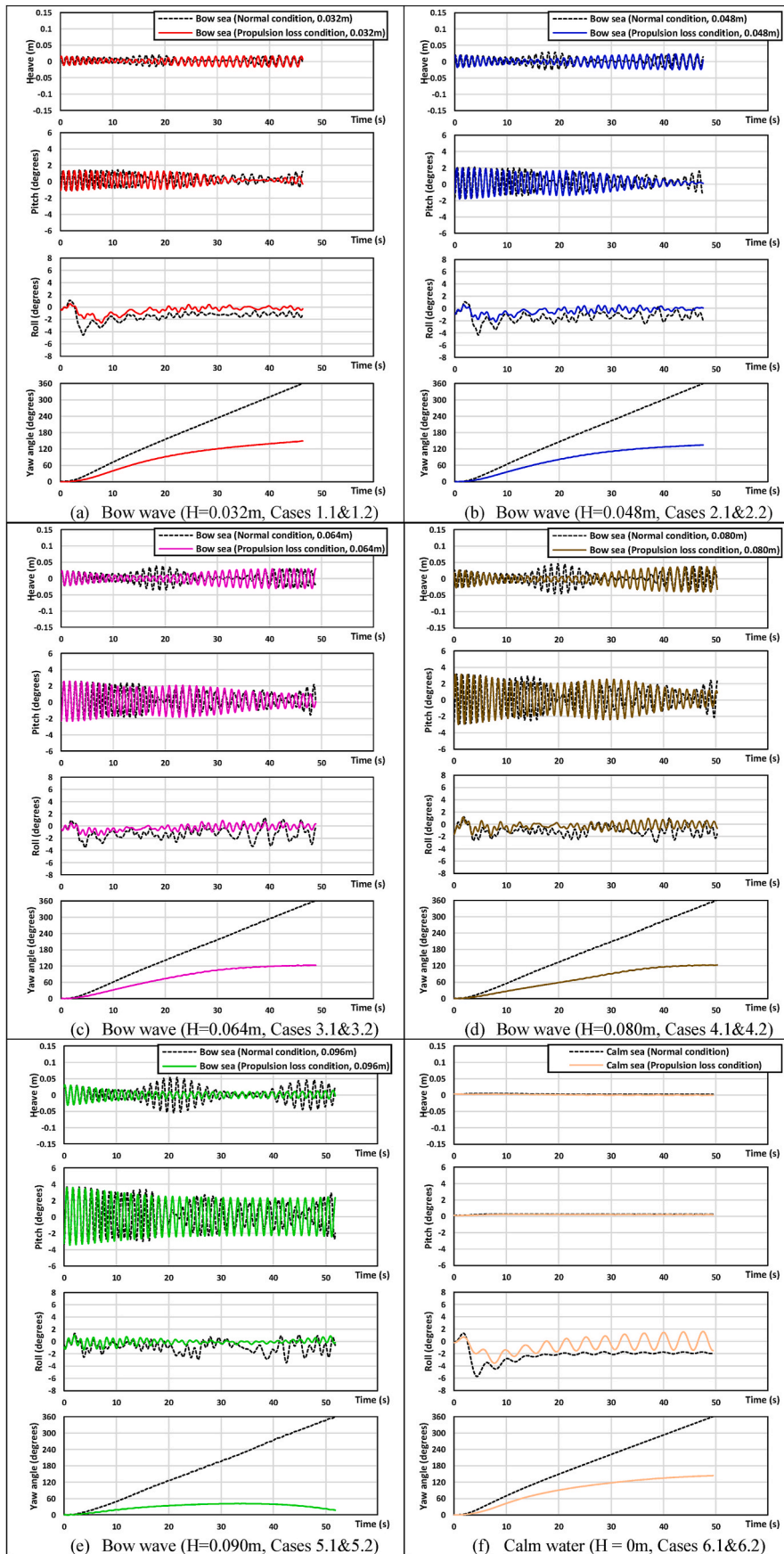
Fig. 11. The temporal changes in the encounter frequencies.

the fluid entering through it were crucial for causing the ship to turn. As conducted in this work, when the rudder blade rotated 35° to the starboard side, it initiated a sequence: the ship initially tilts to the starboard, gravitating towards the trajectory's centre drawn by the ship's turns, propelled by the lift force generated by the rudder. When the ship experiences initial transverse inclination, it is important to emphasize that a significant portion contributing to the roll motion is the rudder lift force, which generates the roll moment. Subsequently, the centrifugal force along with hydrodynamic forces exerted on the hull prompted the ship to tilt towards the outer side. Throughout Cases 1–6, the ship navigating with propulsion loss, consistently demonstrated smaller roll motion amplitudes in comparison to standard operational conditions during manoeuvres. This phenomenon can be ascribed to the diminished rudder lift.

4. Conclusions and discussion

The present study addressed the manoeuvring performance of a ship under both normal operating conditions and propulsion failure scenarios in varying wave heights. It employed an URANS solver integrated with a propeller and rudder controller. Given the recent identification of the most prevalent incident at sea as the loss of ship propulsive power, coupled with the notable increase in propulsion failure occurrences in recent years, it is imperative to evaluate how a ship behaves when experiencing propulsion failure in real seaways to guarantee secure navigation. Therefore, this study aims to provide practical insights into the manoeuvrability of a ship facing sudden thrust loss, thereby advancing the understanding of ship manoeuvring. The main discoveries of this study can be outlined as follows.

(1) Significant disparities in outcomes emerged when the ship attempted a turning manoeuvre under propulsion failure as opposed to normal operational circumstances. Even in calm water devoid of environmental loads (Case 6.2), the ship failed to establish a circular trajectory during the turn. Moreover, with increasing wave heights, it became increasingly clear that executing turns with the ship was nearly impossible.

(2) It was evident that propulsion loss had a significant impact on the speed reduction during turning manoeuvres compared to the velocity encountered by the manoeuvring ship in typical operational circumstances, resulting in notable alterations in critical turning indices.

(3) When examining cases with identical wave heights, it became apparent that the ship's advance appeared greater in instances of propulsion loss compared to normal operational conditions. Upon detailed scrutiny, Case 1 (with a wave height of 2.4 m at full scale) exhibited a 23% increase in ship advance during propulsion failure versus normal operation. Similarly, in Cases 2, 3, and 4 (with wave heights of 3.6 m, 4.8 m, and 6.0 m respectively at full scale), as well as Case 6 (in calm water), increases of 19%, 17%, 12%, and 24% respectively were noted. Notably, in Case 5 (with a full-scale wave height of 7.2 m), the ship failed to complete a 90° turn, precluding the determination of ship advance.

(4) A noticeable difference in the encounter frequency was clear when comparing normal operations to instances of propulsion failure. As a result, these variations in the encounter frequency are likely to affect the differences in the motion responses experienced by the ship under normal operation and propulsive power loss conditions.

(5) The ship operating with propulsion loss consistently showed reduced roll motion compared to standard operational conditions during manoeuvres. This phenomenon can be attributed to the decrease in the fluid velocity entering through the rudder blade, resulting in a decrease in the normal force.

Amidst the diverse research endeavours surrounding Maritime Autonomous Surface Ships (MASS), it is believed that investigating emergencies such as propulsion loss is crucial because propulsion loss events present a direct risk to the safety of ship navigation. The findings of this study on emergency situations can drive the progress and innovation of autonomous navigation technologies for ships. It is crucial to explore solutions that enable ships to navigate safely and efficiently, especially during emergencies, by developing new technologies and systems.

This study has provided a valuable foundation for analysing ship performance under propulsion failure conditions, particularly during turning manoeuvres in rough seas. Additionally, to better prepare for the era of autonomous navigation ships, further investigation into the path-following performance of vessels operating under propulsion failure conditions could enhance the study's overall value.

CRediT authorship contribution statement

Daejeong Kim: Writing – review & editing, Writing – original draft, Validation, Software, Resources, Methodology, Investigation, Formal analysis, Data curation, Conceptualization. **Soonseok Song:** Writing – review & editing, Validation, Methodology, Investigation, Formal analysis, Data curation, Conceptualization. **Tahsin Tezdogan:** Writing – review & editing, Investigation, Conceptualization.

Declaration of competing interest

The authors declare that they have no known competing financial interests or personal relationships that could have appeared to influence the work reported in this paper.

Acknowledgements

References

Broglia, R., Dubbioso, G., Durante, D., Di Mascio, A., 2015. Turning ability analysis of a fully appended twin screw vessel by CFD. Part I: single rudder configuration. Ocean Eng. 105, 275–286.

EMSA, 2023. Annual Overview of Marine Casualties and Incidents 2023.

Hasnan, M.A.A., Yasukawa, H., Hirata, N., Terada, D., Matsuda, A., 2020. Study of ship turning in irregular waves. J. Mar. Sci. Technol. 25, 1024–1043.

ITTC, 2021. The Manoeuvring Committee Final Report and Recommendations to the 29th ITTC.

ITTC, 2011. ITTC - Recommended Procedures and Guidelines : Practical Guidelines for Ship CFD Applications.

Kim, D., Song, S., Jeong, B., Tezdogan, T., 2021a. Numerical evaluation of a ship's manoeuvrability and course keeping control under various wave conditions using CFD. Ocean Eng. 237, 109615.

Kim, D., Song, S., Jeong, B., Tezdogan, T., Incecik, A., 2021b. Unsteady RANS CFD simulations of ship manoeuvrability and course keeping control under various wave height conditions. Appl. Ocean Res. 117, 102940.

Kim, D., Song, S., Sant, T., Demirel, Y.K., Tezdogan, T., 2022a. Nonlinear URANS model for evaluating course keeping and turning capabilities of a vessel with propulsion system failure in waves. Int. J. Nav. Archit. Ocean Eng. 14, 100425.

Kim, D., Song, S., Tezdogan, T., 2021c. Free running CFD simulations to investigate ship manoeuvrability in waves. Ocean Eng. 236 https://doi.org/10.1016/j.oceaneng.2021.109567.

Kim, D., Song, S., Turnock, S., Tezdogan, T., 2023a. Nonlinear URANS model for path-following control problem towards autonomous marine navigation under wave conditions. Ocean Eng. 270, 113681.

Kim, D., Tezdogan, T., 2022. CFD-based hydrodynamic analyses of ship course keeping control and turning performance in irregular waves. Ocean Eng. 248, 110808.

Kim, D., Yim, J., Song, S., Demirel, Y.K., Tezdogan, T., 2022b. A systematic investigation on the manoeuvring performance of a ship performing low-speed manoeuvres in adverse weather conditions using CFD. Ocean Eng. 263, 112364.

Kim, D., Yim, J., Song, S., Park, J.-B., Kim, J., Yu, Y., Elsherbiny, K., Tezdogan, T., 2023b. Path-following control problem for maritime autonomous surface ships (MASS) in adverse weather conditions at low speeds. Ocean Eng. 287, 115860.

Kim, I.-T., Kim, C., Kim, S.-H., Ko, D., Moon, S.-H., Park, H., Kwon, J., Jin, B., 2021. Estimation of the manoeuvrability of the KVLCC2 in calm water using free running simulation based on CFD. Int. J. Nav. Archit. Ocean Eng. 13, 466–477.

Menter, F.R., 1994. Two-equation eddy-viscosity turbulence models for engineering applications. AIAA J. 32, 1598–1605.

Mike Baker, P.E., 2024. Baltimore investigation turns to ship's deadly mechanical failure. The New York Times. URL. https://www.nytimes.com/2024/03/30/us/baltimore-bridge-ship-mechanical.html.

SIMMAN, 2020. Workshop on Verification and Validation of Ship Manoeuvring Simulation Methods.

Wang, J., Zhao, W., Wan, D.C., 2016. Free maneuvering simulation of ONR Tumblehome using overset grid method in naoe-FOAM-SJTU solver. In: Proceedings of 31th Symposium on Naval Hydrodynamics.

ARTICLES FOR FACULTY MEMBERS

NAVIGATIONAL RISK OF CONTAINER FALLS IN THE STRAIT OF MALACCA

Title/Author	Assessment of human error contribution to container loss risk under fault tree analysis and interval type-2 fuzzy logic-based SLIM approach / Erdem, P., Akyuz, E., Aydin, M., Celik, E., & Arslan, O.
Source	*Proceedings of the Institution of Mechanical Engineers Part M: Journal of Engineering for the Maritime Environment* **Volume 238 Issue 3 (2024) Pages 553–566** **https://doi.org/10.1177/14750902231203074** **(Database: SagePub)**

Original Article

Assessment of human error contribution to container loss risk under fault tree analysis and interval type-2 fuzzy logic-based SLIM approach

Pelin Erdem[1] **, Emre Akyuz**[2] **, Muhammet Aydin**[3]**, Erkan Celik**[4] **and Ozcan Arslan**[2]

Abstract

Human is a key element of the safety of life on board ships and a significant contributing factor to most of the accidents and incidents in the maritime industry. At this point, risk analysis plays a critical role in ensuring operational safety and maritime transportation sustainability. This paper aims to systematically evaluate how human errors (HEs) contribute to operational risks. Based on this, Fault Tree Analysis (FTA) is combined under an Interval Type-2 Fuzzy Logic environment with Success Likelihood Index Method (SLIM). Whilst the FTA evaluates the criticality of the operational activities, the Interval Type-2 Fuzzy Sets (IT2FS) deals with vagueness and subjectivity in using experts' judgements, and the SLIM estimates the probabilities for the human error-related basic events. Since container losses can lead to severe damage and catastrophic events in a container terminal, loading operation was investigated as a case study. Safety culture, experience, and fatigue were observed as highly effective factors in crew performance. The obtained results also indicate that this hybrid approach can effectively be applied to determine the operational vulnerabilities in high-risk industries. The paper intends to improve safety control levels and lower losses in the future of maritime container transport besides emphasising the potential consequences of failures and crucial human errors in the operational process.

Introduction

More than 100 million containers are shipped across the globe on containerships per year. According to containerised trade data, the number reached approximately 160.5 million containers in 2019.[1] Based on this, container transportation has become even more important for global maritime trade. However, significant container shipping disasters where hundreds of containers were lost in a single event have occurred in recent years.[2] The disastrous fires and explosions on Maersk Honam,[3,4] MSC Flaminia,[5,6] Hyundai Fortune[6,7] and Hanjin Pennsylvania,[6,8,9] hull fracture on MSC Napoli[5,10,11] and hull girder fracture on Mol Comfort,[5,12] and the breaking of Rena in two,[13,14] collapsed and fallen overboard containers on MSC Zoe[15,16] have caused the worst maritime environmental disasters in the last decade. Besides

the loss of containers severely damaging the marine environment, tragically, some crew members have died because of the accidents.

[1]Department of Naval Architecture, Ocean and Marine Engineering, University of Strathclyde, Glasgow, UK
[2]Department of Maritime Transportation and Management Engineering, Istanbul Technical University, Tuzla, Istanbul, Turkiye
[3]Faculty of Maritime, Recep Tayyip Erdogan University, Rize, Turkiye
[4]Department of Transportation and Logistics, Istanbul University, Avcılar, Istanbul, Turkiye

Corresponding author:
Pelin Erdem, Department of Naval Architecture, Ocean and Marine Engineering, University of Strathclyde, Henry Dyer Building, 100 Montrose Street, Glasgow G40LZ, UK.
Email: pelinulku@hotmail.com

Each operational activity carried out onboard ships includes risks due to the nature of the work. Therefore, identifying the risk factors and minimising them to an acceptable level is paramount to enhancing the safety level.[17] Human error, technical, mechanical, structural failure, and environmental factors are common causes of marine accident risk.[18] As the regulatory body, International Maritime Organization (IMO) emphasises that the human factor plays a crucial role in accidents.[19] The statistics show that more than 80% of shipping casualties are directly related to human error.[20–22] Thereby, human error contribution should be the core point of the quantitative risk analysis (QRA) in maritime operations. A variety of approaches that focus on human error probability (HEP) quantifications have also been implemented in different industries such as offshore,[23–27] aviation,[28] railway,[29–32] nuclear power plants[33–35] and mining.[36]

The maritime industry seeks to reduce losses in the future. However, risk assessments carried out apart from the crew safety performance shall be insufficient in analysing the potential threats. At this point, some impact factors related to the task, individuals or working environment should also be considered while evaluating the HEPs. These relative factors,[37] called performance shaping factors (PSFs), are of paramount influence on human performance negatively or positively.[32]

The SLIM technique considering HEP assessments has been used to determine the human error contribution to operational risks[22,37–40] in the maritime transportation industry. In this study, a quantitative risk analysis is performed by considering the possible human errors in the container loading operation process. In this context, this paper proposed a hybrid approach by incorporating Fault Tree Analysis (FTA) and Interval type-2 fuzzy-based SLIM to evaluate the human contribution to risks and the criticality of the loading operation activities in a container terminal. To achieve this goal, the paper is structured as follows: The first part presents the motivation behind the study and basic literature review on significant container shipping disasters. Because of the substantial role of each method in the study, a brief literature review and the theoretical background of the methods are provided in section 2. Section 3 offers the integration of the proposed approach, while Section 4 illustrates the exemplificative application of the proposed approach to risk of container loss in maritime transportation. Findings and extended discussion are presented in section 5. Finally, the conclusion and research contribution to maritime transport is included in the last section.

Methods

The hybrid approach is proposed to determine the contribution of human error to the risks related with the most critical vulnerabilities in the operational processes.

In this context, the SLIM estimates the HEPs whilst the FTA perform a comprehensive risk assessment. Since there is an ambiguity with the crisp value of probability, the IT2FS deals with vagueness and subjectivity in using experts' judgements.[39,41,42]

IT2FS

The concept of a type-2 fuzzy set was first introduced by Zadeh[43] as an extension of the idea of a conventional fuzzy set called a type-1 fuzzy set (T1FS).[41,44] A fuzzy set states the degree to which an element belongs to a set. In case it is not possible to determine the membership of an element in a set as 0 or 1, the type 1 or type 2 fuzzy sets are utilised. The membership grade for each element of the type-2 fuzzy set (T2FS) is a fuzzy set in [0,1]. On the other hand, a type-1 is a fuzzy set where a membership grade is a crisp number in [0,1].[45,46] The basic principle behind systems is the same for both Type-1 and Type-2. However, T2FS can better express a higher degree of fuzziness and provides more various parameters than T1FS.[45,47]

An interval type-2 fuzzy set (IT2FS) is a special case of the generalised T2FS[41] in which the membership grade of every domain point is a crisp set whose domain is some interval contained in [0,1].[44] Mendel[48] proposed the interval type-2 fuzzy set to describe an imprecise linguistic term, linguistically and quantitatively.[49] The data collected from the experts' linguistic expressions are subjective and have limitations. At this point, the IT2FS can cope with complex conditions and reflects uncertainties better.[44,50,51] IT2FS is rather adequate for utilising in real-case applications compared to generalised T2FS[52] and is commonly used in decision-making problems.[53,54] The IT2FS is applied almost all problems by reason of their reduced computational effort and feasibility.[39,44] Following a description of the T2FS and the IT2FS, the below equations present the mathematical operations' definitions and step-by-step developments, respectively.

Definition 1: A type-2 fuzzy set $\tilde{\tilde{A}}$ in the universe of discourse X can be characterised by a type-2 membership function $\mu_{\tilde{\tilde{A}}}(x,u)$, where J_X denotes an interval in [0, 1] is illustrated as follows[46]:

$$\tilde{\tilde{A}} = \left\{ ((x,u), \mu_{\tilde{\tilde{A}}}(x,u)) | \forall x \in X, \forall u \in J_X \subseteq [0,1], 0 \leqslant \mu_{\tilde{\tilde{A}}}(x,u) \leqslant 1 \right\}$$

In addition, the type-2 fuzzy set $\tilde{\tilde{A}}$ can also be represented as follows when the elements of the fuzzy numbers are continuous[46]:

$$\tilde{\tilde{A}} = \int_{x \in X} \int_{u \in J_X} \mu_{\tilde{\tilde{A}}}(x,u)/(x,u) = \int_{x \in X} \left(\int_{u \in J_X} \mu_{\tilde{\tilde{A}}}(x,u)/u \right) /x$$

Where $J_X \subseteq [0,1]$ and $\iint$ denotes union over all admissible x and u.

Definition 2: Let $\tilde{\tilde{A}}$ be a type-2 fuzzy set in the universe of discourse X represented by the type-2 membership function $\mu_{\tilde{\tilde{A}}}(x,u)$. If all $\mu_{\tilde{\tilde{A}}}(x,u) = 1$, then $\tilde{\tilde{A}}$ is called an interval type-2 fuzzy set and represented as follows[45,46]:

$$\tilde{\tilde{A}} = \int_{x \in X} \int_{u \in J_X} 1/(x,u) = \int_{x \in X} \left(\int_{u \in J_X} 1/u \right) / x,$$

where $J_X \subseteq [0,1]$.

Definition 3: A method utilising the IT2FSs for tackling fuzzy multiple attribute group decision-making problems are presented in this study. In this model, the heights of the upper and the lower membership functions of the IT2FSs and the reference points are characterised as a trapezoidal IT2FS as shown in Figure 1.[46]

A trapezoidal interval type-2 fuzzy set:

$$\tilde{\tilde{A}}_i = \left(\tilde{A}_i^U, \tilde{A}_i^L \right) = \left(\left(a_{i1}^U, a_{i2}^U, a_{i3}^U, a_{i4}^U; H_1(\tilde{A}_i^U), H_2(\tilde{A}_i^U) \right), \left(a_{i1}^L, a_{i2}^L, a_{i3}^L, a_{i4}^L; H_1(\tilde{A}_i^L), H_2(\tilde{A}_i^L) \right) \right)$$

where $\tilde{A}_i^U$ and $\tilde{A}_i^L$ are type-1 fuzzy sets, $a_{i1}^U, a_{i2}^U, a_{i3}^U, a_{i4}^U, a_{i1}^L, a_{i2}^L, a_{i3}^L$ and a_{i4}^L are the reference points of the interval type-2 fuzzy $\tilde{\tilde{A}}_i$; $H_j(\tilde{A}_i^U)$ represents the membership value of the element $a_{i(j+1)}^U$ in the upper trapezoidal membership function, $\tilde{A}_i^U$; $1 \leqslant j \leqslant 2$, $H_j(\tilde{A}_i^L)$ represents the membership value of the element $a_{i(j+1)}^L$ in the lower trapezoidal membership function

$$\tilde{A}_i^L 1 \leqslant j \leqslant 2 H_j(\tilde{A}_i^L),$$

$$H_1(\tilde{A}_i^U) \in [0,1], \ H_2(\tilde{A}_i^U) \in [0,1], H_1(\tilde{A}_i^L) \in [0,1], \ H_2(\tilde{A}_i^L) \in [0,1] \text{ and } 1 \leqslant i \leqslant n.$$

Definition 4: To rank and defuzzify the IT2FSs an extended centre-of-area method is utilised. Accordingly, the equation (1) is implemented in defuzzification process of the IT2FSs.

$$Defuzzified\left(\tilde{\tilde{A}}_i \right) = \frac{\frac{\left(a_{i4}^U - a_{i1}^U \right) + \left(H_1(\tilde{A}_i^U) * a_{i2}^U - a_{i1}^U \right) + \left(H_2(\tilde{A}_i^U) * a_{i3}^U - a_{i1}^U \right)}{4} + a_{i1}^U +}{\frac{\left(a_{i4}^L - a_{i1}^L \right) + \left(H_1(\tilde{A}_i^L) * a_{i2}^L - a_{i1}^L \right) + \left(H_2(\tilde{A}_i^L) * a_{i3}^L - a_{i1}^L \right)}{4} + a_{i1}^L}{2} \tag{1}$$

Mathematical operations using between two IT2FSs for further calculations are also as given below[39,42,55]:
  For the addition operation:

$$\tilde{\tilde{A}}_1 = \left(\tilde{A}_1^U, \tilde{A}_1^L \right) = \left(\left(a_{11}^U, a_{12}^U, a_{13}^U, a_{14}^U; H_1(\tilde{A}_1^U), H_2(\tilde{A}_1^U) \right), \left(a_{11}^L, a_{12}^L, a_{13}^L, a_{14}^L; H_1(\tilde{A}_1^L), H_2(\tilde{A}_1^L) \right) \right)$$

$$\tilde{\tilde{A}}_2 = \left(\tilde{A}_2^U, \tilde{A}_2^L \right) = \left(\left(a_{21}^U, a_{22}^U, a_{23}^U, a_{24}^U; H_1(\tilde{A}_2^U), H_2(\tilde{A}_2^U) \right), \left(a_{21}^L, a_{22}^L, a_{23}^L, a_{24}^L; H_1(\tilde{A}_2^L), H_2(\tilde{A}_2^L) \right) \right)$$

$$\tilde{A}_1 \oplus \tilde{A}_2 = \left(\tilde{A}_1^U, \tilde{A}_1^L \right) \oplus \left(\tilde{A}_2^U, \tilde{A}_2^L \right)$$

$$= \left(\begin{array}{l} \left(a_{11}^U + a_{21}^U, a_{12}^U + a_{22}^U, a_{13}^U + a_{23}^U, a_{14}^U + a_{24}^U; min(H_1(\tilde{A}_1^U), H_1(\tilde{A}_2^U)), min(H_2(\tilde{A}_1^U), H_2(\tilde{A}_2^U)) \right), \\ \left(a_{11}^L + a_{21}^L, a_{12}^L + a_{22}^L, a_{13}^L + a_{23}^L, a_{14}^L + a_{24}^L; min(H_1(\tilde{A}_1^L), H_1(\tilde{A}_2^L)), min(H_2(\tilde{A}_1^L), H_2(\tilde{A}_2^L)) \right) \end{array} \right) \tag{2}$$

For the subtraction operation:
$$\tilde{A}_1 \Theta \tilde{A}_2 = \left(\tilde{A}_1^U, \tilde{A}_1^L \right) \Theta \left(\tilde{A}_2^U, \tilde{A}_2^L \right)$$

$$= \begin{pmatrix} \left(a_{11}^{U} - a_{21}^{U}, a_{12}^{U} - a_{22}^{U}, a_{13}^{U} - a_{23}^{U}, a_{14}^{U} - a_{24}^{U}; min\left(H_1\left(\tilde{A}_1^{U}\right), H_1\left(\tilde{A}_2^{U}\right)\right), min\left(H_2\left(\tilde{A}_1^{U}\right), H_2\left(\tilde{A}_2^{U}\right)\right)\right), \\ \left(a_{11}^{L} - a_{21}^{L}, a_{12}^{L} - a_{22}^{L}, a_{13}^{L} - a_{23}^{L}, a_{14}^{L} - a_{24}^{L}; min\left(H_1\left(\tilde{A}_1^{L}\right), H_1\left(\tilde{A}_2^{L}\right)\right), min\left(H_2\left(\tilde{A}_1^{L}\right), H_2\left(\tilde{A}_2^{L}\right)\right)\right) \end{pmatrix} \tag{3}$$

For the multiplication operation:

$$\tilde{A}_1 \otimes \tilde{A}_2 = \left(\tilde{A}_1^{U}, \tilde{A}_1^{L}\right) \otimes \left(\tilde{A}_2^{U}, \tilde{A}_2^{L}\right)$$

$$= \begin{pmatrix} \left(a_{11}^{U} \times a_{21}^{U}, a_{12}^{U} \times a_{22}^{U}, a_{13}^{U} \times a_{23}^{U}, a_{14}^{U} \times a_{24}^{U}; min\left(H_1\left(\tilde{A}_1^{U}\right), H_1\left(\tilde{A}_2^{U}\right)\right), min\left(H_2\left(\tilde{A}_1^{U}\right), H_2\left(\tilde{A}_2^{U}\right)\right)\right), \\ \left(a_{11}^{L} \times a_{21}^{L}, a_{12}^{L} \times a_{22}^{L}, a_{13}^{L} \times a_{23}^{L}, a_{14}^{L} \times a_{24}^{L}; min\left(H_1\left(\tilde{A}_1^{L}\right), H_1\left(\tilde{A}_2^{L}\right)\right), min\left(H_2\left(\tilde{A}_1^{L}\right), H_2\left(\tilde{A}_2^{L}\right)\right)\right) \end{pmatrix} \tag{4}$$

For the arithmetic operations:

$$k\tilde{\tilde{A}}_1 = \begin{pmatrix} \left(k \times a_{11}^{U}, k \times a_{12}^{U}, k \times a_{13}^{U}, k \times a_{14}^{U}; H_1\left(\tilde{A}_1^{U}\right), H_2\left(\tilde{A}_1^{U}\right)\right), \\ \left(k \times a_{11}^{L}, k \times a_{12}^{L}, k \times a_{13}^{L}, k \times a_{14}^{L}; H_1\left(\tilde{A}_1^{L}\right), H_2\left(\tilde{A}_1^{L}\right)\right) \end{pmatrix} \tag{5}$$

$$\frac{\tilde{\tilde{A}}_1}{k} = \begin{pmatrix} \left(\frac{1}{k} \times a_{11}^{U}, \frac{1}{k} \times a_{12}^{U}, \frac{1}{k} \times a_{13}^{U}, \frac{1}{k} \times a_{14}^{U}; H_1\left(\tilde{A}_1^{U}\right), H_2\left(\tilde{A}_1^{U}\right)\right), \\ \left(\frac{1}{k} \times a_{11}^{L}, \frac{1}{k} \times a_{12}^{L}, \frac{1}{k} \times a_{13}^{L}, \frac{1}{k} \times a_{14}^{L}; H_1\left(\tilde{A}_1^{L}\right), H_2\left(\tilde{A}_1^{L}\right)\right) \end{pmatrix} \tag{6}$$

SLIM

The SLIM[56] was first introduced to estimate the probability of success of specific human actions in nuclear power plants.[57] The fundamental rationale of the SLIM is that the success likelihood of a task is based on the combined effects of a set of performance shaping factors (PSFs) which has a considerable influence on human performance.[58] The SLIM is a simple and flexible approach[24,37,59] that makes use of domain expert judgement to select and weigh the PSFs according to their perceived contribution in a given task for estimating HEPs.[60] Accordingly, the core and crucial step is the formation of a committee of experts to generate the relevant data reliably. Following the quantification of PSFs, a Success Likelihood Index (SLI) is obtained utilising experts' judgements for each action of the specific task.[22,61] Subsequently, the SLI value is calibrated with the human error data to predict the HEP value. The main steps of the method are expressed as follows: (i) PSF derivation, (ii) PSF rating, (iii) PSF weighting, (iv) SLI determination and (v) HEP calculation

The below equation is utilised in the SLI determination process.

$$SLI = \sum_{i=1}^{n} r_i w_i, \qquad 0 \leqslant SLI \leqslant 1 \tag{7}$$

In the equation above, n denotes the PSFs' number, r_i denotes the rating scale of PSFs, and w_i denotes the weight of the PSFs' relative importance.

Accordingly, the conversion of the SLIs to HEP values is achieved by a logarithmic relationship represented in equation (8).

$$Log\ (HEP) = aSLI + b$$

$$\tag{8}$$

In equation (8), a and b are the constants elicited from the HEP values for the sub-tasks with the highest and lowest SLIs.[56]

FTA

Fault Tree Analysis (FTA) is one of the most crucial logic and probabilistic techniques extensively utilised for reliability evaluation and probabilistic risk assessment of complex systems.[62–64] The technique generates a mechanism for efficient system-level risk assessments. As a top-down and deductive failure analysis,[59] the technique identifies the sub-systems essential for the operation of a complex system.[65]

Visualising a conventional fault tree comprises three major graphic symbols: events, logical gates and transfer symbols.[66–68] Several sequential fault combinations that cause the undesired event called the 'top event' (TE) are
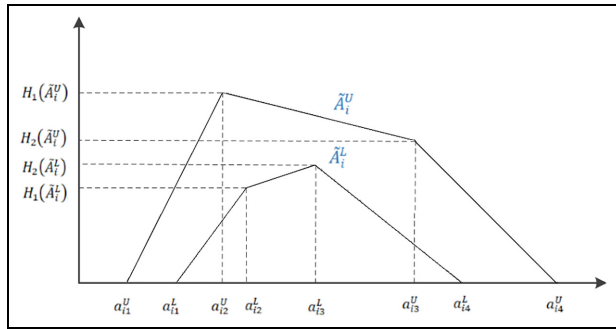
Figure 1. The trapezoidal membership function of IT2FS.

depicted at different system levels. The TE is of enormous significance for the complex system due to cause catastrophic consequences for humans, commodity, and the environment.[69] Therefore, a fault tree is directly focused on the top event of the tree. In line with this purpose, the fault tree represents the logical interrelationships of basic events (BEs), which trigger the main event when they co-occur, and employs Boolean algebra rules. These rules are utilised to acquire one form of the fault tree, called the minimal cut set (MCS), that allows qualitative and quantitative assessments to be performed simply. The MCS specifies the system's structural vulnerability.[69] The logical gates utilised to represent the relationships of events express the relationship type of the input events needed for the output event. The quantification of probabilities occurs according to the MCSs describing the relationships between BEs using 'AND' and 'OR' gates. Accordingly, the equation (9) is utilised to obtain the occurrence probability of the top event associated with the 'AND' gate, where P expresses the occurrence probability of the top event, n expresses the number of the BEs and pi expresses the occurrence probability of basic event i.

$$P = \prod_{i=1}^{n} pi \tag{9}$$

Associated with the 'OR' gate event, the equation (10) is utilised to acquire the top event's occurrence probability:

$$P = 1 - \prod_{i=1}^{n} (1 - pi) \tag{10}$$

The MCSs and overall failure probability of the top event are needed to calculate once the occurrence probabilities of BEs and IEs are gathered. The following equations are used for MCSs.[70,71]

$$TE = MCS_1 + MCS_2 + \ldots + MCS_N = \bigcup_{i=1}^{n_c} MCS \tag{11}$$

The below equations are utilised to calculate the occurrence probability of TE.[71,72]

$$P(T) = P(MCS_1 \cup MCS_2 \cup \ldots \cup MCS_N)$$

$$= P(MCS_1) + P(MCS_2) + \ldots P(MCS_N)$$
$$- (P(MCS_1 \cap MCS_2)$$

$$+ P(MCS_1 \cap MCS_3) + \ldots P(MCS_i \cap MCS_j)\ldots)\ldots$$

$$+ (-1)^{N-1} P(MCS_1 \cap MCS_2 \cap \ldots \cap MCS_N) \tag{12}$$

In the FTA technique, the FV-I (Fussell Vesely Importance Measure) method is utilised to ascertain the importance value of BEs and MCs constructing the TE.[3,73] The following equation is used for the FV-I.

$$I_i^{VF}(t) = \frac{Q_i(t)}{Q_s(t)} \tag{13}$$

where I_i is the importance degree of MCS, $Q_i(t)$ occurrence probability value of MC_i and $Q_S(t)$ states occurrence probability of TE in all MCS.[74]

Integration of methodologies

The integration of methodologies for comprehensive risk analysis is provided in this section. The FTA is combined with the IT2FS-SLIM approach. In this context, Figure 2 illustrates the conceptual framework of the integrated method.

Construction of a FT diagram

The first step of the hybrid approach is to construct a fault tree addressing the events' interaction resulting in container loss. In the process, the FT is developed with references from containership accidents (which occurred last two decades) databases and investigation reports, as well as previous literature, and with the assistance of a group of marine experts. The experts familiar with containership cargo operations on board are involved as consultants due to the lack of failure probability data in the maritime industry.[69] Failures related to crew performance, environmental factors, technical and mechanical failures, and equipment functions are considered altogether for an effective FTA.

Data derivation under the IT2FS-SLIM approach

This section presents the data derivation process to evaluate human error contribution to the operational risks. The evaluation of HEPs in the maritime industry is regarded as onerous due to the scarcity of numerical data.[69,75] The IT2FS-based SLIM approach can generate HEPs, particularly in cases where a lack of numerical data exists. In the SLIM, the marine experts provide professional judgement to bridge the gap. Under the hybrid approach, the probabilities for
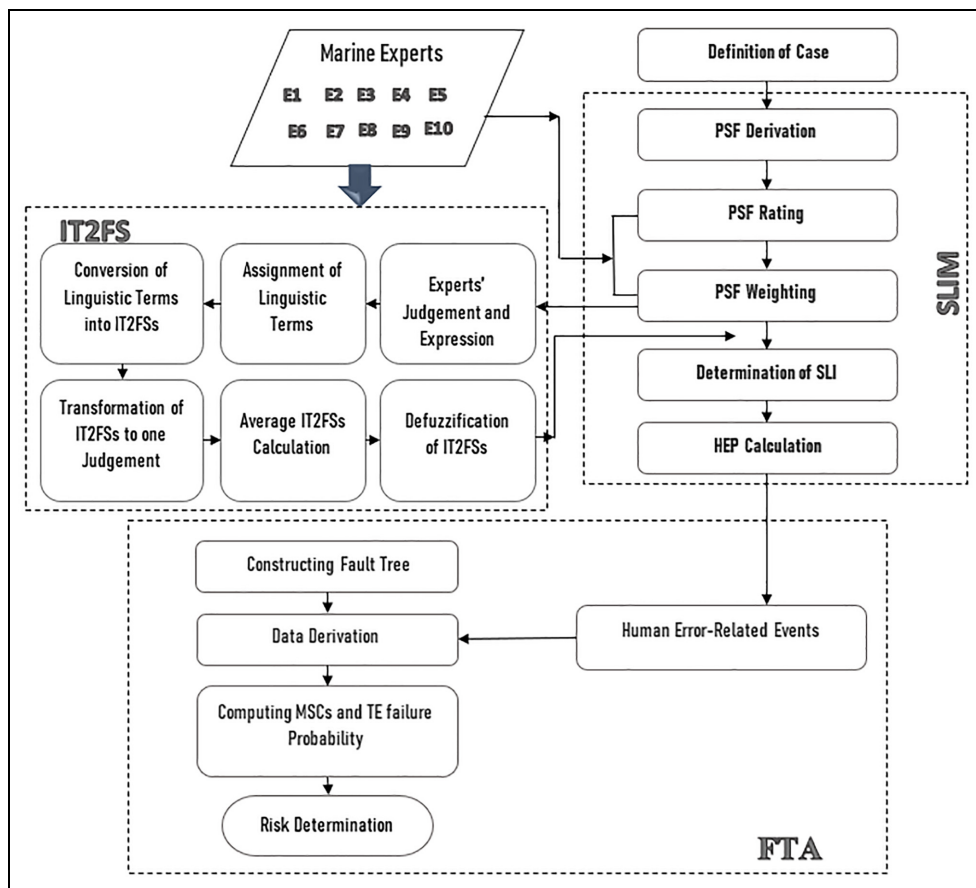
Figure 2. The conceptual framework of the integration.

each human error-related basic event are acquired. Accordingly, the main steps of the process and their brief explanations are as follows.

Step 1. PSF derivation: The PSFs which could trigger human errors such as experience, time availability, fatigue, collaboration quality stress, etc. have a considerable effect on ship crew performance and they are acquired by a group of marine experts.

Step 2. PSF rating: Each PSF is rated by the experts after the derivation process. At this step, a value from 1 to 9 on a linear scale is nominated in order of importance on the related basic event. If a factor has a remarkable impact on the crew performance for the relevant event, value '1' is assigned by marine experts.

Step 3. PSF weighting: Each PSF to trigger human error has a relative contribution compared to others. Accordingly, a relative weight will be assigned for each PSF from one expert to the other.[56] In the conventional SLIM, experts subjectively weigh the PSFs. The weighting process is carried out utilising the interval type-2 fuzzy linguistic scale developed by Chen and Lee[42] to enhance the accuracy and reduce the subjectivity of these judgements.

Step 4. SLI Determination: Following the rating and weighting process of PSFs, the SLI value is calculated using the equation (7). The SLI is a crucial tool for predicting the probability of events in which several human errors may occur.

Step 5. HEP derivation: Once the SLI is calculated, it is then possible to obtain the HEP values of each BE in the FT. The conversion of the SLI values to HEP is accomplished by the logarithmic relationship given in equation (8) and is the fundamental aspect of the SLIM technique.

Computing TE and MCSs failure probabilities

The IT2F-based SLIM approach to performing HEP assessments provides probabilistic outcomes for risk assessment in maritime transportation. The HEPs obtained by utilising the IT2F-SLIM steps are incorporated into the FT of container loss. Based on these outcomes, the failure probability of all BEs is calculated. Thereby, the overall likelihood of the top event (TE) and MCSs are computed for detailed risk analysis.

Model application: The case of container loss risk

This paper evaluates the container loss probability in containership cargo operations based on an FTA

structure under IT2F-SLIM approach is developed to conduct a comprehensive risk analysis.

Problem statement

Several factors ranging from rough seas and heavy weather conditions to more catastrophic events such as collision, explosion, grounding, and hull damage can result in containers being lost at sea.[76] Apart from mentioned events, the likelihood of having other major hazard events such as listing, capsizing, structural fracture, and stack collapse leading to container loss is also significant during the cargo operations at the port period. In this study, containership loading operation is selected to illustrate the applicability of the proposed hybrid approach since it has potential risks for the safety of a container ship, its crew and cargo, shore-based workers, port facilities and the marine environment.

In accordance with non-mandatory and mandatory regulations issued by authorities, to avoid unwanted events, significant items must be checked by the watch-keeping team regularly. Ship stability values (GM, bending moment, torsion moment, drafts, trim and shearing force), stowage plan, visibility line, specific containers such as IMDG, reefers and, OH/OOG, lashing gear, lashings of containers and hatch covers demands great attention[77] throughout the containership cargo operation. In this context, crew performance plays a considerable part in risk analysis in identifying what errors lead to or contribute to the top event. However, whilst determining the human error contributions in the shipboard operations the human error should be treated as a combined outcome of some factors onboard the ship. Besides, failure can sometimes be beyond the crew's control, although rare. Shipper-related issues (i.e. mis declared cargo and incorrectly/poor container packing), port-related issues (issues with hoisting cranes and port storage, poorly stacking containers and poor arrangement of weight distribution) and environmental conditions are also relevant factors in losing containers.

Analysis of respondents

Accident data sets, investigation reports, and empirical studies are the ideal, and key sources for human error prediction.[58] However, the data on maritime transportation is scarce or incomplete due to commercial reasons.[69] To meet this challenge, the SLIM utilises qualified experts' judgements in the decision-making process to predict human errors. In this study, the appraisal of human error contribution to ship operations is evaluated with the participation of 10 qualified experts with substantial seagoing and working experience in containership transportation. Two out of these marine experts also have working experience as operation manager in container terminals. The following criteria were determined to form an expert group in this research; (i) minimum oceangoing Master licence, (ii) minimum 10 years of experience onboard container ship and (iii) physically participated in cargo handling operation on board container ship. At this point, Table 1 contains the profile details of marine experts. The marine experts make professional judgements expressing the PSFs impacts on each human error-related basic event utilising the linguistic statements of defined type-2 fuzzy sets.

Data derivation under the IT2FS-SLIM approach

This section summarises how the HEP data is derived to perform quantitative risk analysis. Since the loss of container operational risk is a concern, Table 2 illustrates the fundamental container handling tasks throughout the operation at a container terminal.

In the study, seven PSFs used are captured from the recent study associated with containership handling operations.[38] Since it has paramount importance to derive appropriate PSFs rather than all PSFs, experience, stress, fatigue, training, time limitation, complexity and safety culture were specified by the Elicitation Review Team (ERT) as effective PSFs on crew performance during the loading operation. A brief description of each PSF included in the HEP assessment is given below, respectively.

- Stress: Negative effect upon seafarer performance to complete the task correctly due to increased anxiety and pressure.
- Experience: Familiarity with the task and knowledge.

Table 1. Marine experts' profile details.

Marine expert ID	Age	Company	Position	Experience (as year)
1	43	Company A	Opr. Manager	14
2	48	Company B	Oceangoing Master	15
3	43	Company C	Oceangoing Master	10
4	41	Company B	Oceangoing Master	18
5	44	Company B	Oceangoing Master	13
6	64	Company C	Oceangoing Master	25
7	43	Company C	Oceangoing Master	22
8	36	Company D	CFS Opr. Manager	10
9	35	Company C	Oceangoing Master	11
10	40	Company C	Oceangoing Master	16

Table 2. Task analysis for container handling operation.

Task	Description of task
1	Equally distributing of weight inside the container
2	Stacking of goods inside the container against to move
3	Properly packing of goods inside container against to degradation/chemical reaction
4	Accurately declaring the type/material of good
5	Accurately declaring the container's weight
6	Tightening/re-tightening loose lashing gear (lashing bars, turnbuckles)
7	Locking the cleats on all sides of all hatch covers
8	Locking all twist locks as appropriate against to move
9	Adhering to the recommended lashing forces
10	Maintaining of the deck fittings (fixed socket, lashing plate, cell guide) against the forces imposed by containers
11	Keeping all lashing equipment (twist lock, cone, bar) qualified and ready for use
12	Selecting the lashing gear compatible with fixed deck fitting
13	Well operating of gantry/mobile crane
14	Container handling by a trained crane operator
15	Port adequateness and opportunities for loading (lights, breakwater, capability, etc.)
16	Being aware of the wind forces throughout operation
17	Preparing of the stowage plan in accordance with the requirements of codes
18	Maintaining proper communication as to the operational process
19	Maintaining proper communication between ship crew and responsible shore personnel
20	Container handling by spreader consisting of a steel frame and four hooks
21	Frequently checking of the stacked containers against leakage
22	Loading of the special-type container in accordance with the requirements
23	Checking of coupled lashing equipment sufficiency against being missing
24	Timely changing in ballast as to the ship's condition
25	Properly activating/deactivating of heeling/ballast system
26	Frequently checking the visibility line and/or steering light sight
27	Adhering to the permissible stack weight
28	Adhering to partial loading quantity
29	Adhering to max GM and stress values
30	Adhering to permissible sequences of masses in stacks

- Training: Expansion of knowledge, performance, and capability of seafarers by activities or actions organised by ship management.
- Fatigue: Extreme tiredness caused by mental/physical workload or illness.
- Time Limitation: Amount of time required for the seafarer to complete the relevant task.
- Complexity: The measure of task difficulty identifies interrelated and interdependent task components.
- Safety Culture: Both individual or group perceptions, attitudes and values that reflect ship management's commitment to safety.

The further step is to determine the PSF rating for each task. The PSFs are rated by marine experts due to the lack of failure data in the shipping industry. The marine experts nominated a rate for each determined task according to the 1–9 linear scale, which reflects their relative judgements. The geometric means of ratings of 10 experts participating in the survey were obtained to simplify the calculation. Accordingly, Table 3 illustrates PSF rates for each task.

After having determined PSFs, the weighting process is performed. The IT2Fs are used for the weighting process of PSFs since it is capable of handling inaccurate information in a logically correct manner. In this context, Table 4 demonstrates the IT2FSs number, and their membership functions related to the linguistic terms for determining the PSFs' importance weight.[42] The next step is to calculate the defuzzified values of PSFs weights. In this context, linguistic variables are converted to the IT2FSs to quantitatively transform the judgements of marine experts. Once the average IT2Fs values are calculated, the defuzzification is conducted using equation (1). Table 5 shows IT2FS, crisp and normalised values of PSFs.[38]

The HEP values are calculated using equations (7) and (8) where a and b are the constants. Given the above equations, Table 6 illustrates the SLI values and derived HEP results.

Quantitative risk assessment for container loss

This section performs quantitative risk analysis for container loss by systematically predicting human error contributions to the operational risks. To achieve this purpose, the FT is constructed by reviewing accident investigation reports, literature, and marine experts' judgement. In the constructed FTA, 30 basic events that will be effective in the realisation of the top event have been determined. At this point, the environmental conditions have been ignored since no environmental obstacle hinders the present real-time containership cargo operation, and the human error contribution was the focal point. Table 7 illustrates the TE, BE and IE for container loss risk in this context.

Three main events cause the top event identified as container loss in the fault tree. These are the failures associated with cargo (IE01), failures associated with lashing (IE02) and failures associated with cargo handling (IE03). Having just one of these three main intermediate events is sufficient to cause container damage. Therefore, IE01, IE02, and IE03 are linked to the TE with the 'OR' gate. Accordingly, Figure 3 depicts the FT diagram for container loss during cargo handling operations in maritime transportation.

From the FT diagram and logic gates, TE (container loss) occurrence probability was calculated by applying equations (9) and (10), respectively. Based on the results, the occurrence probability of TE is found to be 5.54E-01. Accordingly, the MCSs, their occurrence probabilities, and the V–FIM list of MCSs are depicted in Table 8 (equations (11)–(13)).

Table 3. Geometric means of PSF ratings based on the marine experts' evaluations.

Task	Performance shaping factor						
	Stress	Experience	Training	Fatigue	Time Lim.	Complexity	Safety culture
1.	7	3	4	4	2	4	3
2.	7	2	4	4	2	5	3
3.	7	2	3	5	2	4	3
4.	6	2	4	5	4	5	3
5.	5	3	3	6	4	5	2
6.	5	2	3	3	2	3	3
7.	4	3	3	2	3	4	2
8.	4	3	4	3	2	4	2
9.	7	2	3	5	3	4	3
10.	7	2	4	3	3	6	3
11.	5	4	4	3	3	4	3
12.	7	3	4	5	4	4	5
13.	6	3	3	4	2	3	3
14.	5	2	3	3	3	5	4
15.	6	3	4	5	4	4	4
16.	6	2	3	5	4	5	3
17.	5	2	2	3	3	3	3
18.	6	3	3	3	2	5	3
19.	7	3	4	4	2	5	4
20.	4	3	3	3	3	3	2
21.	4	2	3	3	3	4	2
22.	6	3	3	4	4	3	3
23.	3	3	4	3	2	4	2
24.	5	2	3	4	3	4	4
25.	5	2	3	5	3	3	3
26.	4	3	3	3	3	3	2
27.	7	2	3	5	4	4	3
28.	7	2	3	5	3	3	3
29.	6	2	3	5	3	3	3
30.	6	3	4	4	3	3	3

Table 4. Lingusitic terms and their corresponding IT2FSs.

Linguistic assessment	Term	Interval type 2 fuzzy sets
Very low	VL	((0.0;0.0;0.0;0.1;1.0;1.0), (0.0;0.0;0.0;0.05;0.9;0.9))
Low	L	((0.0;0.1;0.1;0.3;1.0;1.0), (0.05;0.1;0.1;0.2;0.9;0.9))
Medium low	ML	((0.1;0.3;0.3;0.5;1.0;1.0), (0.2;0.3;0.3;0.4;0.9;0.9))
Medium	M	((0.3;0.5;0.5;0.7;1.0;1.0), (0.4;0.5;0.5;0.6;0.9;0.9))
Medium high	MH	((0.5;0.7;0.7;0.9;1.0;1.0), (0.6;0.7;0.7;0.8;0.9;0.9))
High	H	((0.7;0.9;0.9;1.0;1.0;1.0), (0.8;0.9;0.9;0.95;0.9;0.9))
Very high	VH	((0.9;1.0;1.0;1.0;1.0;1.0), (0.95;1.0;1.0;1.0;0.9;0.9))

Table 5. Calculated average IT2F values.

PSF	IT2FSs	Crisp value	Normalised value
Stress	((0.36;0.55;0.55;0.73;1;1), (0.46;0.55;0.55;0.64;0.9;0.9))	0.604	0.107
Experience	((0.76;0.92;0.92;0.99;1;1), (0.84;0.92;0.92;0.96;0.9;0.9))	0.929	0.165
Training	((0.42;0.62;0.62;0.8;1;1), (0.52;0.62;0.62;0.71;0.9;0.9))	0.673	0.119
Fatigue	((0.76;0.92;0.92;0.99;1;1), (0.84;0.92;0.92;0.96;0.9;0.9))	0.929	0.165
Time Lim.	((0.72;0.88;0.88;0.96;1;1), (0.8;0.88;0.88;0.92;0.9;0.9))	0.893	0.158
Complexity	((0.38;0.58;0.58;0.77;1;1), (0.48;0.58;0.58;0.68;0.9;0.9))	0.637	0.114
Safety culture	((0.82;0.96;0.96;1;1;1), (0.89;0.96;0.96;0.98;0.9;0.9))	0.957	0.171

Findings and extended discussion

In light of the comprehensive risk assessment for container loss during the loading operation, the top event occurrence probability was calculated as 5.54E-01 which is a rather high. The obtained results show that 55 out of 100 cases may result in container loss due to

Table 6. Calculated HEP values for cargo handling operation.

Task	Calculated SLI	Log-HEP	HEP
1.	3.73	−3.35	4,48E-04
2.	3.75	−3.41	3,86E-04
3.	3.51	−2.73	1,85E-03
4.	3.99	−4.06	8,61E-05
5.	3.89	−3.78	1,65E-04
6.	2.84	−0.86	1,38E-01
7.	2.86	−0.92	1,20E-01
8.	2.95	−1.17	6,72E-02
9.	3.49	−2.68	2,09E-03
10.	3.78	−3.47	3,38E-04
11.	3.76	−3.43	3,70E-04
12.	4.34	−5.04	9,12E-06
13.	3.44	−2.53	2,92E-03
14.	3.40	−2.41	3,87E-03
15.	4.24	−4.77	1,71E-05
16.	3.75	−3.40	3,97E-04
17.	2.88	−0.96	1,09E-01
18.	3.40	−2.41	3,91E-03
19.	3.84	−3.64	2,27E-04
20.	3.04	−1.40	3,95E-02
21.	2.87	−0.94	1,14E-01
22.	3.46	−2.59	2,58E-03
23.	2.87	−0.95	1,13E-01
24.	3.40	−2.42	3,83E-03
25.	3.41	−2.45	3,52E-03
26.	3.04	−1.43	3,76E-02
27.	3.74	−3.37	4,22E-04
28.	3.58	−2.92	1,21E-03
29.	3.50	−2.71	1,94E-03
30.	3.58	−2.92	1,19E-03

Table 7. Fault tree events for the loss of containers.

Event	Description
TE	Container loss
IE1	Failures associated with cargo
IE2	Failures associated with lashing
IE3	Failures associated with cargo handling
IE4	Packing failure
IE5	Misinformation
IE6	Lashing plan (comply with CSM) violation
IE7	Deck-fitting and lashing equipment failure
IE8	Terminal-induced handling failures
IE9	Stowage plan failure
IE10	Communication failure
IE11	Improper handling
IE12	Improper ballast operation
IE13	Stowage plan application failure
BE1	Incorrect weight distribution
BE2	Mobility due to poor stack
BE3	Inaccurate packing
BE4	Misdeclaration/under declaration of the actual type/materials of cargo
BE5	Misdeclaration/under declaration of the actual weight of the container
BE6	Loose lashing gear (lashing bars and turnbuckles)
BE7	Unlocked hatch cleats
BE8	Unlocked twist locks
BE9	Exceeding the recommended lashing forces
BE10	Deck fittings failure
BE11	Broken/bent equipment (twist locks, turnbuckles, bars, etc.)
BE12	Improper equipment for fixed deck fittings
BE13	Gantry/Mobile crane failure
BE14	Operator handling failure
BE15	Port restrictions
BE16	Lack of awareness for wind effect
BE17	Inadequate planning
BE18	Miscommunication as to the operation's actual process
BE19	Lack of communication between crew and stevedore/foreman
BE20	Hook Spreader Usage
BE21	Leakage container loading
BE22	Incorrect special-type container loading
BE23	Missing equipment
BE24	Ballast change failure
BE25	Heeling/ballast system failure
BE26	Exceeding the max. number of containers in each stack
BE27	Exceeding permissible stack weight
BE28	Extreme partial loading
BE29	Exceeding the max GM and stress values
BE30	Neglecting permissible sequences of masses in stacks

the paramount contribution of human error during the loading operation. Since the fault tree structure is a graphic model representing the logical interrelationships of basic events, the possibility of each BE that includes human errors resulting in container loss was calculated to achieve TE occurrence probability. At this point, BE6 (1.38E-01), BE7 (1.20E-01) and BE21 (1.14E-01) with the highest HEP values were found to be the most contributory basic events increasing the risk of TE, respectively.

Further, the occurrence probabilities of the MCSs, the smallest combination of the BEs, were also calculated to identify the structural vulnerability of the system. Based on the results, BE4 (Misdeclaration/under declaration of the actual type/materials of Cargo) and BE5 (Misdeclaration/under declaration of the actual weight of the container) were the basic events that derive the most MCSs (four MCSs for each) among the others.

Lashing gear is a crucial item that needs to be checked by the watchkeeping team properly. Unlocked hatch cover cleats and loose lashings can cause a container stack to move and force on the adjacent stacks while the vessel is underway. Even worse, the forces on the adjacent stacks shall gradually increase and put the lashing equipment under additional load when the vessel rolls. Accordingly, any failure on lashing gear results in container loss due to stack collapse. However, the

increasing effect of factors such as fatigue and limited time, makes the crew more vulnerable to errors, unavoidably.

One of the most significant goals of safe container handling is to minimise the occurrence probability of leaks, spills, or damage. Leakage is a crucial problem in the storage and transport of containers because it may corrode other stacked containers or produce toxic or inflammable fumes if they especially contain dangerous goods. Further, one of the essential parts of the
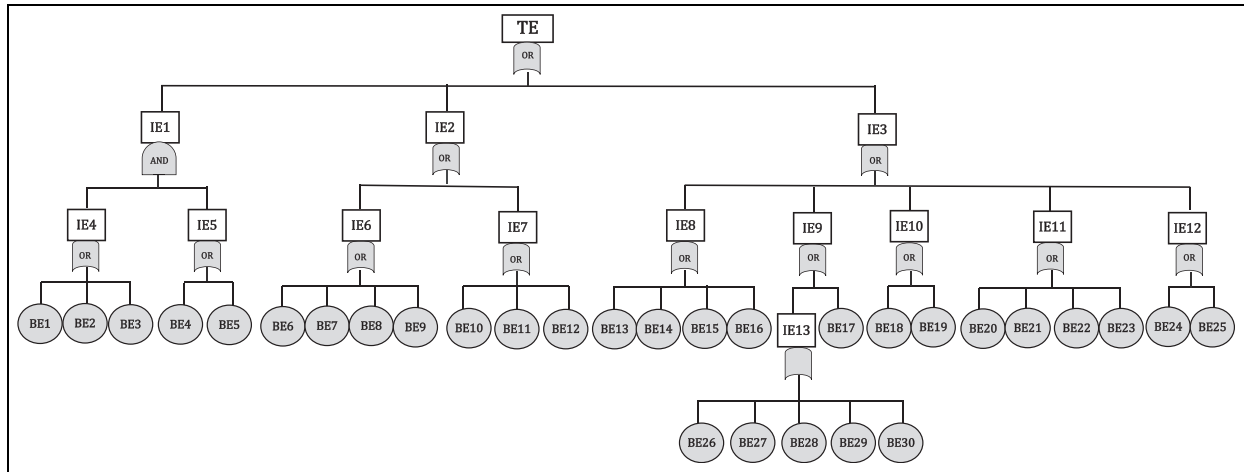
Figure 3. Structure of fault tree for the loss of container at port.

Table 8. Ranking of basic events according to Fussel-Vessely importance.

Basic events	Failure probability of BEs	Number of MCS	MCS elements	FV-I	Ranking
BE1	4,48E-04	3	BE1, BE1BE4, BE1BE5	4.48E-04	20
BE2	3,86E-04	3	BE2, BE2BE4, BE2BE5	3.86E-04	23
BE3	1,85E-03	3	BE3, BE3BE4, BE3BE5	1.85E-03	17
BE4	8,61E-05	4	BE4, BE1BE4, BE2BE4, BE3BE4	8.65E-05	28
BE5	1,65E-04	4	BE5, BE1BE5, BE2BE5, BE3BE5	1.65E-04	27
BE6	1,38E-01	1	BE6	1.38E-01	1
BE7	1,20E-01	1	BE7	1.20E-01	2
BE8	6,72E-02	1	BE8	6.72E-02	6
BE9	2,09E-03	1	BE9	2.09E-03	15
BE10	3,38E-04	1	BE10	3.38E-04	25
BE11	3,70E-04	1	BE11	3.70E-04	24
BE12	9,12E-06	1	BE12	9.12E-06	30
BE13	2,92E-03	1	BE13	2.92E-03	13
BE14	3,87E-03	1	BE14	3.87E-03	10
BE15	1,71E-05	1	BE15	1.71E-05	29
BE16	3,97E-04	1	BE16	3.97E-04	22
BE17	1,09E-01	1	BE17	1.09E-01	5
BE18	3,91E-03	1	BE18	3.91E-03	9
BE19	2,27E-04	1	BE19	2.27E-04	26
BE20	3,95E-02	1	BE20	3.95E-02	7
BE21	1,14E-01	1	BE21	1.14E-01	3
BE22	2,58E-03	1	BE22	2.58E-03	14
BE23	1,13E-01	1	BE23	1.13E-01	4
BE24	3,83E-03	1	BE24	3.83E-03	11
BE25	3,52E-03	1	BE25	3.52E-03	12
BE26	3,76E-02	1	BE26	3.76E-02	8
BE27	4,22E-04	1	BE27	4.22E-04	21
BE28	1,21E-03	1	BE28	1.21E-03	18
BE29	1,94E-03	1	BE29	1.94E-03	16
BE30	1,19E-03	1	BE30	1.19E-03	19

planning is the confirmation that the permissible sequences of masses in stacks are not exceeded. Nevertheless, the weight of the leakage container becomes lighter as time goes by, resulting in container loss due to stack collapse. The primary cause of leakage is rough and inattentive container handling that causes structural damage during cargo operation, in general. Hence, each stowed container should be kept under strict control against any leakage throughout the handling process. At this point, safety culture, fatigue and training were determined as influential factors on human performance in the event of failure.

As for the misdeclared/undeclared cargo, the consequences can be catastrophic in some cases, an example being the disaster that resulted in the loss of the containership 'Sea Elegance' in 2003.[9] The report of the preliminary enquiry revealed that the fire and then explosion onboard originated in a container containing

Calcium Hypochlorite that had not been declared.[78] Tragically, the disaster resulted in the death of one crew member and extensive cargo and vessel damage.

The disastrous explosion occurred in a cargo hold of the containership Hanjin Pennsylvania in 2002[6,8,9] is another unfortunate example of the significance of the subject. The containers filled with fireworks have been mis declared on the manifest. Thereby, the containers listed as having non-hazardous content were incorrectly stacked at the bottom of the hold and did not segregate as appropriate. The ship stayed afloat, but the disaster resulted in the death of two crew members and a substantial loss of cargo.

The consequences of underdeclared weights of containers led to a profound contribution to the catastrophic hull failure of MSC Napoli in 2007.[5,10,11] Essentially, the vessel encountered rough seas that caused her to pitch heavily when on the passage in the English Channel. Following that, a catastrophic failure was suffered from her hull in the way of her engine room and then broke in two. The report by the MAIB (2008) stated a number of factors that contributed to the hull structure failure including the underdeclared weight of containers. All MSC Napoli's containers were weighed again for investigation when beached in the UK, and the total weight of the 137 containers was 312 tonnes heavier than on the manifest. The load on the hull had increased by whipping effect and her hull already did not have sufficient buckling strength in way of the engine room. Although the detected non-compliance level was not evaluated as high, the report by the MAIB[79] identified it as concerning in the occurrence of this catastrophic event.

Conclusion

As a result of container losses from container ships, the maritime industry has taken the issue of safe stowage and securing of containers rather seriously because of the growing global concern over marine disasters. Since the tragic events caused the worst environmental disasters last two decades, the issue of container losses at ships is closely associated with environmental and economic aspects of the maritime transportation industry. At this point, identifying the causes of container losses can provide actionable solutions to reduce losses in future.

Despite the technological improvements, maritime operations remain dangerous for port facilities, vessels, the environment, and human life. Based on this, analysing the operational risk factors, and minimising the threats to an acceptable level is vital to enhance safety. Even though technical and mechanical failures are common causes increasing the risks, human error is found to be the most frequent and significant cause of marine accidents according to the conclusions drawn by the investigation reports.

This paper proposes a hybrid approach incorporating FTA and IT2FS-based SLIM to highlight the overriding importance of human-oriented failures in containership operations. In light of the extended risk analysis on real-time containership loading operation, the occurrence probability of the container loss was found to be 5.54E-01 which is considerably high. In the study, the importance of various factors was also identified as triggering human errors that should be addressed including ineffective safety culture, inadequate experience, fatigue, and limited time. Further, that the proposed approach can effectively be applied to identifying the operational vulnerabilities and critical human errors is concluded.

The fundamental limitation of the research is the scarcity of data. In the framework of the HEP assessment process that should contain both relevant data and real case studies, it is rather difficult to obtain empirical data in the maritime industry. Nevertheless, real data should be captured to validate the acquired results. A set of numerical simulations may also be carried out via risk analysis software in potential future research. This study is expected to provide qualitative and quantitative data on container transportation safety and insight into what measures may be necessary to decrease future losses by quantifying the potential failures in loading operations.

ORCID iDs

Pelin Erdem https://orcid.org/0000-0003-0141-2499
Emre Akyuz https://orcid.org/0000-0002-0071-9619

References

1. UNCTAD. *Review of maritime transport 2019, UNCTAD/RMT/2019/Corr.1*. New York: United Nations Publications, 2020.
2. Alfi A, Shokrzadeh A and Asadi M. Reliability analysis of H-infinity control for a container ship in way-point tracking. *Appl Ocean Res* 2015; 52: 309–316.
3. Wang L, Wang J, Shi M, et al. Critical risk factors in ship fire accidents. *Marit Pol Manage* 2021; 48: 1895–1913.

4. Fan L, Zheng L and Luo M. Effectiveness of port state control inspection using Bayesian network modelling. *Marit Pol Manage* 2022; 49: 1261–18278.

5. Wróbel K, Montewka J and Kujala P. Towards the assessment of potential impact of unmanned vessels on maritime transportation safety. *Reliab Eng Syst Saf* 2017; 165: 155–169.

6. Baalisampang T, Abbassi R, Garaniya V, et al. Review and analysis of fire and explosion accidents in maritime transportation. *Ocean Eng* 2018; 158: 350–366.

7. Ellis J. Analysis of accidents and incidents occurring during transport of packaged dangerous goods by sea. *Saf Sci* 2011; 49(8–9): 1231–1237.

8. Ren D. *Application of HFACS tool for analysis of investigation reports of accidents involving containerized dangerous goods*. Malmö: World Maritime University Dissertations, 377, 2009. http://commons.wmu.se/all_dissertations/377

9. Ellis J. Undeclared dangerous goods — risk implications for maritime transport. *WMU J Marit Affairs* 2010; 9(1): 5–27.

10. Parunov J, Andric J, Corak M, et al. Structural reliability assessment of container ship at the time of accident. *Proc IMechE, Part M: J Engineering for the Maritime Environment* 2015; 229(2): 111–123.

11. Guitart C, Frickers P, Horrillo-Caraballo J, et al. Characterization of sea surface chemical contamination after shipping accidents. *Environ Sci Technol* 2008; 42(7): 2275–2282.

12. Storhaug G. The measured contribution of whipping and springing on the fatigue and extreme loading of container vessels. *Int J Nav Archit Ocean Eng* 2014; 6(4): 1096–1110.

13. Faaui TN, Morgan TKKB and Hikuroa DCH. Ensuring objectivity by applying the Mauri model to assess the post-disaster affected environments of the 2011 MV Rena disaster in the Bay of Plenty, New Zealand. *Ecol Indic* 2017; 79: 228–246.

14. Schiel DR, Ross PM and Battershill CN. Environmental effects of the MVRenashipwreck: cross-disciplinary investigations of oil and debris impacts on a coastal ecosystem. *N Z J Mar Freshwater Res* 2016; 50(1): 1–9.

15. Jo GW. The need for international policy regarding lost containers at sea for reducing marine plastic litter. *J Int Marit Saf Environ Aff Shipp* 2020; 4(3): 80–83.

16. Hwang DJ. The IMO action plan to address marine plastic litter from ships and its follow-up timeline. *J Int Marit Saf Environ Aff Shipp* 2020; 4: 32–39.

17. Goerlandt F, Montewka J, Kuzmin V, et al. A risk-informed ship collision alert system: framework and application. *Saf Sci* 2015; 77: 182–204.

18. Karahalios H. *The management of maritime regulations*. New York, NY: Routledge, 2015.

19. IMO. Human Element Vısıon, Prıncıples and Goals for the Organızatıon, Resolution A. 947(23) Adopted on 27 November 2003 (Agenda item 17).

20. Pazouki K, Forbes N, Norman RA, et al. Investigation on the impact of human-automation interaction in maritime operations. *Ocean Eng* 2018; 153: 297–304.

21. Wiegmann DA and Shappell SA. *A human error approach to aviation accident analysis: the human factors analysis and classification system*. London: Routledge, 2017.

22. Akyuz E. Quantitative human error assessment during abandon ship procedures in maritime transportation. *Ocean Eng* 2016; 120: 21–29.

23. Rozuhan H, Muhammad M and Niazi UM. Probabilistic risk assessment of offshore installation hydrocarbon releases leading to fire and explosion, incorporating system and human reliability analysis. *Appl Ocean Res* 2020; 101: 102282.

24. Islam R and Yu H (eds). Human factors in marine and offshore systems. In: Khan F and Abbassi R (eds) *Offshore process safety*. Cambridge: Elsevier Inc, 2018, pp. 145–167, 1st ed. Vol. 2.

25. Deacon T, Amyotte PR, Khan FI, et al. A framework for human error analysis of offshore evacuations. *Saf Sci* 2013; 51(1): 319–327.

26. Deacon T, Amyotte PR and Khan FI. Human error risk analysis in offshore emergencies. *Saf Sci* 2010; 48(6): 803–818.

27. DiMattia DG, Khan FI and Amyotte PR. Determination of human error probabilities for offshore platform musters. *J Loss Prev Process Ind* 2005; 18(4-6): 488–501.

28. Kunlun S, Yan L and Ming X. A safety approach to predict human error in critical flight tasks. *Procedia Eng* 2011; 17: 52–62.

29. Zhou JL, Lei Y and Chen Y. A hybrid HEART method to estimate human error probabilities in locomotive driving process. *Reliab Eng Syst Saf* 2019; 188: 80–89.

30. Wang W, Liu X and Qin Y. A modified HEART method with FANP for human error assessment in high-speed railway dispatching tasks. *Int J Ind Ergon* 2018; 67: 242–258.

31. Gibson WH, Mills AM and Smith S. Railway action reliability assessment, a railway specific approach to human error quantification. In: Dadashi N, Scott A, Wilson JR, et al. (eds) *Rail human factors. Supporting reliability, safety and cost reduction*. London, Abingdon: Taylor & Francis, 2012, pp.671–676.

32. Grozdanovic M. Usage of human reliability quantification methods. *Int J Occup Saf Ergon* 2005; 11(2): 153–159.

33. Lee SJ, Kim J and Jung W. Quantitative estimation of the human error probability during soft control operations. *Ann Nucl Energy* 2013; 57: 318–326.

34. Kirwan B, Gibson H, Kennedy R, et al. Nuclear Action Reliability Assessment (NARA): a data-based HRA tool. *Probab saf assess manag* 2005; 25: 38–45.

35. Kirwan B. The validation of three human reliability quantification techniques–THERP, HEART and JHEDI: Part III – practical aspects of the usage of the techniques. *Appl Ergon* 1997; 28(1): 27–39.

36. Wang L, Wang Y, Cao Q, et al. A framework for human error risk analysis of coal mine emergency evacuation in China. *J Loss Prev Process Ind* 2014; 30(1): 113–123.

37. Islam R, Abbassi R, Garaniya V, et al. Determination of human error probabilities for the maintenance operations of marine engines. *J Ship Prod Des* 2016; 32(04): 226–234.

38. Erdem P and Akyuz E. An interval type-2 fuzzy SLIM approach to predict human error in maritime transportation. *Ocean Eng* 2021; 232: 109161.

39. Akyuz E and Celik E. The role of human factor in maritime environment risk assessment: a practical application on Ballast Water Treatment (BWT) system in ship. *Hum Ecol Risk Assess* 2018; 24: 653–666.

40. Xi YT and Guo C. A method for marine human error probability estimate: APJE-SLIM. *Appl Mech Mater* 2011; 97-98: 825–830.

41. Akyuz E and Celik E. A modified human reliability analysis for cargo operation in single point mooring (SPM) offshore units. *Appl Ocean Res* 2016; 58: 11–20.

42. Lee LW and Chen SM. Fuzzy multiple attributes group decision-making based on the extension of TOPSIS method and interval type-2 fuzzy sets. In: *2008 International conference on machine learning and cybernetics*, 2008, pp.3260–3265, vol. 6. New York, NY: IEEE.

43. Zadeh LA. The concept of a linguistic variable and its application to approximate reasoning–1. *Inf Sci* 1995; 8: 199–249.

44. Mendel JM. Advances in type-2 fuzzy sets and systems. *Inf Sci* 2007; 177: 84–110.

45. Castillo O and Melin P. *Type-2 fuzzy log.: theory and application.* Springer Berlin: STUDFUZZ, 2008. Vol. 223, pp.145–154.

46. Mendel JM, John RI and Liu F. Interval type-2 fuzzy logic systems made simple. *IEEE Trans Fuzzy Syst* 2006; 14(6): 808–821.

47. N. Karnik N and M. Mendel J. Operations on type-2 fuzzy sets. *Fuzzy Sets Syst* 2001; 122(2): 327–348.

48. Mendel JM. *Uncertain rule-based fuzzy logic systems: introduction and new directions.* Upper Saddle River, NJ: Prentice-Hall, 2001.

49. Solo AMG. Interval type-two fuzzy logic for quantitatively defining imprecise linguistic terms in politics and public policy. In: Information Resources Management Association (ed.) *Research methods: concepts, methodologies, tools, and applications.* IGI Global, 2015, pp.643–651.

50. Demirel H, Akyuz E, Celik E, et al. An interval type-2 fuzzy QUALIFLEX approach to measure performance effectiveness of ballast water treatment (BWT) system on-board ship. *Ships Offshore Struct* 2019; 14(7): 675–683.

51. Celik E, Gul M, Aydin N, et al. A comprehensive review of multi criteria decision making approaches based on interval type-2 fuzzy sets. *Knowl Based Syst* 2015; 85: 329–341.

52. Kahraman C, Öztayşi B, Uçal Sarİ, et al. Fuzzy analytic hierarchy process with interval type-2 fuzzy sets. *Knowl Based Syst* 2014; 59: 48–57.

53. Celik E, Bilisik ON, Erdogan M, et al. An integrated novel interval type-2 fuzzy MCDM method to improve customer satisfaction in public transportation for Istanbul. *Transp Res E Logist Transp Rev* 2013; 58: 28–51.

54. Chen TY, Chang CH and Rachel Lu JF. The extended QUALIFLEX method for multiple criteria decision analysis based on interval type-2 fuzzy sets and applications to medical decision making. *Eur J Oper Res* 2013; 226(3): 615–625.

55. Celik E and Akyuz E. An interval type-2 fuzzy AHP and TOPSIS methods for decision-making problems in maritime transportation engineering: the case of ship loader. *Ocean Eng* 2018; 155: 371–381.

56. Embrey DE, Humphreys PC, Rosa EA, et al. SLIM-MAUD: an approach to assessing human error probabilities using structured expert judgement. NUREG/CR-3518. *US Nuclear Regulatory Commission, Washington, DC, 1984.*

57. Calixto E, Lima GBA and Firmino PRA. Comparing SLIM, SPAR-H and Bayesian network methodologies. *Open J Saf Sci Technol* 2013; 03(02): 31–41.

58. Park KS and Lee JI. A new method for estimating human error probabilities: AHP–SLIM. *Reliab Eng Syst Saf* 2008; 93(4): 578–587.

59. Kirwan B. *A guide to practical human reliability assessment.* London: Taylor & Francis, 1994.

60. Spurgin AJ. *Human reliability assessment theory and practice.* Boca Raton, FL: CRC Press, 2010.

61. Islam R, Yu H, Abbassi R, et al. Development of a monograph for human error likelihood assessment in marine operations. *Saf Sci* 2017; 91: 33–39.

62. Zhang M, Zhang D, Goerlandt F, et al. Use of HFACS and fault tree model for collision risk factors analysis of icebreaker assistance in ice-covered waters. *Saf Sci* 2019; 111: 128–143.

63. Kornecki A and Liu M. Fault tree analysis for safety/security verification in aviation software. *Electronics* 2013; 2(4): 41–56.

64. Mentes A and Helvacioglu IH. An application of fuzzy fault tree analysis for spread mooring systems. *Ocean Engineering* 2011; 38: 285–294.

65. Kristiansen S. *Maritime transportation safety management and risk analysis.* Oxford: Elsevier Butterworth Heinemann, 2005.

66. Kristiansen S. *Maritime transportation: safety management and risk analysis.* New York, NY: Routledge, 2013.

67. Ericson C. *Fault tree analysis – a history Clifton A.* Seattle, WA: Ericson II The Boeing Company, 1999. pp.1–9.

68. Pan H and Yun W. Fault tree analysis with fuzzy gates. *Comput Ind Eng* 1997; 33(3-4): 569–572.

69. Akyuz E, Arslan O and Turan O. Application of fuzzy logic to fault tree and event tree analysis of the risk for cargo liquefaction on board ship. *Appl Ocean Res* 2020; 101: 102238.

70. Arici SS, Akyuz E and Arslan O. Application of fuzzy bow-tie risk analysis to maritime transportation: the case of ship collision during the STS operation. *Ocean Eng* 2020; 217: 107960.

71. Kuzu AC, Akyuz E and Arslan O. Application of fuzzy fault tree analysis (FFTA) to maritime industry: A risk analysing of ship mooring operation. *Ocean Eng* 2019; 179: 128–134.

72. Lavasani SM, Ramzali N, Sabzalipour F, et al. Utilisation of fuzzy fault tree analysis (FFTA) for quantified risk analysis of leakage in abandoned oil and natural-gas wells. *Ocean Eng* 2015; 108: 729–737.

73. Shafiee M, Enjema E and Kolios A. An integrated FTA-FMEA model for risk analysis of engineering systems: a case study of subsea blowout preventers. *Appl Sci* 2019; 9(6): 1192.

74. Aydin M, Camliyurt G, Akyuz E, et al. Analyzing human error contributions to maritime environmental risk in oil/chemical tanker ship. *Hum Ecol Risk Assess* 2021; 27: 1838–1859.

75. Ung ST. Evaluation of human error contribution to oil tanker collision using fault tree analysis and modified fuzzy Bayesian network based CREAM. *Ocean Eng* 2019; 179: 159–172.

76. Aydin M, Akyuz E, Turan O, et al. Validation of risk analysis for ship collision in narrow waters by using fuzzy Bayesian networks approach. *Ocean Eng* 2021; 231: 108973.

77. Larsen R and Pacino D. A heuristic and a benchmark for the stowage planning problem. *Marit Econ Logist* 2021; 23: 94–122.

78. South African Maritime Safety Authority. Report of the preliminary enquiry in- to the explosion and fire onboard the mv "Sea Elegance" on11 October 2003 at the Durban Anchorage. Annex to IMO DSC 10/INF. 2. Durban: South African Maritime Safety Authority; 2004.

79. Marine Accident Investigation Branch. *Annual report.* Southampton: Marine Accident Investigation Branch, 2008. http://www.maib.gov.uk/publications/annual_reports.cfm

ARTICLES FOR FACULTY MEMBERS

NAVIGATIONAL RISK OF CONTAINER FALLS IN THE STRAIT OF MALACCA

Title/Author	Crude oil transportation route choices: A connectivity reliability-based approach / Wang, S., Jia, H., Lu, J., & Yang, D.
Source	*Reliability Engineering and System Safety* **Volume 235 (2023) 109254 Pages 1-11** **https://doi.org/10.1016/j.ress.2023.109254** **(Database: ScienceDirect)**

Crude oil transportation route choices: A connectivity reliability-based approach

Shuang Wang [a], Haiying Jia [b], Jing Lu [a], Dong Yang [c],[*]

[a] College of Transportation Engineering, Dalian Maritime University, Dalian, China
[b] Department of Business and Management Science, Norwegian School of Economics, Norway
[c] Department of Logistics and Maritime Studies, Hong Kong Polytechnic University, Hong Kong

ARTICLE INFO

ABSTRACT

The crucial nodes of maritime transportation routes, such as the Strait of Malacca and the Suez Canal, remain vulnerable to various risk events including political instability and military conflict, piracy and terrorism, and vessel incidents. Existing shipping route choice studies often consider transportation costs and environmental effects, but ignore the connectivity reliability of these straits and canals. In this paper, we develop a bi-objective programming model to determine maritime transportation routes for crude oil, taking both transportation costs and connectivity reliability into consideration. We propose a method to measure the connectivity reliability of straits and canals, which captures the dependence structure of risk events. We apply our model to evaluate Gwadar Port using data covering 1999 to 2021, which is being built to enhance the reliability of Chinese oil imports. We find that the Gwadar Port can substitute for the Lombok Strait only if its connectivity reliability can be improved by 2.4%. In order to fully exploit the strategic advantages of Gwadar Port in substituting for other key straits, its connectivity reliability must be improved by 12.2%. Given the varying dependence of risk events identified in our model, our findings provide rich managerial and policy implications for connectivity reliability improvement.

1. Introduction

Crude oil is an important strategic resource for all countries, but it is unevenly distributed around the world. Maritime transportation is the primary transportation mode of oil distribution, conveying about 90% of the world's total crude oil trade [1]. Recently, the Russia-Ukraine war has actually induced roaring oil prices, e.g., European Brent crude oil prices climbed to $122.71 per barrel in June 2022, which increase 65.44% from December 2021 [2]. And the safety of maritime transportation of crude oil and supply security again attracts a lot of attention, which plays an essential role in economic activity and national security.

While access to crude oil provides the foundation of modern industrial economies, the traditional maritime transportation routes of this vital resource are exposed to a number of risks. The straits and canals so vital to maritime transportation are particularly vulnerable to risk events like piracy and maritime terrorism, vessel incidents, political instability and military conflict [3,4]. A vessel grounding incident caused the blockade of the Suez Canal in 2021, while the Russia-Ukraine

war threatens the safety and reliability of tankers sailing through the Strait of Bosporus. If certain straits or canals are disconnected because of risk events, this directly affects the security of the crude oil supply. When selecting routes for crude oil transportation, it is thus imperative to consider the connectivity reliability of key nodes on top of the transportation cost. Such an approach to route choice better ensures the transportation reliability of the commodity widely regarded as the lifeblood of the global economy.

In previous studies, transportation costs and environmental effects have been widely considered in the construction of route choice models for crude oil transportation [5–9]. Connectivity reliability, meanwhile, remains as yet under-explored. Connectivity reliability broadly refers to the probability that straits and canals will remain connected to the transportation network when subjected to risk events. Notably, the risk events are interrelated by nature [4,10]. The Russia-Ukraine war induces political instability in that region, and threatens the crude oil transportation safety and reliability; in the meanwhile, because of the sanctions against Russia, some old tankers have been purchased by "unknown" buyers to transport crude oil exported by the sanctioned

---

countries, this is also likely to increase the probability of vessel incidents and reduce connectivity reliability [11]. Piracy is also related to the political instability of a region; and heavy weather will restrict pirates from using their small, high-speed boats to attack ships. From this set of factors, researchers have concluded that most piracy will occur in an environment with milder wind and wave conditions [12,13]. The dependence structure between these risk events is one of the most overlooked problems in an investigation of reliability, and an ignorance of the dependent relationships can produce faulty estimations.

The main contributions of this paper are threefold. First, it is a preliminary attempt to consider not just transportation costs, but also the connectivity reliability of straits and canals when choosing routes for crude oil shipping. Second, while many studies of connectivity reliability have been conducted on road networks [14,15], very few have been produced in the field of maritime research. Even among these numerous studies of road networks, the dependence structure between risk events has gone largely ignored. This paper pioneers a more accurate metric for evaluating the connectivity reliability of straits and canals by addressing precisely this interdependence among risk events. Moreover, based on the analysis of these risk dependences, we can estimate the impact of a change in one risk event's likelihood on the likelihood of other risk events, as well as on overall connectivity reliability. From this, we can propose several measures to improve connectivity reliability. Third, we apply our method to a case study of China's crude oil imports. Navigation through Gwadar Port promises to provide an alternative maritime route for China's crude oil imports and thereby to improve energy import reliability. It remains unknown, however, what effects the opening of this new port will have on route choice for Chinese crude oil shipping, and to what extent it will reduce China's dependence on traditional maritime transportation routes. Our proposed method enables us to model the complex consequences of different scenarios.

The rest of this paper is organized as follows: The relevant literature is reviewed in Section 2. Section 3 describes the problem and presents the mathematical formulation of the model, while Section 4 illustrates the efficiency of our model through a case study. The results are analyzed and discussed, followed by the conclusions and implications laid out in Section 5.

2. Literature review

The first stream of literature relevant to our study concerns the maritime transportation of crude oil. Most of the intercontinental crude oil trade is conveyed by ship, and transportation costs are the major consideration in any proposed adjustments to shipping routes [8,9,16]. In addition to the shipping costs, the global trend towards reductions in shipping emissions has led to greater consideration of environmental effects produced by crude oil transportation [17–19].

In the consideration of transportation costs for crude oil, mixed-integer programming models have long been established as the primary method for route selection and voyage scheduling [20,21]. These models are used to determine the best transportation route options, usually with the objective of minimizing total transportation costs [22–24]. Environmental effects are generally considered along with the costs of selecting different routes, and the carbon emissions of crude oil transportation along various possible routes are estimated [25]. In order to model these two factors and identify the best possible routes for oil transportation, either the multi-objective approach [5] or the multi-criteria decision making technique [26,27] is usually proposed. The results of these studies show that environmental emissions do have an impact on route choice [5,27]. Regardless of the different methodological approaches employed by these studies, transportation reliability yet remains largely neglected. The vulnerability of the straits and canals so vital to maritime transportation to disruption demands appropriate attention to connectivity reliability in order to further ensure the security of crude oil transportation.

The second stream of literature of primary concern to us is the body of work specifically related to the evaluation of connectivity reliability. The first measure of a transportation network's connectivity reliability was proposed by Mine and Kawai [14], and considers the probability that specific origin-destination (OD) pairs within a network remain connected when links are subject to complete failures. Binary variables are used to describe the two possible operating states of a link, namely, either full-capacity operation or disconnected. Iida and Wakabayashi [28] extended this measure of terminal connectivity reliability to calculating the connectivity reliability between k nodes and the connectivity reliability of the network as a whole.

Since these initial efforts, the majority of studies related to connectivity reliability have focused on road networks. The methods for calculating network connectivity reliability generally fall into either analytical or approximation methods [29]. Analytical approaches mainly include Boolean algebra [30], graph theory [31], and minimal path and cut set algorithms [15,32,33]. Approximation methods usually rely on Monte Carlo simulations [34]. Notably, several new methods have been recently introduced into the analysis of connectivity reliability in transportation networks. Wu et al. [35] suggested using network connectivity entropy for evaluating connectivity reliability, and conducted a case study of the Nanjing metro network. Liu et al. [36], meanwhile, considered passengers' travel behaviors and employed their acceptable trip time to estimate the connectivity reliability of a rail transit network.

Although the investigation of connectivity reliability in these studies has proven fruitful, all of these studies pay attention to either a road or rail network. From a methodological perspective, this means that the connectivity reliability of individual links or nodes is already known when they calculate a network's connectivity reliability. Simultaneously, the research into connectivity reliability in shipping is largely absent. Recently, the Russia-Ukraine war had great impact on the transportation reliability of crude oil. The war induced high geopolitical risk, and the transportation node's disruption risk increased significantly. Some reports clearly indicated that the war affected the transportation and supply of crude oil [37]. Because of the lack of data, there are few quantitative studies and discussions on this issue yet. It is crucial to develop methods to understand the impact from these risks on the connectivity reliability of crude oil transportation. Although a few studies of the general vulnerability and resilience of maritime transportation networks have been conducted, measures of connectivity reliability specifically remain undeveloped. In practice, these studies of vulnerability and resilience address the effects of disruptions of arcs or nodes on a transportation network in hindsight. Vulnerability specifically refers to the abnormal sensitivity of a transportation network to internal or external risk scenarios, and it measures the increase in costs caused by disruptions [38–40]. Resilience, on the other hand, refers to the ability of a transportation network to recover quickly after one or more severe disruptions. This measure emphasizes the overall performance of a transportation network in responding to damage and returning to a normal state over a period of time. In quantifying resilience, the recovery time becomes one of the important indicators [41–44]. By contrast, calculating the connectivity reliability (the probability that given transportation arcs (i.e., straits and canals) remain connected when subjected to risk events) provides a powerful potential planning and forecasting mechanism that has as yet received little attention in maritime transportation literature. The foundation of such an analysis, that is, the dependence between various risk events has also not been taken into consideration. Any truly applicable measure of connectivity reliability must take into account the interrelation of risk events and the dependence structure between them.

In summary, we propose a multi-objective programming model for shipping route choices. Our work is one of the first studies to consider connectivity reliability as the other significant objective paired with transportation costs. In addition, we develop a vine copula approach, a method that is widely adopted to characterize dependence between

variables, in order to quantify the dependence structure between multiple risk events and evaluate the connectivity reliability of straits and canals. In practice, we apply our model to an urgent problem, which allows us to provide practical and meaningful policy implications that can be referred to widely by decision-makers evaluating energy transportation corridors.

3. Methodology

In this section, we present a bi-objective optimization model of shipping route choices for crude oil that simultaneously considers connectivity reliability and transportation costs. In particular, we apply vine copula, a method that is widely used to model the dependence of interrelated variables, to measure the connectivity reliability of straits and canals.

3.1. Problem description

Fig. 1 shows the maritime transportation network of the global crude oil trade. The main exporters include countries in the Middle East (such as Saudi Arabia and Iraq), African countries (such as Angola and Congo), and Latin American countries such as Brazil (denoted in green). Major importers include Asian countries (such as China and Japan), European

countries (such as the United Kingdom and France), and American countries such as the United States (denoted in yellow). The key straits and canals include the Strait of Hormuz, the Suez Canal, the Bab-el-Mandeb, and the Strait of Malacca, to name only a few (denoted in blue).

We build a simplified schematic diagram of a maritime transportation network for importing crude oil based on Fig. 1 (see Fig. 2) and construct our model of the shipping network. Let $G = (N, A)$ denote the maritime transportation network for crude oil imports, as shown in
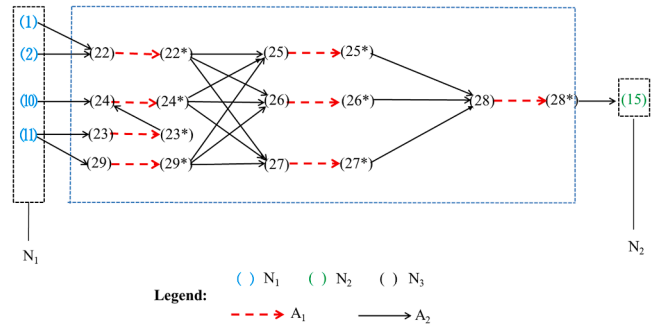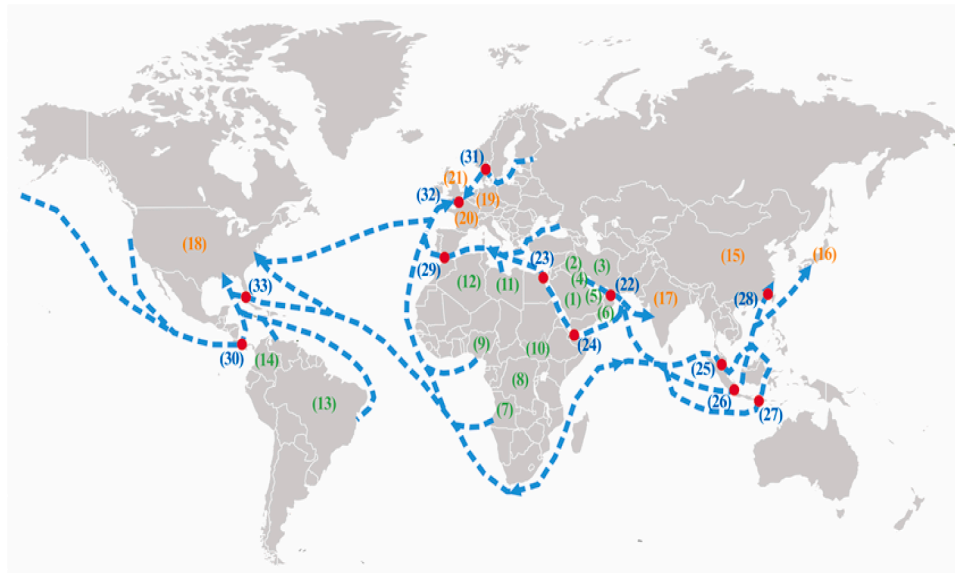

Fig. 2. A schematic diagram of global crude oil transportation network.

(1)	Saudi Arabia	(15)	China	(22)	Strait of Hormuz
(2)	Iraq	(16)	Japan	(23)	Suez Canal
(3)	Iran	(17)	India	(24)	Bab-el-Mandeb
(4)	Kuwait	(18)	United States	(25)	Strait of Malacca
(5)	United Arab Emirates	(19)	Germany	(26)	Sunda Strait
(6)	Oman	(20)	France	(27)	Lombok Strait
(7)	Angola	(21)	United Kingdom	(28)	Taiwan Strait
(8)	Congo			(29)	Strait of Gibraltar
(9)	Nigeria			(30)	Panama Canal
(10)	South Sudan			(31)	Danish Strait
(11)	Libya			(32)	English Channel
(12)	Algeria			(33)	Florida Strait
(13)	Brazil				
(14)	Colombia				

Fig. 1. Maritime transportation network of crude oil.

Fig. 2. N represents the set of nodes, and A the set of arcs. The set of exporters is denoted by N_1, the importer is denoted by N_2, and the set of other nodes in the network is denoted by N_3, where $N = N_1 \cup N_2 \cup N_3$. The set of straits and canals (denoted by A_1) comprises the arc set, and the set of other transportation arcs are denoted by A_2, where $A = A_1 \cup A_2$. The connectivity reliability of arcs $(i,j) \in A_1$ is affected by various risk events, and is within the range of $(0,1)$, while the connectivity reliability of arcs $(i,j) \in A_2$ is 1.

3.2. Mathematical formulation

In this section, we will construct a bi-objective optimization model to solve the maritime transportation route choice problem in a manner that considers both transportation costs and connectivity reliability. We make the following assumptions for model formulation. First, we assume that the transportation cost of an arc is proportional to its length. Second, the shipping company that transports the crude oil imports is regarded as a single entity with a heterogeneous fleet of vessels, including very large crude carriers (VLCCs) and ultra large crude carriers (ULCCs), in addition to Suezmax, Aframax and Panamax vessels. Vessels of each type can only operate along compatible routes. For example, a fully laden VLCC cannot pass through the Suez Canal. Third, the planning horizon is assumed to be one year.

We propose three decision variables in our study. The first is the volume of crude oil transported along each arc. Each arc has its own connectivity reliability and transportation distance (which corresponds to the transportation cost of that arc), and we determine the volume that should be transported via a given arc so as to minimize the total costs and maximize network reliability. This measure is associated with the number of each type of vessel deployed and the volume transported on each route, which are the other two decision variables. The notations used are as follows:

Sets

K	Set of OD pairs
N_1	Set of exporters
N_2	The importer
N_3	Set of other nodes
N	Set of all nodes in the maritime transportation network for crude oil imports, $N = N_1 \cup N_2 \cup N_3$.
A_1	Set of strait and canal arcs
A_2	Set of other arcs
A	Set of all arcs in the maritime transportation network for crude oil imports, $A = A_1 \cup A_2$
L	Set of crude oil vessel types
M	Set of routes for the OD pairs

Parameters

Q_i	Volume of crude oil imported from exporter i
V_l	Number of vessels of the lth type
C_l	Average carrying capacity of a vessel of the lth type
p_{ij}	Transportation cost per ton on arc ij
D	Demand for crude oil
H_k^m	Maximum carrying capacity of a vessel on route m of OD pair k
z_{ij}	Connectivity reliability of arc ij
q_{lm}^k	Cargo-carrying capacity of a vessel of the lth type on route m of OD pair k
c_{lm}^k	Number of round-trip voyages of the lth type vessel on route m of OD pair k
$\delta_{ij}^{m,k}$	$\in \{0,1\}$, 1 if route m of OD pair k uses arc ij, and 0 otherwise

Decision variables

x_{ij}	Volume of crude oil transported on arc ij
f_m^k	Volume of crude oil transported on route m of OD pair k
V_{lm}^k	Number of lth type vessels deployed on route m of OD pair k for transporting imported crude oil

Based on the previous analysis, the model is established as follows.

$$Min \sum_{i \in N} \sum_{j \in N} x_{ij} p_{ij} \tag{1}$$

$$Max \sum_{i \in N} \sum_{j \in N} x_{ij} z_{ij} \tag{2}$$

Subject to

$$\sum_{\substack{j \in N \\ (i,j) \in A}} x_{ij} = Q_i, \ i \in N_1 \tag{3}$$

$$\sum_{\substack{j \in N \\ (j,N_2 \in A)}} x_{jN_2} = \sum_{i \in N_1} Q_i \tag{4}$$

$$\sum_{\substack{j \in N \\ (j,i) \in A}} x_{ji} = \sum_{\substack{j \in N \\ (i,j) \in A}} x_{ij}, \ i \in N_3 \tag{5}$$

$$\sum_{\substack{j \in N \\ (j,N_2) \in A}} x_{jN_2} \geq D \tag{6}$$

$$x_{ij} = \sum_k \sum_m \delta_{ij}^{m,k} f_m^k, \ i \in N, j \in N, k \in K, m \in M \tag{7}$$

$$f_m^k = \sum_l q_{lm}^k c_{lm}^k V_{lm}^k, \ m \in M, k \in K \tag{8}$$

$$q_{lm}^k = \min\{C_l, H_k^m\} \ l \in L, m \in M, k \in K \tag{9}$$

$$\sum_m \sum_k V_{lm}^k \leq V_l, \ l \in L \tag{10}$$

$$x_{ij} \geq 0, \ i \in N, j \in N \tag{11}$$

$$f_m^k \geq 0, V_{lm}^k \geq 0, \text{ and } V_{lm}^k \in Z, l \in L, m \in M, k \in K \tag{12}$$

Objective function (1) minimizes the total transportation costs of crude oil en route from exporters to the importer. Objective function (2) maximizes total connectivity reliability. Constraints (3)-(5) are the flow conservation constraints for x_{ij}. Constraint (3) indicates that, for exporters, the total volume transported from each exporter is equal to its export volume to the importer. Constraint (4) stipulates that the volume transported to the importer is equal to the total import volume from all exporters. Constraint (5) specifies that, for other nodes, the volumes transported to them are equal to the volumes transported out of them. Constraint (6) ensures that the total volume transported to the importer can meet demand. Constraint (7) represents the relationship between the flow of arcs and routes. Constraint (8) indicates that the volume of crude oil transported on route m of OD pair k is related to the number of vessels deployed on that route. In Constraint (9), q_{lm}^k concerns the average carrying capacity of a vessel of the lth type, and it depends on the route along which the vessel is deployed. For example, a fully laden VLCC cannot pass through the Suez Canal; therefore, q_{lm}^k is equal to the smaller value between C_l and H_k^m. Constraint (10) is the vessel fleet constraint and denotes that, for each vessel type, the sum of vessels deployed on all routes should not exceed the total number of that vessel type. Constraints (11) and (12) define the domains of the decision variables.

We introduce w as the carrier's preference toward connectivity reliability, which determines the route choices of a shipping company, and assume $0 \leq w \leq 1$. If the shipping company places more weight on minimizing transportation costs rather than on maximizing reliability, then the value of w will be small. On the other hand, if more emphasis is placed on connectivity reliability at the expense of transportation costs (as can occur in the importation of a strategic resource like crude oil), then the value of w will be large. With the w, the bi-objective model can be transformed into a single-objective programming model, and the trade-off between the two conflicting objectives can be resolved. That is:

$$Min(1-w)\cdot\sum_{i\in N}\sum_{j\in N}p_{ij}^{\wedge}\cdot x_{ij} + w\cdot\sum_{i\in N}\sum_{j\in N}\left(1/z_{ij}\right)^{\wedge}\cdot x_{ij} \tag{13}$$

subject to constraints (3)-(12). Here, $1/z_{ij}$ is the inverse of connectivity reliability, which can be seen as the transportation risk for arc ij, and the problem of maximizing connectivity reliability is solved by minimizing transportation risk. In addition, $p_{ij}^{\wedge}$ and $(1/z_{ij})^{\wedge}$ are the values of min-max normalization processing, which are within the range [0, 1], and the dimensional effects do not exist [45]. We thus have a mixed-integer programming model, which we can solve with Cplex.

3.3. Evaluation of connectivity reliability

From the Global Integrated Shipping Information System (GISIS) and related research reports [3,46], four risk events are commonly identified as significantly affecting the connectivity reliability of straits and canals in the crude oil seaborne trade network. These events are heavy weather, vessel incidents, piracy and maritime terrorism, and political instability and military conflict. Piracy and maritime terrorism, as well as vessel incidents, are the risk events that most directly affect connectivity reliability, although in most cases they do not occur simultaneously. Heavy weather and political instability and military conflict will affect both the occurrence of piracy and maritime terrorism and vessel incidents. Risk events, therefore, are divided into two scenarios. Scenario 1 includes three risk events: piracy and maritime terrorism (ρ), heavy weather during the commission of piracy or maritime terrorism (ω_ρ), and political instability and military conflict (γ). Scenario 2 encompasses the following events: vessel incidents (α), heavy weather at the time of a vessel incident (ω_a), and political instability and military conflict (γ), as shown in Fig. 3.

In addition to establishing the interrelated nature of the various risk events, we further refine the model by referencing the product reliability evaluation method found in Yin et al. [47]. We assume that, given the values of heavy weather and political instability and military conflict, if the number of piracy or vessel incidents is not greater than the critical value, then the straits or canals can be considered connected. Thus, connectivity reliability is a conditional probability that can be obtained by constructing the conditional distribution of various risk events.

Vine copula has been widely used in financial, hydrologic, and engineering fields to model the dependence of interrelated variables. Its advantage over the correlation approach is that it can deal with any non-linearity, asymmetry, and tail dependence of the variables [48,49]. In this paper, we apply vine copula to describe the dependence structure between multiple risk events, and to construct the conditional distribution. Consider a vector $Y_1 = (\gamma, \rho, \omega_\rho)$ of the risk events enumerated in Scenario 1, with the joint distribution function $F = F(\gamma, \rho, \omega_\rho)$, and the marginal distributions of risk events $F_1 = F(\gamma)$, $F_2 = F(\rho)$, $F_3 = F(\omega_\rho)$. According to Sklar's theorem [50], the joint probability distribution of the risk events established in Scenario 1 can be expressed as follows:

$$F(\gamma, \rho, \omega_\rho) = C(F(\gamma), F(\rho), F(\omega_\rho)) \tag{14}$$

The copula function can thus be regarded as the joint distribution function of risk events (γ, ρ, ω_ρ). The copula function reflects information regarding the dependence structure between risk events, and this structure has nothing to do with the marginal distribution of risk events. The copula is a function determined solely by the dependence structure between risk events.
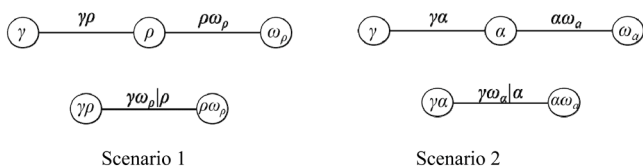

Fig. 3. Risk events in Scenarios 1 and 2.

The joint probability density function of the risk events in Scenario 1 can then be expressed as:

$$f(\gamma, \rho, \omega_\rho) = c(F(\gamma), F(\rho), F(\omega_\rho))\cdot(f(\gamma)\cdot f(\rho)\cdot f(\omega_\rho)) \tag{15}$$

where c indicates copula density. The joint probability density function of the risk events includes two parts: one is the density function of the copula (which contains all of the information about the dependence structure of the risk events) and the other is the product of the marginal density function of each risk event.

Most studies focus on the establishment of bivariate copulae and parameter estimations [51]. It becomes difficult to solve Eq. (15) when the dimension of risk events increases [52]. Vine copulas are graphical models that allow us to decompose Eq. (15) in a hierarchical manner via a series of bivariate copula densities (pair copulas) of risk events, as shown in Fig. 3. Mathematically, we can describe the decomposition of Eq. (15) as follows:

$$\begin{aligned} f(\gamma, \rho, \omega_\rho; \theta) &= f(\gamma)\cdot f(\rho)\cdot f(\omega_\rho)\cdot c_{\gamma\rho}\{F(\gamma), F(\rho)\}\cdot c_{\rho\omega_\rho}\{F(\rho), F(\omega_\rho)\} \\ &\cdot c_{\gamma\omega_\rho|\rho}\{F(\gamma|\rho), F(\omega_\rho|\rho)\} \end{aligned} \tag{16}$$

where $c_{\gamma\rho}$, $c_{\rho\omega\rho}$, and $c_{\gamma\omega_\rho|\rho}$ are the bivariate copula densities of risk events, and θ is the set of all parameters in the vine copula.

The above vine copula construction of risk events involves marginal conditional distributions of the form $F(u|\mathbf{v})$. Furthermore, Joe [53] showed that:

$$F(u|\mathbf{v}) = \frac{\partial C_{u,v_j|\mathbf{v}_{-j}}\{F(u|\mathbf{v}_{-j}), F(v_j|\mathbf{v}_{-j})\}}{\partial F(v_j|\mathbf{v}_{-j})} \tag{17}$$

where v_j is an arbitrarily chosen risk event from events vector $\mathbf{v}$, $\mathbf{v}_{-j}$ is $\mathbf{v}$ excluding this risk event, and $C_{u,vj|v-j}$ is a conditional bivariate copula between pairwise risk events.

More specifically, in the case when $\mathbf{v}$ includes only one risk event:

$$F(u|v) = \frac{\partial C_{uv}\{F(u), F(v)\}}{\partial F(v)} \tag{18}$$

In addition, the function $h(u, v, \Theta)$ is used to represent this conditional distribution function of risk events when u and v are uniform [52]:

$$h(u, v, \Theta) = F(u|v) = \frac{\partial C_{uv}\{F(u), F(v)\}}{\partial F(v)} \tag{19}$$

where the second variable of $h(u, v, \Theta)$ is always the conditional risk event and the set of parameters of the copula of risk events u and v is denoted by Θ.

Therefore, the conditional probability distribution for the risk events outlined in Scenario 1 $F(\rho|\gamma, \omega_\rho)$ can be expressed as:

$$\begin{aligned} F(\rho|\gamma, \omega_\rho) &= \frac{\partial C_{\rho,\gamma|\omega_\rho}\{F(\rho|\omega_\rho), F(\gamma|\omega_\rho)\}}{\partial F(\gamma|\omega_\rho)} \\ &= \frac{\partial C_{\rho,\gamma|\omega_\rho}[h(F(\rho), F(\omega_\rho), \Theta_{\rho\omega_\rho}), h(F(\gamma), F(\omega_\rho), \Theta_{\gamma\omega_\rho})]}{\partial[h(F(\gamma), F(\omega_\rho), \Theta_{\gamma\omega_\rho})]} \end{aligned} \tag{20}$$

It can also be expressed in the following manner:

$$\begin{aligned} F(\rho|\gamma, \omega_\rho) &= h[h(F(\rho), F(\omega_\rho), \Theta_{\rho\omega_\rho}), \\ &\quad h(F(\gamma), F(\omega_\rho), \Theta_{\gamma\omega_\rho}), \Theta_{\rho\gamma|\omega_\rho}] \end{aligned} \tag{21}$$

Similarly, the conditional probability distribution for the risk events described in Scenario 2 $F(\alpha|\gamma, \omega_a)$ can be expressed as:

$$\begin{aligned} F(\alpha|\gamma, \omega_a) &= h[h(F(\alpha), F(\omega_a), \Theta_{\alpha\omega_a}), \\ &\quad h(F(\gamma), F(\omega_a), \Theta_{\gamma\omega_a}), \Theta_{\alpha\gamma|\omega_a}] \end{aligned} \tag{22}$$

As for the choice of bivariate copula types for pair risk events, we consider five commonly used bivariate copulas that can describe different tail dependences of the risk events, namely Gaussian, Student, Frank, Clayton and Gumbel copulas. The Frank copula and Gaussian copula can describe either strong negative or positive dependence

between the risk events, and are symmetric in both their upper and lower tails. The Clayton copula and the Gumbel copula can describe only positive dependence, and the Clayton copula exhibits strong lower tail dependence, while the Gumbel copula exhibits strong upper tail dependence of risk events. The Student copula, meanwhile, is both lower and upper tail dependent [52,54]. The Akaike information criterion (AIC) can calculate which copula best fits the bivariate pair of risk events, so we employ the AIC to select the appropriate type of pair-copula [52].

With regard to the estimation of the parameters of the vine copula, this paper employs stepwise semi-parametric estimators (SSP). The parameters are estimated level by level, plugging in parameters from previous levels at each step [52,55,56]. Based on the estimated parameters of the bivariate copulas, $F(\rho|\gamma, \omega_\rho)$ and $F(\alpha|\gamma, \omega_a)$ can be calculated. We then combine the conditional probabilities of the two scenarios to calculate connectivity reliability. Since piracy and maritime terrorism and vessel incidents are equally important risk events, we assign the same weights to these two conditional probabilities, and derive the connectivity reliability from the sum of these probabilities.

4. Case study

China, as one of the largest importers of crude oil, relies on supplies from multiple countries. Recently, the construction of Gwadar Port in Pakistan has provided China with a new route option. In this section, we will use our model to testify whether the optimal maritime transportation routes include Gwadar Port as an option when the transportation reliability of different channels are considered.

4.1. Problem setting

The China Overseas Port Holding Company took over the operation of Gwadar Port in 2013, and on November 13, 2016, Gwadar Port was officially opened to navigation. Gwadar Port is located at the mouth of the Persian Gulf (about 400 km from the Strait of Hormuz), and is a deep-water port with the capacity to accommodate 80–100,000 DWT oil tankers. China and Pakistan are both interested in the construction of a new crude oil pipeline, such that crude oil from the Middle East, Africa, and Latin America can be transported by sea to Gwadar Port, and then via pipeline to China. Navigation through Gwadar Port is expected to circumvent traditional maritime routes, such as those through the Straits of Malacca.

When determining the major exporters of crude oil to China, we select Saudi Arabia, Iraq, Iran, Kuwait, United Arab Emirates (UAE), and Oman in the Middle East; Angola, Congo, South Sudan, and Libya in Africa; and, Brazil, and Colombia in Latin America [57]. The volumes imported from these countries equate to 67% of China's total imports of crude oil in 2021. The import volumes from these exporters are shown in Table 1. Referring to Fig. 1, the straits, canals, and ports involved in China's crude oil maritime transportation are the Strait of Hormuz, the

Table 1
Import volumes from exporters.

Region	Crude oil exporter	Import volume (tons)
Middle East	Saudi Arabia	87,567,606
	Iraq	54,079,431
	Iran	260,312
	Kuwait	30,163,415
	United Arab Emirates	31,937,527
	Oman	44,815,401
West Africa	Angola	39,154,905
	Congo	8928,017
North Africa	South Sudan	571,894
	Libya	6137,688
Latin America	Brazil	30,301,484
	Colombia	9461,824

Data source: International Trade Center.

Strait of Malacca, the Sunda Strait, the Lombok Strait, the Strait of Gibraltar, the Taiwan Strait, the Bab-el-Mandeb, the Suez Canal, the Panama Canal, Kyaukpyu Port, and Gwadar Port, as shown in Fig. 4. The annual transportation capacities of the China-Pakistan and China-Myanmar crude oil pipelines are 20 and 22 million tons, respectively [58].

We choose four measurements as proxies for the four risk events, as shown in Table 2. Piracy and armed robbery data is collected from the Global Integrated Shipping Information System (GISIS) of the International Maritime Organization (IMO, http://gisis.imo.org/Public/PAR/Default.aspx). According to the coordinate and location information for the piracy, the number of piracy for each strait or canal can be collected. The vessel incidents data is also collected from GISIS. The daily wind speed grid data is collected and the data is produced by the Remote Sensing Systems (http://www.remss.com). It is a spatially complete dataset available every six hours and closely collocated in time and space. Based on the longitude, latitude and time of the piracy or vessel incidents, the wind speed when piracy and armed robbery happened or vessel incidents happened can be obtained. As for the political risk, we refer to the index released by the PRS Group (https://www.prsgroup.com), which can reflect the geopolitical risk of the region where the nodes belong to. For example, with the breakout of the war between Russia and Ukraine, the risk index for the two countries decreased from 59.5 to 52.5, and from 64.5 to 58.5, respectively. Concretely, in our study, the value of the political risk for a strait is represented by the annual average risk value of countries it affiliates to. For example, as for the Malacca Strait, the political risk is expressed as the average of the political risk index of Singapore, Malaysia and Indonesia.

Based on the GISIS, daily wind speed and political risk index database mentioned above, we collect data on each of the four risk events for the 11 straits, canals and ports, and it costs us almost one year for data collection over the course of the period from 1999 to 2021. We take the median number of piracy and vessel incidents in 2021 in the designated straits, canals, and ports as the critical value. We then calculate the conditional probability and the connectivity reliability values using the model proposed in Section 3.3. All calculations are done with *R* software, and the results are listed in Table 3. As shown in Table 3, the connectivity reliability of the Strait of Malacca, the Bab-el-Mandeb and Gwadar Port is relatively low; while the connectivity reliability of the Strait of Gibraltar and the Lombok Strait is high.

Chinese seaborne crude oil imports account for 17.8% of the World's total seaborne oil trade, according to the Clarksons database. We thus multiply the number of vessels of each type in the global fleet by 17.8% in order to estimate the number of each vessel type used to transport Chinese crude oil imports [58]. According to Cheng and Duran [59], a typical, unitary measure of the total transportation cost of oil is within the range of US $1.50–3.00 per barrel of crude oil. We assume that the transportation cost from Iran to China is US $1.50 per barrel of crude oil. Given the transportation distance of each arc within the transportation network and the conversion relationship between tons and barrels of crude oil, we can calculate the transportation cost per ton along each arc of the major routes of Chinese oil imports [57]. Most researchers believe that routing through Gwadar Port provides a cheaper alternative to the traditional maritime transportation routes, such as those through the Strait of Malacca, because the port significantly reduces the transportation distance [60–63]. Therefore, we set the transportation cost of the China-Pakistan and China-Myanmar pipelines according to the transportation distance ratio of pipelines to shipping routes. We assume that the pipelines are constructed by the government [26], and that vessels have already been bought by the shipping company. Thus, for the purposes of our model, we do not consider the fixed investment in pipelines and vessels. The information of each vessel type is shown in Table 4. The number of available operating days per year for each vessel type is assumed to be 345 days [58].
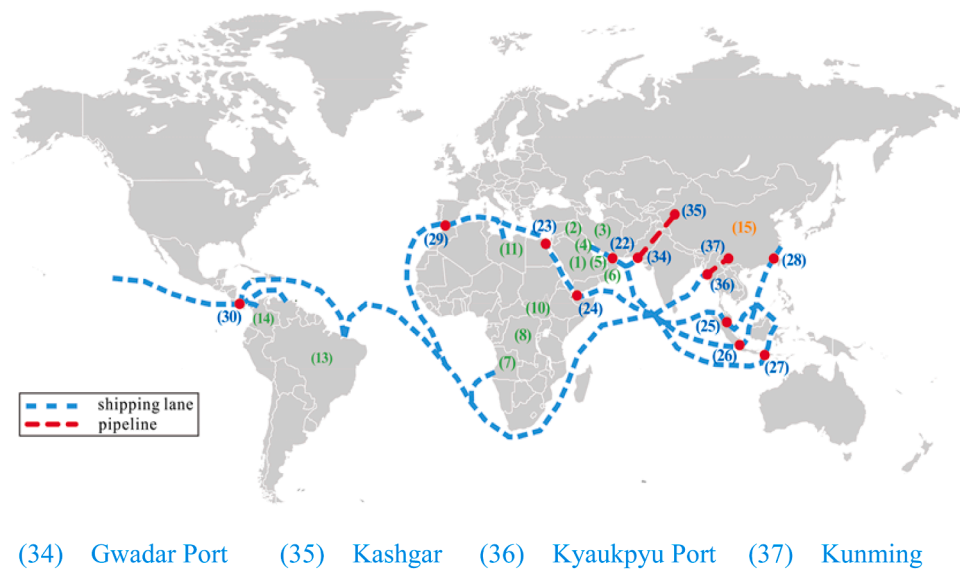
(34) Gwadar Port   (35) Kashgar   (36) Kyaukpyu Port   (37) Kunming

Fig. 4. Maritime transportation network of China's oil imports.

Table 2
Proxies and data sources for risk events.

Risk events	Proxies	Data sources
Piracy and maritime terrorism	Number of piracy and armed robbery	GISIS
Vessel incidents	Number of vessel incidents	GISIS
Heavy weather	Sea surface wind speed	Remote Sensing System
Political instability and military conflict	Political risk index	PRS Group

Note: A higher score in the political risk index indicates lower risk.

Table 3
The connectivity reliability of straits, canals, and ports.

Straits, canals, and ports	Conditional probability in Scenario 1	Conditional probability in Scenario 2	Connectivity reliability
Strait of Malacca	0.2763	0.5212	0.3988
Sunda Strait	0.4279	0.9334	0.6807
Lombok Strait	0.7717	0.8869	0.8293
Taiwan Strait	0.8830	0.6688	0.7759
Strait of Hormuz	0.4538	0.5859	0.5199
Bab-el-Mandeb	0.1599	0.8189	0.4894
Strait of Gibraltar	0.9656	0.6722	0.8189
Suez Canal	0.7076	0.6219	0.6648
Panama Canal	0.7735	0.7525	0.7630
Gwadar Port	0.5074	0.5563	0.5319
Kyaukpyu Port	0.6061	0.7351	0.6706

Table 4
Information for each vessel type.

Vessel type	Average carrying capacity (DWT)	Speed (knots)	Number
VL/ULCC	307,539	15.7	151
Suezmax	155,196	15.1	111
Aframax	107,934	14.9	131
Panamax	72,648	14.9	17

Data source: Clarksons Research Services.

4.2. Results

In this section, we will first analyze the impact of the dependence structure of risk events on connectivity reliability, and then discuss the route choice results.

4.2.1. Impact of dependence structure on connectivity reliability

Based on the model proposed in Section 3.3, the dependence structure of risk events can be calculated as shown in Fig. 5. We use the Malacca and Sunda Straits, along with Gwadar Port, to illustrate the impact of the dependence structure on connectivity reliability.

It can be observed that there are various dependence structures of risk events. Concretely, there is a strong negative dependence between the value of the political risk factor and the number of piracy (e.g., −0.5359 for Gwadar Port). This is expected because, as stated previously, a high score in the political risk index released by the PRS Group represents lower potential political instability, and thus the number of pirate attacks will be smaller. The strong negative dependence between the sea surface wind speed and the number of piracy (−0.6600 for the Malacca Strait, for example) suggests that heavy weather also plays a deterring role in piracy. On the other hand, heavy weather demonstrates a strong positive influence on the number of vessel incidents, as evidenced by the strong positive dependence between them (0.5497 for the Malacca Strait). In terms of political risk and the number of vessel incidents, a relatively weak negative dependence exists between these two risk factors (−0.2312 for the Malacca Strait).

Moreover, the tail dependences between risk events demonstrate variance between the two straits and Gwadar Port. For Gwadar Port, an upper tail dependence exists between sea surface wind speed and vessel incidents (according to the Gumbel copula), which indicates a stronger dependence when two risk events are both more likely to occur. In our case, when sea surface wind speed increases greatly, the probability of vessel incidents also increases significantly also. For the Malacca and Sunda Straits, symmetric tail dependence exists between these two risk events (according to both Gaussian and Frank copulas). This outcome indicates that, regardless of whether these two events are more or less likely to occur, the dependence is the same. Therefore, when in heavy weather near Gwadar Port, relevant precautions should be taken to avoid primarily vessel incidents, which would effectively improve the connectivity reliability of the port. As for political risk and the number of piracy, symmetric tail dependences exist between these two events for both the straits and for Gwadar Port. This suggest that reducing political
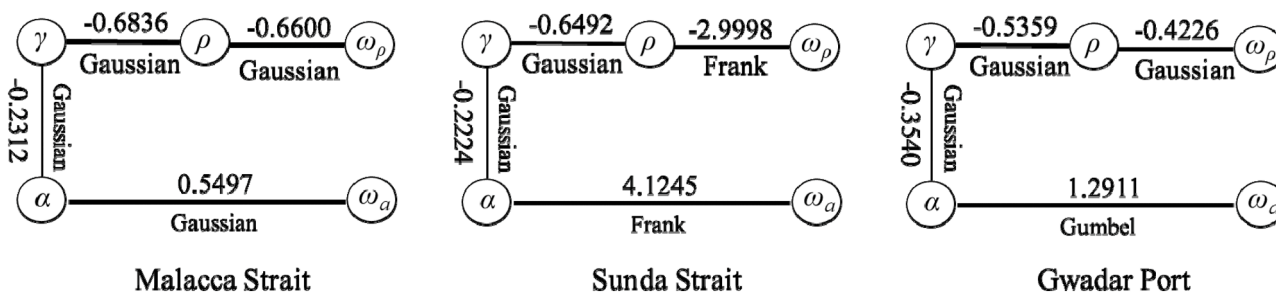
Fig. 5. Dependence structure of risk events.

Note: The parameter value of the Gaussian copula is within the range $(-1,1)$; the parameter value of the Gumbel copula is within the range $[1, +\infty)$; the parameter value of the Frank copula is within the range $(-\infty,0) \cup (0, +\infty)$.

risk should also produce a decreasing rate of pirate attacks and maritime terrorism. From this we can conclude that improvements in local political conditions near one of these nodes will likely improve connectivity reliability.

These results imply that relatively strong dependences do exist between various risk events and that these relationships affect connectivity reliability. Thus, these dependent relationships cannot be ignored when evaluating connectivity reliability; otherwise, it will lead to faulty estimations. In addition, based on the dependence structures identified in this section for Gwadar Port and the two straits, by mitigating the likelihood of certain risk events, we can effectively improve the connectivity reliability of these transportation arcs.

4.2.2. Route choice discussion

In this subsection, we first analyze a carrier's choice of Gwadar Port given different levels of preference for connectivity reliability. Then, we discuss the potential of Gwadar Port as an alternative route for Chinese oil imports through improving its connectivity reliability.

(1) Carrier's preferences toward Gwadar port

The findings shown in Table 5 suggest that the connectivity reliability of Gwadar Port has a crucial influence on its role in the transportation of crude oil to China. Specially, when the carrier has a higher preference toward transportation cost reduction ($w = 0.1$), we observe that 20 million tons of crude oil are transported via routes through Gwadar Port, which is the upper capacity limit of the China-Pakistan pipeline. This is the maximum volume that Gwadar Port can transport, and accounts for 3.9% of China's total crude oil imports. When the carrier's preference toward connectivity reliability and transportation cost is the same ($w = 0.5$), there are also 20 million tons of crude oil transported via routes through Gwadar Port. When the carrier's preference toward connectivity reliability reaches 0.7 (indicating that the carrier has a relatively high preference toward connectivity reliability), routes through Gwadar Port will not be selected. Alternatively, most of the oil will be transported through the Lombok Strait, as routes through the Lombok Strait are more reliable.

(2) The potential of Gwadar Port as an alternative route for oil transportation

As illustrated in Table 5, when $w<0.7$, Gwadar Port is fully utilized; when, however, the carrier demonstrates a higher preference for connectivity reliability ($w \geq 0.7$), Gwadar Port's role as a substitute for traditional transportation routes of crude oil is limited. We must further scrutinize the role of Gwadar Port when w is 0.7, and discuss the necessity of connectivity reliability improvement.

Under this circumstance, according to our model, we calculated that when Gwadar Port's connectivity reliability increases by 2.4%, it provides a viable substitute route and its maximum volume for oil transportation will be utilized if the Lombok strait is disrupted. There are two reasons that help to understand this outcome. First, the connectivity reliability of the Malacca Strait from our data analysis is lower than that of Gwadar Port, and the transportation cost of routes through the Malacca Strait is higher than those through Gwadar Port; thus, when the Lombok Strait is disrupted, routes through Gwadar port will be used rather than those through the Malacca Strait. Second, the cost of routes through Gwadar Port is lower than those through the Sunda Strait, and the difference in reliability between Gwadar Port and the Sunda Strait decreases after improvement of Gwadar Port's connectivity reliability. So, when the Lombok Strait is disrupted, part of the volume originally transported through it will be transferred to Gwadar Port, and the other will be rerouted to the Sunda Strait, as shown in Fig. 6.

When either the Malacca Strait or the Sunda Strait is disrupted, all crude oil will be transported via routes through the Lombok Strait rather than through Gwadar Port, as exhibited in Fig. 6. This is because, although the cost of routes through Gwadar Port is lower than those through the Lombok Strait, the difference in reliability between Gwadar Port and the Lombok Strait remains large after Gwadar Port's connectivity reliability increases by 2.4%. Gwadar Port will thus not be selected by the carrier.

When its connectivity reliability increases by 12.2%, about 3.9% of China's total oil imports are transported via routes through Gwadar Port (i.e., its maximum transportation volume) when the Malacca, Sunda, or Lombok Straits are disrupted, as shown in Fig. 7. As discussed previously, the connectivity reliability of the Lombok Strait is high, and only when Gwadar Port's connectivity reliability is improved by a larger margin can it serve as a route supplement for the Lombok Strait when either the Malacca or Sunda Straits are disrupted. After the improvements, we expect that the substitution effect of Gwadar Port on traditional maritime transportation routes will likewise increase, and that its strategic role will be fully actualized.

Moreover, when the carrier's preference toward connectivity reliability is high ($w = 0.9$), in order to realize Gwadar Port's full potential as a route alternative, its connectivity reliability must be improved by an even larger margin. That is, only when Gwadar Port's connectivity reliability is improved by at least 16.1% can it provide an alternative in the event that the Lombok Strait is disrupted. If either the Malacca or the Sunda Strait is disrupted, Gwadar Port's connectivity reliability must increase by at least 33.6%. The successful development of Gwadar Port would thus increase its overall utility in reducing reliance on key straits, and significantly improve the reliability of crucial oil imports.

Table 5

Volume of crude oil transported through Gwadar Port and the Malacca, Sunda, and Lombok Straits (million tons).

	$w = 0.1$	$w = 0.5$	$w = 0.7$
whether Gwadar Port is selected	Yes	Yes	No
Gwadar Port	20	20	0
Malacca Strait	0	0	0
Sunda Strait	261.6	188	0
Lombok Strait	0	73.6	281.6

Disruption of the Lombok Strait

Disruption of the Sunda Strait

Disruption of the Malacca Strait

Fig. 6. Route choices after Gwadar Port's connectivity reliability increases by 2.4%.

Disruption of the Lombok Strait

Disruption of the Sunda Strait

Disruption of the Malacca Strait

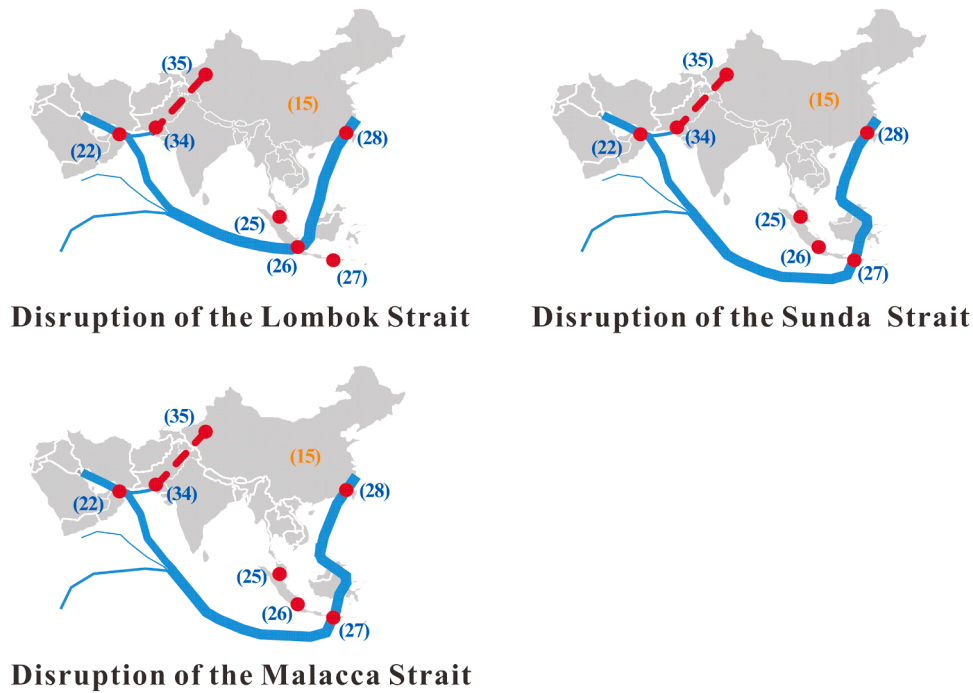**Fig. 7.** Route choices after Gwadar Port's connectivity reliability increases by 12.2%.

Gwadar Port is geographically important to the Middle East and China, and it has a high political risk. The complex ethnic conflicts and religious antagonism within Pakistan precipitate constant political crises and frequent changes in government. Besides, the prevalence of terrorism, and geopolitical maneuvering between international players such as America, India, Iran, and their policy interests in Gwadar Port also pose challenges to Gwadar Port's operations. These lead to a very high level of political risk in Pakistan, and its political risk index is only 47.3 in 2021, which is much smaller than Singapore's 81.7. The high

political risk can induce an increase in piracy and vessel incidents, which reduces the transportation reliability of crude oil through Gwadar Port. Given the dependent relationship between piracy and political risk demonstrated earlier, a reduction of political risk holds substantial promise for improving Gwadar Port's connectivity reliability. In addition, since there is an upper tail dependence between sea surface wind speed and the number of vessel incidents for Gwadar Port, taking better precautionary measures to avoid vessel incidents in heavy weather would also improve Gwadar Port's connectivity reliability.

5. Conclusions and implications

In this study, we develop a maritime transportation route choice model of crude oil that considers both transportation costs and connectivity reliability. In particular, we propose a connectivity reliability evaluation method that establishes the interdependence between risk events. This method both improves the accuracy of connectivity reliability estimation and provides a reference for development decisions made with the improvement of connectivity reliability in mind. We then apply the model to evaluate the effects of Gwadar Port on maritime route choices for imports of crude oil to China. The results show that the dependence relationship varies between different risk events, and the tail dependences between risk events demonstrate variance across straits and canals. As for Gwadar Port, our results demonstrate that its strategic role has not yet been fully realized. When the carrier's preference for connectivity reliability is less than 0.7, Gwadar Port's potential as a substitute route is fully exploited, and the volume of crude oil it handles is equal to the upper capacity limit of the China-Pakistan pipeline. When the carrier's preference for connectivity reliability is higher ($w \geq 0.7$), however, it cannot serve as an alternate route for crude oil transportation due to its low connectivity reliability.

Several managerial insights emerge from this analysis. First, the dependences between risk events are strong, especially for the relationship between political risk and the number of piracy and armed robbery, and the relationship between sea surface wind speed and the number of vessel incidents. Based on these dependences, an amelioration of political instability will likely reduce the number of piracy and maritime terrorism significantly, thus improving connectivity reliability. Likewise, heavy weather is an important determinant of lower connectivity reliability, and carriers and local authorities alike should seek to implement robust precautions. Second, when $w \geq 0.7$, Gwadar Port's existing connectivity reliability constrains its potential to reduce reliance on traditional maritime transportation routes. If Gwadar Port's substitution role for key straits is to be fully realized, its connectivity reliability needs improvement. When the value of w is 0.7–0.9, if Gwadar Port's connectivity reliability is improved by 2.4%–16.1%, it can provide an alternative route when the Lombok Strait is disrupted. If Gwadar Port's connectivity reliability is improved by 12.2%–33.6%, then its role as a reliable alternative to traditional maritime routes through the Malacca, Sunda, and Lombok Straits will be fully realized. In the short and medium term, taking relevant precautions to avoid more vessel incidents in heavy weather, while also promoting a long-term uplift of Pakistan's political condition are likely two effective ways to improve Gwadar Port's connectivity reliability. Additionally, since the volume of crude oil that Gwadar Port can transport is also dependent on the annual capacity of the China-Pakistan pipeline, a larger pipeline capacity would have beneficial ramifications and should be explored by policymakers and investors looking for opportunities to further develop Gwadar Port.

The war between Russia and Ukraine nowadays has great impact on the global crude oil transportation. For example, as for the Strait of Bosporus, the war will raise its geopolitical risks and increase its disruption probability; the likelihood of vessel incidents caused by the abuse of older tankers due to the sanctions against Russia will also increase. These risk events are interrelated and together affect the strait's connectivity reliability. In the future, with more data becomes available, it will be interesting to apply our model to characterize the dependence of these risk events and evaluate the strait's connectivity reliability, then the crude oil transportation flows change can be estimated considering these risks.

Finally, we note the limitations of the present paper, and the opportunities that they provide for future research directions. We did not evaluate the connectivity reliability of pipelines in our study due to the paucity of data related to pipeline security risks. From a methodological perspective, other approaches to the estimation of connectivity reliability for pipelines would be a worthwhile subject of future study.

Besides, for a specific strait or canal, the piracy risk may be higher than vessel incidents, or vice versa. Determining appropriate adjustment parameters to the weights of the two conditional probabilities for specific nodes would also be a possible future extension. Last but not the least, there are multiple ways in defining a risk, the severity of consequence would be considered to define risks in the future study.

CRediT authorship contribution statement

Shuang Wang: Conceptualization, Data curation, Formal analysis, Investigation, Methodology, Validation, Writing – original draft. **Haiying Jia:** Investigation, Methodology, Supervision. **Jing Lu:** Conceptualization, Funding acquisition, Project administration, Resources, Supervision. **Dong Yang:** Conceptualization, Formal analysis, Investigation, Supervision, Validation, Writing – review & editing.

Declaration of Competing Interest

The authors declare that they have no known competing financial interests or personal relationships that could have appeared to influence the work reported in this paper.

Data availability
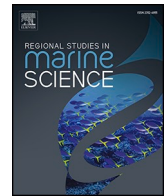
Data will be made available on request.

References

[1] Clarksons Research. Shipping review & outlook. London: Shipping Intelligence Network; 2019.

[2] EIA, 2022. U.S. Energy information administration. https://www.eia.gov/dnav/pet/hist/LeafHandler.ashx?n=PET&s=RBRTE&f=M.

[3] Bailey R, Wellesley L. Chokepoints and vulnerabilities in global food trade. London: Chatham House; 2017.

[4] Emmerson C, Stevens P. Maritime choke points and the global energy System-Charting a way forward. energy, environment and resource governance. Chatham House; 2012.

[5] Atmayudha A, Syauqi A, Purwanto WW. Green logistics of crude oil transportation: a multi-objective optimization approach. Clean Logist Supply Chain 2021;1: 100002.

[6] Jia HY. Crude oil trade and green shipping choices. Transp Res Part D 2018;65: 618–34.

[7] Siddiqui AW, Verma M. A bi-objective approach to routing and scheduling maritime transportation of crude oil. Transp Res Part D 2015;37(8):65–78.

[8] Yahyaoui H, Dahmani N, Krichen S. Sustainable maritime crude oil transportation: a split pickup and split delivery problem with time windows. Procedia Comput Sci 2021;192:4300–9.

[9] Yamashita D, Silva BJV, Morabito R, et al. A multi-start heuristic for the ship routing and scheduling of an oil company. Comput Ind Eng 2019;136:464–76.

[10] Li X, Oh P, Zhou YS, et al. Operational risk identification of maritime surface autonomous ship: a network analysis approach. Transport Policy 2023;130:1–14.

[11] Umar M, Riaz Y, Yousaf I. Impact of Russian-Ukraine war on clean energy, conventional energy, and metal markets: evidence from event study approach. Resour Policy 2022;79:102966.

[12] Jiang MZ, Lu J. The analysis of maritime piracy occurred in Southeast Asia by using Bayesian network. Transp Res Part E 2020;139:101965.

[13] Liu HL, Ren XJ, Yang ZL. Data-driven Bayesian network for risk analysis of global maritime accidents. Reliab Eng Syst Saf 2023;230:108938.

[14] Mine H, Kawai H. Mathematics for reliability analysis. Tokyo: Asakura-shoten; 1982.

[15] Reed S, Löfstrand M, Andrews J. An efficient algorithm for computing exact system and survival signatures of *K*-terminal network reliability. Reliab Eng Syst Saf 2019; 185:429–39.

[16] Wen M, Ropke S, Petersen HL, et al. Full-shipload tramp ship routing and scheduling with variable speeds. Comput Oper Res 2016;70:1–8.

[17] Muhammad S, Long XL. China's seaborne oil import and shipping emissions: the prospect of belt and road initiative. Mar Pollut Bull 2020;158:111422.

[18] Wu M, Li KX, Xiao Y, et al. Carbon Emission Trading Scheme in the shipping sector: drivers, challenges, and impacts. Mar Policy 2022;138:104989.

[19] Zavitsas K, Zis T, Zis MGH. The impact of flexible environmental policy on maritime supply chain resilience. Transp Policy (Oxf) 2018;72:116–28.

[20] Nishi T, Izuno T. Column generation heuristics for ship routing and scheduling problems in crude oil transportation with split deliveries. Comput Chem Eng 2014; 60:329–38.

[21] Pinto T, Alves C, José VDC. Column generation based primal heuristics for routing and loading problems. Electron Notes Discrete Math 2018;64:135–44.

[22] Faury O, Cheaitou A, Givry P. Best maritime transportation option for the Arctic crude oil: a profit decision model. Transp Res Part E 2020;136:101865.

[23] Hennig F, Nygreen B, Christiansen M, et al. Maritime crude oil transportation-a split pickup and split delivery problem. Eur J Oper Res 2012;218(3):764–74.

[24] Hennig F, Nygreen B, Furman KC, et al. Alternative approaches to the crude oil tanker routing and scheduling problem with split pick up and split delivery. Eur J Oper Res 2015;243(1):41–51.

[25] Greene S, Jia HY, Rubio-Domingo G. Well-to-tank carbon emissions from crude oil maritime transportation. Transp Res Part D 2020;88:102587.

[26] Ur Rehman O, Ali Y. Optimality study of China's crude oil imports through China Pakistan economic corridor using fuzzy TOPSIS and Cost-Benefit analysis. Transp Res Part E 2021;148:102246.

[27] Wen X, Ma HL, Choi TM, et al. Impacts of the belt and road initiative on the China-Europe trading route selections. Transp Res Part E 2019;122:581–604.

[28] Iida Y, Wakabayashi H. An approximation method of terminal reliability of a road network using partial minimal path and cut set. Japan: Yokohama: Proceedings of the Fifth WCTR; 1989. p. 367–80.

[29] Rivera-Royero D, Galindo G, Jaller M, et al. Road network performance: a review on relevant concepts. Comput Ind Eng 2022;165:107927.

[30] Wakabayashi H, Iida Y. Upper and lower bounds of terminal reliability of road networks: an efficient method with Boolean algebra. J Nat Dis Sci 1992;14:29–44.

[31] Bell MGH, Iida Y. Transportation network analysis. Ltd: John Wiley & Sons; 1997.

[32] Bai G, Zuo MJ, Tian Z. Search for all d-MPs for all d levels in multistate two-terminal networks. Reliab Eng Syst Saf 2015;142:300–9.

[33] Forghani-elahabad M, Kagan N, Mahdavi-Amiri N. An MP-based approximation algorithm on reliability evaluation of multistate flow networks. Reliab Eng Syst Saf 2019;191:106566.

[34] Zhao HQ, Guo MZ, Zhai CD, et al. Analysis of anti-seismic connectivity reliability of city gas pipeline network based on Monte Carlo method. J Seismol Res 2015;38(2): 292–6.

[35] Wu LS, Tan QM, Zhang YH. Network connectivity entropy and its application on network connectivity reliability. Phys A 2013;392:5536–41.

[36] Liu J, Schonfeld PM, Zhan SG, et al. Measuring and enhancing the connectivity reliability of a rail transit network. Transportmetrica A Transport Science; 2022. In press.

[37] Global Business Outlook. 2022. How the Russia-Ukraine war will shape the global economy. https://www.globalbusinessoutlook.com/.

[38] Liu HL, Tian ZH, Huang AQ, et al. Analysis of vulnerabilities in maritime supply chains. Reliab Eng Syst Saf 2017;169:475–84.

[39] Pan SZ, Yan H, He J, et al. Vulnerability and resilience of transportation systems: a recent literature review. Phys A 2021;581:126235.

[40] Wen T, Gao QY, Chen YW, et al. Exploring the vulnerability of transportation networks by entropy: a case study of Asia-Europe maritime transportation network. Reliab Eng Syst Saf 2022;226:108578.

[41] Ahmadian N, Lim GJ, Cho J, et al. A quantitative approach for assessment and improvement of network resilience. Reliab Eng Syst Saf 2020;200:106977.

[42] Dui HY, Zheng XQ, Wu SM. Resilience analysis of maritime transportation systems based on importance measures. Reliab Eng Syst Saf 2021;209:107461.

[43] Poo MCP, Yang ZL. Optimising the resilience of shipping networks to climate vulnerability. Marit Policy Manag 2022:1–20.

[44] Wang NX, Yuen KF. Resilience assessment of waterway transportation systems: combining system performance and recovery cost. Reliab Eng Syst Saf 2022;226: 108673.

[45] Jain YK, Bhandare SK. Min max normalization based data perturbation method for privacy protection. Int J Comput Commun Technol 2011;2(8):45–50.

[46] EIA. World oil transit chokepoints. U.S. Energy Information Administration; 2017. https://www.eia.gov/beta/international/regions-topics.php?RegionTopicID=WOTC.

[47] Yin JD, Tang JY, Shi YH. Reliability comprehensive evaluation model of product under the correlation failure process of the load shock and performance degradation. Sci Technol Eng 2018;18(13):1–7.

[48] Aas K. Pair-Copula constructions for financial applications: a review. Econometrics 2016;4(4):43.

[49] Farrokhi A, Farzin S, Mousavi SF. Meteorological drought analysis in response to climate change conditions, based on combined four-dimensional vine copulas and data mining (VC-DM). J Hydrol (Amst) 2021;603:127135.

[50] Sklar A. Fonctions de répartition à n dimensions et leurs marges, 8. Publications de l'Institut de Statistique de L'Université de Paris; 1959. p. 229–31.

[51] Marri F, Moutanabbir K. Risk aggregation and capital allocation using a new generalized Archimedean copula. Insurance: Math Econ 2022;102:75–90.

[52] Aas K, Czado C, Frigessi A, et al. Pair copula constructions of multiple dependence. Insurance: Math Econ 2009;44:182–98.

[53] Joe H. Families of m-variate distributions with given margins and m (m − 1) /2 bivariate dependence parameters. Lect Notes-Monogr Ser 1996;28:120–41.

[54] Joe H. Multivariate models and dependence concepts. London: Chapman & Hall; 1997.

[55] Hobæk Haff I. Comparison of estimators for pair-copula constructions. J Multivar Anal 2012;110:91–105.

[56] Hobæk Haff I. Parameter estimation for pair-copula constructions. Bernoulli 2013; 19(2):462–91.

[57] Wang S, Wallace SW, Lu J, et al. Handling financial risks in crude oil imports: taking into account crude oil prices as well as country and transportation risks. Transp Res Part E 2020;133:101824.

[58] Wang S, Yang D, Lu J. A connectivity reliability-cost approach for path selection in the maritime transportation of China's crude oil imports. Marit Policy Manag 2018; 45(5):567–84.

[59] Cheng L, Duran MA. Logistics for world-wide crude oil transportation using discrete event simulation and optimal control. Comput Chem Eng 2004;28(6–7): 897–911.

[60] Guo FF, Huang CF, Wu XL. Strategic analysis on the construction of new energy corridor China–Pakistan–Iran–Turkey. Energy Rep 2019;5:828–41.

[61] Khan SA. Geo-economic imperatives of Gwadar Sea port and Kashgar economic zone for Pakistan and China. IPRI J 2013;13:87–100.

[62] Malik HY. Strategic importance of Gwadar Port. J Polit Stud 2012;19(2):57–69.

[63] Wang JJ, Yau S. Case studies on transport infrastructure projects in belt and road initiative: an actor network theory perspective. J Transp Geogr 2018;71:213–23.

ARTICLES FOR FACULTY MEMBERS

NAVIGATIONAL RISK OF CONTAINER FALLS IN THE STRAIT OF MALACCA

Title/Author	**Evaluation of the factors causing container lost at sea through fuzzy-based Bayesian network / Öztürk, O. B.**
Source	***Regional Studies in Marine Science*** **Volume 73 (2024) 103466 Pages 1-12** **https://doi.org/10.1016/J.RSMA.2024.103466** **(Database: ScienceDirect)**

Evaluation of the factors causing container lost at sea through fuzzy-based Bayesian network

Orkun Burak Öztürk

Department of Maritime Transportation Management Engineering, Turgut Kıran Maritime Faculty, Recep Tayyip Erdogan University, Rize, Türkiye

ARTICLE INFO	ABSTRACT
	To date, many high-profile accidents involving the loss of large numbers of containers overboard have occurred during ocean voyages. It is estimated that an average of 1629 containers are lost at sea each year, and the statistics also highlight that the number of lost shipping containers has increased by two-thirds in the last five years. It is important to consider that falling containers are not only a threat to the safety of shipping but also a potential health and environmental hazard. In this direction, there are ongoing initiatives to improve container handling and reduce the risk of container loss. This paper focuses on container loss at sea, which is a serious risk in terms of marine pollution and financial loss, and seeks to evaluate this problem by identifying its causes. A Fuzzy Bayesian Network (FBN) model is therefore created to provide an approach for determining the factors and weights to be considered by seafarers during container transportation when assessing the causes of a container falling overboard. As a result of the research process, a model for assessing the risk of container falls is developed and the probabilistic relationships between the causes of container falls overboard are revealed. According to the analysis of the model, improper stuffing (15%), misdeclaration of container weight (12.6%), and container structural resistance (11.1%), are the three most risky root causes of container falls. In addition, the most obvious finding to emerge from this study is that the causes of container losses overboard are strictly related to both the process of the lashing and securing of the cargo and to the stability of the ship. Taken together, the results indicate that to prevent container falls at sea, it is crucial to avoid poor stability and ensure proper cargo securing. Consequently, FBN model developed for the study is expected to help improve the safety of container transport and reduce the risk of container loss by providing a comprehensive probabilistic risk analysis of container operations and predicting the risk of container loss if undesirable factors arise.

1. Introduction

Container shipping, an essential component of the maritime industry, carries 80% of the flow of goods transported by ship and plays a progressively significant role in global trade (Surfrider Foundation Europe, 2019). Reports by the United Nations Conference on Trade and Development (UNCTAD) indicate that container transport continues to be significant and is increasingly growing (UNCTAD, 2022, 2019, 2018). The growth of containerization mentioned above is accompanied by various environmental and financial risks. According to studies by the World Shipping Council (WSC), it is estimated that on average around 700 containers are lost at sea each year, excluding catastrophic events (WSC, 2022, 2017, 2014). If catastrophic events are taken into account, an average of 1629 containers are lost each year (WSC, 2022). The statistics show that the number of lost shipping containers has increased by a factor of 2/3 in the last five years. This undesirable situation can

have serious financial and environmental consequences, as well as disrupting supply networks and interrupting product deliveries. It can also pose a health risk to the crew on ships and anyone who comes into contact with lost containers at sea or on land. Efforts are therefore constantly being made to improve container handling and reduce the risk of container loss. The International Maritime Organization (IMO) has developed and adopted a number of requirements for the safe transport and packing and securing of containers and has undertaken significant work to prevent the container loss or problems in container shipping (IMO, 2023).

Drawing on an extensive range of literature, the studies investigate container shipping operations from different perspectives. Among the studies addressing container shipping, the authors have generally been interested in issues related to energy efficiency (Agrawal et al., 2008; Li et al., 2020; Yang et al., 2021; Yiğit, 2022), occupational safety onboard (Akyuz and Celik, 2016; Håvold, 2005; Lu et al., 2012; Lu and Tsai,

2008), marine pollution (Niimi, 2004; Sewwandi et al., 2022),etc. The issue of marine pollution caused by container ships should not only be assessed in terms of fires, collisions, and groundings. It is also important to carefully assess the issue of container losses from ships. The risk of marine pollution resulting from accidents involving container ships is a complex issue due to the wide variety of cargo carried in containers. Following accidents, heavy metals, plastic fibers, fuel spills, and hazardous and noxious substances can contaminate the sea, threaten entire marine habitats, and accumulate through the food chain, ultimately posing a threat to human health (Wan et al., 2022). Turner et al. (2021) published a paper describing observations of an inkjet cartridge spill caused by a container loss at sea. This paper demonstrates that inkjet cartridge spills have had a far-reaching impact, affecting locations as distant as Florida and northern Norway over a four-year period. While the environmental impact of container loss is widely recognized, Saliba et al. (2022) highlighted that there are currently no specific regulations in place to address this issue.

Although extensive research has been carried out on container shipping operations and some good insights have been provided by these studies, far too little attention has been paid to the subject of container loss at sea. In this direction, the study of operational guidelines for the prevention of container loss, carried out by Shigunov (2009), outlined considerations for such operational guidelines, including factors relating to the loss and damage of cargo for a modern container ship. A recent study by Erdem et al. (2023) assessed the role of human error in the risk of container loss. The paper highlighted the potential consequences of failures and critical human errors in the container loading operational process by focusing on the issue of container loss. This paper focuses on container loss at sea, which is a serious risk in terms of marine pollution and financial loss, and seeks to evaluate this problem by identifying its causes. A FBN model is therefore developed to provide an approach for determining the factors and weights to be considered by seafarers when assessing the causes of a container falling overboard. Literature research and expert interviews are conducted to identify the key factors that may influence the causes of container falls. As a result of the interview process, a container fall risk assessment model is developed and the probabilistic relationships between the causes of container falls overboard are revealed. To the best of our knowledge, the literature review did not yield any comprehensive studies on the analysis of the risk of container loss in maritime transport using a Bayesian Network (BN) developed with a fuzzy logic approach.

FBN analysis is an efficient method that is widely used in various maritime fields such as maritime safety, security, logistics, pollution and energy efficiency (Bayazit and Kaptan, 2023; Canbulat et al., 2018; Fan et al., 2020; Hänninen et al., 2014; Kamal and Kutay, 2021; Khan et al., 2022; Liu et al., 2021; Turna, 2022a). The BN approach is often used in risk analysis studies because it can explain the relationships between variables that make up complex systems in terms of quality and quantity (Balmat et al., 2009; Dinis et al., 2020; Jiang et al., 2021; Kevin et al., 2012; Li et al., 2023; Zhou et al., 2022). Furthermore, the BN is used to investigate potential failure issues, while fuzzy logic addresses the uncertainty of expert assessments. This model was selected for the study due to the complexity of container operations, and the requirement for expert assessments of the causes of overboard losses beyond reports. This model helps to establish a comprehensive framework for reasons of container loss. When examining the factors contributing to container loss, the model identifies multiple causes and determines their underlying root nodes. It also presents the probabilities and weights of these root nodes, thus conditional probability calculations are used to draw conclusions about the likelihood of the container falling. In this direction, the FBN model identified for the study is expected to help improve the safety of container transport and reduce the risk of container loss by providing a comprehensive probabilistic risk analysis of container operations.

The overall structure of the study takes the form of five sections, including this introductory section which draws attention to the container loss issue and presents an overview of the literature related to container shipping operations. The second section deals with the cases of containers lost overboard and provides an overview of the issue of container loss. The third section deals with the methodology used in this study. The fourth section presents the results and discussion of the research. The conclusion provides a brief summary, highlights the key findings, and includes suggestions for future research. Overall, the FBN model presented in this study offers an approach to assess the risk of container falls in shipping and to improve the safety of transportation. This paper is primarily intended for seafarers, but should also be considered by maritime policymakers, international organizations, and researchers.

## 2. An overview of the problem of container losses

It has been estimated by the IMO, governments, and marine insurers that up to 10000 shipping containers may fall from cargo ships each year (Frey and De Vogelaere, 2014). Many well-publicized accidents involving large numbers of containers falling overboard have occurred during the voyage. These accidents have caused significant damage to hundreds of other containers onboard, as well as compromising the safety of the ship. It should also be noted that the fallen containers are not only a threat to the safety of navigation but also a potential health and environmental hazard. The table below illustrates the 14-year trend of container loss at sea, and some of the cases of container lost overboard since 2006 (CBC, 2023; CTV, 2022; Frey and De Vogelaere, 2014; GCaptain, 2014; ITJ, 2023; SFR, 2020; The Maritime Executive, 2017; TheShip, 2023; WSC, 2022).

According to the fourteen-year survey in the table above, an average of 1629 containers are lost at sea each year. These results show a significant increase (18%) compared to the average annual loss in the twelve years up to 2019. Total losses averaged 675 per year in the first period (2008–2010) and then quadrupled to 2683 per year in the second period (2011–2013). The yearly average loss throughout the three-year period (2014–2016) was 1390, almost half that of the previous period. The annual loss was almost reduced to 779 in the 2017–2019 period. The two-year average loss for 2020–2021 rose to 3113. In addition, the case summaries related to container loss in Table 1 included the year of the accident, the name of the ship, and the content of the accident. The data show that container loss accidents pose a serious threat to the environment, navigation, and human life. In 2013, more than 4000 containers fell into the water as a result of the Mol Comfort ship breaking in half. After the One Apus accident in 2020, it is estimated that 1816 containers were involved in the catastrophe, of which 64 were dangerous goods. At this point, the average data of the last two years is a notable value that underlines the importance of investigating the causes of container loss incidents. The section of chronological accident data also demonstrates that container losses can result in significant environmental and financial consequences due to the nature of the cargo. In particular, it is important to consider accidents involving large tonnage containerships (MOL Comfort, One Apus, etc.) and to remember that the loss of containers from such ships can be far more devastating than others.

The causes of containers lost overboard are varied and often complicated, although very often basic operational errors are a factor (Gard, 2015). It is believed that more than 50% of lost containers are caused by either ship grounding or structural failure. Moreover, the human factor has been identified as a major problem in lost containers (CargoStore, 2023). The pie chart below shows the immediate causes of container loss, focusing on the number of claims (The Swedish Club, 2020).

As shown in Fig. 1, the claim statistics highlight that the main cause of container loss overboard is related to adverse weather conditions. The remaining factors are insufficient lashing/securing by the shipper, insufficient lashing/securing by the stevedore, insufficient lashing/securing by the vessel, poor tally, loading heavy containers on top of

Table 1
Summary of container lost at sea.
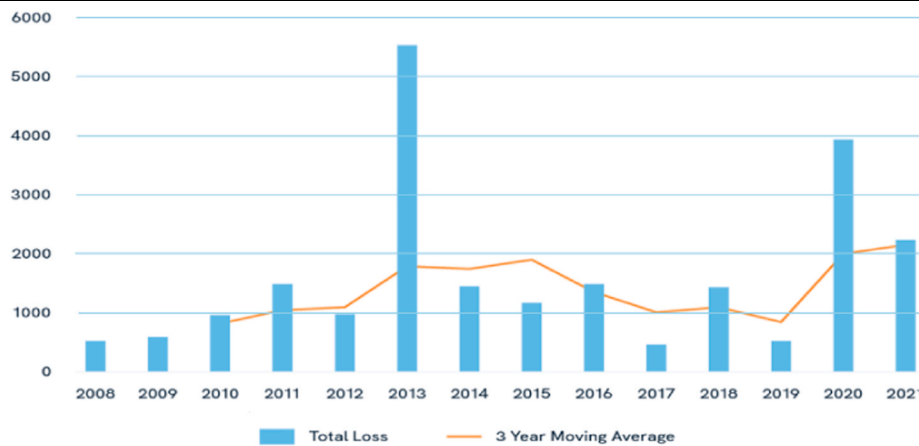
Date of Case	Vessel Name	Content of Accident
2006	Courtney L	One container washed ashore - thousands of bags of crisps washed up on the beach.
2007	MSC Napoli	At least 50 containers lost - Containers containing hazardous materials including nitric acid and airbag inflators.
2011	Rena	After grounding on 5 Oct 2011, 98 (estimated) lost overboard before 8 Jan 2012, 150 (estimated) lost overboard on 8 Jan 2012 off the north coast of New Zealand.
2013	MOL Comfort	4293 containers on board, ship broke in half in 200 miles off the coast of Yemen
2014	Svendborg Maersk	More than 500 containers lost in the Bay of Biscay - posing a threat to fishermen.
2015	El Faro	Total loss of ship (517 containers) with 33 crew in Hurricane Joaquin (Bahamas)
2016	Hanjin Seattle	35 empty containers dumped into the sea off the west coast of southern Vancouver Island - posed a hazard to shipping.
2019	MSC Zoe	280 containers lost in heavy weather between Portugal and Germany, littering the shores of the Wadden Islands with toys, furniture and smashed televisions.
2020	One Apus	An estimated 1816 containers lost or dislodged from their lashings during the ship's voyage from Yantian in China to Long Beach in the USA - 64 of the 1816 containers carried dangerous goods.
2021	Zim Kingston	Lost 109 shipping containers in heavy seas off Victoria - two containers contained hazardous chemicals, contaminated inflatable toys, vacuum cleaner parts, bicycle helmets, coolers and urinal mats.
2022	Dyros	Lost around 90 containers in the North Pacific - nine of these containers were marked as hazardous cargo and contained lithium-ion batteries packed with equipment.
2023	MSC Shristi	46 empty containers fall overboard approximately 350 nautical miles east of Bermuda
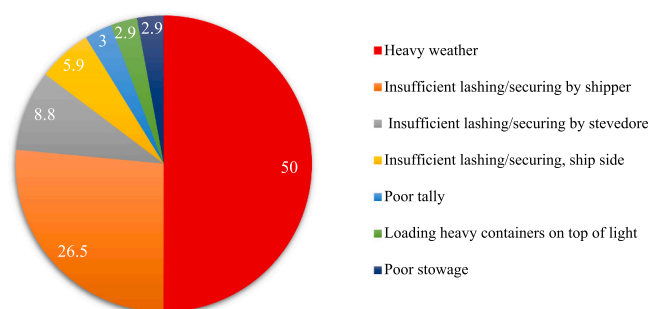
Fig. 1. Immediate causes of container loss – number of claims %.

light, and poor stowage respectively. With all of the above in mind, the following factors such as misdeclaration of container weight (IMO, 2023), insufficient cargo planning prior to loading operations, and poor condition of lashing equipment (Burthem and Brown, 2016; Offshore Energy, 2023), inverse placement- heavy containers on top of light containers, the problem of stacking height or weight, and poor structural resistance (Frey and De Vogelaere, 2014; Murdoch and Tozer, 2012), improper lashing and securing according to cargo securing manual, and improper container stuffing (The Swedish Club, 2020), poor ship stability (Cheng and Hirdaris, 2012), adverse weather conditions (CargoStore, 2023), etc. have been identified as the root causes of container loss overboard.

Although reports on container losses are published regularly, the data reported is often controversial. The reports do not cover all container ships in the maritime trade, some incidents are not reported and it is believed that some companies do not report in order to avoid legal obligations (ShippingKnowledge, 2017; The Maritime Post, 2022). Furthermore, the reports may ignore incidents involving the dropping of containers which do not cause problems in terms of pollution of the coastline and which do not contain hazardous cargo (ContainersMax, 2023; GatewayContainers, 2024).

There are also a number of initiatives in the maritime industry to improve container safety and reduce such losses. These initiatives aim to minimize the environmental impact of lost containers, reduce and prevent the risk of container falls, and ensure that cargo is transported safely. The International Convention for the Safety of Life at Sea (SOLAS) includes requirements for stowage and securing of cargo (such as containers) in Chapter VI on cargo transport. SOLAS Chapter VII (IMDG Code) contains provisions for dangerous cargo such as packing, container transport, and stowage (SOLAS, 1974). SOLAS also requires the verification of the gross mass of a filled container to prevent the misdeclaration of the gross weight of containerized cargo in 2016 (VGM Rules, 2014). The International Convention for Safe Containers (CSC) provides acceptable test procedures and related strength requirements for the transport and handling of containers (CSC, 1972). To provide an international standard to promote the safe stowage and securing of cargo, the Code of Safe Practice for Cargo Stowage and Securing (CSS Code) was adopted (CSS Code, 1991).

IMO, in cooperation with the International Labour Organization (ILO) and the United Nations Economic Commission for Europe (UNECE), has developed a non-mandatory code for the handling and

packing of cargo transport units for maritime and land transportation (CTU Code, 2014). The International Organization for Standardization (ISO) has updated basic standards for container handling and securing equipment (ISO, 2017, 2016). The studies of the organizations dealing with container loss are not limited to these, but have also been taken into account by SOLAS Chapter V - reporting procedure of container loss, MARPOL Annexes - reporting, pollution and prevention, ICS Guidelines - safe transport of containers, IACS Rules - lashing and securing of containers, etc (IACS, 2015; ICS, 2008; MARPOL, 1978; MSC, 2022; SOLAS, 1974). The WSC and member lines have also initiated the MARIN Top Tier project to reduce the risk of containers being lost overboard (WSC, 2021). In addition to the mentioned work, IMO has also adopted some regulations to cover liability and compensation for damage, such as pollution, caused by ships (HNS, 1996; LLMC, 2004; NICRW, 2007).

3. Material and methods

3.1. Fuzzy Bayesian networks

This paper employs a FBN method to define and evaluate the risks that may affect container falls overboard. BN is a graph model that allows for causal inference, the representation of uncertainty using conditional probability functions, and the exposure of probabilistic relationships between variables (Chang et al., 2021; Şakar and Zorba, 2017). Since BN has both qualitative and quantitative components in terms of explaining the relationship between variables, it is ideal for contextual reasoning (Holický et al., 2013; Khakzad et al., 2011). The qualitative component of a BN is represented by a directed acyclic graph, where each node represents a variable in the system, and the arcs between nodes represent the cause-effect relationships or dependencies between the variables. The quantitative component of the BN is provided by the conditional probability table (CPT), which specifies the relationships between each node and its parent nodes (Cai et al., 2013). The CPT, which is associated with each node and deals with the determination of numerical values, serves as a representation of the

quantitative approach in the BN (Turna, 2022b).

In summary, the BN combines the qualitative representation of the system with the quantitative relationships between the variables. The basic BN modeling approach usually consists of three main stages: identifying the influencing factors, generating the qualitative and quantitative components, and validating the model (Baksh et al., 2018; Goerlandt and Montewka, 2015). The research flowchart can be summarized in the following five steps (see Fig. 2).

The Bayesian probability theory underpins the inference principle of BNs. In theory, the CPT and marginal probability of the root nodes can be composed of statistical data, expert judgment, or a combination of both (Yang et al., 2008). Determining the probability of the network nodes is a critical step in generating significant outcomes from the BN structure. Bayes' Theory essentially assesses the probability of an event based on prior conditions that may be significant to that event. Algorithms for inference Eq. (1)=The joint probability distribution of a set of variables, Eq. (2) = The marginal probability computation for X_i are listed below equations (U refers to the universe of variables $X_1, X_2..., X_n n \geq 1$) (Díez-Mesa et al., 2018; Heckerman et al., 1995; Mahadevan et al., 2001).

$$P(U) = \prod_{i=1}^{n} P(X_i | \quad P_a \quad (X_i)) \qquad (1)$$

$$P(X_i) = \sum_{X_j \quad j \neq i} P(U) \qquad (2)$$

Using new data designated as evidence defined as (E), BN calculates the posterior probability of events based on Bayes' theorem, as shown in Eq. (3) (Jing et al., 2008; Zarei et al., 2019).

$$P\left(U\backslash E\right) = \frac{P(U, E)}{P(E)} = \frac{P(U, E)}{\sum_U P(U, E)} \qquad (3)$$

In order to address some limitations arising from the application of crisp probabilities in BN, this study develops a BN based on fuzzy set
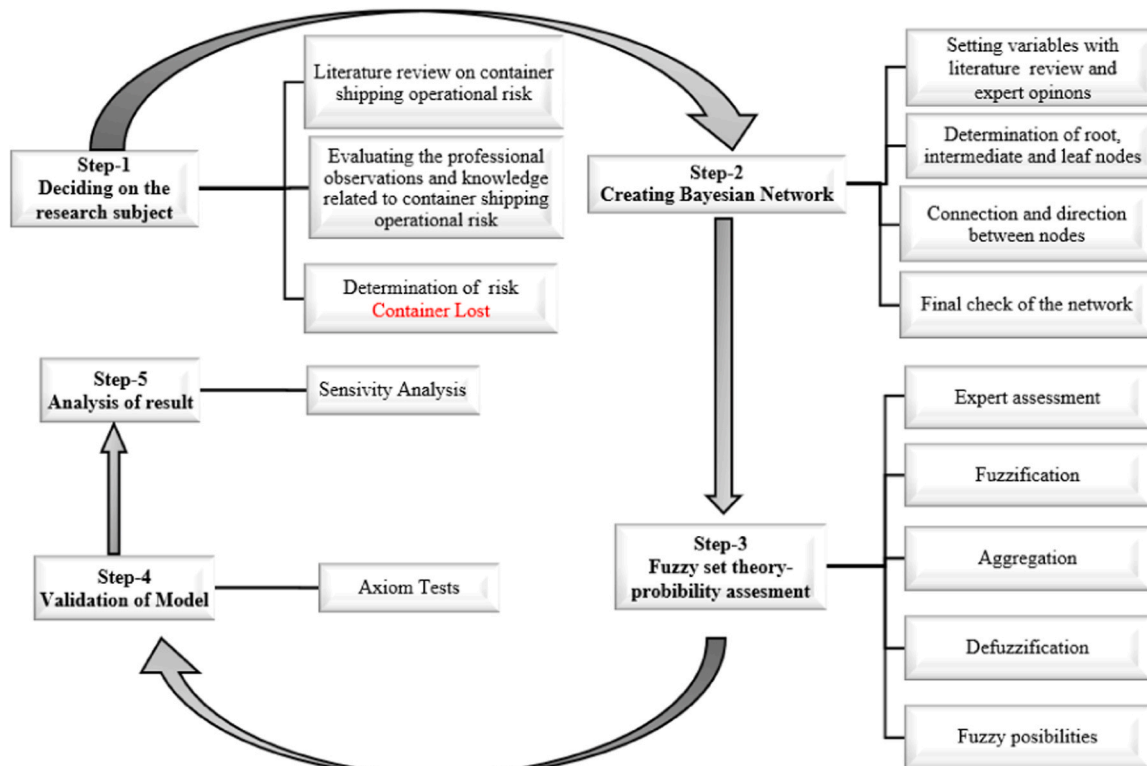

Fig. 2. FBN research flowchart.

theory. Fuzzy set theory is a research method that can deal with ambiguous and subjective assessments, and it can measure the linguistic aspects of available data and opinions for individual or group decision-making (Shan et al., 2015). The concept of 'linguistic variables' is very effective in dealing with circumstances that are too vague or ill-defined to be reasonably characterized by conventional quantitative expressions (Zadeh, 1965). Probabilistic assessment requires historical data on events in order to identify the events that cause the research topic and the causal relationships between these events. When retrospective information is not available or it is costly to obtain new information, it is an acceptable approach to use expert judgment. In addition, expert evaluations are widely used as acceptable data in the scientific community (Cooke and Goossens, 2000). Expert elicitation is essentially a scientific consensus methodology, often used to calculate the probabilities of vague events. This method is a solution for dealing with uncertainty and lack of sufficient data and provides useful information for risk assessment (Ramzali et al., 2015). In the absence of experimental or historical data, expert judgments serve as the primary data source for Bayesian network construction and are utilized to parameterize network interactions (Zhang et al., 2018). To provide marginal probabilities of root nodes and conditional probability values of intermediate events, the fuzzy set theory works successfully in decision-making stages using expert judgments (Senol and Yasli, 2021; Yazdi and Kabir, 2017).

Since there is not enough data for this study to calculate conditional probabilities, conditional probabilities were determined based on expert judgments. A heterogeneous expert group that consists of academicians and seafarers was incorporated into this study. The key point in selecting an expert is that all experts have seagoing experience on container ships. The number of experts in the current study was limited to five because including many expert opinions in studies might lead to negative marginal values (Clemen and Winkler, 1999). These experts were selected on the basis of their professional title, competence, service time, and level of education. Each parameter was ranked into five levels. Then, the weight scores of the experts were calculated using Eq. (4) (Rajakarunakaran et al., 2015). Table 2 presents the decision weight scores of the experts.

Weighting Factor of Expert $(W\mu)$

$$= \frac{Weighting\ score\ of\ the\ expert}{In\ all\ weight\ score\ of\ experts} \quad (4)$$

Once these experts were identified, they were asked to provide a detailed critique of the network structure and a linguistic evaluation of the nodes. Then, to take into account the weighting of the experts' differences, steps of fuzzification, aggregation, and defuzzification were performed on the experts' judgments in the context of fuzzy set theory. Due to its accuracy in transforming precise numbers into fuzzy numbers (Ross, 2000), the triangle membership function (Wang, 1997) was used to define linguistic variables in this study. In addition, the linguistic measurement scale (Bayazit and Kaptan, 2023; Rajakarunakaran et al., 2015) was used to assess the probability distribution of the uncertainty of the nodes. The membership function of triangular fuzzy numbers (Eq. 5) and the fuzzy linguistic measurement scale (Table 3) are given below.

Table 3
Fuzzy linguistic scale.

Failure possibilities	Triangular fuzzy numbers		
	a_1	a_2	a_3
Very low (VL)	0.00	0.04	0.08
Low (L)	0.07	0.13	0.19
Medium low (ML)	0.17	0.27	0.37
Medium (M)	0.35	0.50	0.65
Medium high (MH)	0.63	0.73	0.83
High (H)	0.81	0.87	0.93
Very high (VH)	0.92	0.96	1.00

$$\mu_{\tilde{A}}(x) = \begin{cases} 0; x \leq a_1 \\ \dfrac{(x-a_1)}{a_2-a_1}; a_1 \leq x \leq a_2 \\ \dfrac{(a_3-x)}{a_3-a_2}; a_2 \leq x \leq a_3 \\ 0; x \geq a_3 \end{cases} \quad (5)$$

Collecting and reconciling of experts' judgments is the key point because of the different backgrounds of the experts. To achieve consensus, expert judgments should be formed as a single term. For this reason, an algorithm called the similarity aggregation method has been proposed to merge the findings of heterogeneous expert groups (Hsu and Chen, 1996). The judgments of each expert are expressed in linguistic terms formulated as E_u (u= 1,... m).

(1) Calculation of the degree of agreement between expert judgments: Eq.(6) describes the similarity function from $\tilde{A}_1$ to $\tilde{A}_2$. $\tilde{A}_1 = (a_{11}, a_{12}, a_{13})$ and $\tilde{A}_2 = (a_{21}, a_{22}, a_{23})$ are two standard triangular fuzzy numbers.

$$S\left(\tilde{A}_1, \tilde{A}_2\right) = 1 - (1/3)\sum_{i=1}^{3}|a_{1i} - a_{2i}| \quad (6)$$

(2) Calculation of the average agreement (AA) degree between expert judgments: Eq. (7) describes the AA degree of M experts.

$$AA(E_u) = \frac{1}{M-1}\sum_{\substack{U \neq V\ v=1}}^{M} S\left(\tilde{A}_1, \tilde{A}_2\right) \quad (7)$$

(3) Calculation of the degree of relative agreement (RA): Eq. (8) describes the RA degree of M number of experts.

$$RA(E_u) \frac{AA(E_U)}{\sum_{u=1}^{M} AA(E_U)} \quad (8)$$

(4) Calculation of the consensus coefficient (CC): Eq. (9) describes the CC of experts.

$$CC(E_U) = \beta.w(E_U) + (1-\beta).RA(E_U) \quad (9)$$

$\beta\ (0 \leq \beta \leq 1)$ is the proposed method's relaxing factor. In this study, $\beta = 0.5$ was considered.

(5) Aggregation of expert judgements: Eq. (10) calculates the aggregated expert judgements.

Table 2
Experts' details and weight factor.

Expert	Profession Title	Competency	Service Time (year)	Education Level	Weight Score				Total Score	Weight Factor
E_1	Academician	Master	10	Master	5	5	4	4	18	0.23
E_2	First Officer	Master	5	Bachelor	3	5	3	3	14	0.18
E_3	Academician	OOW	3	Doctorate	5	3	2	5	15	0.19
E_4	Captain	Master	15	Bachelor	4	5	5	3	17	0.21
E_5	Captain	Master	13	Bachelor	4	5	4	3	16	0.20

$$\widetilde{R}_{AG} = CC(E_1) \times \widetilde{R}_1 + CC(E_2) \times \widetilde{R}_2 + \ldots + CC(E_M) \times \widetilde{R}_M \qquad (10)$$

(6) Defuzzification: The purpose of this step is to extract measurable values from fuzzy numbers. The fuzzy values obtained in this step should be converted into a crisp score for use in calculating Bayesian network probabilities (fuzzy possibility score). In this study, the fuzzy possibility values of each basic event were computed using a widely utilized 'center of area' technique. Eq. (11) is utilized for the triangular fuzzy number, $\widetilde{A} = (a_1, a_2, a_3)$, in the defuzzification stages.

$$X = \frac{\int_{a_1}^{a_2} \frac{x-a_1}{a_2-a_1} x dx + \int_{a_2}^{a_3} \frac{a_3-x}{a_3-a_2} x dx}{\int_{a_1}^{a_2} \frac{x-a_1}{a_2-a_1} dx + \int_{a_2}^{a_3} \frac{a_3-x}{a_3-a_2} dx} = \frac{1}{3}(a_1 + a_2 + a_3) \qquad (11)$$

3.2. The FBN model on container loss

The FBN was used in this section to model the causes of container loss in container shipping. Before applying the method, it was necessary to identify the causes of container loss overboard in order to build the BN. Literature reviews and expert consultations were conducted to achieve this objective. The terms container loss and container fall from overboard are used synonymously in this model. The causes of container fall from overboard are represented by the BN graph in Fig. 3.

From the figure above we can see that the Bayesian network has been constructed from a total of 36 nodes covering the most possible causes of container falling overboard during navigation. The network nodes consist of 22 root nodes (colored green), 15 intermediate nodes (colored yellow, grey, blue, and orange) and 1 leaf node (colored red) according to their hierarchical rank. The GeNIe Academic version 4.0 software was used to model this network. The definitions of the root nodes in the model are shown in Table 4.

Following the creation of the BN structure, the marginal and conditional probability tables for the nodes were constructed. Due to the lack of data and the desire to delve deeper into the causes of container loss, the marginal and conditional probabilities for the nodes were calculated using fuzzy applications based on the judgments of five experts (see Table 2 for the expert panel). After the linguistic expressions derived from the expert judgments were fuzzied using Eqs. (6), (7), (8), and (9), the aggregated expert judgments were calculated using Eq. (10) and defuzzified using Eq. (11-12).

The expert decisions of probabilities on root nodes of the paper are shown in Table 5. In addition, the experts provide fuzzy conditional probabilities of the intermediate and leaf nodes. Table 6 also presents an example of the calculation of conditional probabilities, which takes into account calculation error (exist or non) and lack of loadmaster calibration (exist or non) in terms of stability calculation (inadequate or adequate).

As a result of these steps, the marginal probabilities of the root nodes were obtained. Likewise, the fuzzy conditional probabilities for the intermediate and leaf nodes were also calculated from the experts' evaluations.

3.3. Model validation

Validation of the model is essential in terms of confidence in the results after the conditional probabilities in the constructed network have been calculated. The literature demonstrates that there are several techniques to determine the validity of the model. According to a widely recognized method that is also employed in this study, the following three axioms need to be verified (Pristrom et al., 2016; Rathnayaka et al., 2012; Zhang et al., 2013).

The Axiom 1 part of Table 7 presents that the network behaves as expected and that increasing or decreasing the value of each parent
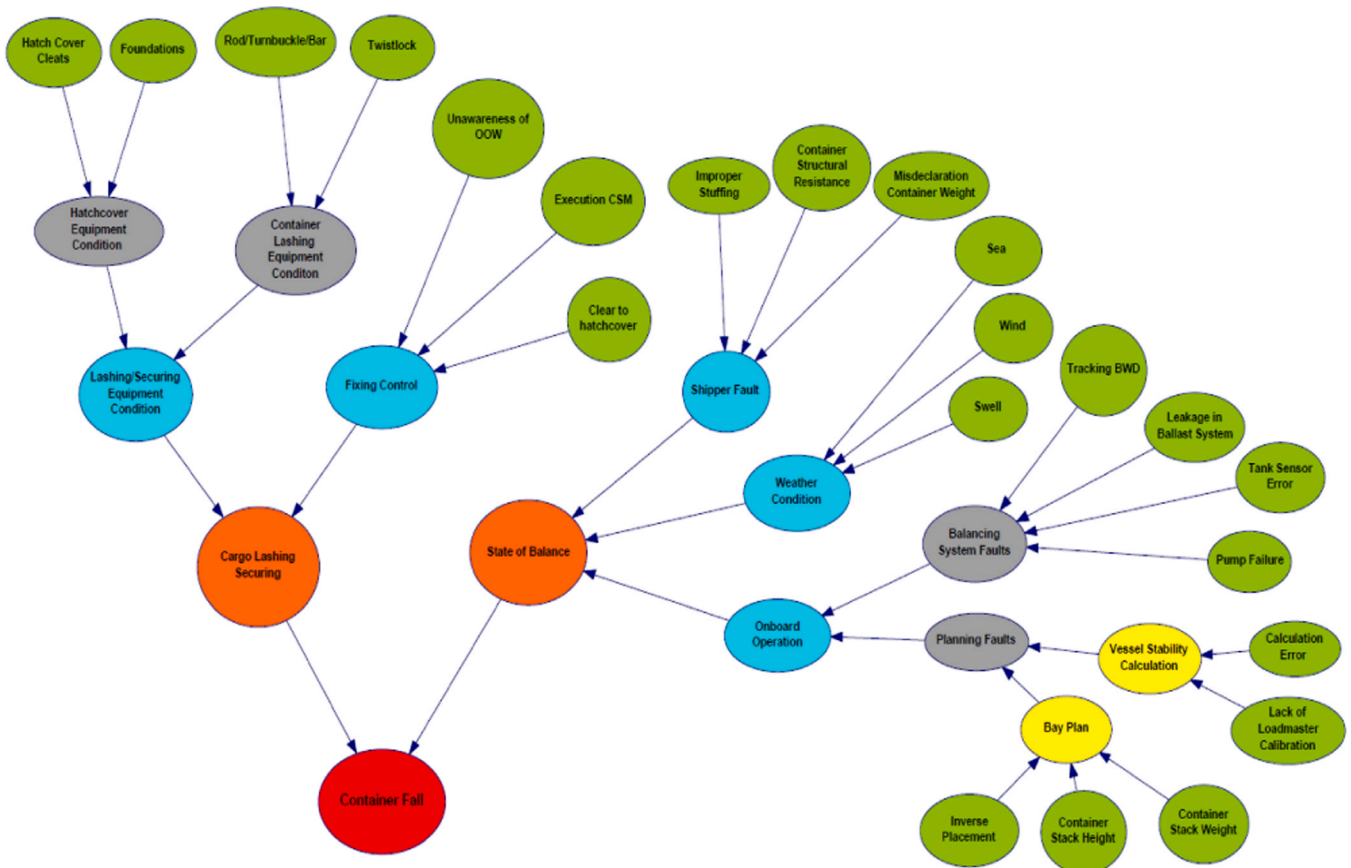

Fig. 3. Bayesian network model for container loss.

Table 4
Definition of the root nodes.

Root Nodes	Definition
Hatch cover cleats	Hatch cover cleats should be in good condition.
Foundations	Hatch cover foundations should be in good condition.
Rod, turnbuckle, bar	Rod, turnbuckle and bar should be in good condition.
Twistlock	Twistlocks should be in good condition.
Unawareness of OOW	Watchkeeping officer should be aware of cargo that is not secured.
Execution CSM	Securing operations should be in accordance with the ship's container securing manual.
Clear hatch cover	Clearing of hatch cover control (securing) should be adequate.
Improper stuffing	Cargo in containers should not be haphazardly arranged and should be braced.
Container structural resistance	Containers should have favourable structural conditions.
Misdecleration container weight	It is believed that shippers sometimes ignore container weight limits.
Sea	The components of weather conditions such as sea state,
Wind	wind force and swell heights can cause ships to roll,
Swell	sway, pitch, yaw and heave, but each has a different effect on the ship.
Tracking BWD	The ballast water diagram monitor should be tracked with care.
Leakage in ballast system	It should be ensured that there is no leakage in the ballast system.
Tank sensor error	It should be known that the tank sensors show the water levels without error.
Pump failure	Failure of the ballast pump may cause unstable conditions.
Calculation error	Ship stability calculations should be done carefully.
Lack of loadmaster calibration	Calibration of the loadmaster is critical to obtaining the correct stability values.
Container stack weight	The limit of container stack weight should not be exceeded in the bay plan.
Container stack height	The height of the container stack should be taken into account.
Inverse placement	Heavier containers should be placed on the lower tiers.

node's 'inadequate onboard operation' changes probabilities at the child nodes. If the 'balancing system' faults become a high-risk value, the probability of 'inadequate onboard operation' increases from 41.9% to 70.2%. Likewise, if the 'balancing system fault' is a low-risk level, the probability of an 'inadequate onboard operation' decreases to 22.5%. The Axiom 2 test shows the change in probabilities for the 'weather

condition' node according to changes in its parent variables 'sea state', 'wind force', and 'swell size'. As can be seen from the line shapes, there are no outliers or sharp knees. Due to alterations in the probability of 'high sea state', 'strong wind ', or 'high swell', there is a consistent change in the probability of 'adverse weather conditions'. The Axiom 3 test presents that the collective influence of parents is greater than the effect of each parent independently for a child node with more than one parent node. In addition, validation steps have also been carried out for the whole model, and it was seen that the results are in harmony with the requirements of the axiom tests.

3.4. Sensitivity Analysis

Sensitivity analysis, also known as variance analysis, changes the prior probability values of the variables within the formed network so that the influence of each node on the target node can be examined. It highlights the network's key preventive measures and helps predict system risk in the event of a severe adverse scenario (Uğurlu et al., 2020). Sensitivity analysis ensures that the probability of the leaf node (target) can be evaluated according to the probability of elimination or realization of the identified causes. In other words, the Bayesian network analyzes the effect of changes in the inputs (root node, intermediate node) on the leaf node (Bayazit and Kaptan, 2023). The sensitivity analysis performed for each root and intermediate node in the present research is presented in Table 8.

It can be seen from the data in Table 8 that 22 root nodes are labeled with the abbreviation 'RN 1–22', and the remaining 13 intermediate nodes are also numbered by colour such as 'YIN 1–2', 'GIN1–4', 'BIN1–5', and 'OIN1–2'. In addition, the table also shows the node names, prior states, and the degree of influence of the root or intermediate nodes on the leaf nodes. The next section of the research deals with

Table 6
Conditional probabilities of vessel stability calculation.

Calculation Error	Loadmaster Calibration	Vessel Stability Calculation	
		Inadequte	Adequate
Exist	Exist	0.994	0.006
Exist	Non	0.568	0.432
Non	Exist	0.424	0.576
Non	Non	0.005	0.995

Table 5
The expert decisions of probabilities and FPS (fuzzy probabilities scores) on root nodes.

All Nodes		States		Experts Evaluation for States 1					Final Evaluation Scores
		State 1	State 2	1	2	3	4	5	
Hatch cover cleats		Poor	Good	M	VH	M	MH	MH	0.676
Foundations		Poor	Good	MH	MH	MH	M	MH	0.686
Rod, turnbuckle, bar		Poor	Good	ML	MH	MH	L	M	0.468
Twistlock		Poor	Good	MH	MH	MH	L	M	0.581
Unawareness of OOW		Exist	Non	H	M	H	ML	H	0.695
Execution CSM		Inadequate	Adequate	VH	VH	H	ML	ML	0.680
Clear hatch cover		Inadequate	Adequate	VH	L	M	VL	MH	0.474
Improper stuffing		Exist	Non	MH	ML	VH	VL	MH	0.566
Container structural resistance		Poor	Good	VL	L	ML	L	MH	0.234
Misdecleration container weight	Exist		Non	MH	M	H	ML	VH	0.675
Sea		High	Low	MH	M	MH	MH	M	0.642
Wind		High	Low	H	M	MH	MH	M	0.670
Swell		High	Low	MH	M	MH	MH	M	0.642
Tracking BWD		Inadequate	Adequate	L	L	M	L	L	0.192
Leakage in ballast system		Exist	Non	ML	L	MH	ML	M	0.370
Tank sensor error		Exist	Non	VH	VH	H	M	H	0.840
Pump failure		Exist	Non	H	L	M	ML	M	0.453
Calculation error		Exist	Non	VH	L	M	ML	ML	0.404
Lack of loadmaster calibration		Exist	Non	H	L	M	L	ML	0.362
Container stack weight		High	Low	MH	L	MH	M	MH	0.591
Container stack height		High	Low	L	VL	ML	ML	M	0.241
Inverse placement		Exist	Non	MH	ML	M	M	MH	0.555

Table 7
Validation tests of the model.

Axiom 1 "Onboard Operation-Inadequate"			Axiom 2 "Weather Condition"	

Condition	Parent Nodes	Child Node
Exist	Balancing System Faults	Onboard Operation Failure
	Prior %	41.9
	100%	70.2
	0%	22.5
Exist	Planning Faults	Onboard Operation Failure
	Prior %	41.9
	100%	70.4
	0%	20.6

Axiom 2 for the node Weather Condition

Probability of Weather Condition "Exist" (y-axis) vs Weather Condition (x-axis) — Sea State, Wind, Swell

Axiom 3 "Bay Plan"
Parent Nodes

Inverse Placement %	Container Stack Height %	Container Stack Weight %	Child node Bay Plan Inadequat%	Percentage Variation %
55.5	24.0	59.1	46.6	0
100	24.0	59.1	69.3	48.7
55.5	100	59.1	76.7	64.6
55.5	24.0	100	67.0	43.8
100	100	100	99.9	114.4

Table 8
Sensitivity analysis results.

	Node No	Name of Nodes Affecting the Container Fall	Condition 1st	Prior %	Container Fall Prior %	Change 0%	Change 100%	Effect %
Root nodes (R)	RN1	Improper stuffing	Exist	56.6	48.3	39.8	54.8	15.0
	RN2	Misdecleration container weight	Exist	67.5	48.3	39.8	52.4	12.6
	RN3	Container structural resistance	Poor	23.4	48.3	45.7	56.8	11.1
	RN4	Leakage in ballast system	Exist	37.0	48.3	44.4	54.9	10.5
	RN5	Sea state	High	64.3	48.3	41.6	52.0	10.4
	RN6	Swell	High	64.3	48.3	43.0	51.2	8.2
	RN7	Tracking ballast water diagram	Inadequate	19.2	48.3	46.7	54.8	8.1
	RN8	Wind	High	67.0	48.3	43.3	50.8	7.5
	RN9	Twistlock	Poor	58.1	48.3	44.8	50.9	6.1
	RN10	Tank sensor error	Exist	84.0	48.3	43.3	49.3	6.0
	RN11	Pump failure	Exist	45.4	48.3	45.6	51.5	5.9
	RN12	Calculation error	Exist	40.5	48.3	46.0	51.7	5.7
	RN13	Unawareness of OOW	Exist	70.0	48.3	44.4	50.0	5.6
	RN14	Clear hatch cover	Inadequate	47.4	48.3	45.8	51.0	5.2
	RN15	Inverse placement	Exist	55.5	48.3	45.4	50.6	5.2
	RN16	Container stack weight	High	59.1	48.3	45.3	50.4	5.1
	RN17	Lack of loadmaster calibration	Exist	36.3	48.3	46.7	51.0	4.3
	RN18	Container stack height	High	24.0	48.3	47.3	51.3	4.0
	RN19	Execution CSM	Inadequate	68.0	48.3	45.7	49.5	3.8
	RN20	Rod, turnbuckle, bar	Poor	46.8	48.3	47.0	49.7	2.7
	RN21	Foundations	Poor	68.6	48.3	46.6	49.1	2.5
	RN22	Hatch cover cleats	Poor	67.6	48.3	46.8	49.0	2.2
Intermediate nodes(acc. different groups) (yellow-Y/ grey-G/ blue-B/ orange-O)	YIN1	Vessel stability calculation	Inadequate	38.6	48.3	44.4	54.5	10.1
	YIN2	Bay plan	Inadequate	46.6	48.3	43.6	53.7	10.1
	GIN1	Planning faults	Exist	42.8	48.3	39.4	60.2	20.8
	GIN2	Balancing system faults	Exist	40.6	48.3	40.2	60.1	19.9
	GIN3	Container lashing equip. cond.	Poor	54.5	48.3	43.4	52.4	8.0
	GIN4	Hatch cover equipment condition	Poor	66.8	48.3	44.9	50.0	5.1
	BIN1	Onboard operation	Inadequate	41.9	48.3	30.9	72.5	41.6
	BIN2	Shipper fault	Exist	49.1	48.3	34.2	62.9	28.7
	BIN3	Weather condition	Adverse	68.5	48.3	33.9	54.9	21.0
	BIN4	Lashing/securing equip. cond.	Poor	48.2	48.3	41.4	55.6	14.2
	BIN5	Fixing control	Improper	57.2	48.3	41.3	53.5	12.2
	OIN1	State of balance	Inadequate	49.5	48.3	13.0	84.2	71.2
	OIN2	Cargo lashing and securing	Inadequate	50.6	48.3	34.6	61.6	27.0

the findings from the sensitivity analysis table and the model network.

4. Results and Discussion

This study is set out with the aim of determining the causes and assessing the risk of container falls in shipping. The model of the study mainly provides a significant foresight into the risk of container falls. In this respect, the causes of the fall of the container mentioned in the model have been analyzed in terms of their sensitivity to this risk. Before returning to the sensitivity analysis results given in Table 6, it is necessary to present the possibility of a loss of a container. The figure below illustrates in detail the fuzzy Bayesian model of the current study, which was created with expert judgments. Fig. 4.

The BN model created in the current research demonstrates the factors causing the container loss overboard and the relationship between these factors. This enables users of the network to assess the causes of container loss overboard and predict the risk of container loss if undesirable factors arise. The adequacy of the state of balance and the lashing and securing of the cargo determines the risk of a container falling as configured through the network structure. According to the FBN analysis results, the probability of a container falling from overboard was found to be 48%. This probability value is derived from the experts' assessment of the root causes of the network. It can be seen that the most likely cause is 'tank sensor error' (84%), while the least likely cause is inadequate 'tracking of the ballast water monitoring system' (19%). Looking at the two parent nodes (cargo lashing and securing - state of balance) of the child node (the container fall), it can be seen that the probability of both parent nodes being inadequate is around 50%. Although the BN provides information on the probability of an incident, the evaluation of the weighting of the causal factors, their effect on each other, and their impact on the top event (container fall), rather than the probability of occurrence of the risk, in the light of the data in the sensitivity table, will provide valuable perspectives on the results of the Bayesian network. Therefore, a detailed analysis of the sensitivity table (Table 6) should be conducted at this stage.

The related results obtained from the sensitivity analysis of the

container fall are set out in Table 6. The effect column in Table 6 can be used to evaluate the impact level of factors on container fall. The results of the sensitivity analysis reveal the riskiest factors separately as root and intermediate nodes. According to the sensitivity analysis, "improper stuffing (15%)", "misdeclaration of container weight (12.6%)", and "container structural resistance (11.1%)", are the three most risky causes of container falls. The most important root node here is the variable "improper stuffing", which can lead to a container overboard probability of between approximately 39.8% and a maximum of 54.8%. Besides, the lowest effective root node is "poor hatch cover cleats", which can increase the probability of a container falling overboard by approximately 2.2%. The parent nodes of container fall, "state of balance" (71.2%), and "cargo lashing and securing" (27.0%), have a significant influence on container loss. Hence "the state of balance" node caused the highest effect for the variable "container fall". Apart from these nodes, the most significant intermediate causes are the "inadequate onboard operation" node (41.6%), the "shipper fault" node (28.7%), and the "weather conditions" node (21.0%). The lowest effective intermediate node is also the "poor condition of hatch cover equipment" which increases the probability of a container fall by about 5.1%.

A more striking result to emerge from the data in the sensitivity table is that the effect of the onboard operation node has a very high rate. Accordingly, it is necessary to thoroughly examine in detail the onboard operation fault node, which contains nine root causes. In the onboard operation node, four root causes (leakage in ballast system 10.5%, inadequate tracking of ballast water diagram-8.1%, tank sensor error 6.0%, and pump failure 5.9%) that are related to the balancing system faults are effective root causes of a container falling. This situation should be considered by seafarers, as a leak in the ballast system may also cause other environmental problems. In the same vein, it is necessary to examine the planning fault node in the onboard operation node. There are a total of 5 root causes that cause the planning fault. These root causes seem to be effective (4%- 5.7%) on falling containers. Although this value seems to be a low rate, it emphasizes that the ship's crew should carefully control the cargo operation planning process.

The weather node which consists of 3 root nodes has a remarkable
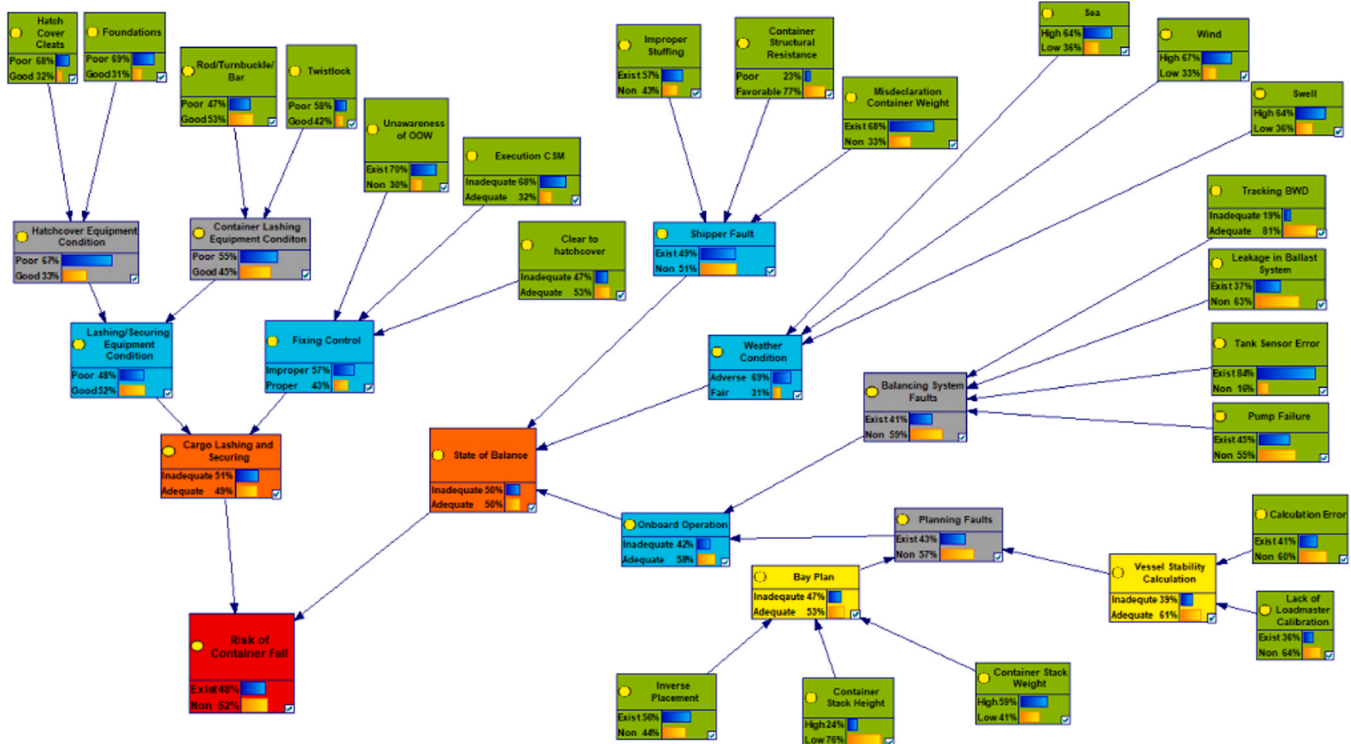

Fig. 4. FBN model including the probability of container fall.

value of 21.0%. From the lowest to the highest level of the "sea, swell, and wind conditions" influence the probability of container fall changes with percentages of 10.4, 8.2, and 7.5 values, respectively. In the "shipper fault node", three root causes, "improper stuffing", "container structural resistance", and "misdeclaration of container weight" are the significant root causes of a container falling. This node is not associated with the ship but is related to the shore, shipper, or terminal. Because both of the above nodes cannot be directly controlled by the ship, the root causes need to be carefully investigated.

When the container lashing and securing node section of the container fall is examined, 7 root nodes stand out under the fixing controls and lashing equipment condition nodes. The most significant root node here is the variable "twistlock" which may lead to a likelihood for a container fall of approximately the rate of 6.1%. The remaining root nodes of the "cargo lashing and securing node" affect the container fall as follows: "Unawareness of the officer of watchkeeping (5.6%)", "clear hatch cover (5.2%)", "execution CSM (3.8%)", "rod, turnbuckle, bar (2.7%)", "foundations (2.5%)", and "hatch cover cleats (2.2%)". The intermediate nodes of the same section that are colored blue (lashing and securing equipment condition, and fixing control), and gray (container lashing equipment condition, and hatch cover equipment condition) can cause a probability range of 14.2%, 12.2%, 8.0%, and 5.1%, respectively for the variable 'container fall'. As "twistlock" is the main influencing root node for the 'container lashing equipment condition' node, it is apparent that the parent nodes of this node contribute significantly to the 'container fall' probabilities. Therefore, this finding should be interpreted with caution because the twistlocks which lock the container together and provide stability to the stack, play a crucial role in ensuring the lashing and securing of the cargo on deck.

Very little has been found in the literature on the evaluating causes of container loss at sea, therefore, the present study was designed to determine the causes of the container fall from overboard and to make a risk assessment in relation to these causes. As mentioned in Section 2 of the current study, it is known that there are a variety of causes of container loss at sea. The Swedish Club's claims statistics reveal that the primary cause is navigation in adverse weather conditions combined with the crew's failure to adjust speed and/or course. Moreover, the report points to other causes of container loss such as inadequate securing and lashing of cargo, incorrect cargo stuffing and misdeclaration of cargo, inappropriate stowage planning, and excessive metacentric height (GM) (The Swedish Club, 2020). In this respect, both the report (Fig. 1) and the current study identify similar reasons for the fall of containers. The report shows that the "weather condition" is the main cause of the loss of containers. However, our study identifies "improper stuffing" as the most effective cause of container falls. In this study, weather conditions are evaluated under 3 different nodes: sea state, swell state, and wind severity. The effects of these factors are 10.4%, 8.2%, and 7.5% respectively (a total of 26.1%), which can be interpreted as the most effective cause in terms of container fall. It is important to note that the data in the reports only consist of claims, and therefore, unreported situations should also be considered.

Similarly, the WSC report lists some of the common causes of container loss as: misdeclared container weights, faulty connections between containers, heavier containers placed on top of lighter containers, stacking height, improperly loaded container contents, etc (WSC, 2022). These causes are largely consistent with the causes of the study's network model. However, this study did not use any risk assessment approach for container loss, and provides information on causes and results for several case studies.

Shigunov (2009) highlights some considerations regarding cargo loss and damage for a container ship in adverse weather conditions. These issues were evaluated in terms of cargo movements and accelerations, standard limits, lashing systems, and proper container stacking. In addition, the findings of the current study are consistent with those of Erdem et al. (2023) who assessed human error contribution to container loss risk. The results of this study revealed that 55 out of 100 cases may

result in container loss due to the major contribution of human error during the process of loading operation. Furthermore, the misdeclaration of the actual weight of the container is underlined as a crucial structural vulnerability. The current study reveals that the risk of container loss is 48%, and misdeclaration of container weight is the significant root cause of a container falling in terms of the shipper fault node. The present findings appear to be consistent with this research, which was aimed at reducing cargo loss. In view of all that has been mentioned so far, the main findings and the principal issues that have arisen in the mentioned works corroborate the findings of the current study. The combination of findings provides some support for preventing container loss at sea. In this context, it is essential for safe container shipping to ensure that the cargo is stable and properly secured.

5. Conclusion

To prevent containers from falling overboard, it is essential to understand the whole process of cargo handling on a container ship. This can be done by identifying the causes of container loss. Therefore, the present study was designed to identify the root causes of container loss at sea. The FBN was then modeled to assess the risk of container loss at sea. In this way, the relationship between the factors that cause container loss at sea and their consequences can be scrutinized.

The most obvious finding to emerge from this study is that the root causes of container falling overboard are related to both cargo lashing and securing processes and ship stability. Furthermore, it should be taken into account that the deficiencies caused by the shipper are the most effective root causes of the probability of container loss in the study. Since this situation is not directly associated with ship operations, it should be considered by all maritime stakeholders. The causes of container falling overboard can frequently be attributed to a series of multiple failures, rather than a single cause but improving awareness of these issues among both ship crew and shore workers will serve to prevent accidents.

It is considered that highlighting the most common causes of container loss overboard and creating a model for evaluating the risk of container fall in the current study will be beneficial for loss prevention initiatives of maritime transportation. The components of the maritime transportation community will be able to understand how container loss occurs, and what measures can be taken to prevent this harmful incident. Nobody can completely remove the difficulties of adverse weather conditions or the possibility of ship casualties at sea, however, the safety of maritime container transport may be improved with care and cooperation from all those involved in shipping, packing, handling, weighing, stowing, lashing, and securing containers. Overall, the prevention of container loss requires a combination of proper planning, implementation of safety measures, and regular maintenance and inspection.

Finally, a number of important limitations need to be considered for this study. Firstly, the opinions of a limited number of seafarers were used in the model. Increasing the number of experts in the studies would help us to establish a greater degree of accuracy on this issue. Secondly, the study only investigated the causes of container falls overboard during voyages, but it is considered that the risk of container falls should also be evaluated for port operations in detail.

Recommendations

The results of this study have a number of important implications for the prevention of container loss. In this direction, here are some recommendations for preventing container loss:

i. Proper lashing and securing, ii. Regular maintenance and inspection of container lashing and securing equipment, iii. Regular maintenance and inspection of containers, and improved container design, iv. Consideration of the container weight restrictions, v. Proper weight distribution, vi. Improved weather forecasting and route planning, vii. Improved monitoring (GPS tracking) and reporting technology, viii.

Proper crew training, ix. Proper weight distribution, x. Preventing misdeclaration of container weight, xi. Proper stowage planning, xii. Proper balancing.

As a result, exercising qualified seamanship in shipping will help to reduce container loss and their associated maritime pollution risk and high cost. The goal of the container shipping industry should remain to keep container losses at sea as close to zero as possible. Within this framework, initiatives on container losses should aim to promote safer and more sustainable shipping practices and to reduce the impact of container losses on the environment and the shipping industry.

CRediT authorship contribution statement

The author confirms sole responsibility for the following: study conception and design, data collection, analysis and interpretation of results, and manuscript preparation.

Declaration of Competing Interest

The authors declares that they have no known competing financial interests or personal relationships that could have appeared to influence the work reported in this paper.

Data Availability

Data will be made available on request.

References

Agrawal, H., Malloy, Q.G.J., Welch, W.A., Wayne Miller, J., Cocker, D.R., 2008. In-use gaseous and particulate matter emissions from a modern ocean going container vessel. Atmos. Environ. 42, 5504–5510. https://doi.org/10.1016/J.ATMOSENV.2008.02.053.

Akyuz, E., Celik, M., 2016. A hybrid human error probability determination approach: The case of cargo loading operation in oil/chemical tanker ship. J. Loss Prev. Process Ind. 43, 424–431. https://doi.org/10.1016/j.jlp.2016.06.020.

Baksh, A.A., Abbassi, R., Garaniya, V., Khan, F., 2018. Marine transportation risk assessment using Bayesian Network: Application to Arctic waters. Ocean Eng. 159, 422–436. https://doi.org/10.1016/J.OCEANENG.2018.04.024.

Balmat, J.F., Lafont, F., Maifret, R., Pessel, N., 2009. MAritime RISk Assessment (MARISA), a fuzzy approach to define an individual ship risk factor. Ocean Eng. 36, 1278–1286. https://doi.org/10.1016/J.OCEANENG.2009.07.003.

Bayazit, O., Kaptan, M., 2023. Evaluation of the risk of pollution caused by ship operations through bow-tie-based fuzzy Bayesian network. J. Clean. Prod. 382, 135386 https://doi.org/10.1016/J.JCLEPRO.2022.135386.

Burthem, S., Brown, A., 2016. Container Shipping And Ports: An Overview.

Cai, B., Liu, Y., Liu, Z., Tian, X., Zhang, Y., Ji, R., 2013. Application of Bayesian Networks in Quantitative Risk Assessment of Subsea Blowout Preventer Operations. Risk Anal. 33, 1293–1311. https://doi.org/10.1111/J.1539-6924.2012.01918.X.

Canbulat, O., Aymelek, M., Turan, O., Boulougouris, E., 2018. A Bayesian Belief Network Model for Integrated Energy Efficiency of Shipping 257–273. https://doi.org/10.1007/978-3-319-74576-3_19.

CargoStore, 2023. How Many Containers Are Lost At Sea?. https://cargostore.com/how-many-containers-are-lost-at-sea/ (accessed 5.2.23).

CBC, 2023. CBC.ca - watch, listen, and discover with Canada's Public Broadcaster, https://www.cbc.ca/ (accessed 4.28.23).

Chang, C.H., Kontovas, C., Yu, Q., Yang, Z., 2021. Risk assessment of the operations of maritime autonomous surface ships. Reliab. Eng. Syst. Saf. 207, 107324 https://doi.org/10.1016/J.RESS.2020.107324.

Cheng, F., Hirdaris, S., 2012. Improvement of Ship Safety through Stability Research and Innovations. Proc. 11th Int. Conf. Stab. Ships Ocean Veh. 23–28. https://doi.org/10.13140/RG.2.1.2996.8724.

Clemen, R.T., Winkler, R.L., 1999. Combining probability distributions from experts in risk analysis. Risk Anal. 19, 187–203. https://doi.org/10.1023/A:1006917509560/METRICS.

ContainersMax, 2023. How Many Shipping Containers Are Lost At Sea?. ⟨https://www.containersmax.com/how-many-shipping-containers-are-lost-at-sea/⟩.

Cooke, R.M., Goossens, L.H.J., 2000. Procedures Guide for Structural Expert Judgement in Accident Consequence Modelling. Radiat. Prot. Dosim. 90, 303–309. https://doi.org/10.1093/OXFORDJOURNALS.RPD.A033152.

CSC, 1972. International Convention for Safe Containers (CSC, 1972).

C.S.S. Code, 1991. Code of Safe Practice for Cargo Stowage and Securing (CSS Code).

C.T.U. Code, 2014. IMO/ILO/UNECE Code of Practice for Packing of Cargo Transport Units (CTU Code).

CTV, 2022. MV Zim Kingston's lost cargo containers | CTV News. https://vancouverisland.ctvnews.ca/mv-zim-kingston-s-lost-cargo-containers-still-a-deep-concern-for-vancouver-island-communities-1.5791612 (accessed 4.28.23).

Díez-Mesa, F., de Oña, R., de Oña, J., 2018. Bayesian networks and structural equation modelling to develop service quality models: Metro of Seville case study. Transp. Res. Part A Policy Pract. 118, 1–13. https://doi.org/10.1016/J.TRA.2018.08.012.

Dinis, D., Teixeira, A.P., Guedes Soares, C., 2020. Probabilistic approach for characterising the static risk of ships using Bayesian networks. Reliab. Eng. Syst. Saf. 203, 107073 https://doi.org/10.1016/J.RESS.2020.107073.

Erdem, P., Akyuz, E., Aydin, M., Celik, E., Arslan, O., 2023. Assessment of human error contribution to container loss risk under fault tree analysis and interval type-2 fuzzy logic-based SLIM approach. Proc. Inst. Mech. Eng. Part M J. Eng. Marit. Environ. https://doi.org/10.1177/14750902231203074.

Fan, S., Yang, Z., Blanco-Davis, E., Zhang, J., Yan, X., 2020. Analysis of maritime transport accidents using Bayesian networks. https://doi.org/10.1177/1748006×19900850 234, 439–454. https://doi.org/10.1177/1748006×19900850.

Frey, T., De Vogelaere, A, 2014. The Containerized Shipping Industry and the Phenomenon of Containers Lost at Sea-Marine Sanctuaries Conservation Series ONMS-14-07.

Gard, 2015. Cause and prevention of container loss at sea. https://www.gard.no/web/updates/content/20856543/cause-and-prevention-of-container-loss-at-sea-.

GatewayContainers, 2024. Shipping Containers Lost At Sea – Where Do They Go?. https://www.gatewaycontainersales.com.au/blog/shipping-containers-lost-at-sea-where-do-they-go/.

GCaptain, 2014. Maersk Tasked with Finding Hundreds of Missing Containers in Bay of Biscay. https://gcaptain.com/tag/containers-lost-at-sea/ (accessed 28.8.23).

Goerlandt, F., Montewka, J., 2015. Maritime transportation risk analysis: Review and analysis in light of some foundational issues. Reliab. Eng. Syst. Saf. 138, 115–134. https://doi.org/10.1016/J.RESS.2015.01.025.

Hänninen, M., Valdez Banda, O.A., Kujala, P., 2014. Bayesian network model of maritime safety management. Expert Syst. Appl. 41, 7837–7846. https://doi.org/10.1016/J.ESWA.2014.06.029.

Håvold, J.I., 2005. Safety-culture in a Norwegian shipping company. J. Saf. Res. 36, 441–458. https://doi.org/10.1016/J.JSR.2005.08.005.

Heckerman, D., Geiger, D., Chickering, D.M., 1995. Learning Bayesian networks: The combination of knowledge and statistical data. Mach. Learn. 1995 203 20, 197–243. https://doi.org/10.1007/BF00994016.

HNS, 1996. International Convention on Liability and Compensation for Damage in Connection with the Carriage of Hazardous and Noxious Substances by Sea (HNS).

Holický, M., Marková, J., Sýkora, M., 2013. Forensic assessment of a bridge downfall using Bayesian networks. Eng. Fail. Anal. 30, 1–9. https://doi.org/10.1016/J.Engfailanal.2012.12.014.

Hsu, H.M., Chen, C.T., 1996. Aggregation of fuzzy opinions under group decision making. Fuzzy Sets Syst. 79, 279–285. https://doi.org/10.1016/0165-0114(95)00185-9.

IACS, 2015. Rules for Classification of sea-going steel ships.

ICS, 2008. Safe Transport of Containers by Sea.

IMO, 2023. Safe transport of containers. https://www.imo.org/en/MediaCentre/HotTopics/Pages/container-default.aspx (accessed 4.28.23).

ISO, 2017. ISO 3874:2017 Series 1 freight containers- Handling and securing.

ISO, 2016. ISO 1161:2016 Series 1 freight containers-Corner and intermediate fittings-Specifications.

ITJ, 2023. "Svendborg Maersk" loses containers off Spain. https://m.transportjournal.com/en/artikeldetail/svendborg-maersk-loses-containers-off-spain.html (accessed 4.28.23).

Jiang, D., Wu, B., Cheng, Z., Xue, J., van Gelder, P.M., 2021. Towards a probabilistic model for estimation of grounding accidents in fluctuating backwater zone of the Three Gorges Reservoir. Reliab. Eng. Syst. Saf. 205, 107239 https://doi.org/10.1016/J.RESS.2020.107239.

Jing, Y., Pavlović, V., Rehg, J.M., 2008. Boosted Bayesian network classifiers. Mach. Learn. 73, 155–184. https://doi.org/10.1007/S10994-008-5065-7/METRICS.

Kamal, B., Kutay, Ş., 2021. Assessment of causal mechanism of ship bunkering oil pollution. Ocean Coast. Manag. 215, 105939 https://doi.org/10.1016/J.Ocecoaman.2021.105939.

Kevin, X., Jingbo, L., Hee Seok, Y., Zaili, B., Jin, W, Y., 2012. Bayesian network with quantitative input for maritime risk analysis. Transp. A Transp. Sci. 10, 89–118. https://doi.org/10.1080/18128602.2012.675527.

Khakzad, N., Khan, F., Amyotte, P., 2011. Safety analysis in process facilities: Comparison of fault tree and Bayesian network approaches. Reliab. Eng. Syst. Saf. 96, 925–932. https://doi.org/10.1016/J.RESS.2011.03.012.

Khan, R.U., Yin, J., Mustafa, F.S., Wang, S., 2022. Analyzing human factor involvement in sustainable hazardous cargo port operations. Ocean Eng. 250, 111028 https://doi.org/10.1016/j.oceaneng.2022.111028.

Li, H., Ren, X., Yang, Z., 2023. Data-driven Bayesian network for risk analysis of global maritime accidents. Reliab. Eng. Syst. Saf. 230, 108938 https://doi.org/10.1016/J.RESS.2022.108938.

Li, X., Sun, B., Guo, C., Du, W., Li, Y., 2020. Speed optimization of a container ship on a given route considering voluntary speed loss and emissions. Appl. Ocean Res. 94 https://doi.org/10.1016/J.APOR.2019.101995.

Liu, J., Duru, O., Law, A.W.K., 2021. Assessment of atmospheric pollutant emissions with maritime energy strategies using bayesian simulations and time series forecasting. Environ. Pollut. 270, 116068 https://doi.org/10.1016/J.ENVPOL.2020.116068.

LLMC, 2004. Convention on Limitation of Liability for Maritime Claims (LLMC). https://www.imo.org/en/About/Conventions/Pages/Convention-on-Limitation-of-Liability-for-Maritime-Claims-(LLMC).aspx.

Lu, C.S., Lai, K.H., Lun, Y.H.V., Cheng, T.C.E., 2012. Effects of national culture on human failures in container shipping: The moderating role of Confucian dynamism. Accid. Anal. Prev. 49, 457–469. https://doi.org/10.1016/J.AAP.2012.03.018.

Lu, C.S., Tsai, C.L., 2008. The effects of safety climate on vessel accidents in the container shipping context. Accid. Anal. Prev. 40, 594–601. https://doi.org/10.1016/J.AAP.2007.08.015.

Mahadevan, S., Zhang, R., Smith, N., 2001. Bayesian networks for system reliability reassessment. Struct. Saf. 23, 231–251. https://doi.org/10.1016/S0167-4730(01)00017-0.

MARPOL, 1978. International Convention for the Prevention of Pollution from Ships (MARPOL).
  2022 MSC, 2022. Development of Measures Regarding the Detection and Mandatory Reporting of Containers Lost at Sea that May Enhance The Positioning, Tracking and Recovery of Such Containers.

Murdoch, E., Tozer, D., 2012. A Masters Guide to Container Securing, 2nd ed. Lloyd's Register nad The Standad Club, London.

NICRW, 2007. Nairobi International Convention on the Removal of Wrecks, 2007. https://www.imo.org/en/About/Conventions/Pages/Nairobi-International-Convention-on-the-Removal-of-the-Removal-of-Wrecks.aspx.

Niimi, A.J., 2004. Role of container vessels in the introduction of exotic species. Mar. Pollut. Bull. 49, 778–782. https://doi.org/10.1016/J.MARPOLBUL.2004.06.006.

Offshore Energy, 2023. Why Containers Get Lost at Sea? - Offshore Energy. https://www.offshore-energy.biz/why-containers-get-lost-at-sea/ (accessed 5.2.23).

Pristrom, S., Yang, Z., Wang, J., Yan, X., 2016. A novel flexible model for piracy and robbery assessment of merchant ship operations. Reliab. Eng. Syst. Saf. 155, 196–211. https://doi.org/10.1016/J.RESS.2016.07.001.

Rajakarunakaran, S., Maniram Kumar, A., Arumuga Prabhu, V., 2015. Applications of fuzzy faulty tree analysis and expert elicitation for evaluation of risks in LPG refuelling station. J. Loss Prev. Process Ind. https://doi.org/10.1016/J.JLP.2014.11.016.

Ramzali, N., Lavasani, M.R.M., Ghodousi, J., 2015. Safety barriers analysis of offshore drilling system by employing Fuzzy Event Tree Analysis. Saf. Sci. 78, 49–59. https://doi.org/10.1016/J.SSCI.2015.04.004.

Rathnayaka, S., Khan, F., Amyotte, P., 2012. Accident modeling approach for safety assessment in an LNG processing facility. J. Loss Prev. Process Ind. 25, 414–423. https://doi.org/10.1016/J.JLP.2011.09.006.

Ross, T.J., 2000. Membership Functions, Fuzzification and Defuzzification 48–77. https://doi.org/10.1007/978-3-7908-1859-8_3.

Şakar, C., Zorba, Y., 2017. A Study on Safety and Risk Assessment of Dangerous Cargo Operations in Oil/Chemical Tankers. J. ETA Marit. Sci. 5, 396–413. https://doi.org/10.5505/JEMS.2017.09226.

Saliba, M., Frantzi, S., van Beukering, P., 2022. Shipping spills and plastic pollution: A review of maritime governance in the North Sea. Mar. Pollut. Bull. 181, 113939 https://doi.org/10.1016/j.marpolbul.2022.113939.

Senol, Y.E., Yasli, F., 2021. A risk analysis study for chemical cargo tank cleaning process using Fuzzy Bayesian Network. Ocean Eng. 235, 109360 https://doi.org/10.1016/J.OCEANENG.2021.109360.

Sewwandi, M., Hettithanthri, O., Egodage, S.M., Amarathunga, A.A.D., Vithanage, M., 2022. Unprecedented marine microplastic contamination from the X-Press Pearl container vessel disaster. Sci. Total Environ. 828, 154374 https://doi.org/10.1016/j.scitotenv.2022.154374.

SFR, 2020. ONE Apus - Container stack collapse - Update https://www.shippingandfreightresource.com/one-apus-container-stack-collapse-update-7th-dec/ (accessed 4.28.23).

Shan, M., Chan, A.P.C., Le, Y., Xia, B., Hu, Y., 2015. Measuring Corruption in Public Construction Projects in China. J. Prof. Issues Eng. Educ. Pract. 141 https://doi.org/10.1061/(ASCE)EI.1943-5541.0000241.

Shigunov, V., 2009. Operational Guidance for Prevention of Container Loss, in: Proceedings of the 10th International Conference on Stability of Ships and Ocean Vehicles (STAB2009). pp. 473–482.

ShippingKnowledge, 2017. Why and How Many of Cargo Containers are Lost at Sea? https://shippingknowledge.com/container-shipping/many-cargo-containers-lost-sea/.

SOLAS, 1974. Int. Conv. Saf. Life Sea. Int. Conv. Saf. Life Sea 1974.

Surfrider Foundation Europe, 2019. 10 proposals to prevent container losses Table of contents.

The Maritime Executive, 2017. Dramatic Drop in Containers Lost at Sea. https://maritime-executive.com/article/dramatic-drop-in-containers-lost-at-sea (accessed 4.28.23).

The Maritime Post, 2022. Lost at Sea: How Shipping Containers' Pollution affects Marine Life. https://themaritimepost.com/2022/02/how-lost-containers-affecting-marine-life/.

The Swedish Club, 2020. Container focus-Preventing the loss of containers at sea.

TheShip, 2023. How Many Shipping Containers Are Lost at Sea Every Year?. https://theship.ai/blog/how-many-shipping-containers-are-lost-at-sea-every-year/ (accessed 4.28.23).

Turna, İ., 2022a. A safety risk assessment for ship boarding parties from fuzzy Bayesian networks perspective. https://doi.org/10.1080/03088839.2022.2112780. https://doi.org/10.1080/03088839.2022.2112780.

Turna, İ., 2022b. A Fuzzy Bayesian approach for 'Appraisal' of ship voyage plans. https://doi.org/10.1080/17445302.2022.2077279. https://doi.org/10.1080/17445302.2022.2077279.

Turner, A., Williams, T., Pitchford, T., 2021. Transport, weathering and pollution of plastic from container losses at sea: Observations from a spillage of inkjet cartridges in the North Atlantic Ocean. Environ. Pollut. 284, 117131 https://doi.org/10.1016/J.ENVPOL.2021.117131.

Uğurlu, F., Yıldız, S., Boran, M., Uğurlu, Ö., Wang, J., 2020. Analysis of fishing vessel accidents with Bayesian network and Chi-square methods. Ocean Eng. 198, 106956 https://doi.org/10.1016/J.OCEANENG.2020.106956.

UNCTAD, 2022. Review of Maritime Transport 2022, Review of Maritime Transport.

UNCTAD, 2019. Review of Maritime Transport 2019.

UNCTAD, 2018. United Nations Conf. on Trade and Develop., Review of Maritime Transport 2018, in: United Nations Conf. on Trade and Develop., Review of Maritime Transport 2018.

V.G.M. Rules, 2014. Verification of the gross mass of a packed container. https://www.imo.org/en/OurWork/Safety/Pages/Verification-of-the-gross-mass.aspx (accessed 5.4.23).

Wan, S., Yang, X., Chen, X., Qu, Z., An, C., Zhang, B., Lee, K., Bi, H., 2022. Emerging marine pollution from container ship accidents: Risk characteristics, response strategies, and regulation advancements. J. Clean. Prod. 376, 134266 https://doi.org/10.1016/J.JCLEPRO.2022.134266.

Wang, W.J., 1997. New similarity measures on fuzzy sets and on elements. Fuzzy Sets Syst. 85, 305–309. https://doi.org/10.1016/0165-0114(95)00365-7.

WSC, 2022. Containers Lost at Sea 2022 Update.

WSC, 2021. Marin Top Tier-Securing Container Safety, https://www.marin.nl/en/jips/toptier (accessed 5.4.23).

WSC, 2017. Containers Lost At Sea – 2017 Update.

WSC, 2014. Survey Results for Containers Lost At Sea – 2014 Update.

Yang, J., Tang, T., Jiang, Y., Karavalakis, G., Durbin, T.D., Wayne Miller, J., Cocker, D.R., Johnson, K.C., 2021. Controlling emissions from an ocean-going container vessel with a wet scrubber system. Fuel 304, 121323. https://doi.org/10.1016/J.FUEL.2021.121323.

Yang, Z., Bonsall, S., Wang, J., 2008. Fuzzy rule-based Bayesian reasoning approach for prioritization of failures in FMEA. IEEE Trans. Reliab. 57, 517–528. https://doi.org/10.1109/TR.2008.928208.

Yazdi, M., Kabir, S., 2017. A fuzzy Bayesian network approach for risk analysis in process industries. Process Saf. Environ. Prot. 111, 507–519. https://doi.org/10.1016/J.PSEP.2017.08.015.

Yiğit, K., 2022. Evaluation of energy efficiency potentials from generator operations on vessels. Energy 257, 124687. https://doi.org/10.1016/J.ENERGY.2022.124687.

Zadeh, L.A., 1965. Fuzzy sets. Inf. Control 8, 338–353. https://doi.org/10.1016/S0019-9958(65)90241-X.

Zarei, E., Yazdi, M., Abbassi, R., Khan, F., 2019. A hybrid model for human factor analysis in process accidents: FBN-HFACS. J. Loss Prev. Process Ind. 57, 142–155. https://doi.org/10.1016/J.JLP.2018.11.015.

Zhang, D., Yan, X.P., Yang, Z.L., Wall, A., Wang, J., 2013. Incorporation of formal safety assessment and Bayesian network in navigational risk estimation of the Yangtze River. Reliab. Eng. Syst. Saf. 118, 93–105. https://doi.org/10.1016/J.RESS.2013.04.006.

Zhang, G., Thai, V.V., Yuen, K.F., Loh, H.S., Zhou, Q., 2018. Addressing the epistemic uncertainty in maritime accidents modelling using Bayesian network with interval probabilities. Saf. Sci. 102, 211–225. https://doi.org/10.1016/J.SSCI.2017.10.016.

Zhou, Y., Li, X., Yuen, K.F., 2022. Holistic risk assessment of container shipping service based on Bayesian Network Modelling. Reliab. Eng. Syst. Saf. 220, 108305 https://doi.org/10.1016/J.RESS.2021.108305.

ARTICLES FOR FACULTY MEMBERS

NAVIGATIONAL RISK OF CONTAINER FALLS IN THE STRAIT OF MALACCA

Title/Author	Exploring spatial patterns and environmental risk factors for global maritime accidents: A 20-year analysis / Zhou, X., Ruan, X., Wang, H., & Zhou, G.
Source	*Ocean Engineering* Volume 286 Part 1 (2023) 115628 Pages 1-10 https://doi.org/10.1016/j.oceaneng.2023.115628 (Database: ScienceDirect)

Exploring spatial patterns and environmental risk factors for global maritime accidents: A 20-year analysis

Xiao Zhou [a,*], Xiaoguang Ruan [b], Han Wang [c], Guoqing Zhou [d]

[a] *College of Urban and Environmental Sciences, Central China Normal University, Wuhan 430079, China*
[b] *College of Geomatics and Municipal Engineering, Zhejiang University of Water Resources and Electric Power, Hangzhou 310018, China*
[c] *Institute of Remote Sensing and Geographic Information System, School of Earth and Space Sciences, Peking University, Beijing 100871, China*
[d] *Guangxi Key Laboratory of Spatial Information and Geomatics, Guilin University of Technology, Guilin 541004, China*

ABSTRACT

The global shipping industry faces increasingly complex safety challenges due to the rapid growth of international maritime trade. This study develops a novel framework that combines spatial density analysis and machine learning (i.e., extreme gradient boosting model) to investigate the evolutionary patterns of global maritime accidents during 2001–2020 from both spatial and temporal dimensions, and then identifies key environmental risk factors affecting maritime safety. The results show that the number of global maritime accidents exhibits fluctuations between 2001 and 2019, with a significant decrease observed in 2020. Furthermore, the distribution of global maritime accidents shows significant spatial variation over different time periods. Denmark's sea areas have high accident rates between 2001 and 2005, while concentrated accidents are observed in the seas around the United Kingdom, Denmark, and China between 2006 and 2010. From 2011 to 2015, Europe's accident-prone areas increase, but fewer accidents are reported along China's east coast. The Strait of Malacca is also an accident-prone area from 2016 to 2020. In addition, wave height, sea surface temperature, wind speed, water depth, and precipitation are identified as key environmental risk factors affecting maritime safety. These findings can inform strategies and mitigation plans to improve navigational safety in the global shipping industry.

1. Introduction

Economic globalization has accelerated the growth of the global shipping industry over the past decade. Shipping accounts for about 90% of global trade (Zhou, 2022). However, with the rapid increase in the size and number of ships, maritime accidents are expected to become more frequent, resulting in significant casualties and environmental damage (Knapp and Heij, 2017; Zhou et al., 2020c). From 2014 to 2021, the European Maritime Safety Agency (EMSA) recorded a total of 21,173 marine casualties and incidents, causing 6,155 injuries, 563 fatalities, 495 pollution cases, and the loss of 177 ships (EMSA, 2022). Maritime safety has become a growing concern for maritime authorities, shipping companies, and the general public. The International Maritime Organization (IMO) has consistently demonstrated its commitment to improving maritime safety through the promulgation of a plethora of laws, regulations, and guidelines (Huang et al., 2023). Therefore, research on maritime accidents is crucial to improve maritime safety and reduce fatalities and property losses (Zhou et al., 2019).

The knowledge gained from maritime accidents has served as a cornerstone in the development of modern maritime safety management practices (Chen et al., 2020). Researchers typically focus on the three aspects of maritime accidents (Liu et al., 2021; Zhang et al., 2021; Wang et al., 2022): (1) statistical characteristics analysis (Hassel et al., 2011; Bye and Almklov, 2019), (2) accident consequences and influencing factors (Jin, 2014; Afenyo et al., 2017), and (3) risk assessment (Antão and Soares, 2019; Zhou et al., 2020a). In the last decade, spatial data from remote sensing and GPS have increased, providing basic data for maritime accident studies globally. It has been shown that maritime accidents tend to occur in specific geographical locations (Huang et al., 2013). Therefore, Spatial-based maritime accident studies have gained popularity in recent years and have contributed to a better understanding of marine accident patterns (e.g., Acharya et al., 2017; Zhang et al., 2021; Wang et al., 2022). However, most of these studies have focused on a limited area of the ocean (Zhang et al., 2021), and there is a lack of investigation into the spatial and temporal evolutionary patterns of marine accidents. In addition, few studies have identified the
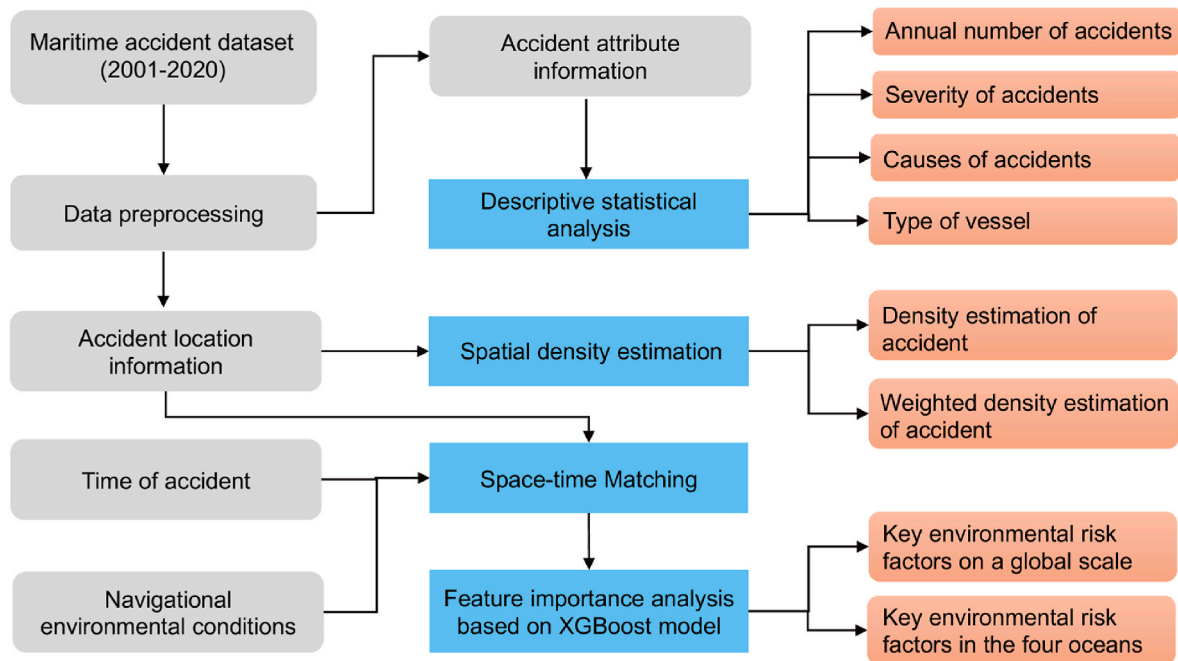

Fig. 1. The process flow of the proposed methodological framework.

environmental risk factors that affect the navigational safety of ships, considering the spatial heterogeneity.

To address the above research gaps, this study develops a novel framework combining spatial density analysis and machine learning (i. e., extreme gradient boosting (XGBoost) model) to investigate the evolutionary patterns of global maritime accidents during 2001–2020 from both spatial and temporal dimensions, and then identify the key environmental risk factors affecting the navigational safety of ships. The findings of this study may assist relevant authorities in developing customized safety plans, allocating research and rescue resources, and making more precise decisions. The rest of this study is organized as follows. Section 2 summarizes the related studies. In Section 3, the methodological framework is proposed, and the data used in this study are described. Sections 4 and 5 present the results and discussion, respectively. The conclusions are given in Section 6.

2. Literature review

2.1. Analysis of spatial patterns of maritime accident

Studies on maritime accidents have primarily focused on statistical analysis, accident consequences and influencing mechanisms, and risk assessment (Liu et al., 2021; Zhang et al., 2021; Wang et al., 2022). Since accidents are highly correlated with their locations, geospatial techniques have been used in recent years to investigate the spatial patterns of maritime accidents.

In this regard, some scholars have made helpful contributions. For example, Acharya et al. (2017) collected a database of accidents that occurred in the coastal areas around Korea from 2007 to 2014 and used buffer and cluster analysis to investigate the distribution of maritime accidents. Isnan (2021) utilized Geographical Information Systems (GIS) tools to determine the accident-prone areas in Malaysian waters. In addition, Yildiz et al. (2022) generated maritime accident density maps in Istanbul Strait and Dover Strait by using accident reports between 2004 and 2020 and applying GIS tools. However, a global analysis of maritime accidents is particularly rare. One example is Zhang et al. (2021), who used Kernel Density Estimation (KDE) and K-means clustering methods to explore the spatial patterns and characteristics of global maritime accidents from 2003 to 2018. Another example is Wang

et al. (2022), who developed a framework to integrate density analysis and clustering analysis to reveal the distribution characteristics of global maritime accidents during 2010–2019.

Although there has been considerable progress in spatial-based studies of maritime accidents, these studies have primarily focused on limited maritime areas (Zhang et al., 2021). Others have analyzed accident-prone areas without further examining the spatial and temporal evolution of maritime accidents. For maritime safety management, it is crucial to conduct a global perspective analysis of the spatio-temporal evolution of maritime accidents.

2.2. Identification of risk influencing factors

Studying the risk factors that affect the safety of ships can help identify their causes and effects and provide more detailed policy recommendations to governments. Researchers have used various methods to numerically analyze the relationships between factors contributing to marine casualties. Statistical models are among the most commonly used approaches in previous studies. For example, Weng and Yang (2015) used binary logistic regression to examine the probability of fatal accidents and found that accidents occur more frequently during adverse weather and darkness. Fu et al. (2016) presented a causal probabilistic model to calculate the probability of a ship becoming stuck in Arctic waters. The model analyzed several risk factors, including wave height and wind speed. Bye and Aalberg (2018) applied logistic regression analysis to identify the critical factors associated with maritime accidents in Norwegian waters. In addition, Wang et al. (2021) developed a framework based on fault tree analysis and Bayesian network to investigate the key risk factors in ship fire accidents. Similarly, Sokukcu and Sakar (2022) conducted a probabilistic risk analysis of collision accidents and identified important risk factors. Eski and Tavacioglu (2022) combined the entropy weight method with the grey relational analysis to assess the influencing factors of crew fatalities and serious injuries.

In recent years, the emergence of machine learning has provided an alternative approach to improving maritime risk management. Mendonça et al. (2022) indicated that machine learning models accelerate data interpretation and uncover hidden patterns. Compared to traditional methods, machine learning models can better determine the

likelihood and consequences of maritime accidents using ship position data, accident data, and other relevant information (Rawson and Brito, 2023). Munim et al. (2020) conducted a bibliometric analysis of artificial intelligence applications in the marine industry and identified four underlying research fields: digital transformation, AIS data analysis, energy efficiency, and predictive analytics. However, few studies have attempted to use these techniques to assess maritime risks and specifically identify key risk factors (Rawson and Brito, 2023). Therefore, this study aims to explore the relationship between accident events and environmental risk factors using machine learning algorithms and then identify key risk factors.

3. Methodology and data

The proposed methodological framework is shown in Fig. 1. First, global marine accident data for the period 2001–2020 were collected from the Global Integrated Shipping Information System database. Any garbled records were either corrected or eliminated. In addition, the original dataset contained a total of 22 fields, many of which were found to be irrelevant or unusable for the present study and were subsequently removed. As a result, a refined dataset consisting of 8,338 accident records with 6 relevant fields was obtained after the aforementioned data manipulation process. The 6 fields used in this research include the type of casualty, time of accident, initial event, type of vessel, latitude, and longitude. Descriptive statistical analysis was performed on the accident attribute information to explore the general characteristics of marine accidents. Subsequently, records without latitude and longitude information were filtered out, resulting in a total of 5,537 accident records. These records were then imported into ArcGIS software for spatial density estimation, which can identify accident-prone areas worldwide and their evolutionary patterns. Then, the nine key factors of the navigational environment were selected and related data were collected. Finally, space-time matching between marine accidents and their corresponding navigation environments was performed, and an XGBoost model was used to identify key environmental risk factors.

3.1. Point density estimation

This study refers to the existing literature (Huang et al., 2013; Zhang et al., 2021) and proposes that maritime accidents exhibit spatial patterns, with variations in accident characteristics across different regions. Furthermore, it is assumed that historical data can effectively capture the underlying patterns and distributions of maritime accidents (Akbari et al., 2018). As a result, identifying areas with high accident frequency can help national or maritime organizations to develop targeted safety strategies, allocate maritime rescue resources, and improve overall maritime safety.

The point density estimation is one of the most commonly used spatial analysis tools for observing how samples are distributed in a study area. In point density analysis, each grid has a neighborhood around its center, which can be circular, rectangular, or another shape. The point density is obtained by adding the number of points within a neighborhood, and this sum is then divided by the area of the neighborhood (Yeh et al., 2017). This analysis creates a density surface using points, which is then mathematically converted into a raster surface (Zhou et al., 2023). The accident density of each grid can be calculated as follows:

$$PD = \frac{\sum\limits_{j \in A} N_j}{S_A} \tag{1}$$

where PD represents the accident density, N_j represents the j-th accident point, and S_A represents the area of neighborhood A.

The size of the grid cell is crucial, as larger cells result in coarse data representation, while smaller cells result in excessive non-accident cells (Zhang et al., 2021). Previous studies on maritime accidents have used different grid cell sizes such as 0.1°, 0.5°, and 2° (Ugurlu et al., 2013; Zhang et al., 2021). This study tests the grid size in the range of 0.1°–2° with a step size of 0.1°. The results show that a cell size of 0.5° is chosen, which ensures accuracy and mitigates the occurrence of a significant number of non-accident cells. This parameter choice is consistent with Zhang et al. (2021).

To consider the effect of accident severity, a more comprehensive density estimation can be obtained by taking the severity of the accident as a weight for each accident. In the Global Integrated Shipping Information System database, maritime accidents are categorized into three levels: very serious, serious, and less serious. According to the severity of the accident, accidents with very serious, serious, and less serious levels are weighed by 3, 2, and 1, respectively (Wang et al., 2022). Therefore, the weighted accident density of each grid can be calculated as follows:

$$WPD = \frac{\sum\limits_{j \in A} N_j * w_j}{S_A} \tag{2}$$

where WPD represents the weighted accident density, *and w_j represents* the weight of the j-th accident point.

3.2. XGBoost model

The XGBoost is one of the most widely used machine learning models for solving classification and regression problems (Rawson et al., 2022). The XGBoost algorithm can be described as follows: using a dataset with n examples and m features, the ensemble general tree model generates predictions that are the sum of predictions made by independent trees (Yun et al., 2021). The equation is as follows:

$$\widehat{y}_i = \sum\nolimits_{k=1}^{K} f_k(x_i), f_k \in F \tag{3}$$

where $\widehat{y}_i$ indicates the predicted value, F indicates the space of regression trees. There are independent weights and tree structures for each f_k. To obtain optimal parameters, the objective function is minimized as follows:

$$L = \sum_i l(\widehat{y}_i, y_i) + \sum_k \Omega(f_k) \tag{4}$$

where l indicates a differentiable convex loss function. $\Omega(f)$ indicates a model complexity for regularization.

In addition, the XGBoost can identify key features based on the importance score ranking. The algorithm determines importance by "gain," "weight," or "cover" (Song et al., 2023). Here, feature importance is set by "weight." Weight refers to the number of times a feature is used for splitting data across trees. In this study, we selected nine environmental risk factors as features after an extensive review of studies related to maritime accidents (e.g., Wang et al., 2014; Khan et al., 2018; Qian et al., 2020; Zhou et al., 2020a; Rawson et al., 2022), These nine risk factors are as follows: (1) water depth, (2) wind speed, (3) significant wave height, (4) precipitation, (5) sea ice cover, (6) snowfall, (7) sea surface temperature, (8) distance to coastline, and (9) distance to port.

3.3. Data collection

(1) Maritime accident data

The IMO develops the Global Integrated Shipping Information System database, which includes modules such as marine casualties and incidents, ship fuel oil consumption, and a global search and rescue plan. This database is widely used in marine studies due to its transparency, usability, availability, and clearly defined structures (Zhang et al., 2021). For this study, we collected global ship accident data from the marine casualties and incidents module during the period 2001–2020, obtaining a total of 8,338 historical records. This dataset contains

Table 1

Navigation environment data used in this study.

Name	Source	Time	Output
Water depth	Global gridded bathymetric data (https://www.gebco.net/)	2019	Water depth
10-m wind speed	European Center for Medium-Range Weather Forecasts (https://www.ecmwf.int)	2001–2020	Wind speed
Significant wave height			Significant wave height
Precipitation			Precipitation
Sea-ice cover			Sea ice cover
Snowfall			Snowfall
Sea surface temperature			Sea surface temperature
Coastline	Global Self-consistent, Hierarchical, High-resolution Geography Database (https://www.ngdc.noaa.gov/mgg/shorelines/)	2017	Distance to Coastline
Port	World seaports catalogue, marine and seaports marketplace (http://ports.com/)	2020	Distance to port

several fields, and six key fields, including type of casualty, time of accident, initial event, type of vessel, latitude, and longitude, are used for descriptive analysis. Additionally, due to the loss of location information in some records, further spatial analysis was conducted on 5,537 accident records with complete coordinates.

(2) Navigation environment data

One of the objectives of this study is to analyze the risks associated with environmental conditions such as meteorological environment, topographic condition, and hydrological environment. Table 1 shows the data collected on the navigation environment.

4. Results

4.1. Characteristics of global maritime accidents

Fig. 2A illustrates the annual number of global maritime accidents from 2001 to 2020, showing a trend of fluctuation throughout this time period. However, there is a significant decrease in accidents in 2020. This can be attributed to the impact of COVID-19 on the global economy, which resulted in a noticeable decrease in trade activities (Saviolakis and Pazarzis, 2021; Chua et al., 2022). Maritime transportation accounts for approximately 90% of global trade (Zhou, 2022). With the decrease in maritime activities, the number of maritime accidents has also decreased. The IMO categorizes maritime accidents into three severity levels: very serious, serious, and less serious. As shown in Fig. 2B, in the past twenty years, the proportion of very serious accidents and serious accidents accounts for 48.9% and 41.2%, respectively, while the proportion of less serious accidents is only 9.9%. To analyze the changes in the proportion of these three severity levels over time, we further divided the data into 5-year periods. The percentage of very serious accidents increases, while the percentage of serious accidents shows a downward trend. Less serious accidents account for only a small percentage of the total across all four-time intervals.

To prevent and investigate maritime accidents, it is crucial to identify the initial events that lead to these accidents. Fig. 3A displays the proportion of different initial events that cause maritime accidents from 2001 to 2020. The most common causes of maritime accidents are collision, stranding or grounding, and fire or explosion, accounting for 22.1%, 19.7%, and 16.7%, respectively. In addition, rare initial events such as foundering, hull failure, and missing have been grouped together under "Others," which accounts for 19.8% of the total number of accidents. The distribution of initial events across four-time intervals indicates a decreasing trend for some types of initial events (e.g., stranding or grounding), while the proportion of accidents with initial events labeled as "Others" shows an increasing trend. This suggests that the causes of maritime accidents are becoming more complex.

Furthermore, an analysis of maritime accidents based on the types of ships involved (Fig. 3B) reveals that general cargo ships are involved in the highest number of accidents (24.9%) from 2001 to 2020. Fish
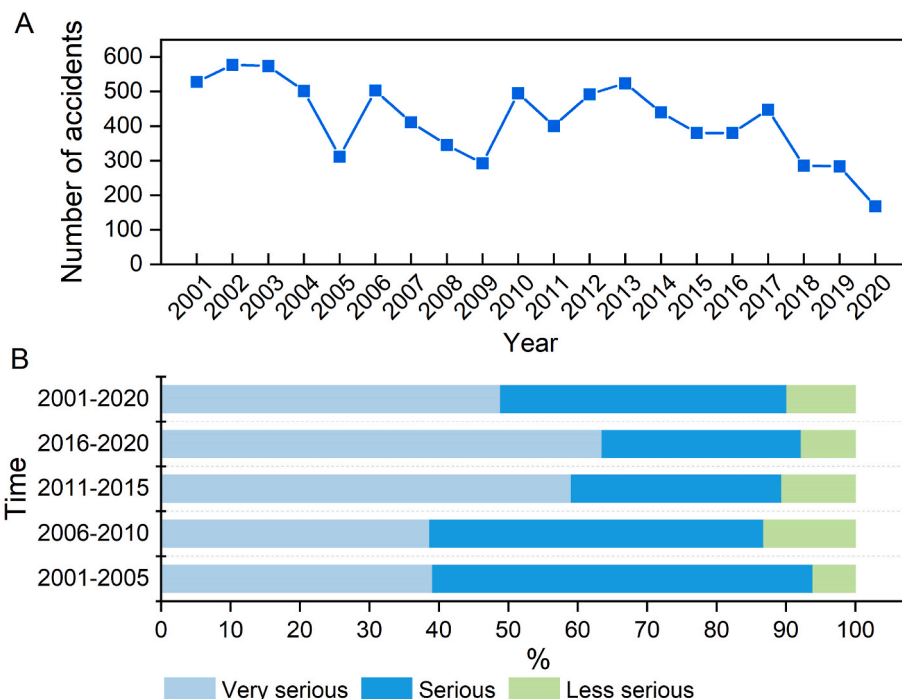

Fig. 2. The annual number of maritime accidents (A) and their severity levels based on casualty effects (B).
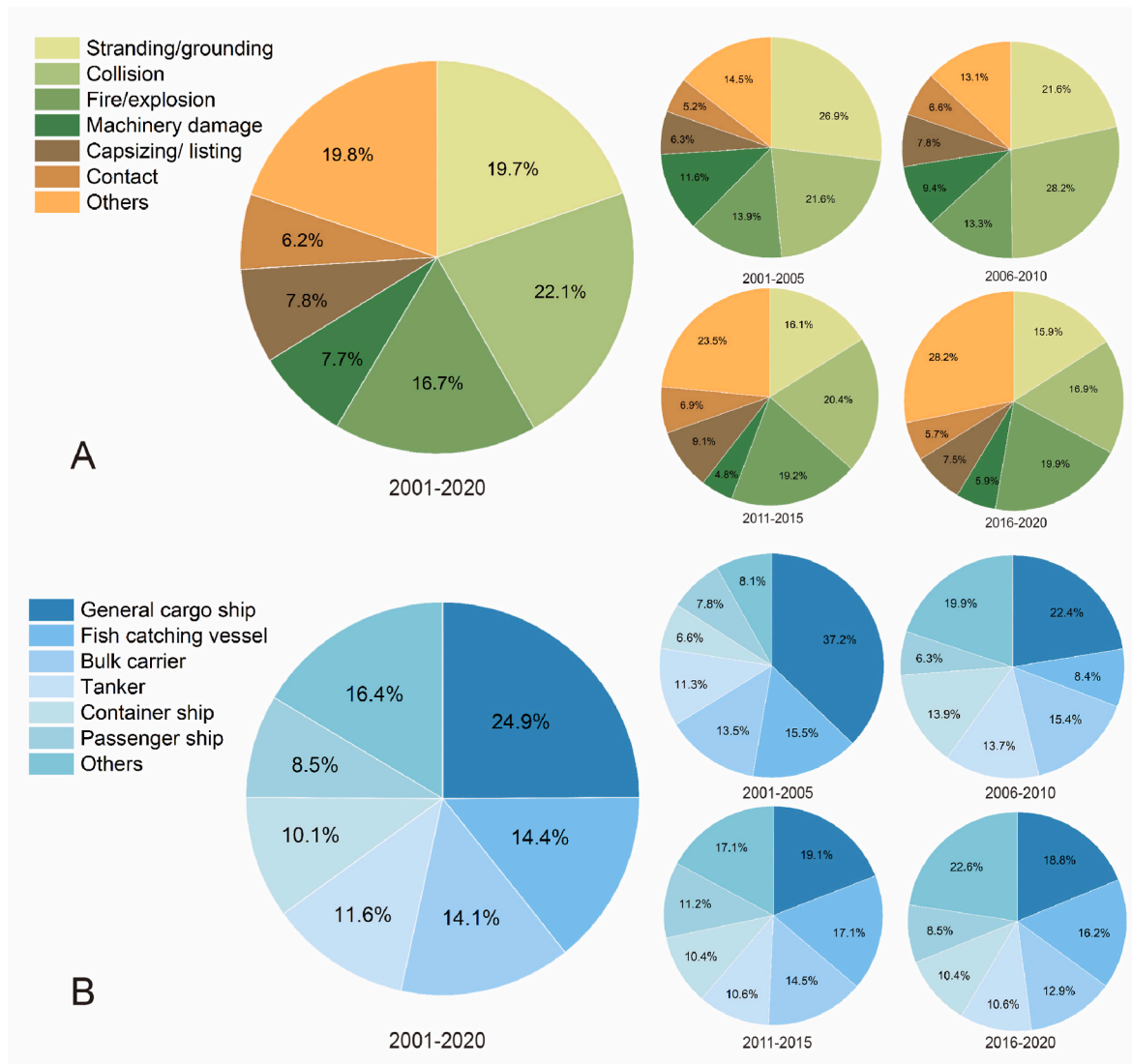
Fig. 3. The distribution of initial events (A) and the ship types (B) involved in maritime accidents.

catching vessels, bulk carriers, tankers, and container ships also have relatively high accident frequencies, accounting for more than 10% of all accidents respectively. The group of "Others" (e.g., cement carrier, research survey vessel, offshore construction vessel, etc.) also constitutes a significant proportion (16.4%) of maritime accidents. Examining the ship type distribution of global maritime accidents for each 5-year period shows a gradual decrease in the proportion of general cargo ships involved in accidents, despite being the most numerous types of ship in the past two decades. On the other hand, the group of "Others" has an upward trend, indicating that with the growing diversification of marine activities, the types of ships involved in maritime accidents are gradually increasing, making search and rescue operations increasingly complicated.

4.2. Spatial distributions of global maritime accidents

Fig. 4A shows the density estimation of global maritime accidents from 2001 to 2020. The density values were divided into six categories using the natural breaks classification method, indicating different levels of density. Higher density values correspond to areas where accidents are more likely to occur. As illustrated in Fig. 4A, the seas around the UK, the seas around Denmark, the northern Mediterranean Sea, parts of the Black Sea, parts of the seas around China, and the Strait of

Malacca have high accident density, indicating that these areas are prone to maritime accidents. The spatial distribution of maritime accidents in these areas can be attributed to several reasons, such as high ship traffic density, dangerous navigable waters, and adverse weather conditions. For example, the coastal waters of China and the west coast of Europe have a high volume of small vessels navigating the area (Wang et al., 2022). The Mediterranean Sea is an important waterway that connects Europe and Asia, as well as Europe and Africa, but its coastline is winding and contains numerous islands, making navigation through the area challenging and increasing the likelihood of accidents (Zhang et al., 2021).

When considering the influence of accident severity, the weighted density of global maritime accidents is calculated, as shown in Fig. 4B. By comparing Fig. 4A and B, additional high-risk seas are identified, including the Gulf of Guinea, the Persian Gulf, the sea areas around Mumbai, and the coastal areas of Vietnam, Japan, and South Korea. This means that these areas have experienced a high number of serious or very serious maritime accidents. In addition, when considering the severity of the accident, the range of density distribution centers is larger, indicating that both the number of accidents and the percentage of serious or very serious accidents are higher in these sea areas than in other regions.

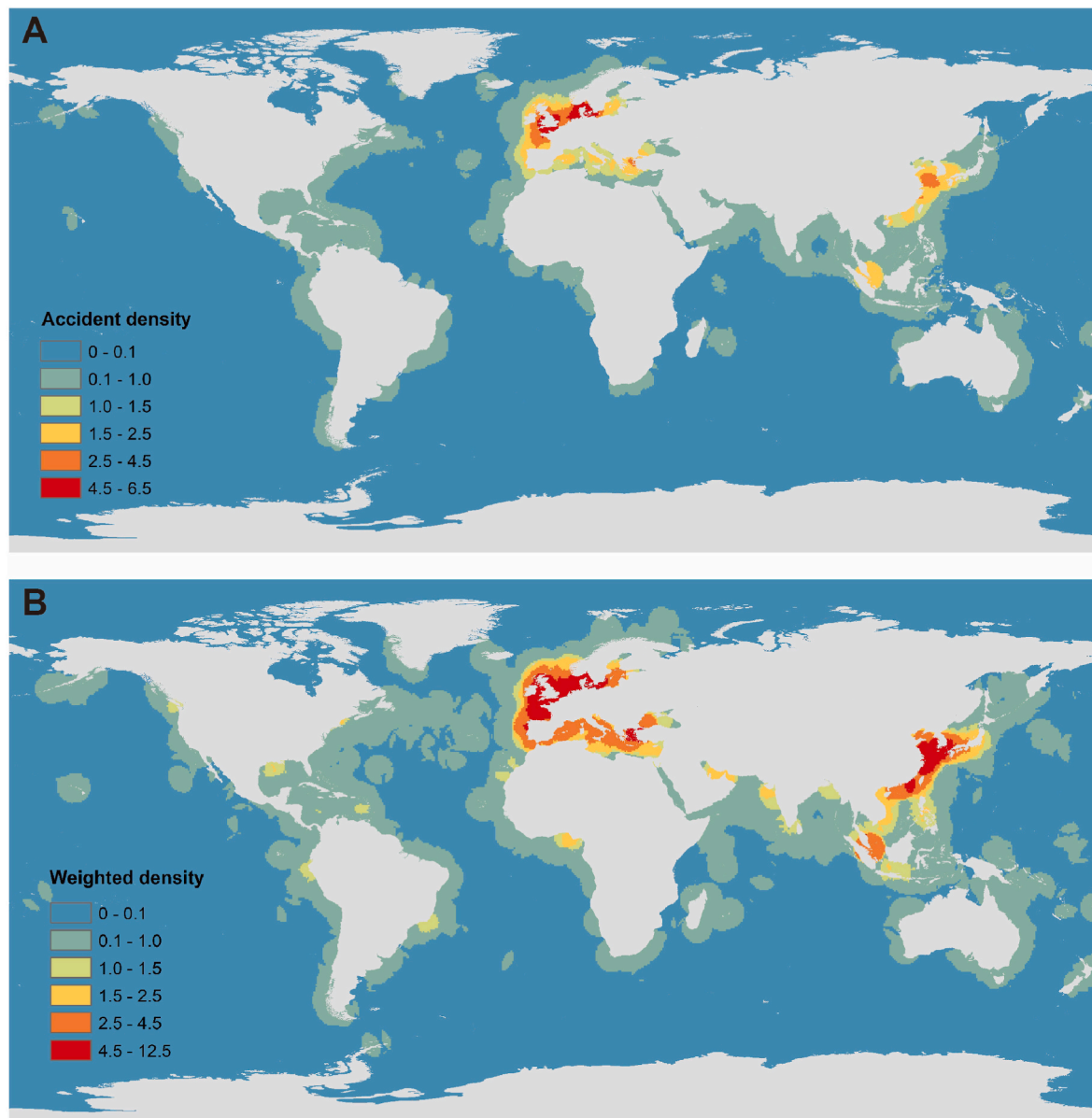Fig. 5 further illustrates the estimated density of global maritime

Fig. 4. Density estimation of global maritime accidents without (A) and with (B) considering the accident severity.

accidents for each 5-year period (i.e., 2001–2005, 2006–2010, 2011–2015, and 2016–2020) while considering the severity of the accident. The accident-prone areas during 2001–2005 were primarily located in the sea areas around Denmark, whereas those during 2006–2010 were concentrated in the seas around the UK, sea areas around Denmark, and parts of the sea areas around China. Between 2011 and 2015, the range of accident-prone areas expanded substantially in the European region, but the accident density on the east coast of China was significantly reduced. In addition to the high-risk areas mentioned earlier, the Strait of Malacca was also identified as an accident-prone region from 2016 to 2020. Therefore, it is essential to pay attention to these changes to ensure maritime safety in the future.

4.3. Environmental risk factor analysis

The XGBoost model is applied to identify the key factors related to accident severity levels. The parameter settings for the XGBoost model were determined based on the principle of achieving the highest accuracy on the test set. We used the XGBoost Python package to conduct this

process. The specific parameter settings are as follows: learning_rate = 0.03, max_depth = 10, n_estimators = 200, and subsample = 0.5. The remaining parameters are set to their default values. To rank the importance of all input features, the feature importance scores (F score) for each feature were calculated. A higher F score indicates a greater importance of a given feature. Fig. 6 shows the feature importance rankings for the global ocean and its major basins (i.e., the Atlantic Ocean, Pacific Ocean, Indian Ocean, and Arctic Ocean). The Southern Ocean is omitted because of limited samples. As shown in Fig. 6A, the most important factor for global maritime accidents is "significant wave height," followed by "sea surface temperature," "wind speed," "water depth," "precipitation, " and others. Although the ranking of importance varies slightly in the four major ocean basins, the key factors remain the same, as shown in Fig. 6B–E. This means that different waters have different environmental hazards that must be considered in advance to prevent maritime accidents.

The key factors identified by the XGBoost model have different impacts on the safety of ship navigation. Water depth is crucial for the safe navigation of a ship, as low bathymetry can cause ships to run aground
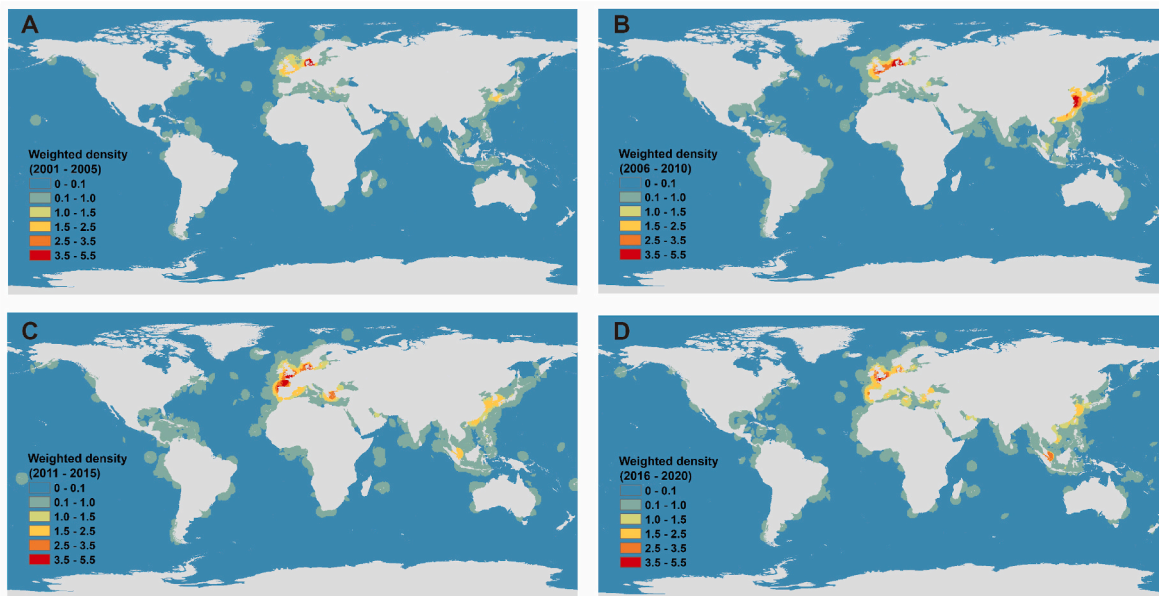
Fig. 5. Density estimation of global maritime accidents with considering accident severity for each 5-years period. A: 2001–2005; B: 2006–2010; C: 2011–2015; and D: 2016–2020.

(Zhou et al., 2020b). Weather events have a significant impact on many maritime socio-economic activities (Rodríguez-Martín et al., 2022). Strong winds can induce lateral drift or leeway in ships, particularly at low speeds, while waves can affect both the depth and width of a channel, with parallel waves affecting heave and pitch, and oblique waves affecting roll and yaw (Briggs et al., 2003). Precipitation can reduce the visibility of a ship's crew members, making it harder to see other vessels, navigational aids, and potential hazards in the water, thereby increasing the risk of collisions, groundings, and other accidents (Zhou, 2022). Sea surface temperature can significantly affect ship navigation safety by affecting water density, weather patterns, and the survival time of a person in the water (Li et al., 2022).

Although at the bottom of the list in terms of feature importance, four factors (i.e., distance to shoreline, distance to port, snowfall, and sea ice cover) also affect the safety of ship navigation. Ships near coastlines and ports are at greater risk due to the high level of social and economic activities in these areas (Zhou et al., 2020a). In addition, as the Arctic route continues to open, an increasing number of vessels are seeking to use it for commercial voyages to reduce transportation costs. However, ships navigating Arctic waters are faced with greater uncertainties due to the heavy snowfall and sea ice compared to ordinary waters (Li et al., 2022). For example, the hull structure and stability of ships can be affected by ice (Kruke and Auestad, 2021).

5. Discussion

Improving maritime safety is essential for promoting global economic and trade development. In this study, we developed a new framework to investigate the evolutionary patterns of global maritime accidents from 2001 to 2020. Our analysis revealed fluctuating accident trends over the years, with a notable decline in 2020. Furthermore, we observed significant spatial variation in the distribution of accidents across different time periods. Previous studies have analyzed the spatial distribution patterns of maritime accidents in different time periods (e. g., Huang et al., 2013; Zhang et al., 2021; Wang et al., 2022). These studies have identified accident hotspots such as the waters around the United Kingdom, the coastal regions of East Asian countries, and the Mediterranean region. However, we not only confirmed these findings, but also investigated the temporal and spatial evolution patterns of global maritime accidents during the period 2001–2020. Our results

revealed significant spatial disparities in global maritime accidents over different time periods, as shown in Fig. 5. This novel finding emphasizes the importance of monitoring changes in accident hotspots over time to ensure the effectiveness of maritime safety measures.

Maritime risk assessment is essential for the development of effective risk reduction policies and strategies. Identifying the key factors and their relative importance is critical to accurately assessing the risk of maritime accidents. Multi-criteria decision making is one of the most commonly used methods for maritime risk assessment. For example, Yu et al. (2022) and Zhou et al. (2020a) used the Analytic Hierarchy Process decision-making method to obtain the weights of risk factors based on expert judgment. However, the weight calculation based on expert judgment may be more subjective, leading to uncertainty in the evaluation process (Xie et al., 2022). In this study, big data and the XGBoost model were used to identify the main environmental risk factors affecting the safety of ship navigation. Compared to traditional weighting approaches, the utilization of the XGBoost model allows for handling complex variable interactions, contributing to accurate risk factor identification.

The chosen approach can significantly impact the results of the study. In addition to the method described in the study, there exist several viable alternatives. These include clustering analysis, regression analysis, and time series analysis. Clustering analysis involves the use of techniques such as k-means to identify accident-prone areas (Wang et al., 2022). Regression analysis can also be used to identify key risk factors (Lu and Tsai, 2008). Time series analysis investigates the temporal patterns of accidents (Zhang et al., 2021). However, the proposed approach offers several advantages over the feasible alternatives mentioned above. First, spatial density estimation provides a comprehensive view of accident-prone areas worldwide, taking into account both the number and severity of accidents. Consequently, the results can provide insights into the global accident distribution, which may differ from localized analyses. Second, the use of the XGBoost model in this study is advantageous because of its ability to handle complex interactions between variables. Maritime accidents can be influenced by a variety of environmental factors, and accurate identification of key risk factors requires consideration of these intricate relationships. The XGBoost model's ability to capture nonlinear interactions and feature importance increases the accuracy of identifying critical environmental risk factors. Rawson et al. (2022) highlight that XGBoost exhibits higher
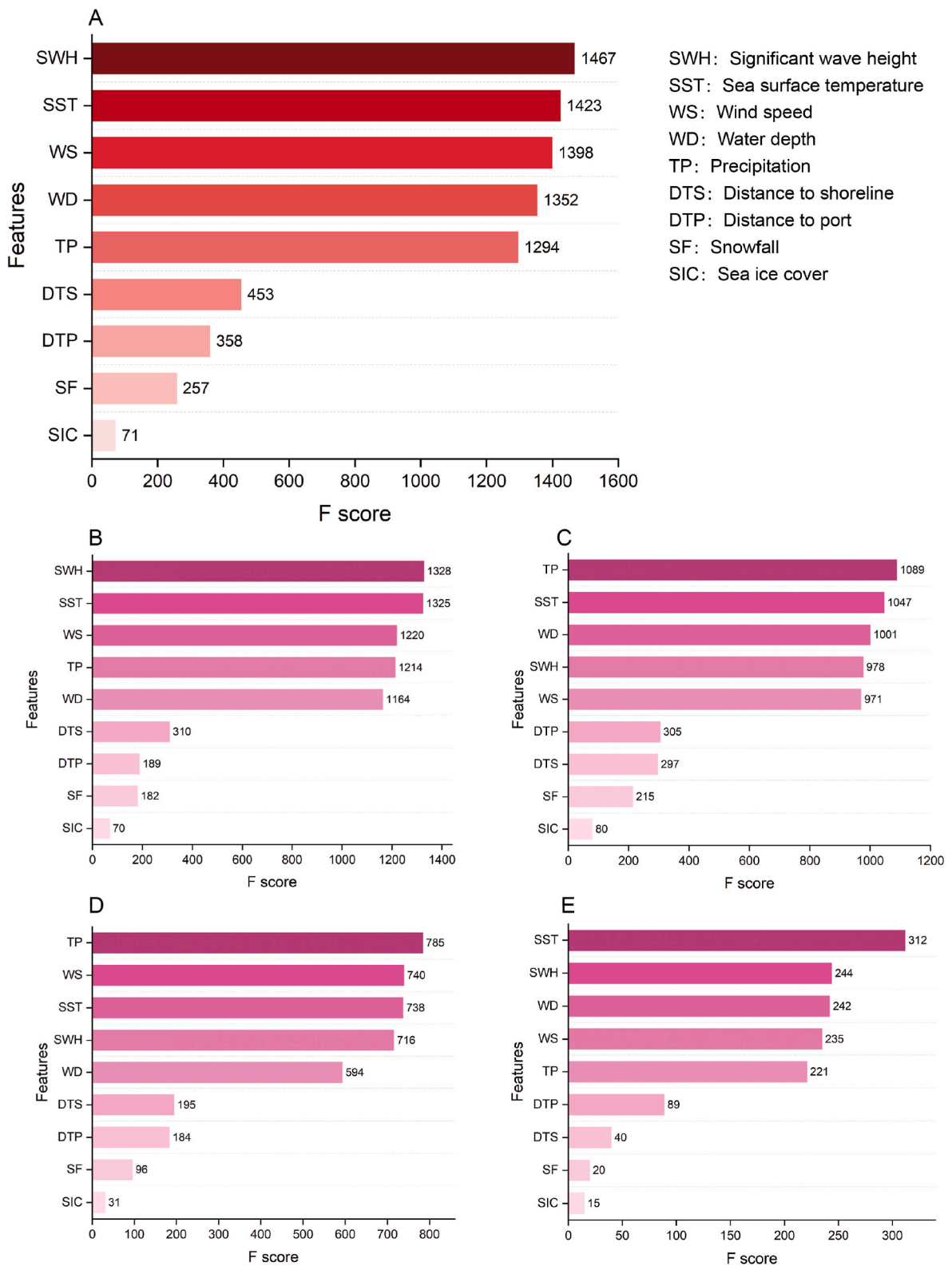
SWH： Significant wave height
SST： Sea surface temperature
WS： Wind speed
WD： Water depth
TP： Precipitation
DTS： Distance to shoreline
DTP： Distance to port
SF： Snowfall
SIC： Sea ice cover

Fig. 6. The ranks of feature importance. A: Global Ocean; B: Atlantic Ocean; C: Pacific Ocean; D: Indian Ocean; E: Arctic Ocean.

performance in maritime risk analysis compared to other machine learning algorithms. In addition, the combination of descriptive statistical analysis, spatial density estimation, and machine learning techniques provides a comprehensive understanding of the characteristics, patterns, and risk factors of maritime accidents.

Nevertheless, there are several limitations to this study. First, while

maritime accident data were obtained from the Global Integrated Shipping Information System, it's possible that additional valuable information could have been obtained from other reputable sources, such as Lloyd's List Intelligence. This suggests that the completeness of maritime accident data could be further improved by collecting additional data from such sources. Second, this study primarily focuses on

environmental risk factors because of the significant uncertainties associated with quantifying internal factors related to technical malfunctions or human-caused errors. However, operational or human factors may also play a critical role in the occurrence of maritime accidents. Therefore, future works should investigate additional influencing factors from different dimensions, which could shed additional light on the overall risk profile of the maritime industry. Despite these limitations, this study provides valuable insights into the spatial and temporal patterns of maritime accidents and identifies key environmental risk factors affecting maritime safety.

6. Conclusions

This study aims to develop a novel framework by integrating spatial density analysis with machine learning, specifically the XGBoost model. The framework is utilized to analyze global maritime accidents during the period of 2001–2020 in terms of their spatial and temporal aspects. In addition, the primary environmental risk factors affecting the safety of ships' navigation are determined. Based on the analysis, the conclusions are as follows:

(1) The number of global maritime accidents showed a fluctuating trend from 2001 to 2019, with a significant decrease observed in 2020. Moreover, the proportion of very serious accidents has shown an increasing trend over time. Collision, stranding or grounding, and fire or explosion were found to be the primary causes of maritime accidents during 2001–2020, collectively accounting for 58.5% of all accidents. General cargo ships were the most frequently involved in accidents (24.9%), followed by fish catching vessels, bulk carriers, tankers, and container ships. Additionally, there is an increasing trend in the proportion of initial events or ship types classified as "Others", indicating a growing complexity in the causes of maritime accidents.

(2) Accident-prone sea areas include the seas around the UK, the sea areas around Denmark, the northern Mediterranean Sea, parts of the Black Sea, the sea areas around China, and the Strait of Malacca. Considering the influence of accident severity, some new high-risk sea areas have been identified, including the Gulf of Guinea, the Persian Gulf, the part of the sea areas around Mumbai, and the coastal areas of Vietnam, Japan, and South Korea.

(3) Global maritime accidents exhibit significant spatial variation across different time periods. During the period from 2001 to 2005, the sea areas around Denmark had a higher frequency of maritime accidents. However, from 2006 to 2010, the concentration of accident-prone regions expanded to include the seas surrounding the United Kingdom and parts of the sea areas around Denmark and China. Between 2011 and 2015, the accident-prone regions in Europe underwent a substantial increase in range, while the density of accidents along the east coast of China demonstrated a noticeable decrease. In addition to the aforementioned accident-prone regions, the Strait of Malacca also emerged as a region with a high frequency of maritime accidents from 2016 to 2020.

(4) The key environmental risk factors that affect the navigational safety of ships include wave height, sea surface temperature, wind speed, water depth, and precipitation. Furthermore, while there may be slight variations in ranking across the four major ocean basins, the underlying key factors driving environmental hazards remain consistent. This suggests that the primary hazards in various bodies of water may differ, and proactive measures should be taken to address these hazards in advance.

This study makes three main contributions. First, the study introduces a novel framework that combines spatial density analysis and machine learning techniques, specifically the XGBoost model. This framework allows for a more comprehensive analysis of maritime accidents by exploiting spatial information and using advanced machine learning algorithms. Second, we conduct an investigation of the evolutionary patterns of global maritime accidents in both spatial and temporal dimensions. By examining the evolutionary patterns, the study can provide a deeper understanding of how maritime accidents have changed over time. Third, by considering spatial heterogeneity, we uncover the specific environmental factors that contribute to maritime accidents. This provides valuable insights for policy makers, maritime authorities, and stakeholders in developing targeted strategies and interventions to mitigate the identified risk factors and enhance maritime safety.

CRediT authorship contribution statement

Xiao Zhou: Conceptualization, Methodology, Formal analysis, Investigation, Writing – original draft, Writing – review & editing, Funding acquisition. **Xiaoguang Ruan:** Conceptualization, Software, Writing – review & editing, Funding acquisition. **Han Wang:** Visualization, Data curation, Validation. **Guoqing Zhou:** Methodology, Supervision.

Declaration of competing interest

The authors declare that they have no known competing financial interests or personal relationships that could have appeared to influence the work reported in this paper.

Data availability

Data will be made available on request.

References

Acharya, T.D., Yoo, K.W., Lee, D.H., 2017. GIS-based spatio-temporal analysis of marine accidents database in the coastal zone of Korea. J. Coast Res. 79 (10079), 114–118.

Afenyo, M., Khan, F., Veitch, B., Yang, M., 2017. Arctic shipping accident scenario analysis using Bayesian Network approach. Ocean Eng. 133, 224–230.

Akbari, A., Eiselt, H.A., Pelot, R., 2018. A maritime search and rescue location analysis considering multiple criteria, with simulated demand. INFOR 56 (1), 92–114.

Antão, P., Soares, C.G., 2019. Analysis of the influence of human errors on the occurrence of coastal ship accidents in different wave conditions using Bayesian Belief Networks. Accid. Anal. Prev. 133, 105262.

Briggs, M.J., Borgman, L.E., Bratteland, E., 2003. Probability assessment for deep-draft navigation channel design. Coast. Eng. 48 (1), 29–50.

Bye, R.J., Aalberg, A.L., 2018. Maritime navigation accidents and risk indicators: an exploratory statistical analysis using AIS data and accident reports. Reliab. Eng. Syst. Saf. 176, 174–186.

Bye, R.J., Almklov, P.G., 2019. Normalization of maritime accident data using AIS. Mar. Pol. 109, 103675.

Chen, J., Di, Z., Shi, J., Shu, Y., Wan, Z., Song, L., Zhang, W., 2020. Marine oil spill pollution causes and governance: a case study of Sanchi tanker collision and explosion. J. Clean. Prod. 273, 122978.

Chua, J.Y., Foo, R., Tan, K.H., Yuen, K.F., 2022. Maritime resilience during the COVID-19 pandemic: impacts and solutions. Continuity Resilience Rev. 4, 124–143.

EMSA, 2022. Annual Overview of Marine Casualties and Incidents. https://www.emsa. europa.eu/we-do/safety/accident-investigation/items.html?cid=141&id=4867. (Accessed 11 July 2023).

Eski, Ö., Tavacioglu, L., 2022. Evaluation of factors influencing maritime dangerous cargo transport accidents-induced crew fatalities and serious injuries. Civ. Eng. J. 8 (10), 2084–2095.

Fu, S., Zhang, D., Montewka, J., Yan, X., Zio, E., 2016. Towards a probabilistic model for predicting ship besetting in ice in Arctic waters. Reliab. Eng. Syst. Saf. 155, 124–136.

Hassel, M., Asbjørnslett, B.E., Hole, L.P., 2011. Underreporting of maritime accidents to vessel accident databases. Accid. Anal. Prev. 43 (6), 2053–2063.

Huang, D.Z., Hu, H., Li, Y.Z., 2013. Spatial analysis of maritime accidents using the geographic information system. Transport. Res. Rec. 2326 (1), 39–44.

Huang, X., Wen, Y., Zhang, F., Han, H., Huang, Y., Sui, Z., 2023. A review on risk assessment methods for maritime transport. Ocean Eng. 279, 114577.

Isnan, S., 2021. Application of GIS: maritime accident analysis in Malaysian waters using Kernel density function. Trans. Marit. Sci. 10 (2), 348–354.

Jin, D., 2014. The determinants of fishing vessel accident severity. Accid. Anal. Prev. 66, 1–7.

Khan, B., Khan, F., Veitch, B., Yang, M., 2018. An operational risk analysis tool to analyze marine transportation in Arctic waters. Reliab. Eng. Syst. Saf. 169, 485–502.

Knapp, S., Heij, C., 2017. Evaluation of total risk exposure and insurance premiums in the maritime industry. Transport. Res. Transport Environ. 54, 321–334.

Kruke, B.I., Auestad, A.C., 2021. Emergency preparedness and rescue in Arctic waters. Saf. Sci. 136, 105163.

Li, Z., Hu, S., Zhu, X., Gao, G., Yao, C., Han, B., 2022. Using DBN and evidence-based reasoning to develop a risk performance model to interfere ship navigation process safety in Arctic waters. Process Saf. Environ. 162, 357–372.

Liu, K., Yu, Q., Yuan, Z., Yang, Z., Shu, Y., 2021. A systematic analysis for maritime accidents causation in Chinese coastal waters using machine learning approaches. Ocean Coast Manag. 213, 105859.

Lu, C.S., Tsai, C.L., 2008. The effects of safety climate on vessel accidents in the container shipping context. Accid. Anal. Prev. 40 (2), 594–601.

Mendonça, Y.V., Naranjo, P.G.V., Pinto, D.C., 2022. The role of technology in the learning process: a decision tree-based model using machine learning. Emerg. Sci. J. 6, 280–295.

Munim, Z.H., Dushenko, M., Jimenez, V.J., Shakil, M.H., Imset, M., 2020. Big data and artificial intelligence in the maritime industry: a bibliometric review and future research directions. Marit. Pol. Manag. 47 (5), 577–597.

Qian, H., Zhang, R., Zhang, Y.J., 2020. Dynamic risk assessment of natural environment based on Dynamic Bayesian Network for key nodes of the arctic Northwest Passage. Ocean Eng. 203, 107205.

Rawson, A., Brito, M., 2023. A survey of the opportunities and challenges of supervised machine learning in maritime risk analysis. Transport Rev. 43 (1), 108–130.

Rawson, A., Brito, M., Sabeur, Z., 2022. Spatial modeling of maritime risk using machine learning. Risk Anal. 42 (10), 2291–2311.

Rodríguez-Martín, J., Cruz-Pérez, N., Santamarta, J.C., 2022. Maritime climate in the canary islands and its implications for the construction of coastal infrastructures. Civ. Eng. J. 8 (1).

Saviolakis, P., Pazarzis, M., 2021. The effect of Covid-19 pandemic on the maritime industry and the role of the ship registries. Emerg. Sci. J. 5, 77–85.

Sokukcu, M., Sakar, C., 2022. Risk analysis of collision accidents during underway STS berthing maneuver through integrating fault tree analysis (FTA) into Bayesian network (BN). Appl. Ocean Res. 126, 103290.

Song, T., Yan, Q., Fan, C., Meng, J., Wu, Y., Zhang, J., 2023. Significant wave height retrieval using XGBoost from polarimetric gaofen-3 SAR and feature importance analysis. Rem. Sens. 15 (1), 149.

Ugurlu, O., Yildirim, U., Yuksekyildiz, E., 2013. Marine accident analysis with GIS. J. Shipp. Ocean Eng. 3 (1–2), 21.

Wang, H., Liu, Z., Liu, Z., Wang, X., Wang, J., 2022. GIS-based analysis on the spatial patterns of global maritime accidents. Ocean Eng. 245, 110569.

Wang, J., Li, M., Liu, Y., Zhang, H., Zou, W., Cheng, L., 2014. Safety assessment of shipping routes in the South China Sea based on the fuzzy analytic hierarchy process. Saf. Sci. 62, 46–57.

Wang, L., Wang, J., Shi, M., Fu, S., Zhu, M., 2021. Critical risk factors in ship fire accidents. Marit. Pol. Manag. 48 (6), 895–913.

Weng, J., Yang, D., 2015. Investigation of shipping accident injury severity and mortality. Accid. Anal. Prev. 76, 92–101.

Xie, L., Zhang, R., Zhan, J., Li, S., Shama, A., Zhan, R., Wang, T., Lv, J., Bao, X., Wu, R., 2022. Wildfire risk assessment in Liangshan Prefecture, China based on an integration machine learning algorithm. Rem. Sens. 14 (18), 4592.

Yeh, C.H., Lin, M.L., Chan, Y.C., Chang, K.J., Hsieh, Y.C., 2017. Dip-slope mapping of sedimentary terrain using polygon auto-tracing and airborne LiDAR topographic data. Eng. Geol. 222, 236–249.

Yildiz, S., Uğurlu, Ö., Loughney, S., Wang, J., Tonoğlu, F., 2022. Spatial and statistical analysis of operational conditions influencing accident formation in narrow waterways: a Case Study of Istanbul Strait and Dover Strait. Ocean Eng. 265, 112647.

Yu, Q., Teixeira, A.P., Liu, K., Soares, C.G., 2022. Framework and application of multi-criteria ship collision risk assessment. Ocean Eng. 250, 111006.

Yun, K.K., Yoon, S.W., Won, D., 2021. Prediction of stock price direction using a hybrid GA-XGBoost algorithm with a three-stage feature engineering process. Expert Syst. Appl. 186, 115716.

Zhang, Y., Sun, X., Chen, J., Cheng, C., 2021. Spatial patterns and characteristics of global maritime accidents. Reliab. Eng. Syst. Saf. 206, 107310.

Zhou, X., 2022. A comprehensive framework for assessing navigation risk and deploying maritime emergency resources in the South China Sea. Ocean Eng. 248, 110797.

Zhou, X., Cheng, L., Li, M., 2020a. Assessing and mapping maritime transportation risk based on spatial fuzzy multi-criteria decision making: a case study in the South China sea. Ocean Eng. 208, 107403.

Zhou, X., Cheng, L., Li, W., Zhang, C., Zhang, F., Zeng, F., Yan, Z., Li, M., 2020b. A comprehensive path planning framework for patrolling marine environment. Appl. Ocean Res. 100, 102155.

Zhou, X., Cheng, L., Min, K., Zuo, X., Yan, Z., Ruan, X., Chu, S., Li, M., 2020c. A framework for assessing the capability of maritime search and rescue in the south China sea. Int. J. Disaster Risk Reduc. 47, 101568.

Zhou, X., Cheng, L., Zhang, F., Yan, Z., Ruan, X., Min, K., Li, M., 2019. Integrating island spatial information and integer optimization for locating maritime search and rescue bases: a case study in the South China Sea. ISPRS Int. J. Geo-Inf. 8 (2), 88.

Zhou, X., Dong, Q., Huang, Z., Yin, G., Zhou, G., Liu, Y., 2023. The spatially varying effects of built environment characteristics on the integrated usage of dockless bike-sharing and public transport. Sustain. Cities Soc. 89, 104348.

ARTICLES FOR FACULTY MEMBERS

NAVIGATIONAL RISK OF CONTAINER FALLS IN THE STRAIT OF MALACCA

Title/Author	**Simulating the impact of the sustained melting arctic on the global container sea–rail intermodal shipping / Sun, Z., Zhang, R., & Zhu, T.**
Source	*Sustainability (Switzerland)* **Volume 14 Issue 19 (2022) 12214 Pages 1-19** **https://doi.org/10.3390/su141912214** **(Database: MDPI)**

Article

Simulating the Impact of the Sustained Melting Arctic on the Global Container Sea–Rail Intermodal Shipping

Zhuo Sun [1,*] **, Ran Zhang** [2] **and Tao Zhu** [1]

1   College of Transportation Engineering, Dalian Maritime University, Dalian 116026, China
2   College of Maritime Economics and Management, Dalian Maritime University, Dalian 116026, China
*   Correspondence: mixwind@gmail.com

Abstract: Global warming trends and the rapid reduction of summer Arctic sea ice extent have increased the feasibility of transarctic transport. How the process of glacier melting affects the existing containerized sea–rail shipping network and container flow assignment has become a challenging economic and policy issue. This paper first examines the meteorological influences on glacier melting and the assignment of container flow over the existing sea–rail network. Then, a three-layer simulation framework is constructed, with the upper layer simulating glacier melting based on the raster grid, the middle layer combining a grid and topology analysis to simulate the evolution of the global sea–rail network and the lower layer establishing a concave cost network flow model to simulate the container flow assignment. Finally, we use MicroCity to achieve the dynamic optimization and simulation of global container flow assignment, solving the large-scale sea–rail shipping network traffic assignment problem. The simulation results show that the proposed model and solution algorithm are feasible and effective, revealing the variation of container flow assignment in the global sea–rail shipping network under different Arctic ice melting scenarios. For instance, in the summer of 2050, the Arctic routes will share the global container flows, resulting in a significant reduction of container flows in the Malacca Strait, Suez Canal and Panama Canal.

Keywords: Arctic routes; container flow assignment; sea ice extent; sea–rail intermodal network

1. Introduction

Maritime transport is the most important mode of transportation in international trade and is also a key element in promoting international trade and global economic integration [1,2]. According to the United Nations Conference on Trade and Development (UNCTAD), seaborne trade has grown at a compound annual rate of 2.9% over the past 20 years. The total global seaborne trade volume reached 10.7 billion tons in 2020. Meanwhile, container trade volume has been growing annually, reaching 149 million twenty-foot equivalent units (TEUs) in 2020 [3]. The volume of container trade between East Asia, North America and Europe accounts for nearly 40% of the global container trade. At present, liner shipping companies mainly transport between these regions via the Suez Canal and Panama Canal. As the demand for inter-regional trade continues to grow, the navigational problems of traditional waterways are becoming increasingly apparent. Affected by factors such as waiting time for canal passage, canal tolls and capacity limitations, shipping companies are seeking new routes to replace traditional routes. Transarctic routes shorten the spatial distance between regions, and the potential economic and strategic value of the Arctic routes has received widespread attention from the international community [4,5].

Arctic routes consist of two sets of waterways in the Arctic region: the Northern Sea Route (NSR) and the Northwest Passage (NWP). The NSR starts from the Bering Strait in the east and passes through the northern waters of Russia to the Kara Sea in the west, connecting East Asia and Northern Europe. The NWP begins in the Labrador Sea in the east, passes through the Canadian Arctic Islands and ends in the Bering Strait in the

west, connecting the Atlantic and Pacific [4]. Compared to traditional routes, the new routes can shorten sailing distances by up to 40%. When overcoming sea ice obstacles, transportation through the Arctic routes is better than traditional routes in terms of time, cost and safety [6].

Arctic sea ice melting is continuous and complicated. Satellite mapping shows that Arctic sea ice has exhibited a continuous trend of shrinkage since 1979. Arctic sea ice extent hit record lows several times, and the ice thickness and volume are also decreasing rapidly [7]. The National Snow and Ice Data Center (NSIDC) report indicated that Arctic sea ice shrank to 4.72 million square kilometers on September 16, 2021, ranking in the bottom 2 of the last 15 years of satellite records. Figure 1 shows a comparison of sea ice concentrations in September 1990 and September 2020. Dark blue areas are open water. All icy areas have a sea ice concentration of at least 15%, with the highest concentration in the opaque white areas. The yellow outline shows the median sea ice extent in September as observed by satellites. We can see a significant reduction in Arctic sea ice extent in 2020. In addition, climate scenario simulations show that global warming is amplified in the Arctic [8]. Sea ice melting reduces the albedo of solar radiation in the area, and seawater then absorbs heat more efficiently, thus intensifying the melting of sea ice. Arctic sea ice shrinkage is accelerating due to the combined effects of atmospheric circulation and greenhouse gases [8,9]. Meanwhile, Arctic sea ice changes show seasonal characteristics. About 70% of the floating ice in the Arctic consists of seasonal sea ice that grows rapidly during the winter and melts during the summer. Sea ice extent reaches a yearly maximum in March and then gradually decreases to a yearly minimum in September [10]. The navigable mileage of the Arctic shipping lanes varies under different sea ice conditions constraints. Therefore, it is necessary to examine the sea ice melt trends and the feasibility of Arctic routes under different melt phases.
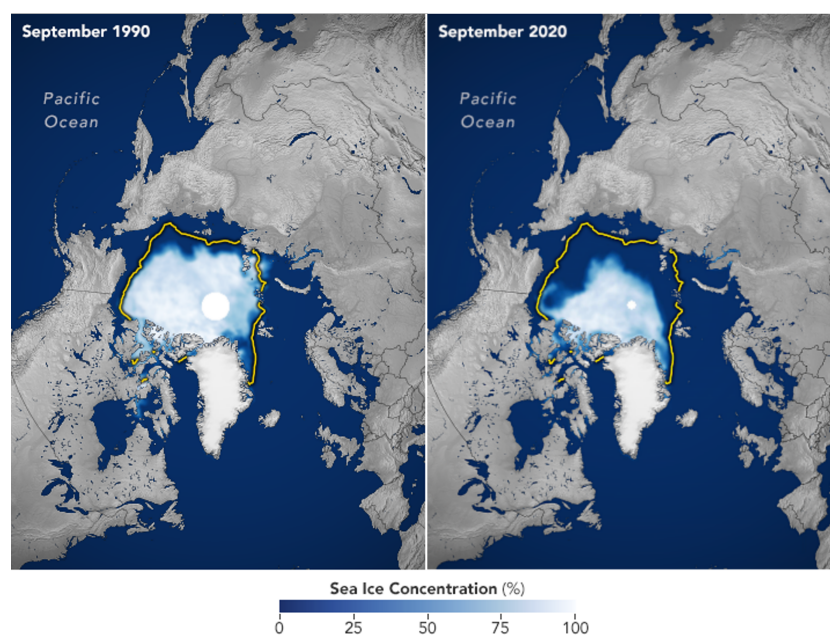
Figure 1. Arctic sea ice concentration between September 1990 and September 2020 (Source: NASA data).

In recent years, with the continuous improvement and extension of the rail network, the transshipment process between railways and ports has been more convenient, and the volume of sea–rail intermodal transport has gradually been increasing. Sea–rail intermodal transport combines the advantages of both modes and can carry large amounts of cargo with a high network stability [11,12]. After the opening of the Arctic routes, the new routes will be connected to the traditional routes as well as to the rail network, forming a new sea–rail shipping network. The new sea–rail network will increase inter-regional

connectivity and facilitate international trade exchanges, which will inevitably cause drastic changes in freight traffic in the network. Considering the risk, emission and cost factors, liner companies will adjust their fleet deployment according to the new route network and choose more economical transportation methods [13–15]. The problem of Arctic sea–rail container assignment is worth studying, both from an economic and stability point of view. As pointed out earlier, with the continuous reduction of sea ice extent, the Arctic shipping lanes are gradually revealed. Changes in the shipping lanes affect the shipping network and the assignment of freight demand in the network, so it is essential to analyze the changes in the sea–rail intermodal network and the container flow assignment in the context of Arctic ice melting.

Studies on Arctic routes began at the end of the last century and have focused on the history of Arctic navigation, the climate of the Arctic region and international laws related to Arctic navigation [4,5]. Until the last decade, studies on the economic value of transarctic transport have emerged, addressing the economic feasibility of Arctic routes and their impact on the economy and trade [6,16]. Arctic navigation will change the structure of the maritime network, which will affect freight flows in the network. However, few have considered the impact of Arctic navigation on the container flows in the shipping network. Therefore, this study is motivated to narrow the research gap by answering the following questions: (1) How will the container flows in the global sea–rail shipping network change with the opening of the Arctic routes? (2) Considering the impact of continued sea ice melt on the navigability of the Arctic shipping lanes, what are the trends in container flows on the routes? Hence, the paper aims to examine the impact of continued Arctic ice melt on global container sea–rail network and the container flows in the network. First, we simulate the melting of Arctic glaciers by 2050 using sea ice data from three Coupled Model Intercomparison Project 5 (CMIP5) models under the medium forcing emission scenario (Representative Concentration Pathway (RCP) 4.5). Then, with the melting of sea ice, new navigable shipping lanes are emerging in the Arctic. The new shipping routes can be combined with the existing maritime and rail networks to form a new container sea–rail intermodal network. Finally, we simulate the assignment of container flows in the global sea–rail intermodal network with a concave cost network flow model and solve it with the shortest path algorithm.

Our contribution to the existing literature is mainly twofold. On the one hand, it is one of the few studies in the field of global container transport research that considers the Arctic routes to construct a containerized sea–rail network with global coverage. Moreover, although existing studies have examined the economic feasibility of the Arctic routes, there has been little exploration of freight traffic along the Arctic routes. Our study innovatively considers the Arctic ice melt-based container flow assignment problem to analyze the changes in container flows due to network changes. On the other hand, carriers will choose more economical modes of transportation and adjust their business strategies in the face of new route networks. Our study can provide theoretical implications for carriers. Meanwhile, the calculation results reveal the future trend of freight traffic, which can provide a basis for decision-making for the future planning and development of ports and the country.

The remainder of this paper is organized as follows. Section 2 reviews the literature on Arctic routes and on the container flow assignment. Section 3 presents a simulation framework to analyze the impact of sea ice melt on the global containerized sea–rail network and the assignment of container flows. Section 4 presents the numerical analysis results and discussion. The final section lists conclusions and suggestions for future research.

2. Literature Review

In this section, we first review the research on Arctic routes in Section 2.1. Section 2.2 provides an overview of relevant studies on container flow assignment problems. Finally, we list the differences between current and existing studies.

2.1. Arctic Routes

The Arctic region is covered with snow and ice all year round and the low-temperature environment restricts maritime traffic. The exploration of navigable conditions for the Arctic is the basis for further analysis of transarctic transport's feasibility and economic value [7]. Arctic navigation factors include meteorological, hydrological and facility conditions. Among them, sea ice is considered essential in limiting the opening and commercial exploitation of Arctic shipping lanes [9]. Available monitoring data show that Arctic sea ice continues to melt with no apparent pattern and that there are significant interannual differences in the distribution of sea ice in the Arctic shipping lanes. Sea ice has great variability and uncertainty, and the literature has monitored and simulated the modeling of sea ice extent and thickness. Because of the large temperature difference between summer and winter in the Arctic, it is highly unlikely that the Arctic routes will be navigable before the mid-21st century, so scholars prefer to study the summer sea ice extent of the Arctic. The methods used include statistical models, sea-ice–ocean models and atmosphere–ocean general circulation models. Furthermore, linear regression models can be used, using past observations for statistical or training purposes and then predicting future sea ice conditions [10,17].

Among existing studies on sea ice changes and the navigability of Arctic shipping lanes, Lefebvre and Goosse [18] further confirmed the possibility of the Arctic routes by analyzing the change of sea ice area in the 21st century using several atmosphere–ocean general circulation models (AOGCMs). Laliberté et al. [19] used 42 models and 91 simulations of the CMIP5 forced Representative Concentration Pathways (RCP) 8.5 to examine changes in sea ice areas between June and October. The results showed that eastern Arctic waters will experience a more extended period of ice-free conditions earlier in the century. Jahn et al. [20] argued that accurately predicting an ice-free summer in the Arctic was complex, considering the effects of uncertainties in sea ice volume, trends, area, extent and thickness. Considering that transarctic transport is influenced by changes in temperature, seawater temperature, wind direction and wind speed, Zhang et al. [21] evaluated the development of transarctic transport on the basis of mining big data.

The existence of sea ice creates routing difficulties and increases navigation risks. Numerous studies have considered the impact of different ice scenarios on the economic viability of the Arctic. Sibul and Jin [6] focused on environmental parameters, assessing the impact of three factors—ice thickness, ice conditions and ice class—on the cost of transarctic transport. Xu et al. [22] discussed a seasonal NSR/SCR-combined shipping service pattern. The model considered changes in sea ice extent, which was more reasonable for assessing Arctic container shipping. Cheaitou [23] analyzed the impact of ice thickness changes on the economic and environmental attractiveness of the NSR. In studies considering the impact of sea ice melt on trade, Bensassi et al. [16] predicted the changes in future Arctic sea ice extent by using CMIP5 and discussed the impact of climate change and distance shortening on international trade.

2.2. Container Flow Assignment

In recent years, many scholars have studied the problem of assigning container traffic to single-mode and multimode networks [24]. Shibasaki and Kawasaki [25] constructed an international containerized cargo network assignment model and applied it to analyze three countries in South Asia to analyze the impact of logistics policy changes on network flows. Rosell et al. [26] developed a combined mode-split/traffic assignment model to assess the share of freight traffic between train–road modes, using the European rail network as an example. In the study of applying assignment solutions to maritime networks, Bell et al. [27] proposed a global maritime container assignment model, considering sailing time, service frequency and port capacity effects on full and empty container flow assignment. Bell et al. [28] presented a cost-based container allocation model to minimize container handling costs, container rental and inventory costs. Song and Dong [29] considered a joint optimization problem of freight assignment and empty container repositioning

in the planning of a shipping network with multiple service routes, multiple deployed vessels and multiple regular voyages. Sun and Zheng [30] established a cargo flow assignment model with a concave function as the objective function to analyze the cargo flow assignment of empty and loaded containers in the global shipping network. Lin and Huang [31] developed a model to analyze the international liner shipping network and estimate the changes in container flows under different scenarios to predict future maritime network development trends. Ozcan et al. [32] took a Turkish liner shipping agency as their object of study to investigate its shipment assignment and vessel scheduling problems. A mixed-integer linear programming model was developed and solved with a two-stage algorithm. With the gradual depth of research, some scholars pointed out that the container flow assignment problem referred to a series of container transport activities, including container loading and unloading, transport between different routes or combined transport between different modes of transport, etc. [33,34].

However, most studies on container flow assignment are based only on existing maritime networks, and only a few scholars have considered new shipping networks in the context of Arctic navigation. Lin and Chang [35] constructed a time-network-based model to analyze the NSR ship routing and freight assignment problem and developed a Lagrangian relaxation based decomposition algorithm. Zeng [36] analyzed the market share of the NSR, SCR and railway transport between China and Europe using a multi-indicator logit model and discussed the trend of NSR market share under different scenarios.

2.3. Summary

Existing studies have mainly focused on assessing historical sea ice data trends or discussed Arctic routes' navigation feasibility and economic value. Although the issue of container assignment has attracted much attention, few scholars have discussed container assignment after the opening of the Arctic routes. Moreover, sea ice melting is gradually improving the navigation conditions in the Arctic, and the effects are sustained. Few studies have analyzed the impact of changes in sea ice extent on the shipping network pattern and container flow in the shipping network. Moreover, existing studies have only explored the impact of the Arctic routes on container flows in the current maritime network without considering the changes in container flows in the inland transportation network. This paper aims to focus on the assignment of container flows in the global sea–rail intermodal network under the changing ice conditions in the Arctic region. Based on the analysis of the influencing factors of sea ice melting and the existing sea–rail intermodal network, a simulation framework of container flow assignment in the shipping network is established. By simulating the assignment of container flows, we explore the changes in the global sea–rail intermodal network and container flows under the influence of Arctic ice melt. The findings will not only bring direct economic benefits to shipping companies but also provide a basis for decision-making for future planning and development of ports and countries.

3. Methodology

In this section, we propose a simulation framework to analyze how global container flows are assigned after the Arctic navigation. Figure 2 shows the framework structure, containing three layers. In the upper layer, we estimate the future Arctic sea ice concentration based on the atmosphere–ocean coupled models of CMIP5. The obtained sea ice concentration data are transferred to the middle layer as input information to determine whether the transarctic shipping lanes are covered by sea ice. The sea ice melting gradually reveals the shipping lanes and changes the shipping network. In the middle layer, we can get a new global sea–rail intermodal network considering sea ice extent changes. We construct a concave cost network flow model in the lower layer to minimize the total transportation costs. By assigning container demand to the new global sea–rail intermodal network, changes in container flow assignment in the context of Arctic ice melt can be assessed.
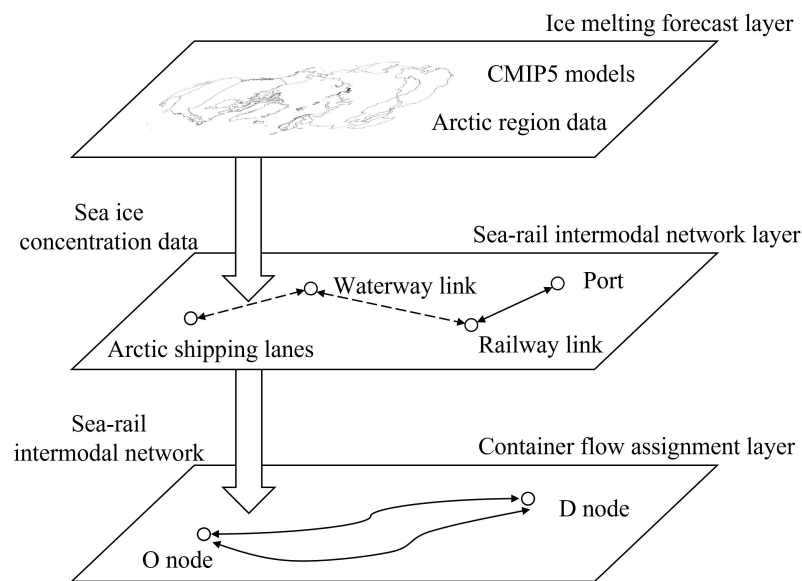
Figure 2. Simulation framework.

3.1. Ice Melting Forecast

Arctic sea ice melting is a complex process. Considering the coupling relationship between sea ice and atmosphere, we estimated the Arctic climate with the help of the CMIP database in this module. The fifth phase of the International Coupling Model Comparison Program has carried out climate analysis under different scenarios through several global atmosphere–ocean coupled models (AOGCMs) in 35 countries, including future short-term climate change projections (to 2035) and future long-term climate change projections (to 2100–2300) [7]. This paper adopted the global AOGCMs mentioned in the Fifth Assessment Report of the Intergovernmental Panel on Climate Change (IPCC AR5) as the prediction model for Arctic ice melting.

The AOGCM consists of three parts: atmospheric circulation model, the sea ice circulation model and the coupler, which can well reflect the dynamic process of heat exchange between atmosphere and ocean as well as the formation and melting cycle of sea ice. Thus, when using the AOGCMs to study the distribution of ice and snow on the sea surface, it is not only necessary to consider the energy conversion between the sea ice surface and the atmosphere but also the influence of the sea–air flow on the ice and snow, the melting of the sea ice itself and the formation of new ice.

The Representative Concentration Pathways (RCPS) are the emission scenario developed by the IPCC AR5, which was developed to combine climate, atmospheric circulation, carbon emissions and socioeconomic factors to provide a specific analysis of the impacts of climate change in the Arctic [37]. This paper used the RCP 4.5 typical emission scenario and selected sea ice concentration data from three AOGCMs in CMIP5, MRI-CGCM3, ACCESS1-3 and CNRM-CM5.

Based on the sea ice concentration data output from each model prediction, the dividing line between Arctic seawater and sea ice cover was further determined. To reduce the prediction model error, this paper used the boundary between seawater and sea ice determined by more than 50% of the selected models as the standard and finally determined the edge of sea ice extent.

3.2. Sea–Rail Intermodal Network

To optimize and simulate the assignment of container flows in the global sea–rail intermodal network, we used Microcity to connect the maritime network with the rail network. The network consisted of transport links and port nodes. Some ports had rail transit stations, which were the basis for connecting maritime and rail networks. In addition, the NSR and the NWP were also added to the global sea–rail intermodal network. Then,

the entire network was topologically processed to obtain the specific path distance between nodes. To avoid the error between the calculated path distance on the plane and the actual path distance, we used the radian formula to refine the distance data further. Finally, container demand between global ports was obtained from a shipping company, and subsequently, the container demand, shipping distance, passing capacity and other related data of major ports were stored in the global sea–rail intermodal network correspondingly. Since the container flow assignment model considered not only the flow assignment of full containers but also the flow assignment of empty containers, a two-way container shipping network covering both eastbound and westbound was established. Figure 3 shows the constructed global container sea–rail intermodal network containing the NSR and the NWP. To easily distinguish the routes, different colors are set for different links of the container shipping network, with pink indicating the trans-Arctic links, dark blue indicating the traditional waterway links and light blue indicating the railway links.
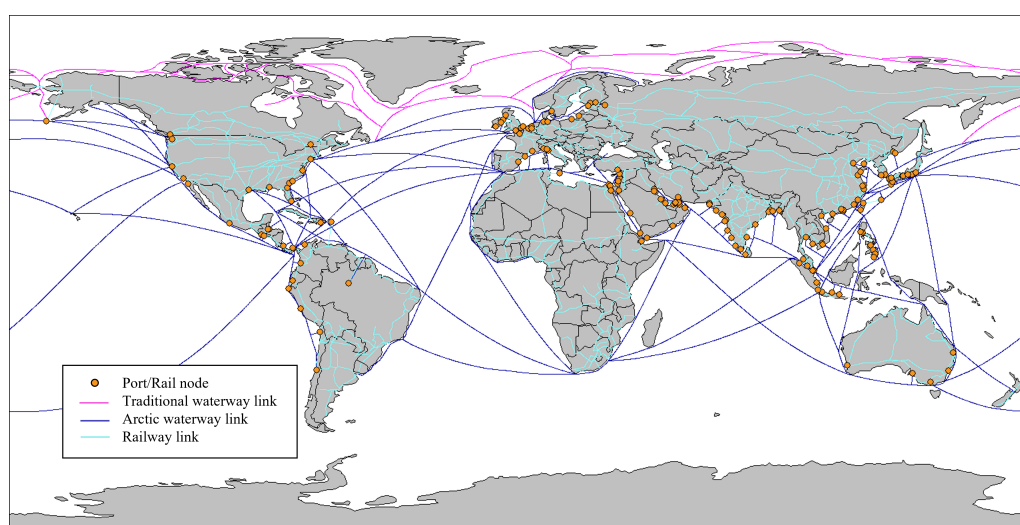
**Figure 3.** Global container sea–rail intermodal network.

3.3. Container Flow Assignment

3.3.1. Problem Description

Arctic routes provide new transport channels for international trade exchanges. Shipping companies can choose Arctic routes for cargo transportation, which will cause changes in cargo flows in the shipping network. To analyze the assignment of global container flows after the opening of Arctic routes, we established a sea–rail intermodal network container flow assignment model from the perspective of transportation cost and aimed at the minimum cost of the whole transportation process for path selection. The model not only considered meeting the cargo demand but also considered the problem of empty container repositioning due to the unbalanced cargo demand between regions.

We constructed a global container sea–rail intermodal network consisting of maritime and rail networks, and its abstract network is shown in Figure 4. Topologically, the shipping network was described by a graph, denoted by $G(V, A)$. V indicates the set of nodes and A indicates the set of links in the network. There were three types of nodes: port nodes, ordinary nodes and dummy nodes. It was assumed that the ordinary nodes were the intersections of navigable waterways. Each port node was linked to an ordinary node via a waterway link. Some of the port nodes had transshipment rail nodes within them, and these ports were the linking points between the maritime network and rail network. The full container demands originated and terminated at port nodes. Considering the imbalance between container supply and demand in the network, we added dummy nodes as supply and demand points for excess empty containers to solve the problem of empty container repositioning. The set of links included waterway links, railway links and dummy links.

Waterway links connected various ports. Dummy links connected ports and dummy empty container surplus or deficit nodes.
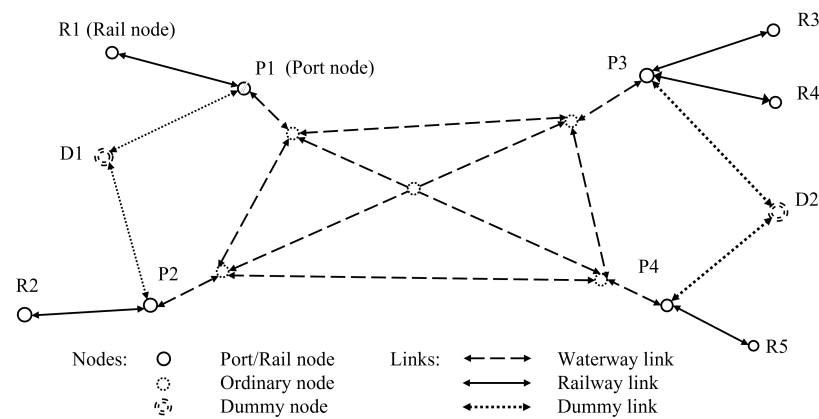
Figure 4. An illustrative sail–rail intermodal network.

For a better understanding, an an example is given of a shipping network with 10 container demands from port 1 (P1) to port 4 (P4) and 15 container demands from port 2 (P2) to port 3 (P3), respectively. After the container transportation demand is met, port 1 and port 2 will experience empty container demand, while port 3 and port 4 will generate excess empty containers. Thus, empty containers need to be repositioned. The remaining empty containers will be concentrated in dummy node 2 through the dummy link, and all empty container demand will be concentrated in dummy node 1. Thus, the normal OD demand from dummy node 2 to 1 is established. We set the capacity of links D1-P1 and P4-D2 to 10 and the capacity of links D1-P2 and P3-D2 to 15.

To simplify the problem, we propose the following assumptions in this study: (1) It is assumed that the liner shipping company does not have its fleet, and all the ships used for transport come from the charter market. (2) Container types include twenty-foot and forty-foot equivalent unit containers. Full and empty containers are transferred throughout the network to meet the fixed demand between various port nodes. (3) The shipping costs mainly include capital cost and voyage cost. Specifically, charter costs, fuel costs during the voyage and container handling costs are calculated. In the rail network, railway freight is mainly considered. The cost of the dummy link is assumed to be zero. In addition, the transshipment costs of the nodes are not considered. (4) Each link has a capacity limit. The demand of the port determines the capacity of the waterway links connecting to the ports. The capacity of other waterway links is assumed to be very large. The capacity of the dummy links is set to the corresponding excess or shortage of the container volume.

3.3.2. Mathematical Model

For discussion convenience, we summarize the notations used in this paper in Table 1 below.

Before presenting the mathematical formulation, we first established the network's cost functions for the waterway and railway links.

Shipping costs in the maritime network include costs incurred during voyages and costs incurred in ports. The model proposed in this paper considered the cost of loading and unloading containers at the port, including both full containers and empty containers. In addition, the voyage cost and charter cost were also considered. $c_{ij}(\cdot)$ is the charter cost function of the link (i, j), $v_{ij}(\cdot)$ is the voyage cost function of the link (i, j). The shipping costs C_1 in the network can be expressed as:

$$C_1 = \sum_{(i,j)\in A} c_{ij} \left(\sum_{k_f\in K_f} y_f x_{ij}^f + \sum_{k_e\in K_e} y_e x_{ij}^e \right) + \sum_{(i,j)\in A} v_{ij} \left(\sum_{k_f\in K_f} y_f x_{ij}^f + \sum_{k_e\in K_e} y_e x_{ij}^e \right)$$
$$+ \sum_{(i,j)\in A} \sum_{k_f\in K_f} h_{ij}^f x_{ij}^f + \sum_{(i,j)\in A} \sum_{k_e\in K_e} h_{ij}^e x_{ij}^e \tag{1}$$

Compared to shipping costs, rail costs are much simpler. Since national governments generally set railway freight rates, the principles of calculating the cost of railway costs are uniform. Total freight is the product of container freight rate, weight billed and mileage. Similarly, full containers and empty containers are considered in the railway network. The rail costs C_2 in the network can be expressed as:

$$C_2 = \sum_{(i,j)\in \bar{A}} R_{ij}^f x_{ij}^f dis_{ij} + \sum_{(i,j)\in \bar{A}} R_{ij}^e x_{ij}^e dis_{ij} \tag{2}$$

The container flow assignment problem can be formulated as follows:

$$\min C_1 + C_2 \tag{3}$$

$$\sum_j x_{ij}^f - x_{ji}^f = d_i^f, \forall i \in v, k_f \in K_f \tag{4}$$

$$\sum_j x_{ij}^e - x_{ji}^e = d_i^e, \forall i \in v, k_e \in K_e \tag{5}$$

$$\sum_{k_f\in K_f} y^f x_{ij}^f + \sum_{k_e\in K_e} y^e x_{ij}^e \leq u_{ij}, \forall (i,j) \in B \tag{6}$$

$$x_{ij}^f \geq 0, \forall (i,j) \in B \tag{7}$$

$$x_{ij}^e \geq 0, \forall (i,j) \in B \tag{8}$$

$$d_i^f = \begin{cases} q_i^f, & \text{if } i = r \in O \\ -q_r^f, & \text{if } i = s \in D \\ 0, & \text{otherwise} \end{cases} \tag{9}$$

$$d_i^e = \begin{cases} q_i^e, & \text{if } i = r \in O \\ -q_r^e, & \text{if } i = s \in D \\ 0, & \text{otherwise} \end{cases} \tag{10}$$

The objective function (3) is the sum of the shipping cost and the railway cost of container shipping. Equations (4) and (5) ensure that each node flow is conserved. Equation (6) limits the container flow of each link to its maximum passing capacity. Equations (7) and (8) restrict the decision variable to be non-negative. Equations (9) and (10) indicate that the node surplus at the origin and destination ports should meet the port's container demand.

Table 1. Notations.

Sets	
V	Set of port nodes and rail nodes
P	Set of port nodes, including empty container remaining virtual nodes and empty container demand virtual nodes, $P \subseteq V$
O	Set of origin ports, $O \subseteq P$
D	Set of destination ports, $D \subseteq P$
B	Set of links, where $B = A \cup \bar{A}$
A	Set of waterway links
$\bar{A}$	Set of railway links
Parameters	
K_f	Type of full containers
K_e	Type of empty containers
y_f	Volume-sharing factor for full containers of type f
y_e	Volume-sharing factor for empty containers of type e
u_{ij}	Capacity of link (i, j)
dis_{ij}	Distance of link (i, j)
h_{ij}^f	Loading and unloading cost of full containers of type f on link (i, j)
h_{ij}^e	Loading and unloading cost of empty containers of type e on link (i, j)
R_{ij}^f	Freight rates for full containers of type f on link (i, j)
R_{ij}^e	Freight rates for empty containers of type e on link (i, j)
d_i^f	Net flow of full containers of type f at node i
d_i^e	Net flow of empty containers of type e at node i
q_i^f	Demand for full containers of type f at node i
q_i^e	Demand for empty containers of type e at node i
Decision variable	
x_{ij}^f	Flow of full containers of type f on link (i, j)
x_{ij}^e	Flow of empty containers of type e on link (i, j)

3.4. Solution Method

Based on the shortest path cargo flow assignment method, this paper regarded the transportation cost on each path as impedance and changed the path impedance of different transportation modes, then realized the cargo flow assignment of the global container shipping network. The shortest path cargo flow assignment method is not constrained by conditions such as geographical limitations and path capacity. It usually assigns the cargo flow demand between all ports to the corresponding shortest path of the cargo flow in the shipping network. The shortest path cargo flow assignment method is more convenient and faster than the mathematical model cargo flow assignment method in dealing with large-scale shipping networks' cargo flow assignment problems. In addition, this method is consistent with the empirical fact that trains and ships on railways and waterways mostly choose the shortest route for transportation.

The planning and simulation of the container flow assignment of the network were carried out in line with the specific process design shown in Figure 5.

Step 0: Establish a global container shipping network based on the current shipping network and container demand between ports. In the initial step of the simulation, the Arctic sea ice extent in March 2020 is used as the initial state, and the time interval is six months. Based on the temporal variation of Arctic ice melt, the system generates Arctic Sea ice extent every six months based on the predicted data.

Step 1: Determine whether the Arctic route is covered by sea ice based on the sea ice extent. If the Arctic route is blocked, go to Step 2. Otherwise, it is proved that the Arctic route is navigable and repeat Step 1 until all Arctic routes are reviewed. Then, go to Step 3.

Step 2: When the Arctic route is covered by sea ice and is not navigable, this route is deleted, and a new container shipping network is generated.

Step 3: Based on the established model, the flow assignment is performed separately for full containers and empty containers. When the demand for empty and full containers

reaches equilibrium among all ports, the result of container flow assignment under Arctic sea ice extent is output, and then go to Step 4.

Step 4: Determine whether the forecast period is reached (September 2050). If the expected time is not reached, return to Step 0. Otherwise, terminate the procedure and report the results.
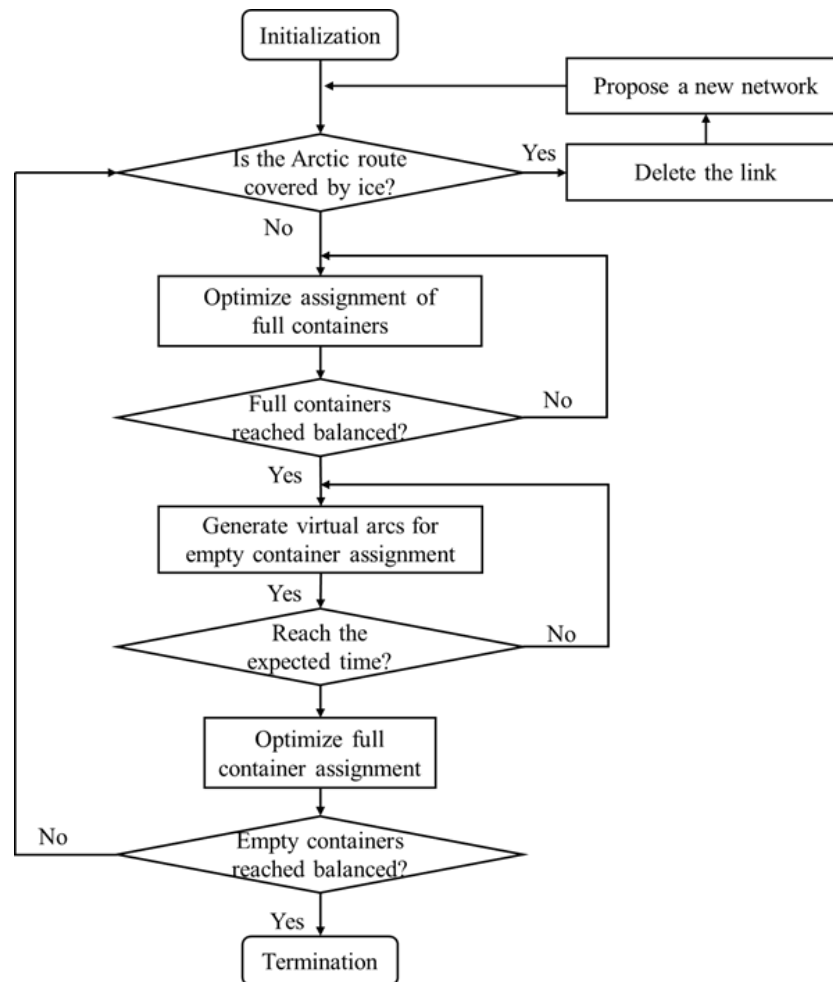
**Figure 5.** Flowchart of the simulated process.

4. Numerical Examples

4.1. Data Collection and Processing

4.1.1. Sea Ice Forecast

Arctic sea ice concentration was processed in the form of gridded data, and the models applied were MRI-CGCM3, ACCESS1-3 and CNRM-CM5. This paper selected 2020, 2030 and 2050 as the forecast time for analysis. Moreover, to compare the ice melt in different seasons in the Arctic, March and September were selected as the observation periods in winter and summer, respectively. To facilitate data processing, this paper addressed sea ice concentration in the form of gridded data. By establishing the horizontal and vertical coordinates of longitude and latitude, the earth's surface was divided into 360 × 360 grids. Since the sea ice concentration was the ratio of the sea ice coverage area in a single network cell to the total area of the entire grid, the data value ranged from 0 to 100, with 0 representing no sea ice coverage and 100 representing complete sea ice coverage.

We use Microcity combined with the three models of MRI-CGCM3, ACCESS1-3 and CNRM-CM5 for the prediction. Sea ice concentration generated different colors based on a linear relationship. It can be observed from Figure 6 that the results of sea ice cover predicted by different models are similar, but there are still differences. Taking

the prediction results for September 2050 as an example, the simulation results using the MRI-CGCM3 model show a narrow ice extent in the Arctic, while the simulation results using the CNRM-CM5 model show a much larger extent.
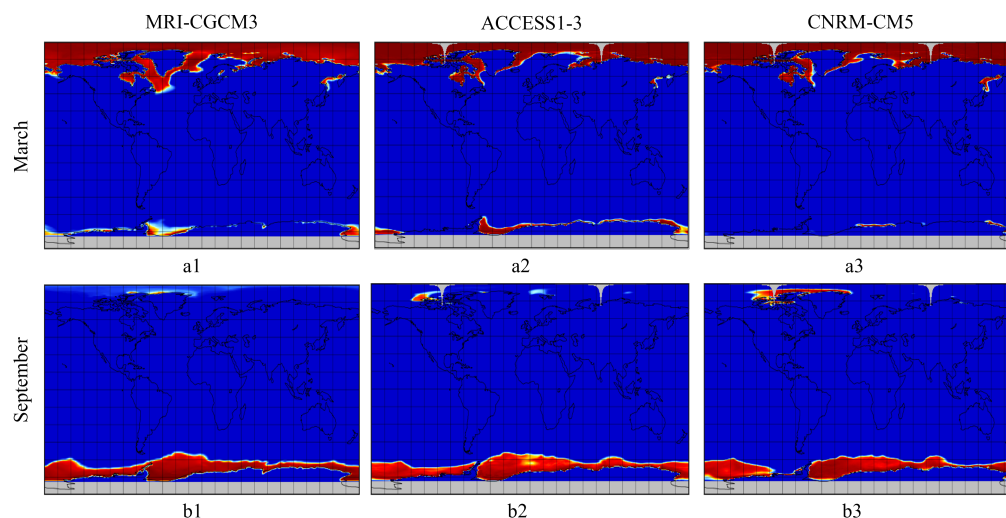
Figure 6. Sea-ice predictions in 2050 ((**a1**–**a3**) indicate the predicted Arctic sea ice extent in March 2050 using different models; (**b1**–**b3**) indicate the predicted Arctic sea ice extent in September 2050 using different models).

To reduce the error, the results of the three models were comprehensively processed and we selected the results reflected in more than 50% of the models as the standard. The sea ice concentration of 15% was used as the boundary between the presence or absence of sea ice [38]. Comparing b1 and b3 in Figure 7, it can be found that compared to 2020, the sea ice extent in the Arctic area in 2050 was significantly reduced and the navigable area was expanded.

It can be seen from the results that the extent of Arctic sea ice will gradually shrink in the future. Although the winter ice situation represented by March changed little and the Arctic region will still be covered by ice and snow in the future, the ice and snow around Greenland will disappear in summer. The ice in Russia's northern seas is disappearing, and by 2050, Russia's northern seas could meet navigable conditions for Arctic routes. Therefore, from the perspective of geographical conditions, the opening of the Arctic routes in the future is feasible and will have a non-negligible impact on the assignment of cargo flows in the global container shipping network.

4.1.2. Transportation Costs

The sea–rail intermodal network includes waterway and railway links, so the container transportation cost is also composed of maritime and rail costs.

Considering the limitation of the Panama Canal waterway, we uniformly chose Panamax container ships as the carriers in the shipping network. We took a 5000 TEU ship as a sample ship with a gross tonnage of 53,453 t, a length of 294.1 m, a draft of 13.5 m and a main engine power of 55,917 kW. The ship had an economic ship speed of 20 knots and a maximum ship speed of 22 knots [39]. The main engine fuel consumption rate was fixed at 185 (g/KWh). Other relevant data were calculated under full load conditions. Container shipping cost is mainly divided into capital cost, operating cost and voyage cost. The capital cost is the charter cost of the shipping company and was set at USD 19,000 per day [39]. Referring to the operating and management costs of the Panama Canal, the operating cost was assumed to be USD 5000 per day. In the voyage cost, we mainly calculated fuel cost and port charges. Fuel cost is related to fuel price and fuel consumption, and the fuel consumption depends on the ship's speed and its main engine parameters. According to the Bunker Index, the average price of the set fuel IFO 380 is USD 400 per ton.

Port charges include all costs incurred by the ship in entering and leaving the port, channel and berthing. We focused on container handling costs, which vary from port to port. To simplify the calculation, we assumed a uniform price of USD 50 per TEU [40].

Compared to maritime transport, the cost of rail freight is simpler to calculate. The rail cost of container transportation can be defined as the product of container freight rate, weight and mileage. The mileage is the shortest path between two nodes of the rail network. Since container freight rates are related to the mileage within the country, they may vary among different countries. We classified each country by continent and set different container freight rates for different continents. To facilitate the calculation, we converted the weight of the container according to its dimensional standards. The weight of a twenty-foot container is 22 tons, and the weight of a forty-foot container is 27 tons.
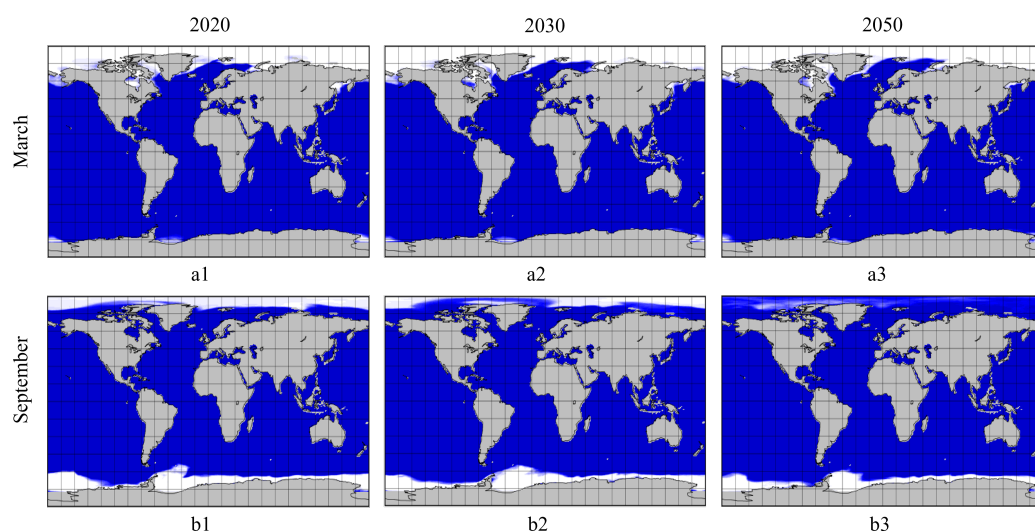

Figure 7. The comprehensive forecast results of Arctic sea ice ((**a1**–**a3**) indicate the sea ice extent in March for 2020, 2030 and 2050, respectively; (**b1**–**b3**) indicate the sea ice extent in September for 2020, 2030 and 2050, respectively).

4.2. Results Analysis

4.2.1. Impact of Arctic Routes on Flow Assignment

With the optimization and simulation of the container flow assignment model, we obtained the container flow assignment results of the global container sea-rail intermodal network. Figures 8 and 9 show the results of container flow assignment when not considering and considering the Arctic routes, respectively. The NSR and the NWP share about 4% of the global container flow after opening the Arctic routes. Comparing Figures 8 and 9, it can be found that the container flow of the traditional routes changes after the Arctic navigation. Especially, the container flow through the Malacca Strait, the Mandeb Strait and the Hormuz Strait is greatly reduced. In addition, the opening of the Arctic routes has little impact on the assignment of container flow in the rail network, with a slight decrease in container flows through the Eurasian Land Bridge. A further analysis found that opening the Arctic routes would reduce container flow on 34% of the routes in the network. Among the routes with reduced container flows, waterway links account for 52% and railway links account for 19%. Therefore, the Arctic routes have a more significant impact on the assignment of container flows in the maritime network.
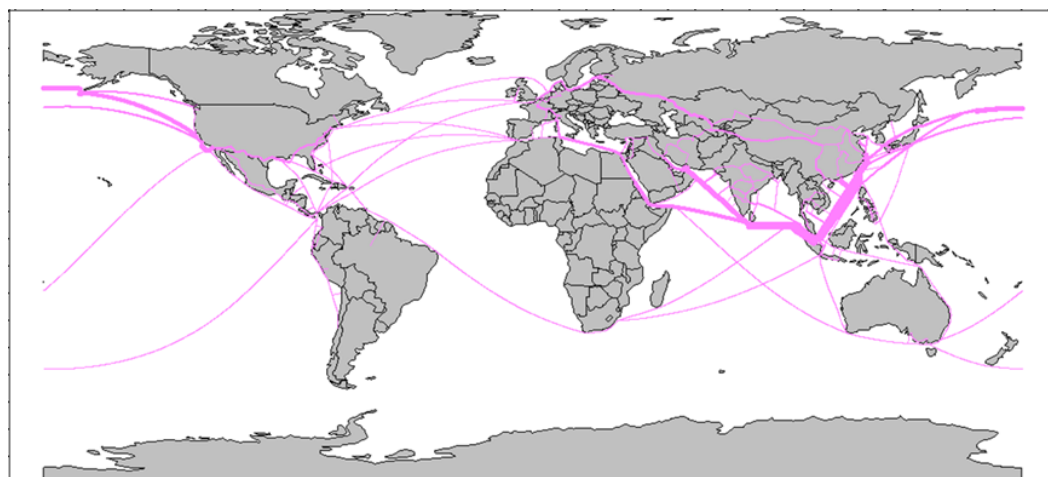
Figure 8. Simulation results of container flow assignment without considering the Arctic routes.
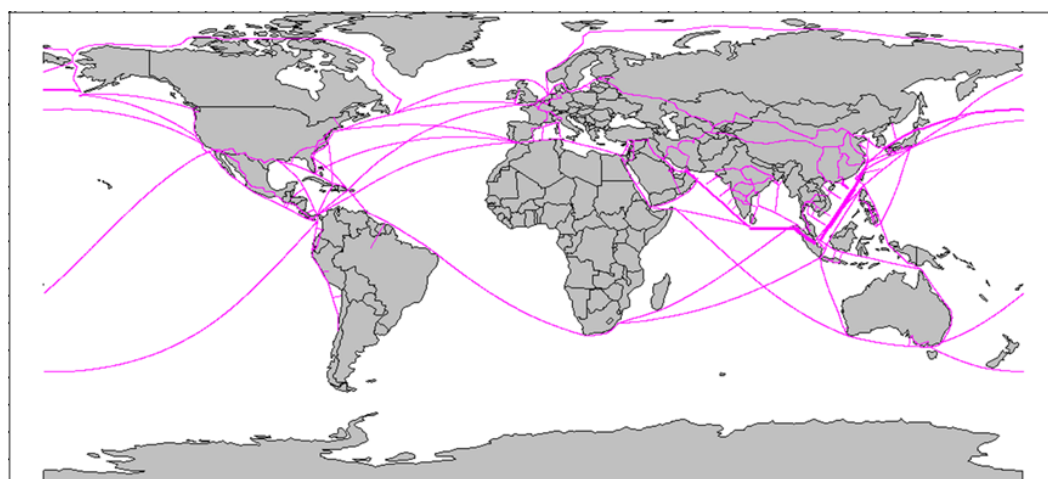
Figure 9. Simulation results of container flow assignment considering the Arctic routes as fully navigable.

To illustrate the changes in container flows assignment in the network after the Arctic navigation, we present the container flows for some routes. As can be seen in Table 2, there is a decreasing trend in the container flow of the major waterways passing through Singapore. Moreover, container flow from Rotterdam to the Suez waterway decreases from 9188 TEU to 6857 TEU per day, while container traffic from the Suez waterway to Hong Kong shows a slight increase. In addition, the Panama Seaway is also negatively affected, with reduced container traffic on the Vancouver–Balboa route decreasing by 1122 TEU per day. After considering transarctic transport, the route from Shanghai to New York via the NWP is assigned 2354 TEU per day, while the route from Busan to Boston via the NWP is assigned 1064 TEU per day. In the railway links, container flow in the Eurasian Land Bridge and the New Eurasian Land Bridge presents a decrease of 12% and 16%. In addition, the total cost of global container transport is reduced by 0.5%. The Arctic routes not only have an important impact on the assignment of container flows in the global shipping network, but they are also able to reduce the total cost of container shipping and bring more competitiveness to container shipping companies.

Table 2. Changes in container flow assignment after the Arctic navigation (TEU/day).
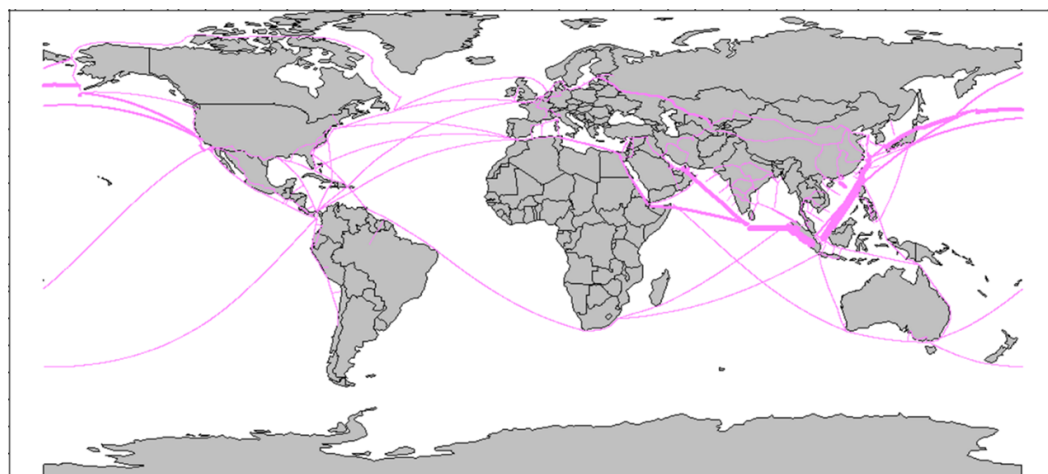
	Current Container Flow Assignment	Container Flow Assignment Including Arctic Routes
Waterway		
Yokohama–Singapore	4972	4443
Shanghai–Singapore	18,634	15,236
Pusan–Singapore	6245	5143
Manila–Singapore	8435	7899
Balboa–New York	7253	4060
Rotterdam–Suez Canal	9188	6857
Suez Canal–Hong Kong	7464	7568
Vancouver–Balboa	3363	2241
Seattle–Balboa	8643	6256
Miami–Hamburg	1135	1008
Shanghai–New York (via NWP)	0	2354
Busan–Boston (via NWP)	0	1064
Railway		
Eurasian Land Bridge	4136	3653
New Eurasian Land Bridge	3274	2751

4.2.2. Impact of Ice Conditions on Flow Assignment

With global warming and changes in Arctic ice melt, parts of the Arctic routes will become navigable. Since the feasibility of Arctic navigation in winter is low, this paper focuses on the Arctic summer ice melt and analyzes the changes in global container flows assignment. Figure 10 shows the results of the global container flow assignment when trans-Arctic transport is considered in the summer of 2020. We can see that only the NWP is navigable in 2020. While in 2050, when the Arctic route is fully navigable in summer, there will be some container traffic on both the NWP and the NSR (Figure 9). In terms of container flows, the NWP carries 1% of total global container flows in the summer of 2020, while in the summer of 2050 when the Arctic is fully navigable, all Arctic routes can carry 4% of total global container traffic.

Compared with the result of the 2020 summer container flow assignment, 27% of the railway links experience a reduction in the container flow, but more than 50% of the railway links see no change in flows. Conversely, 47% of the waterway links in the maritime network reduce container flow, while 16% of the waterway links have no change in flow. In addition, in terms of the distribution of the affected routes, the Asia–Europe and the Asia–North America routes show a significant decrease in cargo flow. Among them, the container flow through the Malacca Strait and the Panama Canal decreases by more than 50%, and the container flow through the Mandeb Strait and the Suez Canal decreases by more than 40%. At the same time, compared to 2020, the total transportation costs of the global shipping network will be reduced by about 0.3% when the Arctic is fully navigable in 2050. Therefore, as the Arctic ice melts, the impact of the Arctic routes on the assignment of container flows in the global shipping network also changes.

We selected the main waterways as the research subjects and present the variation of container flows in the main hub ports along the waterways, as shown is Table 3. In the Malacca Straits, container flow in Singapore and Penang gradually decreases as the Arctic routes become fully navigable. By 2050, the container flow in the two ports drops by 24% and 26%, respectively. As an essential port in the Mandeb Strait, Djibouti suffers the negative impact of Arctic navigation, reducing container flow from 2534 TEU in 2020 to 1607 TEU in 2050. Similarly, container flow in Balboa along the Panama Canal shows a decreasing trend. For ports along other main routes, container flow in the Rotterdam Port remains unchanged, and container flow in Colombo and Seattle declines significantly.

Figure 10. Simulation results of container flow assignment considering trans-Arctic transport in 2020.

Table 3. Changes in container flow at main ports (TEU/day).

	2020	**2050**
Singapore	98,537	74,574
Penang	2024	1505
Djibouti	2534	1607
Balboa	17,224	9634
Huston	27,365	20,046
Colombo	15,545	12,076
Hamburg	30,012	29,745
Seattle	13,654	11,345

5. Conclusions

Arctic sea ice is melting at an accelerated rate due to climate warming, and it is a key factor limiting the Arctic navigation. The progressive opening of Arctic shipping lanes will change the layout of the maritime network, which in turn will affect the container flows in the network. This paper investigated the container flow assignment in the global sea–rail intermodal shipping network under the change of Arctic sea ice. To solve the above problem, we simulated future changes in sea ice extent using the CMIP5 models, proposed a network flow assignment model to simulate the assignment of container flows in the new global sea–rail intermodal network and solved it with an algorithm.

Our results introduced the following conclusions. First, from the transportation cost side, the opening of the Arctic routes will reduce the total global container transportation costs by 0.5%, which can bring more competitiveness to container shipping enterprises. Secondly, the Arctic routes will compete with traditional routes and share the container flows in traditional routes. Waterways such as the Straits of Malacca and the Suez Canal will be the most negatively impacted, with a significant reduction in container traffic. Thirdly, besides the important impact on the maritime network, the Arctic navigation also leads to a reduction in container flow on the rail network. Compared to the maritime network, the rail network is less affected. Taking the Eurasian Land Bridge as an example, its container flow will be reduced by about 12% after the opening of the Arctic routes. Finally, because the Arctic routes are still severely constrained by ice and snow in winter, and the seasonality of navigation is obvious, the proportion of container flows undertaken in the global container shipping network is still very limited. However, with global warming, the sailing time of the Arctic routes will be expected to be extended annually. The impact of the Arctic routes on the global container shipping network will continue to expand.

Theoretically, our paper considered the feasibility of Arctic navigability after the melting of sea ice, established a global container sea–rail intermodal shipping network including the Arctic routes and assigned the container flow based on the shipping network.

In practice, our research can provide valuable management insights for liner shipping companies, port operators and government decision-makers. Specifically, liner companies should make timely adjustments to the shipping network according to the navigability of the Arctic shipping lanes. According to the characteristics of the Arctic shipping lanes at different periods, liner companies can consider deploying different capacities and vessel sizes to reduce transportation costs by using transarctic transportation. For port operators, the Arctic navigation will change the freight flow in the global shipping network, and the port throughput will change with it. The hub position of the southern hemisphere ports will be challenged by the northern ports due to the northward shift of container traffic after the opening of the Arctic routes. For the ports that may benefit from the Arctic routes, they should accelerate the improvement of the sea–rail shipping network of the ports and actively play a transportation hub function. For ports with declining freight volumes, such as Singapore and Penang, they should adjust their port development strategies in time to actively face the economic impact of changes in network traffic. The Arctic route will shorten the distance of maritime trade and increase the efficiency of inter-regional transport. The governments can pursue their strategic interests in the Arctic region and strategically position themselves for a better use of the Arctic routes to facilitate trade development.

It should be noted that the study has some limitations and needs to be improved in future studies. On the one hand, this study did not consider the passage capacity of the shipping lanes. We only analyzed whether the Arctic routes could be opened as sea ice melts. In practice, the extent of Arctic ice melt affects the width of the Arctic shipping lanes, and thus limits the volume of cargo passing through. Further research on Arctic shipping capacity will help to consider the problem of cargo flow in the Arctic more realistically. On the other hand, this study simplified the calculation of transportation costs. We only considered the main container transportation costs, while the actual transportation cost factors are more complex. Future studies need to further refine the classification of transportation costs to consider factors such as container transshipment costs, Arctic route transit costs, etc.

References

1. Elmi, Z.; Singh, P.; Meriga, V.K.; Goniewicz, K.; Borowska-Stefańska, M.; Wiśniewski, S.; Dulebenets, M.A. Uncertainties in liner shipping and ship schedule recovery: A state-of-the-art review. *J. Mar. Sci. Eng.* **2022**, *10*, 563. [CrossRef]
2. Abioye, O.F.; Dulebenets, M.A.; Kavoosi, M.; Pasha, J.; Theophilus, O. Vessel schedule recovery in liner shipping: Modeling alternative recovery options. *IEEE Trans. Intell. Transp. Syst.* **2020**, *22*, 6420–6434. [CrossRef]
3. UNCTAD. *Review of Maritime Transport 2021*; United Nations: New York, NY, USA, 2022; OCLC: 1291391335.
4. Wang, Z.; Silberman, J.A.; Corbett, J.J. Container vessels diversion pattern to trans-Arctic shipping routes and GHG emission abatement potential. *Marit. Policy Manag.* **2021**, *48*, 543–562. [CrossRef]
5. Theocharis, D.; Pettit, S.; Rodrigues, V.S.; Haider, J. Arctic shipping: A systematic literature review of comparative studies. *J. Transp. Geogr.* **2018**, *69*, 112–128. [CrossRef]
6. Sibul, G.; Jin, J.G. Evaluating the feasibility of combined use of the Northern Sea Route and the Suez Canal Route considering ice parameters. *Transp. Res. Part A Policy Pract.* **2021**, *147*, 350–369. [CrossRef]

7.   Khon, V.C.; Mokhov, I. Arctic climate changes and possible conditions of Arctic navigation in the 21st century. *Izv. Atmos. Ocean. Phys.* **2010**, *46*, 14–20. [CrossRef]

8.   Döscher, R.; Vihma, T.; Maksimovich, E. Recent advances in understanding the Arctic climate system state and change from a sea ice perspective: A review. *Atmos. Chem. Phys.* **2014**, *14*, 13571–13600. [CrossRef]

9.   Guemas, V.; Blanchard-Wrigglesworth, E.; Chevallier, M.; Day, J.J.; Déqué, M.; Doblas-Reyes, F.J.; Fučkar, N.S.; Germe, A.; Hawkins, E.; Keeley, S.; et al. A review on Arctic sea-ice predictability and prediction on seasonal to decadal time-scales. *Q. J. R. Meteorol. Soc.* **2016**, *142*, 546–561. [CrossRef]

10. Ng, A.K.; Andrews, J.; Babb, D.; Lin, Y.; Becker, A. Implications of climate change for shipping: Opening the Arctic seas. *Wiley Interdiscip. Rev. Clim. Chang.* **2018**, *9*, e507. [CrossRef]

11. Kim, G.S.; Lee, S.W.; Seo, Y.J.; Kim, A.R. Multimodal transportation via TSR for effective Northern logistics: Perspectives of Korean logistics companies. *Marit. Bus. Rev.* **2020**, *5*, 291–308. [CrossRef]

12. Seo, Y.J.; Chen, F.; Roh, S.Y. Multimodal transportation: The case of laptop from Chongqing in China to Rotterdam in Europe. *Asian J. Shipp. Logist.* **2017**, *33*, 155–165. [CrossRef]

13. Romano, A.; Yang, Z. Decarbonisation of shipping: A state of the art survey for 2000–2020. *Ocean. Coast. Manag.* **2021**, *214*, 105936. [CrossRef]

14. Dulebenets, M.A. Multi-objective collaborative agreements amongst shipping lines and marine terminal operators for sustainable and environmental-friendly ship schedule design. *J. Clean. Prod.* **2022**, *342*, 130897. [CrossRef]

15. Baştuğ, S.; Haralambides, H.; Esmer, S.; Eminoğlu, E. Port competitiveness: Do container terminal operators and liner shipping companies see eye to eye? *Mar. Policy* **2022**, *135*, 104866. [CrossRef]

16. Bensassi, S.; Stroeve, J.C.; Martínez-Zarzoso, I.; Barrett, A.P. Melting ice, growing trade? Melting ice, growing trade? In *Elementa: Science of the Anthropocene*; University of California Press: Berkeley, CA, USA, 2016; Volume 4.

17. Meng, Q.; Zhang, Y.; Xu, M. Viability of transarctic shipping routes: A literature review from the navigational and commercial perspectives. *Marit. Policy Manag.* **2017**, *44*, 16–41. [CrossRef]

18. Lefebvre, W.; Goosse, H. Analysis of the projected regional sea-ice changes in the Southern Ocean during the twenty-first century. *Clim. Dyn.* **2008**, *30*, 59–76. [CrossRef]

19. Laliberté, F.; Howell, S.; Kushner, P. Regional variability of a projected sea ice-free Arctic during the summer months. *Geophys. Res. Lett.* **2016**, *43*, 256–263. [CrossRef]

20. Jahn, A.; Kay, J.E.; Holland, M.M.; Hall, D.M. How predictable is the timing of a summer ice-free Arctic? *Geophys. Res. Lett.* **2016**, *43*, 9113–9120. [CrossRef]

21. Zhang, Z.; Huisingh, D.; Song, M. Exploitation of trans-Arctic maritime transportation. *J. Clean. Prod.* **2019**, *212*, 960–973. [CrossRef]

22. Xu, H.; Yang, D.; Weng, J. Economic feasibility of an NSR/SCR-combined container service on the Asia-Europe lane: A new approach dynamically considering sea ice extent. *Marit. Policy Manag.* **2018**, *45*, 514–529. [CrossRef]

23. Cheaitou, A.; Faury, O.; Cariou, P.; Hamdan, S.; Fabbri, G. Economic and environmental impacts of Arctic shipping: A probabilistic approach. *Transp. Res. Part Transp. Environ.* **2020**, *89*, 102606. [CrossRef]

24. Corman, F.; Viti, F.; Negenborn, R.R. Equilibrium models in multimodal container transport systems. *Flex. Serv. Manuf. J.* **2017**, *29*, 125–153. [CrossRef]

25. Shibasaki, R.; Kawasaki, T. International intermodal container shipping network in South Asia: Modelling and policy simulations. *Int. J. Shipp. Transp. Logist.* **2021**, *13*, 70–101. [CrossRef]

26. Rosell, F.; Codina, E.; Montero, L. A combined and robust modal-split/traffic assignment model for rail and road freight transport. *Eur. J. Oper. Res.* **2022**, *303*, 688–698. [CrossRef]

27. Bell, M.G.; Liu, X.; Angeloudis, P.; Fonzone, A.; Hosseinloo, S.H. A frequency-based maritime container assignment model. *Transp. Res. Part Methodol.* **2011**, *45*, 1152–1161. [CrossRef]

28. Bell, M.G.; Liu, X.; Rioult, J.; Angeloudis, P. A cost-based maritime container assignment model. *Transp. Res. Part B Methodol.* **2013**, *58*, 58–70. [CrossRef]

29. Song, D.P.; Dong, J.X. Cargo routing and empty container repositioning in multiple shipping service routes. *Transp. Res. Part B Methodol.* **2012**, *46*, 1556–1575.

30. Sun, Z.; Zheng, J. Finding potential hub locations for liner shipping. *Transp. Res. Part B Methodol.* **2016**, *93*, 750–761. [CrossRef]

31. Lin, D.Y.; Huang, K.L. An equilibrium-based network model for international container flows. *Marit. Policy Manag.* **2017**, *44*, 1034–1055. [CrossRef]

32. Ozcan, S.; Eliiyi, D.T.; Reinhardt, L.B. Cargo allocation and vessel scheduling on liner shipping with synchronization of transshipments. *Appl. Math. Model.* **2020**, *77*, 235–252. [CrossRef]

33. Wang, H.; Zhang, X.; Wang, S. A joint optimization model for liner container cargo assignment problem using state-augmented shipping network framework. *Transp. Res. Part C Emerg. Technol.* **2016**, *68*, 425–446. [CrossRef]

34. Karsten, C.V.; Pisinger, D.; Ropke, S.; Brouer, B.D. The time constrained multi-commodity network flow problem and its application to liner shipping network design. *Transp. Res. Part E Logist. Transp. Rev.* **2015**, *76*, 122–138. [CrossRef]

35. Lin, D.Y.; Chang, Y.T. Ship routing and freight assignment problem for liner shipping: Application to the Northern Sea Route planning problem. *Transp. Res. Part E Logist. Transp. Rev.* **2018**, *110*, 47–70. [CrossRef]

36. Zeng, Q.; Lu, T.; Lin, K.C.; Yuen, K.F.; Li, K.X. The competitiveness of Arctic shipping over Suez Canal and China-Europe railway. *Transp. Policy* **2020**, *86*, 34–43. [CrossRef]
37. Aksenov , Y.; Popova, E.E.; Yool, A.; Nurser, A.G.; Williams, T.D.; Bertino, L.; Bergh, J. On the future navigability of Arctic sea routes: High-resolution projections of the Arctic Ocean and sea ice. *Mar. Policy* **2017**, *75*, 300–317. [CrossRef]
38. Parkinson, C.L.; Cavalieri, D.J. Arctic sea ice variability and trends, 1979–2006. *J. Geophys. Res. Ocean.* **2008**, *113*. [CrossRef]
39. Clarksons. Shipping Intelligence Network. Available online: https://www.clarksons.net/ (accessed on 6 August 2022).
40. Shibasaki, R.; Iijima, T.; Kawakami, T.; Kadono, T.; Shishido, T. Network assignment model of integrating maritime and hinterland container shipping: Application to Central America. *Marit. Econ. Logist.* **2017**, *19*, 234–273. [CrossRef]

ARTICLES FOR FACULTY MEMBERS

NAVIGATIONAL RISK OF CONTAINER FALLS IN THE STRAIT OF MALACCA

Title/Author	**Quantitive HAZOP and D-S evidence theory-fault tree analysis approach to predict fire and explosion risk in inert gas system on-board tanker ship / Durukan, O., Akyuz, E., Destanoğlu, O., Arslanoğlu, Y., & Sezer, S. I.**
Source	***Ocean Engineering*** **Volume 308 (2024) 118274 Pages 1-12** **https://doi.org/10.1016/J.OCEANENG.2024.118274** **(Database: ScienceDirect)**

27th October 2024

Research paper

Quantitive HAZOP and D-S evidence theory-fault tree analysis approach to predict fire and explosion risk in inert gas system on-board tanker ship

Ozcan Durukan [a,b,*], Emre Akyuz [b], Orhan Destanoğlu [c], Yasin Arslanoğlu [b], Sukru Ilke Sezer [b,d]

[a] Galatasaray University, Maritime Vocational School, 34349, Besiktas, Istanbul, Turkey
[b] Istanbul Technical University, Maritime Faculty, 34940, Tuzla, Istanbul, Turkey
[c] Istanbul University-Cerrahpasa, Institute of Forensic Sciences and Legal Medicine, 34320, Istanbul, Turkey
[d] Iskenderun Technical University, Faculty of Barbaros Hayrettin Naval Architecture and Maritime, 31200, Iskenderun, Hatay, Turkey

ABSTRACT

Tanker ships carry volatile cargo, presenting inherent risks of fire and explosion. Inert gas systems (IGS) are pivotal in mitigating risks by displacing oxygen in cargo tanks. However, failure of IGS components may lead to fatal consequences such as loss of life and marine pollution. This paper prompts a systematic approach integrating Quantitative Hazard and Operability (HAZOP) analysis under D-S (Dempster–Shafer) evidence theory and Fault Tree Analysis (FTA) to predict and quantify the fire and explosion risk associated with IGS malfunction on tanker ships. The methodology systematically evaluates failure probabilities, and consequences using HAZOP to identify critical scenarios. D-S evidence theory is employed to address uncertainties and incorporate expert knowledge into the analysis. FTA is applied to model fault propagation and assesses the likelihood of fire and explosion events based on the identified failure scenarios. A case study is presented to demonstrate the application of the proposed methodology, illustrating effectiveness in identifying high-risk scenarios and providing insights for enhancing operational safety minimising the risk of IGS on tanker ships. The findings show that the risk of fire and explosion in the inert gas system due to the high concentration of oxygen entering the tank was found to be 2.86E-01. Besides its robust theoretical background, the findings of the paper provide the utmost contribution to ship crew, ship inspectors, HSEQ managers and safety professionals for proactive risk mitigation strategies, contributing to the advancement of safety management practices in the maritime industry.

1. Introduction

Safety is always on the agenda in the maritime industry. It's about protecting the marine environment, human life and economic interests. Staying safe at sea is undoubtedly the most important consideration for seafarers. It is well known that the sea can be so attractive that it frightens people. It can suddenly change its deceptive structure and turn into the biggest nightmare ever seen (Formela et al., 2019). Collisions, falling objects, deterioration of structural integrity, equipment failure, stranding, leaks, fires, explosions and many other inherent risks exist in the marine and offshore industry (Ok, 2019). An accident involving fire is one of the most serious and deadly incidents that can occur on a ship (Soner et al., 2015). Given the hazardous nature of the cargoes they carry and the special requirements for handling them, tankers are exposed to high risks (Arslan and Er, 2008; Elidolu et al., 2022). Most tanker fires and explosions are caused by gases coming into contact with

an ignition source in the tank atmosphere where flammable and explosive gases, such as oil vapour, are not adequately removed (Ahn et al., 2021). In order to prevent fire, cutting the air with flammable materials can be applied. Inert gas is used to cut off the contact of flammable materials with air (Yasa et al., 2016). The Maritime Safety Committee (MSC), organised by the IMO, has approved amendments to the SOLAS Convention concerning the use of inert gas systems on new tankers and on existing tankers of more than 20,000 deadweight tonnage when carrying cargoes with a low flash point (Akyuz, 2015). Despite continuous developments in technology and maritime safety management, maritime accidents continue to occur, causing great harm to people and the environment. Between 2010 and 2019, there were 26071 accidents, of which 951 resulted in total casualties (Safety and shipping review, 2020), according to Lloyd's List Intelligence Accident Statistics (Shi et al., 2021).

There are few studies in the literature on inert gas systems, which are

important for fire safety, especially in tankers. However, studies are available which look at the protective gas system from various angles. Akyuz (2015) presented an approach to quantify the probability of human error in the gas inerting operation of crude oil tankers. Unlike traditional HEP assessment methods, the study utilises a quantitative approach to systematically estimate human error for specified tasks and to determine the desired level of safety control on crude oil tanker vessels. Thomas and Skjong (2009) aimed to elaborate on the effectiveness of N2 inert gas systems (IGS) for chemical tankers and conventional fuel burning type inert gas systems (IGS) for oil tankers in reducing the risk associated with cargo tank fire and explosions on chemical and oil tankers smaller than 20,000 DWT. Accordingly, the Gross Cost of Avoiding Fatality (GCAF) and Net Cost of Avoiding Fatality (NCAF) are calculated using the standard FSA method recognised by the International Maritime Organization (IMO). In addition, the Cost to Avoid One Tonne of Oil Spill (CATS) was applied to understand the cost effectiveness of IGSs in preventing environmental pollution. Milkovic et al. (2021) addressed the fact that many of the terminals where Long Range 2 tankers used for the carriage of petroleum products operate cargo cannot use their full capacity due to technological obsolescence and the fact that they are built for medium-range and Long Range 1 tankers. In their study, using analysis and synthesis methods, comparative methods and elements of the mathematical method, they describe a possible solution to this problem using the environmentally friendly START/STOP operating mode of an inert gas generator. Malakhov et al. (2020) presented alternatives for the development of a new technology for the ventilation of cargo holds during inert gas operation on tankers. Yasa et al. (2016) emphasised the importance of inert gas in terms of fire prevention and fighting, especially in tanker ships, and its conditions were examined. Okafor et al. (2012) evaluated the On-Board Inert Gas Generation System (OBIGGS) using a genetic algorithm. Functional hazard assessment (FHA), preliminary system safety assessment (PSSA), fault tree analysis (FTA) and failure mode and effect critical analysis (FMECA) were used in the study. Chiang et al. (2009) investigated the flammability characteristics of methanol under operating conditions during processing. The effects of N2 and CO2 as different inertising gases on the safety related parameters determined in the study were discussed and explained. Mountford et al. (2006) investigated the extent to which existing inert gas technology can be used for fire risk reduction, fire prevention or extinguishment on RN surface warships, based on the significant reduction in fire and explosion incidents on tankers. A phased assessment of ship-specific operating procedures, compartment design and emergency scenarios was carried out, taking into account general criteria such as the remaining life of the ship and the fire risk of the compartments. Aydin et al. (2021) aim to perform a systematic probabilistic analysis of the risk of asphyxiation during the gas inerting process on a chemical tanker ship. In the study, a detailed probabilistic risk assessment was performed using Bayesian network and fuzzy logic methods that can calculate the conditional probability of each basic and intermediate node of the process. Fang et al. (2022) contributed to the understanding of the inerting mechanism of N2 and CO2 in coal and the evaluation of their inerting performance. In the study, an experimental procedure for replacing oxygen with inert gas was applied in coal, consisting of a preparation stage, a vacuum pumping stage, a free space volume determination, an oxygen adsorption stage and a replacement stage. Siswantoro et al. (2020) provided an overview of the modification of the seawater scrubber system in the inert gas system of tankers from seawater utilisation to freshwater. A basic research framework such as problem formulation, literature review, design, calculation, verification and conclusions were applied as a methodology in the research.

Inert gas systems, which have an important role in terms of safety in the maritime transport sector, are accepted with the existing safety measures and are not sufficiently analysed. The main purpose of this study is to make a risk analysis of the diagram of an inert gas system currently used for the safety of the inerting process and to find the accident potential of the system-induced malfunctions during the inerting

operation. For the analysis, an inert gas system diagram in which the inert gas is obtained from the main or auxiliary boilers was chosen for examination. Thus, revealing the operational risks that the mentioned inert gas systems, which have a more complex structure and are mostly used in crude oil tanker ships, may have, with combined risk assessment systems, will contribute to increasing operational safety in the sector and fills an important gap in the literature. The novelty of the article is to reveal the hidden risks of inert gas systems with standard operating conditions.

In the first step, a descriptive and cross-sectional study was conducted to identify potential hazards that could cause a ship's inert gas system to malfunction and assess risks on a ship. To this end, the HAZOP (Hazard, and Operability Analysis) method, which provides qualitative and quantitative results, has been used for the detection, analysis and elimination of failures that may occur in the inert gas system and associated equipment.

In the second step, the top event was selected from the possible outcomes of the HAZOP risk analysis and root cause analysis was performed using Fault Tree Analysis (FTA). At this stage, the intermediate and main events were evaluated as possible causes obtained by the HAZOP method. Finally, the probabilities of the root causes were calculated using the D-S evidence HEART approach. These probabilities were used in the fault tree analysis.

2. Methodology

This section describes the methods used in the research.

2.1. Hazard and operability analysis (HAZOP)

A systematic design analysis, HAZOP, has been developed for an understanding of the operational problems and potential hazards of the system (Ay et al., 2022; Mokhtarname et al., 2022). It is a highly scientific and disciplined process for the monitoring of process plants that are in contact with hazardous substances. Originally developed and then modified to improve hazard identification capabilities, it was designed to detect defects and deviations that could lead to obvious events such as explosions, fires and toxic releases (Solukloei et al., 2022).

HAZOP is based on a theory that dangerous events result from deviations from design and operational targets. Such deviations are easily identified using a set of 'guide words' as a systematic list of divergent perspectives. This approach helps to capture the imagination of team members as they identify potential deviations, which is a unique feature of the HAZOP methodology (PQRI, 2014). Fig. 1 shows the HAZOP procedure (Silvianita et al., 2015).

Many factors have an influence on the success or failure of a HAZOP. An attempt has been made to generalise these factors as follows (Crawley and Tyler, 2015a).

- Accuracy and consistency of the data used (drawings, etc.) to support the work done
- The intuition and technical skills of the team
- The capability of the team to focus on more serious hazards

2.2. Fault tree analysis (FTA)

Fault Tree Analysis is a systematic, deductive approach to analysis, working from the occurrence of a failure to the identification of its root causes (Gharahasanlou et al., 2014). Accordingly, the fault tree diagram begins with the undesired event i.e. top event. Then, intermediate events and basic events that cause the top event to occur are identified. The relationship between events is presented through logic gates. The constructed fault tree diagram provides an understanding of the path leading to the top event (Sezer et al., 2023). In other words, by providing a quantitative analysis of the system and showing the relationships between the top event and the basic events, the FTA shows the probability
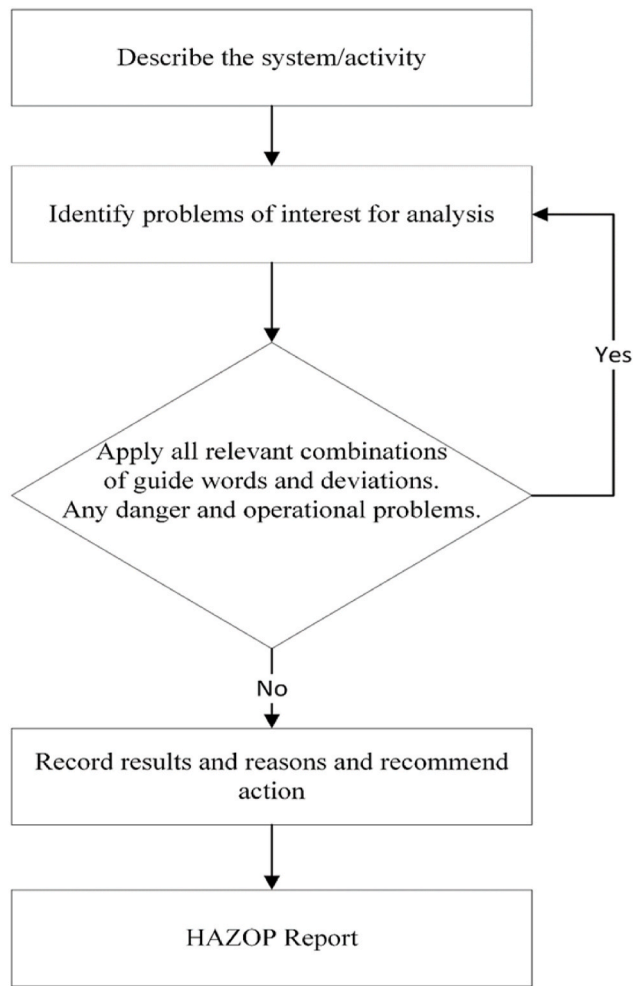
Fig. 1. HAZOP procedure.

of failure and calculates the level of system reliability based on a logical diagram (Gachlou et al., 2019). The application steps of this technique are (Fuentes-Bargues et al., 2017) basically: i.) Define the top event, ii.) Creating fault tree diagram, iii.) Qualitative evaluation, iv.) Quantitative evaluation.

2.3. D-S evidence HEART

D-S evidence theory (Shahriar et al., 2012) is a robust tool to fuse information from various sources and handle uncertainty. The method has been widely applied in different disciplines to transform judgements/decisions into meaningful data (Guo et al., 2023; Liu and Zhang, 2020). On the other hand, HEART (Human Error Assessment and Reduction Technique) is a practical tool to predict human error probability systematically for a specific task (Sezer et al., 2023; Williams, 1988). The hybrid method combining D-S evidence and HEART is used to calculate the occurrence probability of basic events in FT since the data-set is of paramount importance to calculate risk. By integrating D-S evidence theory into the HEART approach, consistency in APOA calculation is increased and data from multiple experts can be aggregated (Sezer et al., 2022). The basic steps of the D-S evidence HEART method consist of; i.) Task analysis, ii.) Scenario definition, iii.) GTT (generic task type) and EPC (error producing condition) selection, iv.) APOA (assessed proportion of affect) calculation and v.) HEP calculation.

2.4. Integration of methods

A cross-sectional study using the HAZOP method, which presents qualitative and quantitative results, provides detailed and sufficient information about the risk of the issue under consideration. Accordingly, the TE of FT can be selected. In addition, the detailed analysis provided by the HAZOP method helps to identify the BEs. The FT represents the root cause analysis using logic gates. Then, the probabilities of the BEs are determined using the D-S evidence based HEART method and the analysis is quantified by calculating the probability of the TE. In traditional FTA, the probability of the top event occurring is calculated based on the failure probability of the basic events. The probabilities of basic events are exact values. Probabilities are not dependent on actual data due to data scarcity. Therefore, they are obtained from expert judgements. The D-S evidence theory-based HEART approach is used to overcome subjectivity and uncertainty arising from expert judgements. Thus, the probability of the top event can be calculated more accurately. The conceptual framework of the approach is shown in Fig. 2 (Sezer et al., 2023).

2.4.1. Determining process parameter and deviation

HAZOP is derived from a theory based on the assumption that hazard events occur as a result of deviations from the design or operational objectives. Such deviations are easily identified using sets of 'keywords' as a systematic listing of a wide range of deviation perspectives (PQRI, 2014). Using the HAZOP keywords listed in Table 1, we create these potentially problematic deviations. (Aspinall, 2006; Suzuki et al., 2021).

While some recommendations can be made with regard to the keywords to be considered, this is not the case with regard to the parameters. For each system under consideration, the parameters must be selected by the responsible teams. Table 2 gives examples of possible parameters for process operations (Crawley and Tyler, 2015b).

2.4.2. Identifying possible causes and consequences

The HAZOP concept is the brainstorming of the design of the facility by a multidisciplinary team, following the experience of the team leaders and the structure provided by the guide words during the facility review meetings (Dunjó et al., 2010). The main advantage of these brainstorms is that they stimulate creativity and generate ideas. The interaction of the team and the different experiences they have had in the past are the source of this creativity, so the participation of all team members is necessary and team members should avoid criticising each other when putting forward ideas. When a particular point in the design, called a node, is examined by the team using guide words, the deviations in the process parameters are analysed in detail for each node. Guide words are used as guidelines to control the design in every conceivable way. The best time to perform a HAZOP analysis is when the design is fairly robust. (Kotek and Tabas, 2012).

The success or failure of the HAZOP depends on many elements.

- The completeness and accuracy of the data and drawings used to create the work.
- Intuition and technical skills of the team
- The ability of the team to focus on the more serious risks that have been identified

2.4.3. Constructing FT diagram

A fault tree is usually a logic diagram that symbolises the relationships between the failure events of a system that are caused by a combination of faults. Logic gates and events are used to show how the states of the components are in relation to the state of the whole system (Peeters et al., 2018). The causal effects that are defined deductively are organised logically. Following the most significant event, the causal factors and the logical relationships between them are then presented in a tree diagram, as in Table 3 (Fuentes-Bargues et al., 2017).

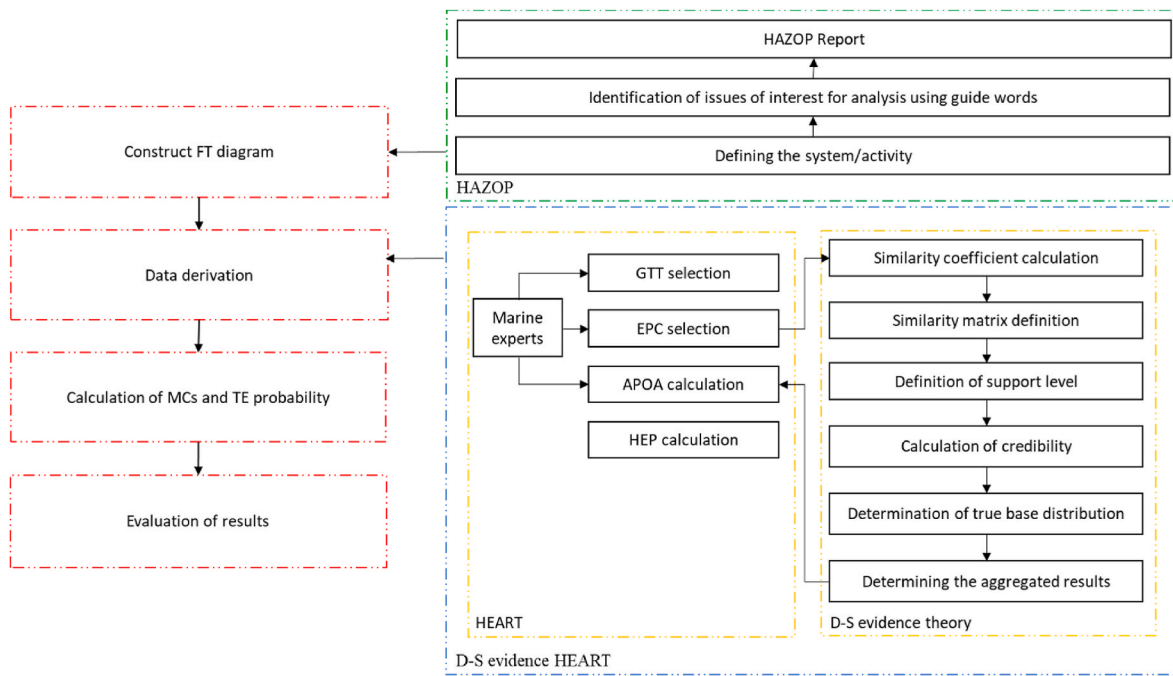Logical links, the branch of the failure tree, consist of gates using the

Fig. 2. Conceptual framework of the approach.

Table 1
Guide words of HAZOP.

Guide words	Interpretations	Examples
No	Task not completed	Operator skips next step
Less	Do less than what needs to be done	Completion of less than required amount due to not opening all valves at once
More	Do more than just action	A larger amount was completed due to the fact that the valves were opened more than they should.
Reverse	Do the reverse of what should be done	Reversal of the previous action as a result of closing the valves instead of opening them.
Part of	Not all tasks required to be done in action have been done	Skipping some of the actions in the step.
As well as	Do something else in addition to the task that needs to be done	Additional material is processed by opening the additional valve.
Other than	Do something other than the task that needs to be done	Wrong material processed by opening wrong valve.
Sooner	Perform the action before the time specified	Very fast action by changing the order of the steps
Later	Perform the action after the specified time	Very slow action by changing the order of the steps
Other	Different factors which may influence the action	Change of shift working

Table 2
Examples of parameters used in process operations.

Pressure	pH	Operate	Monitoring
Flow	Reaction	Phase	Signal
Mixing	Composition	Speed	Start/stop
Stirring	Temperature	Transfer	Aging
Particle size	Addition	Measure	Maintain
Level	Sequence	Control	Diagnostics
Time	Separation	Viscosity	Services

Table 3
Guide words, deviations, and explanations.

Symbol	Meaning	Description
	AND gate	The output event occurs only if all input events occur.
	OR gate	Output event occurs if any of the input events occur
	Basic event	The primary cause is the failure of an unidentified component and has the highest level of detail in the fault tree.
	Undeveloped event	Failure of a component with an undeveloped primary cause due to lack of knowledge
	Intermediate event	A fault event that happens due to one or more predecessors causes action by means of logic gates.

only occur if all events at input (Ai) occur simultaneously. The probability of an output event at such a gate is calculated using Equation (1) (Markulik et al., 2021).

$$P(\mathrm{G}) = \prod_{i=1}^{n} P(\mathrm{A_i}) \tag{1}$$

The "OR" gate is "negative" - a negative event occurs at output P(G) and any event occurs at an input (Ai). Using equation (2), the probability of an event occurring at the output of such gates is calculated.

$$P(G) = 1 - \prod_{i=1}^{n} (1 - P(\mathrm{Ai})) \tag{2}$$

The completed FT diagram can be analysed both qualitatively and quantitatively. Using Boolean algebra, the top event can be evaluated quantitatively by deriving an expression in terms of combinations of

logical symbols (AND) and (OR). Each door has an entry and an entry event. The "AND" gate uses a logical sum representing the combination of unrelated events. "It is positive" - A negative event at output P(G) will

primary events. In the quantitative part, the probability of the top event occurring is expressed in terms of the probability of the primary events occurring or the minimum cutoff sets (Khakzad et al., 2011).

2.4.4. Calculating failure probabilities of BEs

D-S evidence HEART model is applied to calculate probabilities of BEs in the constructed fault tree diagram. After the BEs are determined for the relevant process, the D-S evidence HEART model is conducted in three steps. These are; i) GTT and EPC selection, ii) APOA calculation, iii) HEP calculation (Sezer et al., 2023).

Firstly, for each BE, one of the nine GTTs defined from A to M in the HEART methodology is selected according to the consensus of the experts. Thus, the generic error probability (GEP) value is determined. Then, experts select from thirty-eight EPCs that affect human performance. If experts select more than one EPC, the APOA calculation is performed. Experts may assess the same EPCs differently when more than one EPC is selected. In this context, different assessments of different experts (e_p) are aggregated by applying modified D-S evidence theory. The aggregation process is applied based on crossmerging. The following equations are used for the aggregation process (Sezer et al., 2023).

$$sim(e_p, e_q) = \frac{\sum\limits_{EPC_l \cap EPC_m \neq \varnothing} e_p(EPC_l)e_q(EPC_m)}{\sqrt{\left(\sum \left(e_p(EPC_l)\right)^2\right) \cdot \left(\sum \left(e_q(EPC_m)\right)^2\right)}} \quad (3)$$

In Equation (3), the similarity coefficient ($sim(e_p, e_q)$) between the experts is computed using the assessments of the experts. e_p and e_q express the opinion of two different experts. Then the support degree ($\sup(e_p)$) and credibility ($Crd(e_p)$) of the experts is obtained through Equations (4) and (5) (Uflaz et al., 2022; Sezer et al., 2023).

$$\sup(e_p) = \sum_{q=1,q\neq p}^{n} sim(e_p, e_q) \quad (p = 1, 2, \ldots n) \quad (4)$$

$$Crd(e_p) = \frac{\sup(e_p)}{\sum\limits_{p=1}^{n} \sup(e_p)} \quad (p = 1, 2, \ldots n) \quad (5)$$

In Equation (4), the sum of the similarities between the e_p and other experts is the support degree of the e_p. In this way, the support degree for each expert opinion is determined. The credibility of each expert is determined by applying the normalization process in Equation (5). Finally, the basic true distribution of the EPCs ($e_c(EPC_t)$) is calculated using Equation (6) and the aggregated APOA ($\overline{APOA}_t$) is defined by conducting Equation (7). Equation (8) is applied to calculate the HEP value (Uflaz et al., 2022; Sezer et al., 2023).

$$e_c(EPC_t) = \sum_{p=1}^{n} e_p(EPC_t) \cdot Crd(e_p) \quad (t = 1, 2, \ldots, 38) \quad (6)$$

$$\overline{APOA}_t = e(EPC_t) = \frac{e_c(EPC_t)^2}{\sum\limits_{t=1}^{n} e_c(EPC_t)^2} \quad (t = 1, 2, \ldots, 38) \quad (7)$$

$$HEP = GEP \times \left\{ \prod_t [(EPC_t - 1)\overline{APOA}_t + 1] \right\} \quad (8)$$

2.4.5. Calculating failure probability of TE and MCS

D-S evidence HEART modelling is adopted to calculate the occurrence probability of BE in the FT diagram. Based on the calculating failure probability of BEs, the occurrence probability of TE is calculated. Thereby, the overall likelihood of the top event (TE) and MCSs are computed for detailed risk analysis.

3. Illustrative example: fire and explosion risk in inert gas system on-board tanker ship

This section shows how a detailed quantitative risk analysis is performed to predict potential fire and explosion risk in tanker ship.

3.1. Inert gas system on-board tanker ships

An IG system is designed to prevent tanks from burning or exploding. It is not a fixed fire-fighting system. However, it can be used to help control fires and prevent explosions (ICS, 2020). The main use of inert gas is for the control of the atmosphere in a cargo tank in order to prevent the formation of flammable mixtures. The most important requirement for inert gas is a low oxygen content. Apart from this, the composition of inert gas can vary (ICS, 2020). Oxygen levels vary depending on the type of cargo and volatile and flammable gases. For example, the maximum oxygen level for a hydrocarbon gas-emitting cargo is 11%, since the gas it emits does not react with oxygen. On the other hand, for a cargo that emits hydrogen gas, the maximum oxygen content is 5%, according to the International Convention for the Safety of Life at Sea (Solukloei et al., 2022; Yazir et al., 2021).

A characteristic diagram of a flue gas inerting system is shown in Fig. 3. In this system, dirty and hot gas passes from the boiler through a shut-off valve located at the boiler suction to the scrubber and demister. At this stage, the gas is cooled and purified. It is then transferred to the cargo tanks by blowers through the deck water seal, check valve and deck isolation valve. The flow to the cargo tank is regulated by a gas pressure regulating valve located downstream of the blowers. In addition, a liquid-filled pressure/vacuum breaker is installed in the circuit to prevent any damage to the cargo tanks caused by excessive pressure or vacuum. A vent is installed between the deck isolate/one-way valve and the gas pressure regulating valve to vent any leaks that may occur when the system is not in use (IMO, 1990).

The inert gas circuit runs from the deck isolating valve forward along the entire cargo deck. This allows inert gas to be supplied to the cargo tanks during operations such as cargo discharge, deballasting, tank cleaning and topping up the gas pressure in the tank for other stages of the voyage. From the main inert gas line, lateral lines emerge from the top of each cargo tank (IMO, 1990).

Flammable mixtures in the inert gas system can cause fire and explosion with catastrophic consequences for ship crew, marine environment and goods. Therefore, assessing the risk of fire and explosion in the inert gas system and taking preventive measures is very significant for maritime safety practitioners. In this context, this paper systematically estimates the risk related to this issue and provides recommendations for enhancing safety at sea.

3.2. Analysis of respondents

Expert judgement can provide assurance of accuracy when a dataset is not available (Rae and Alexander, 2017). Due to the scarcity of data in the maritime industry, expert judgement is generally used. This allows the data set to be practically collected. In this paper, expert judgement was used for the HAZOP analysis, the construction of the FT diagram and the calculation of the probabilities of BEs. Five marine experts participated in the study. The experts have carried out many operations with the inert gas system. They therefore have extensive knowledge and experience of the inert gas system. They are able to provide a high-level assessment. The marine expert profiles consist of ocean-going masters, academics and chief officers. Table 4 presents experts' essential information.

3.3. Empirical risk analysis

HAZOP is used as a hybrid of the FTA methods to perform a systematic analysis, which provides a detailed understanding of the
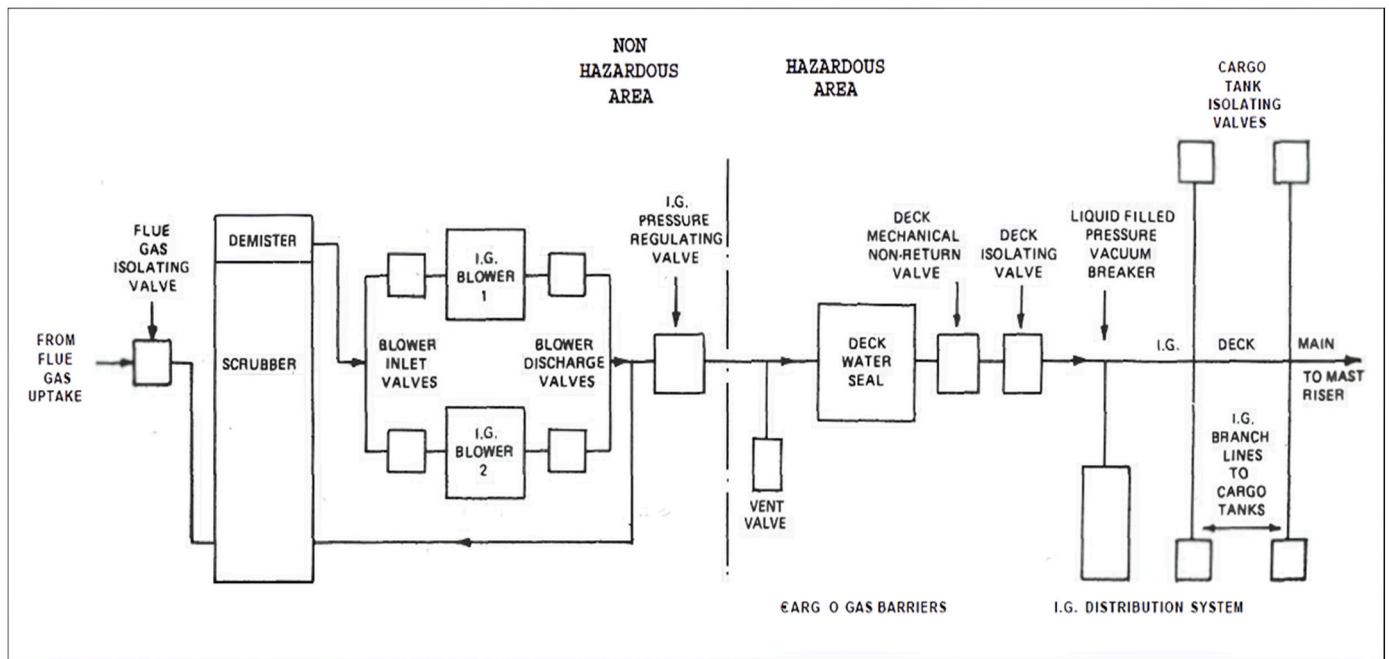
Fig. 3. A typical arrangement for an inert gas system.

Table 4
Profile of marine experts participating in the study.

Expert	Position	Education	Experience	Information
1	Oceangoing Master	BSc.	9 years	This expert is actively engaged in working aboard tanker ships and manages frequent cargo operations.
2	Oceangoing Master	BSc.	10 years	This seasoned professional, equipped with extensive expertise in inert gas systems, commanded inert gas operations. He is acquainted with the necessary procedures throughout these operations.
3	Oceangoing Chief Officer	BSc.	8 years	He works on board and is responsible for cargo operations. He has extensive knowledge and experience in cargo operations. He provides instructions to the ship's officers regarding safe cargo operations.
4	Academician	PhD.	7 years	This expert is a former oceangoing chief officer onboard. He has extensive experience in cargo operations. He works at a university as an academician and conducts research on the safety of tanker ships.
5	Academician	MSc.	5 years	She served as an oceangoing chief officer aboard ships. She performed studies focused on risk analysis.

operational process of inert gas system on-board tanker ship. The D-S HEART method was used to determine the required failure probabilities in the FT diagram. The first step is to form a HAZOP team of ten marine experts responsible for using and controlling the inert gas systems concerned on crude oil tanker ships. Then, using a sketch taken from crude oil tankers, the diagram of the system is drawn. The diagram of the system is divided by the HAZOP team into five separate nodes which are shown in Fig. 4.

The operational nodes split by the HAZOP team and listed below are also assessed by the HAZOP team against their intended operational functions using guide words.

● Node 1: Boiler to the scrubber unit (Table 5)
● Node 2: Scrubber unit to deck seal (Table 5)
● Node 3: Deck Seal to cargo tank (Table 5)
● Node 4: Seawater supply and drain line of scrubber unit (Table 5)
● Node 5: Seawater supply unit of deck seal unit (Table 5)

After having created the HAZOP work sheet, risk analysis of fire and explosion risk in inert gas system on-board tanker ship is performed under FT analysis. The top event of the FT diagram is created by using the research output of HAZOP analysis, where the gas with high oxygen concentration at node 3 of the inert gas diagram entered the cargo tanks and the risk of fire and explosion occurred. The FT diagram is created based on marine expert judgements under Class and P&I circulars, inert gas system manual, accident investigation report and ISGOTT. Accordingly, Fig. 5 shows an FT diagram covering the top event (TE), intermediates (IE) and basic events (BE) for fire and explosion risk in inert gas system on-board tanker ship. Table 6 gives definitions of the FT diagram including TE, IE and BE.

Since data scarcity is one of the most significant challenges for the maritime industry, quantification of the BE in the diagram is performed based on the marine expert's judgement. To achieve this purpose, a robust D-S evidence HEART modelling is applied. Hence, marine experts' judgements are transformed into meaningful crisp values. The operational task sequence for inert gas system in tanker ship is illustrated in Table 7 in conjunction with relevant BEs.

According to Fig. 5 and Table 7, the D-S evidence HEART model is applied and the probabilities of each BE are calculated according to
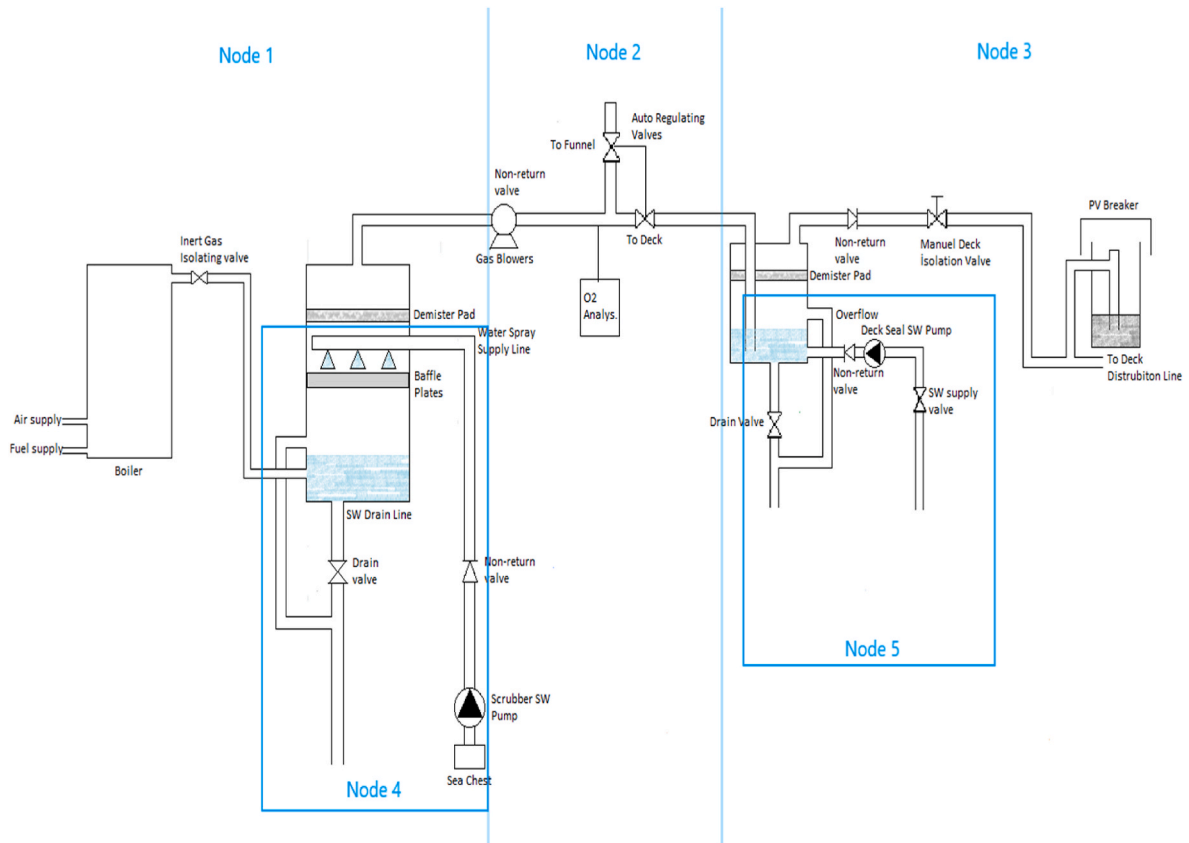
Fig. 4. Diagram of an inert gas system with operational nodes.

equations (3)–(8). In this context, Table 8 lists the HEP values (occurrence probability) of BEs. In addition, the results of the APOA calculations as well as the GTT and EPCs determined by the experts for each BE are shown in Table 8.

According to the FT diagram and logic gates, the occurrence probability of the TE (Fire and explosion risk in inert gas system due to high concentration of oxygen enters into tank) is calculated as per equations (1) and (2) respectively. The results show that the occurrence probability of TE is 2.86E-01. In the FT, the calculation of minimal cut sets (MCSs) is of paramount as they are a group of sets consisting of the smallest combinations of BE which result in the occurrence of the TE (Arici et al., 2020). The MCS represents all how the BE may cause the TE (Vesely et al., 1981). In the FTA method, the Fussel Vesely Importance Measure (FV–I) method is frequently used to determine the significance value of BEs and MCSs forming the top event (Sezer et al., 2023; Shahriar et al., 2012). Thus, the TE sensitivity for each MCS can be calculated. Table 9 illustrates MCSs, their occurrence probabilities and the FV-I list of MCSs.

$$I_i^{FV}(t) = \frac{Q_i(t)}{Q_S(t)} \qquad (9)$$

$$TE = MCS_1 + MCS_2 + \ldots + MCS_N = \bigcup_{i=1}^{n_c} MCS \qquad (10)$$

3.4. Findings and extended discussions

According to the comprehensive analysis, the risk of fire and explosion in the inert gas system due to the high concentration of oxygen entering the tank was found to be 2.86E-01, which is an overall high rate. Root cause analysis was carried out and an attempt was made to identify the causes that played a significant role in the occurrence of TE in order to understand the failure pattern. In this context, Table 8 shows the probabilities of the root causes involved in the occurrence of TE.

Table 8 shows that BE10 (incorrect air and fuel line pressure measurement) is the most effective cause of TE. The boiler operates on the principle of temperature/pressure increase by atomisation and ignition of air and fuel in the boiler furnace (Ceylan and Celik, 2024; Taylor, 1990). Flue gas oxygen concentration is the concentration of oxygen after the boiler has burned the flue gas. If the oxygen content is too high, the loss of exhaust gas is high; if it is too low, the loss of incomplete combustion of chemical fuel is high, leading to waste of fuel, so it must be kept within an appropriate range (Lingfang and Yechi, 2012). A boiler is one of the most operationally problematic auxiliary machinery of the ship due to fuel quality, combustion problems and systemic failures despite the equipment that ensures proper operation. Under this condition, in order to send the appropriate inert gas in terms of oxygen

$$P(T) = P(MCS_1 \cup MCS_2 \cup \ldots \cup MCS_N) = P(MCS_1) + P(MCS_2) + \ldots P(MCS_N) - (P(MCS_1 \cap MCS_2)$$
$$+ P(MCS_1 \cap MCS_3) + \ldots P(MCS_i \cap MCS_j) \ldots) \ldots$$
$$+ (-1)^{N-1} P(MCS_1 \cap MCS_2 \cap \ldots \cap MCS_N) \qquad (11)$$

Table 5
HAZOP worksheet for all nodes.

No	Guide Words	Deviation	Possible Cause	Consequence	Action Required
1	None	No flow	(1) Line blockage	Loss of time, high soot concentration in inert gas lines.	(1.1.1) Institute regular patrolling & inspection of boiler uptake line. (1.1.2) Install on/off indicator on the valve. (1.1.3) Install pressure gauge on the line before boiler uptake valve.
2	More of	More heat	(2) Excess fuel supply in boiler (3) Fuel, air auto regulating valve malfunction	Structural damage to the scrubber and inert line.	(1.2.1) Install heat sensor and thermometer on scrubber unit and institute regular check heat inside the scrubber tower. (1.2.2.) Install fuel pressure gauge on fuel line of boiler (1.2.3) Institute regular inspection and maintenance for Fuel auto regulating valve.
3	Part of	High O2 concentration in IG	(4) Excess air supply in boiler As for (3)	Gas with a high percentage of oxygen coming out of the boiler	(1.3.1) Install pressure gauge on air supply line of boiler (1.3.2) Check O2 level from boiler regularly. Covered by (1.2.3)
		High SO2 concentration in IG	(5) Poor fuel quality As for (2) As for (3)	Gas with a high percentage of SO2 coming out of the boiler	(1.3.3) Performing regular fuel analysis. Covered by (1.2.2) and (1.2.3)
4	Reverse	SW flow from scrubber to boiler	(6) High water level in scrubber unit	Boiler malfunction.	(1.4.1) Install high level alarm on scrubber unit (1.4.2) Institute regular check for water level in scrubber unit.
5	Other	Maintenance	(7) Gas leakage from boiler, IG line and/or scrubber tower.	Toxic gas release to public space.	(1.5.1) Performing pressure test to IG line regularly. (1.5.2) Check pressure continuously during operation. (1.5.3) Install atmosphere monitoring system in engine room.
6	None	No flow	(8) Line blockage (9) Inert gas fans' failure (10) High water level inside the scrubber tower (11) Blockage on baffle plates in scrubber tower (12) O2 concentration in IG more than 5% as per SOLAS (13) Failure of automatic diverting valves and/or O2 analyser	Exposure of scrubber and line to unsuitable conditions.	(2.6.1) Install pressure gauge on output line of scrubber. (2.6.2) Institute regular check and/or test for inert gas fans' condition. (2.6.3) Install high level alarm on scrubber unit. (2.6.4) Check and clean inside the scrubber tower regularly. Covered by (1.2.3), (1.3.1), (1.3.2) (2.6.5) Check and test automatic diverting valves regularly (2.6.6) Check O2 analyser with reference gas detector regularly (2.6.7) Calibrate the O2 analyser with test gas before every inerting operation
7	Less of	Less flow	As for (8), (9) and (10)	Exposure of scrubber and line to unsuitable conditions.	Covered by (2.6.2), (2.6.3) and (2.6.4)
8	More of	More heat	(14) Insufficient cooling water inside the scrubber tower	Exposure high temperature of the line and the elements on the line	(2.8.1) Institute regular inspection to the sea water line of scrubber tower. (2.8.2) Install pressure and flow gauge on sea water line of scrubber tower.
9	Part of	High SO2 concentration in IG	(15) Baffle plates in the scrubber unit in poor condition. (16) Poor fuel quality	Release of gas containing high SO2 to the atmosphere	(2.9.1) Performing regular fuel analysis. (2.9.2) Inspect baffle plates condition regularly. (2.9.3) Install fixed gas measurement device on IG output line of scrubber tower.
10	More than	Soot	As for (15) and (16)	Air pollution, Soot piles up in the IG line.	Covered by (2.9.1), (2.9.2) and (2.9.3)
11	Other	Maintenance	(17) Gas leakage from IG line, fans	Toxic gas release to public space.	(2.11.1) Performing pressure test to IG line regularly. (2.11.2) Check pressure continuously during operation. (2.11.3) Install atmosphere monitoring system in engine room.
12	None	No flow	(18) More water level inside deck seal unit	Loss of time	(3.12.2) Install high level alarm on deck seal unit
13	More of	More pressure	(19) Excessive working condition of the IG fans. (20) High oil level inside the PV breaker.	Exposing the IG line to high pressure, Oil spill on main deck	(3.13.1) Institute starting and using procedure for IG fans (3.13.2) Check oil level of PV breaker. (3.13.3) Establish patrol on deck with the IG system on (3.13.4) Keep an oil spill kit ready near the PV breaker Covered by (3.12.2)
14	Less of	Less flow	(21) Jammed deck isolation valve (22) More cargo tank supply valve open than the system can handle As for (18)	Loss of time	(3.14.2) Institute regular check and test for deck isolation valve (3.14.3) Check all tanks' supply valve and institute tank inerting procedure
15	As well as	Water	(23) Demister pads in deck seal in poor condition	Water entering the cargo tank	(3.15.1) Check, clean and renew demister pads regularly. (3.15.2) Install filter for water output of deck seal

Table 5 (*continued*)

| No	Guide Words	Deviation	Possible Cause	Consequence	Action Required
		Soot	(24) Low water level inside deck seal (25) Uncleaned deck seal unit	Soot entering the cargo tank	(3.15.3) Install low level alarm on deck seal (3.15.4) Check and clean deck seal regularly
16	Part of	High O2 concentration in IG	(26) Failure of O2 analyser As for (3) and (4)	Inert gas with high oxygen content entering the cargo tank	Covered by (2.6.6) and (2.6.7)
17	Reverse	Cargo vapour flow in opposite direction	(27) Non-return valve error (28) High cargo tank pressure	Equipment damage	(3.16.1) Check tanks' pressure before operation. (3.16.2) Check non-return valve condition regularly
18	None	No flow	(29) Scrubber sw pump failure (30) SW supply valve failure (31) Damaged non-return valve	Insufficient water level in scrubber tower, Loss of time	(4.18.1) Install pressure gauge on sw supply line of scrubber tower
19	More of	More back pressure	(32) High sea water level in scrubber tower (33) SW drain line blockage	Demister pad damage	Covered by (3.12.2)
20	Less of	Less flow	As for 29, 30 and 32	Insufficient water level in scrubber tower, Loss of time	Covered by (3.12.2) and (4.18.1)
21	As well as	Impurities in sea water	(34) Sea chest in poor condition	Quick contamination in scrubber tower and structural damage	(4.21.1) Regular inspection and cleaning of the sea chest.
22	Reverse	SW flow in opposite direction	(35) High back pressure due to high water level in scrubber unit As for 31	Scrubber sw pump damage	Covered by (3.12.2) and (4.18.1)
23	None	No flow	(29) Deck seal sw pump failure (30) SW supply valve failure (31) Damaged non-return valve	Insufficient amount of water in the deck seal, Loss of time	(5.23.1) Install pressure gauge on sw supply line of deck seal
24	More of	More back pressure	(32) High sea water level in deck seal (33) SW drain line blockage	Demister pad damage	Covered by (3.12.2)
25	Less of	Less flow	As for 29, 30 and 32	Insufficient amount of water in the deck seal, Loss of time	Covered by (3.12.2) and (5.23.1)
26	As well as	Impurities in sea water	(34) Sea chest in poor condition	Quick contamination in deck seal and structural damage	Covered by (4.21.1)
27	Reverse	SW flow in opposite direction	(35) High back pressure due to high water level in deck seal As for 31	Deck seal sw pump damage	Covered by (3.12.2) and (4.18.1)
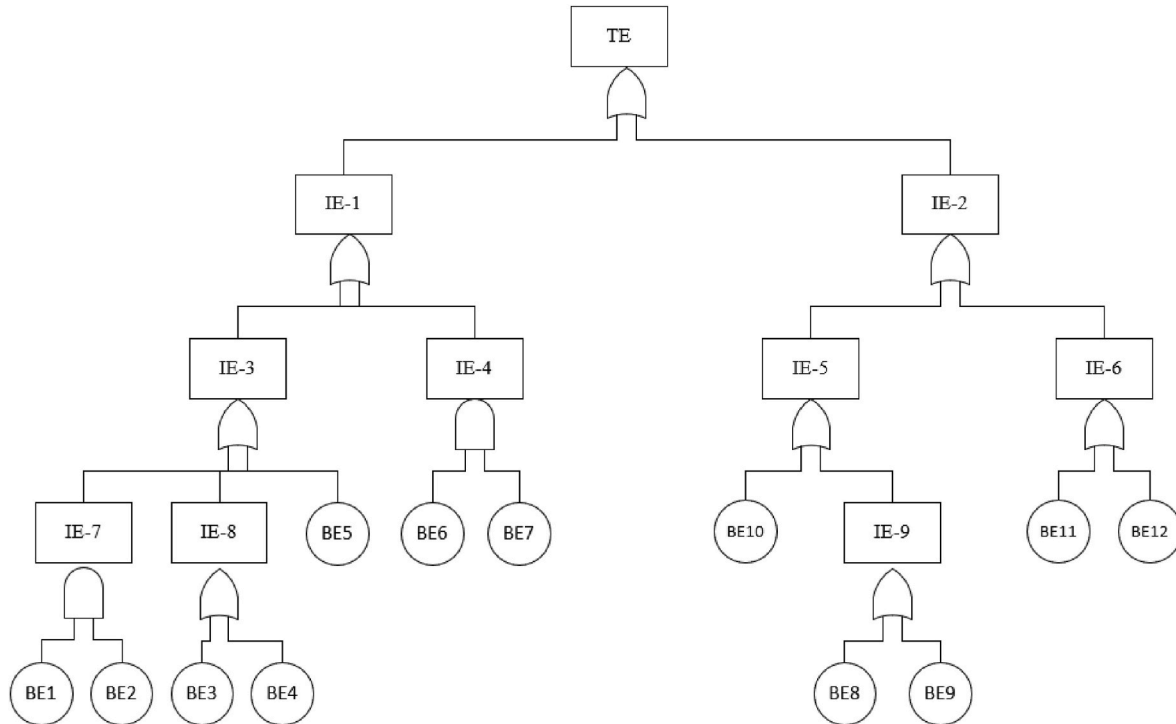
Fig. 5. Fault tree diagram.

concentration to the cargo tanks in the inerting operation, the appropriate inert gas must first be produced in the boiler. For this reason, it is understood that the combustion of the air and fuel mixture in the boiler is one of the most important steps of the process. The amount of fuel and air entering the boiler is provided by automatic adjustment valves. Any error and/or dysfunction that may occur in these valves will directly affect the combustion efficiency and change the character of the gas to be formed and thus the first link of the error chain will have occurred. In

Table 6
Definition of TE, IE and BE in FT diagram.

Event	Definitions
TE	Fire and explosion risk in inert gas system due to high concentration of oxygen enters into tank
IE-1	Auto diverter valves error
IE-2	Output of inert gas with high oxygen content from boiler
IE-3	Oxygen analyser error
IE-4	Defective auto diverter valves
IE-5	Excess air supply into boiler
IE-6	Inadequate combustion in boiler
IE-7	Uncalibrated oxygen analyser
IE-8	Sensor failure
IE-9	Auto fuel air supply valve error
BE-1	Lack of experience/knowledge of responsible staff
BE-2	Lack of planned maintenance
BE-3	Wrong calibration
BE-4	Using defective/incorrect test gas
BE-5	Computing failure
BE-6	Unsuitable operational condition
BE-7	Lack of planned maintenance
BE-8	Computing failure
BE-9	Defective valve system
BE-10	Incorrect pressure measurement on air and fuel line
BE-11	Computing failure
BE-12	Poor condition of boiler

Table 7
Operational task sequence for the inert gas system in tanker ship.

Event No.	Task definition
BE-1	Make sure that the personnel who carry out the calibration of the O2 analyser have sufficient knowledge and/or have the necessary certificates.
BE-2	Make sure that the planned maintenance is done on time and correctly and recording it.
BE-3	Ensure that calibration process is done correctly.
BE-4	Monitor a suitable and useable test gas is used for calibration.
BE-5	Check if computing system of oxygen analyser is working properly.
BE-6	Monitor that automatic diverter valves are working properly.
BE-7	Make sure that the maintenance of automatic diverter valves is done regularly.
BE-8	Monitor that computing system of fuel/air supply valve is working properly.
BE-9	Make sure that automatic fuel air supply valve is in good condition.
BE-10	Check that if pressures of the fuel and air lines are correct.
BE-11	Monitor that computing system of boiler is working properly.
BE-12	Make sure that boiler is clean and in proper condition.

Table 8
HEP and $\overline{APOA}$ calculation results for BEs.

No	GTT	EPC/s	$\overline{APOA}$	HEP
BE-1	G	EPC 10	0.026	1.91E-03
		EPC 12	0.216	
		EPC 15	0.715	
		EPC 18	0.042	
BE-2	E	EPC 13	0.066	6.87E-02
		EPC 16	0.934	
BE-3	F	EPC 10	0.343	1.71E-02
		EPC 15	0.620	
		EPC 17	0.036	
BE-4	E	EPC 15	0.489	6.89E-02
		EPC 19	0.494	
		EPC 21	0.017	
BE-5	F	EPC 13	0.105	4.54E-03
		EPC 16	0.075	
		EPC 23	0.820	
BE-6	E	EPC 19	0.035	3.32E-02
		EPC 23	0.965	
BE-7	E	EPC 13	0.110	7.39E-02
		EPC 16	0.890	
BE-8	F	EPC 15	0.401	7.35E-03
		EPC 23	0.599	
BE-9	E	EPC 16	0.707	4.49E-02
		EPC 17	0.293	
BE-10	D	EPC 17	0.090	1.64E-01
		EPC 23	0.910	
BE-11	F	EPC 15	0.209	6.27E-03
		EPC 23	0.791	
BE-12	G	EPC 11	0.858	2.48E-03
		EPC 13	0.134	
		EPC 21	0.008	

Table 9
MCS probabilities and importance values as per FV-I.

MCS no	MCS	MSC Probabilities	FV-I	Ranking
MCS$_1$	BE1BE2	1.31E-04	4.59E-04	10
MCS$_2$	BE3	1.71E-02	5.98E-02	4
MCS$_3$	BE4	6.89E-02	2.41E-01	2
MCS$_4$	BE5	4.54E-03	1.59E-02	7
MCS$_5$	BE6BE7	2.45E-03	8.58E-03	9
MCS$_6$	BE8	7.35E-03	2.57E-02	5
MCS$_7$	BE9	4.49E-02	1.57E-01	3
MCS$_8$	BE10	1.64E-01	5.73E-01	1
MCS$_9$	BE11	6.27E-03	2.19E-02	6
MCS$_{10}$	BE12	2.48E-03	8.67E-03	8

addition, the quality of the fuel sent to the boiler also has a significant effect on the character of the gas formed. In the elimination of this error, the chief engineer responsible for the operation and the personnel under his supervision should have accurate information about every stage of the operation and constantly monitor the system. On the other hand, if any it is very important to continuously monitor the pressure gauges between auto diverter valves and boiler entrance in operational and systemic terms, and if not, to install extra pressure gauges on the circuit in order to have accurate/up-to-date information.

Another control point in front of the gas coming out of the boiler with high oxygen concentration is the automatic diverter valves operating according to the oxygen analyser command. Inert gas with high oxygen concentration is sent to the chimney by means of automatic diverter valves and discharged. At this stage, it is foreseen that the malfunctions that may occur in the automatic diverter valves may cause gas that is not suitable for inerting operation to enter the cargo tanks and BE7 (lack of planned maintenance) is determined as the next critical failure for these valves. Onboard maintenance is an important part of the maintenance

activities of conventional ships. It includes regular or routine checks and services that can be performed by crews every day without disrupting operations (Deris et al., 1999; Yang et al., 2023). Planned maintenance activities are the activities that should continue uninterruptedly under ship conditions and their correct execution is tried to be secured by the ISM Code. However, as a result of the intensity of operations and contracted working dynamics, situations such as failure to standardise knowledge and experience in changing teams may cause disruptions in maintenance activities and/or incorrect maintenance and maintenance services. Ensuring regular and accurate control of these valves, which are an important transition point for inert gas, with extra records, supervision by the responsible engineer that the team maintaining such equipment has the correct information about the equipment, and finally, continuous surveillance during operation.

The second critical fault in the incorrect operation of the automatic diverter valves is receiving incorrect data from the oxygen analyser. Since it is known that the oxygen analyser will make incorrect measurements due to a system failure and/or incorrect calibration, BE4 (Defective/incorrect test gas use) was determined as the third critical error. Nonconformities such as the test gas used in the calibration of the oxygen analyser not being correct, sufficient and useable (expired, not stored under suitable conditions, etc.) may cause the oxygen analyser to

be incorrectly calibrated and make incorrect measurements. Incorrect gas measurement or no gas measurement at all is a significant cause of fire incidents in the maritime industry. It is very important to ensure that the personnel carrying out the measurements are trained and experienced, and that the equipment used to carry out the measurements is fit for purpose. This type of error can be avoided by making sure that the oxygen analyser is correctly calibrated using the appropriate test gases. Training and experience of the responsible personnel and checking the calibrated equipment from several different angles are important.

Another important point is to analyse the clusters of BE, i.e. MCS, that lead to the formation of TE. Table 9 shows the probabilities of the top ten MCS in the system and their ranking among themselves. Accordingly, TE is strongly influenced by BE10 (Incorrect pressure measurement in the air and fuel line), i.e. MCS8, which has the highest probability of occurrence. BE4 (Using defective/incorrect test gas) with the second highest probability of occurrence, i.e. (MCS3), and finally BE9 (Defective valve system) with the third highest probability of occurrence, i.e. MCS 7, are other important clusters involved in the occurrence of TE. BE10 and BE4 have been discussed in detail above under this heading.

BE9 (Defective valve system) is another critical MCS leading to the occurrence of TE. The valve system, which automatically adjusts the fuel and air inlet to the boiler, adjusts the oil and air circuit pressures by processing the data received from the circuits in a computing system. A faulty valve system can cause different amounts of air and fuel to enter the boiler, changing the character of the gas generated for the inerting operation. In the case of excessive air intake, the O_2 concentration in the generated gas will be high and this will again constitute the first link in the fault chain. The proper functioning of the valve system mentioned above can be possible to a large extent by regular and correct planned maintenance by knowledgeable and experienced responsible persons. On the other hand, close monitoring of the function of the system during operation allows early action to be taken in case of a malfunction that may occur.

In the light of what has been discussed above, in an environment where everything is in place for a fire to start, it can be seen that the malfunctions that are likely to occur in the inert gas circuit, which is designed to eliminate the possibility of fire by breaking the oxygen edge of the fire triangle, pose a high risk of fire and explosion in the system. The theoretical infrastructure of this study can be digitalised and made applicable before starting to work with inert gas. This allows measuring the risk of the process, analysing existing risks and deciding on preventive measures before the process has even been started. It is also possible to apply the combined risk analysis methods to other circuits on the ship, which carry operational risk and/or involve critical processes.

4. Conclusion

This paper presented a systematic approach for predicting and quantifying fire and explosion risks in inert gas systems (IGS) on-board tanker ships under HAZOP with D-S evidence theory - Fault Tree Analysis (FTA). Through the systematic evaluation of potential failure modes and their consequences using HAZOP analysis, critical scenarios were identified, providing a comprehensive understanding of the risk landscape associated with IGS malfunction. The incorporation of D-S evidence theory addressed uncertainties inherent in the analysis, allowing for the integration of expert knowledge and improving the reliability of risk assessments. A specific case study, fire and explosion risk in an inert gas system on-board tanker ship, is demonstrated to predict risk in quantitatively. According to the findings, the occurrence probability of TE (Fire and explosion risk in inert gas system due to high concentration of oxygen enters into tank) is found 2.86E-01. The findings of the research hold promise for enhancing safety standards and reducing the likelihood of fire and explosion incidents on tanker ships, ultimately ensuring the protection of personnel, cargo, and the marine environment.

Although the experts are experienced in inert gas systems in the maritime industry and the operations carried out through this system, the number of maritime experts can be considered as a limitation of the study. Another limitation of the study is that the study's findings have not been compared to other models because of data scarcity. Future research may include validating the findings with another robust risk assessment approach. Also, the results can be compared with the data obtained from the simulation environment. Besides further research will focus on refining the quantitative aspects of the analysis, such as improving the accuracy of failure probability estimates and considering dynamic factors that may influence risk levels. Additionally, exploring the applicability of the proposed approach to other maritime systems and expanding its scope to include environmental and economic considerations would be valuable for comprehensive risk management in the shipping industry.

CRediT authorship contribution statement

Ozcan Durukan: Writing – original draft, Resources, Methodology, Investigation, Formal analysis, Data curation. **Emre Akyuz:** Writing – review & editing, Supervision, Conceptualization. **Orhan Destanoğlu:** Supervision. **Yasin Arslanoğlu:** Writing – review & editing, Supervision, Conceptualization. **Sukru Ilke Sezer:** Writing – original draft, Methodology, Investigation, Formal analysis, Data curation.

Declaration of competing interest

The authors declare that they have no known competing financial interests or personal relationships that could have appeared to influence the work reported in this paper.

Data availability

No data was used for the research described in the article.

References

Ahn, Y.J., Yu, Y.U., Kim, J.K., 2021. Accident cause factor of fires and explosions in tankers using fault tree analysis. J. Mar. Sci. Eng. 9 (8) https://doi.org/10.3390/jmse9080844.

Akyuz, E., 2015. Quantification of human error probability towards the gas inerting process on-board crude oil tankers. Saf. Sci. 80, 77–86. https://doi.org/10.1016/j.ssci.2015.07.018.

Arici, S.S., Akyuz, E., Arslan, O., 2020. Application of fuzzy bow-tie risk analysis to maritime transportation: the case of ship collision during the STS operation. Ocean Eng. 217, 107960.

Arslan, O., Er, I.D., 2008. SWOT analysis for safer carriage of bulk liquid chemicals in tankers. J. Hazard Mater. 154 (1–3), 901–913. https://doi.org/10.1016/j.jhazmat.2007.10.113.

Aspinall, P., 2006. HAZOPS AND HUMAN FACTORS.

Ay, C., Güler, T., Bal Beşikçi, E., 2022. Implementation of ARAMIS methodology in the risk assessment of chemical tankers: the case of loading operation. Ocean Eng. 261 https://doi.org/10.1016/j.oceaneng.2022.112211.

Aydin, M., Arici, S.S., Akyuz, E., Arslan, O., 2021. A probabilistic risk assessment for asphyxiation during gas inerting process in chemical tanker ship. Process Saf. Environ. Protect. 155, 532–542. https://doi.org/10.1016/j.psep.2021.09.038.

Ceylan, B.O., Celik, M.S., 2024. Operational risk assessment of marine boiler plant for on-board systems safety. Appl. Ocean Res. 144 https://doi.org/10.1016/j.apor.2024.103914.

Chiang, C.C., Lee, J.C., Chang, Y.M., Chuang, C.F., Shu, C.M., 2009. Inert effects on the flammability characteristics of methanol by nitrogen or carbon dioxide. J. Therm. Anal. Calorimetry 96 (3), 759–763. https://doi.org/10.1007/s10973-009-0028-1.

Crawley, F., Tyler, B., 2015a. Factors for a successful HAZOP study. In: HAZOP: Guide to Best Practice. Elsevier, pp. 92–94. https://doi.org/10.1016/b978-0-323-39460-4.00012-8.

Crawley, F., Tyler, B., 2015b. The detailed HAZOP study procedure. In: HAZOP: Guide to Best Practice. Elsevier, pp. 13–28. https://doi.org/10.1016/b978-0-323-39460-4.00004-9.

Deris, S., Omatu, S., Ohta, H., Cdr, L., Kutar, S., Samat, P.A., 1999. Theory and Methodology Ship Maintenance Scheduling by Genetic Algorithm and Constraint-Based Reasoning.

Dunjó, J., Fthenakis, V., Vílchez, J.A., Arnaldos, J., 2010. Hazard and operability (HAZOP) analysis. A literature review. J. Hazard Mater. 173 (Issues 1–3), 19–32. https://doi.org/10.1016/j.jhazmat.2009.08.076.

Elidolu, G., Akyuz, E., Arslan, O., Arslanoğlu, Y., 2022. Quantitative failure analysis for static electricity-related explosion and fire accidents on tanker vessels under fuzzy bow-tie CREAM approach. Eng. Fail. Anal. 131 https://doi.org/10.1016/j.engfailanal.2021.105917.

Fang, X., Wang, H., Tan, B., Wang, F., Zhuang Shao, Z., Cheng, G., Yao, H., 2022. Experimental comparison study of CO2 and N2 inerted loose coal based on atmospheric pressure gas replacement. Fuel 328. https://doi.org/10.1016/j.fuel.2022.125347.

Formela, K., Neumann, T., Weintrit, A., 2019. Overview of definitions of maritime safety, safety at sea, navigational safety and safety in general. TransNav 13 (2), 285–290. https://doi.org/10.12716/1001.13.02.03.

Fuentes-Bargues, J.L., González-Cruz, M.C., González-Gaya, C., Baixauli-Pérez, M.P., 2017. Risk analysis of a fuel storage terminal using HAZOP and FTA. Int. J. Environ. Res. Publ. Health 14 (7). https://doi.org/10.3390/ijerph14070705.

Gachlou, M., Roozbahani, A., Banihabib, M.E., 2019. Comprehensive risk assessment of river basins using Fault Tree Analysis. J. Hydrol. 577 https://doi.org/10.1016/j.jhydrol.2019.123974.

Gharahasanlou, A.N., Mokhtarei, A., Khodayarei, A., Ataei, M., 2014. Fault tree analysis of failure cause of crushing plant and mixing bed hall at Khoy cement factory in Iran. Case Studies in Engineering Failure Analysis 2 (1), 33–38. https://doi.org/10.1016/j.csefa.2013.12.006.

Guo, Y., Jin, Y., Hu, S., Yang, Z., Xi, Y., Han, B., 2023. Risk evolution analysis of ship pilotage operation by an integrated model of FRAM and DBN. Reliab. Eng. Syst. Saf. 229, 108850.

ICS OCIMF, 2020. International Safety Guide for Oil Tankers and Terminals (ISGOTT), sixth ed.

IMO, 1990. Inert Gas Systems (Third). International Maritime Organization.

Khakzad, N., Khan, F., Amyotte, P., 2011. Safety analysis in process facilities: comparison of fault tree and Bayesian network approaches. Reliab. Eng. Syst. Saf. 96 (8), 925–932. https://doi.org/10.1016/j.ress.2011.03.012.

Kotek, L., Tabas, M., 2012. HAZOP study with qualitative risk analysis for prioritization of corrective and preventive actions. Procedia Eng. 42, 808–815. https://doi.org/10.1016/j.proeng.2012.07.473.

Lingfang, S., Yechi, W., 2012. Soft-sensing of oxygen content of flue gas based on mixed model. Energy Proc. 17, 221–226. https://doi.org/10.1016/j.egypro.2012.02.087.

Liu, P., Zhang, X., 2020. A new hesitant fuzzy linguistic approach for multiple attribute decision making based on Dempster–Shafer evidence theory. Applied Soft Computing Journal 86, 105897.

Malakhov, O.V., Kolegaev, M.O., Brazhnik, I.D., Saveleva, O.S., Malakhova, D.O., 2020. New forced ventilation technology for inert gas system on tankers. Int. J. Innovative Technol. Explor. Eng. 4, 2278–3075. https://doi.org/10.35940/ijitee.D1933.029420.

Markulik, S., Šolc, M., Petrík, J., Balážiková, M., Blaško, P., Kliment, J., Bezák, M., 2021. Application of fta analysis for calculation of the probability of the failure of the pressure leaching process. Appl. Sci. 11 (15) https://doi.org/10.3390/app11156731.

Milkovic, M., Krmek, I., Kristic, M., Sirotic, M., 2021. The possibility of the inert gas generator environmental operation mode utilization on long range 2 oil tankers during discharge operation. Nase More 68 (2), 131–136. https://doi.org/10.17818/NM/2021/2.9.

Mokhtarname, R., Safavi, A.A., Urbas, L., Salimi, F., Zerafat, M.M., Harasi, N., 2022. Application of multivariable process monitoring techniques to HAZOP studies of complex processes. J. Loss Prev. Process. Ind. 74 https://doi.org/10.1016/j.jlp.2021.104674.

Mountford, L.P., MimechE, B., Suen, K.O., MimechE MioR Mashrae, Ce, Goodall, L.M., Ceng MimarEst, Be, 2006. To what Extent Can Existing Inert Gas Technology Be Used to Provide Fire Protection on RN Surface Ships.

Ok, D., 2019. Enhancement of safety and design in cargo handling spaces to prevent accidental fire or explosion in oil tankers and FPSOs. In: Journal of Ship Production and Design, 35. Society of Naval Architects and Marine Engineers, pp. 299–308. https://doi.org/10.5957/JSPD.05180018, 4.

Okafor, E.G., Sun, Y.-C., Lu, Z., 2012. Safety Assessment of an On Board Inert Gas Generating System. Recent Patent Eng 6 (1), 70–79. https://doi.org/10.2174/187221212799436736.

Peeters, J.F.W., Basten, R.J.I., Tinga, T., 2018. Improving failure analysis efficiency by combining FTA and FMEA in a recursive manner. Reliab. Eng. Syst. Saf. 172, 36–44. https://doi.org/10.1016/j.ress.2017.11.024.

PQRI, 2014. Hazard & Operability Analysis (HAZOP) 1 Overview.

Rae, A., Alexander, R., 2017. Forecasts or fortune-telling: when are expert judgements of safety risk valid? Saf. Sci. 99, 156–165. https://doi.org/10.1016/j.ssci.2017.02.018.

Sezer, S.I., Akyuz, E., Arslan, O., 2022. An extended HEART Dempster–Shafer evidence theory approach to assess human reliability for the gas freeing process on chemical tankers. Reliab. Eng. Syst. Saf. 220, 108275 https://doi.org/10.1016/j.ress.2021.108275.

Sezer, S.I., Camliyurt, G., Aydin, M., Akyuz, E., Gardoni, P., 2023. A bow-tie extended DS evidence-HEART modelling for risk analysis of cargo tank cracks on oil/chemical tanker. Reliab. Eng. Syst. Saf. 237, 109346 https://doi.org/10.1016/j.ress.2023.109346.

Shahriar, A., Sadiq, R., Tesfamariam, S., 2012. Risk analysis for oil & gas pipelines: a sustainability assessment approach using fuzzy based bow-tie analysis. J. Loss Prev. Process. Ind. 25, 505–523. https://doi.org/10.1016/j.jlp.2011.12.007.

Shi, X., Zhuang, H., Xu, D., 2021. Structured survey of human factor-related maritime accident research. In: Ocean Engineering, 237. Elsevier Ltd. https://doi.org/10.1016/j.oceaneng.2021.109561.

Silvianita, Khamidi, M.F., Rochani, I., Chamelia, D.M., 2015. Hazard and operability analysis (HAZOP) of mobile mooring system. Procedia Earth and Planetary Science 14, 208–212. https://doi.org/10.1016/j.proeps.2015.07.103.

Siswantoro, N., Prastowo, H., Rosyadi, F.Z., 2020. Modification of seawater scrubber system into freshwater of inert gas system on the crude oil tanker 85,000 DWT. International Journal of Marine Engineering Innovation and Research 5 (Issue 2).

Solukloei, H.R.J., Nematifard, S., Hesami, A., Mohammadi, H., Kamalinia, M., 2022. A fuzzy-HAZOP/ant colony system methodology to identify combined fire, explosion, and toxic release risk in the process industries. Expert Syst. Appl. 192 https://doi.org/10.1016/j.eswa.2021.116418.

Soner, O., Asan, U., Celik, M., 2015. Use of HFACS-FCM in fire prevention modelling on board ships. Saf. Sci. 77, 25–41. https://doi.org/10.1016/j.ssci.2015.03.007.

Suzuki, T., Izato, Y. ichiro, Miyake, A., 2021. Identification of accident scenarios caused by internal factors using HAZOP to assess an organic hydride hydrogen refueling station involving methylcyclohexane. J. Loss Prev. Process. Ind. 71 https://doi.org/10.1016/j.jlp.2021.104479.

Taylor, D.A., 1990. Introduction to Marine Engineering. Butterworths.

Thomas, M., Skjong, R., 2009. Cost benefit analysis of inert gas systems for chemical and product tankers. In: 28th International Conference on Ocean, Offshore and Arctic Engineering. In: https://proceedings.asmedigitalcollection.asme.org.

Uflaz, E., Sezer, S.I., Akyuz, E., Arslan, O., Kurt, R.E., 2022. A human reliability analysis for ship to ship LNG bunkering process under DS evidence fusion HEART approach. J. Loss Prev. Process. Ind. 80, 104887.

Vesely, W.E., Goldberg, F.F., Roberts, N.H., Haasl, D.F., 1981. Fault Tree Handbook. Nuclear Regulatory Commission, Washington DC.

Williams, J.C., 1988. A data-based method for assessing and reducing human error to improve operational performance. In: Proceedings of IEEE 4th Conference on Human Factor and Power Plants. Monterey, California, pp. 436–453.

Yang, R., Vatn, J., Utne, I.B., 2023. Dynamic maintenance planning for autonomous marine systems (AMS) and operations. Ocean Eng. 278 https://doi.org/10.1016/j.oceaneng.2023.114492.

Yasa, H., Fatih, Ergin M., Ayfer, Ergin, Güler, Alkan, 2016. Importance of Inert Gases for Chemical Transportation, pp. 825–831.

Yazir, D., Sahin, B., Alkac, M., 2021. Selection of an inert gas system for the transportation of direct reduced iron. Math. Probl Eng. https://doi.org/10.1155/2021/8529724, 2021.

ABOUT UMT FACULTY

S D I

Selective Dissemination of Information (SDI) service is a current-awareness service offered by the PSNZ for UMT Faculty Members. The contents selection criteria include current publications (last 5 years), highly cited and most viewed/downloaded documents. The contents with pdf full text from subscribed databases are organized and compiled according to a monthly theme which is determined based on the topics of specified interest.

For more information or further assistance, kindly contact us at 09-6684185/4298 or email to psnz@umt.edu.my/sh_akmal@umt.edu.my

Thank you.